ABSTRACT

Title of dissertation: EXPERIMENTAL ATOMIC SPECTROSCOPY OF IRON GROUP ELEMENTS FOR ASTROPHYSICS

Jacob Wolfgang Ward
Doctor of Philosophy, 2021

Dissertation directed by: Dr. Gillian Nave
Department of Physics

The quality of modern astrophysical spectra has made it clear that there is a lack of sufficiently accurate and robust laboratory atomic reference data sets. Particularly for spectra of the iron-group elements, the growing demand for critically evaluated sets of comprehensive atomic data is a direct result of advancing stellar astrophysics models and fundamental physics problems probing beyond the standard model. My thesis reports on my critical evaluation of the Ni V spectrum and the recent laboratory measurements I have conducted to improve the state of available reference data for astrophysical applications that rely on observations of Ni V. Additionally, I report my laboratory measurements of Fe II branching fraction values in the UV/VUV.

Using high-resolution grating spectroscopy at the National Institute of Standards and Technology, I have carried out an analysis of quadruply ionized iron and nickel (Fe V & Ni V) in the vacuum ultraviolet (VUV) region by both recording new spectra and critically evaluating previously published data sets. My analysis

has resulted in highly accurate wavelengths, presented with calculated oscillator strengths, for roughly 1500 Ni V lines, 200 of which have uncertainties that are almost an order of magnitude lower than in previous publications. Additionally, I present over 300 Ni V energy levels derived from my evaluated wavelengths. This section of my thesis focuses on the large improvements made in the analysis of Ni V, but my work also strongly supports the previous evaluations of Fe V by another author. With the extreme accuracy requirements of modern astrophysics problems, confirming the wavelength scale and uncertainty evaluation of previous Fe V data sets is still significant.

In addition to the above work, my thesis also presents measurements of singly ionized iron (Fe II) branching fractions (BFs) in the VUV using high-resolution Fourier-transform spectroscopy. BFs are essential values for interpreting complex astrophysical spectra, but are notoriously difficult to measure in the VUV; for this reason, VUV BFs of Fe II have only been reported by one other research group for just seven levels. My thesis reports accurate BFs for 11 Fe II levels, involving approximately 100 spectral lines (16 in the VUV), which roughly doubles the amount of reported Fe II BFs in VUV.

EXPERIMENTAL ATOMIC SPECTROSCOPY OF IRON GROUP ELEMENTS FOR ASTROPHYSICS

by

Jacob Wolfgang Ward

Dissertation submitted to the Faculty of the Graduate School of the
University of Maryland, College Park in partial fulfillment
of the requirements for the degree of
Doctor of Philosophy
in the subject of Physics
2021

Advisory Committee:
Dr. Gillian Nave, Advisor
Professor Steve Rolston, Chair
Professor Trey Porto
Professor Ronald Walsworth
Professor Wendell Hill

Dedication

To my most wonderful wife, Christie, your strength and love are my most precious gifts. I thank you for all you have helped me become. You are my shining light.

Acknowledgments

Gill, it has been my honor to work with you. You have mentored me though the majority of my early career and I feel immensely lucky for it. We have shared many conversations in our sparsely occupied section of the lab and they have helped me navigate the challenges I've faced in trying to become a better physicist. Our time together has taught me a great deal of atomic physics and spectroscopy. It has also taught me that determination in the lab is invaluable and that I can breathe new life into almost anything with enough elbow grease (or vacuum grease). I am so grateful for your support, patience, and insights. I am also simply thankful for the time we were able to share together at picnics, star parties, and coffee breaks.

To my family, thank you for the love and support. It meant a great deal to me that I knew I could always call and you would lend me your ear. To my parents, thank you for instilling in me a love for learning and giving me the opportunities to pursue it. The sacrifices you made to support me are bearing fruit, and I thank you for it. To my sisters, thank you for being my advocates, friends, and inspirations. Emily, I hope to be as strong for my family as you are. Gabby, I hope to be as kind and loving as you are.

To the NIST Atomic Spectroscopy Group, I have so enjoyed my time working with you. I have learned more from you all than I could have hoped to during my stay at NIST. More so than any other place I have worked, you have created a welcoming and inclusive group that helped me feel supported in my various endeavour at NIST. Thank you for the much needed conversations and coffee, they helped me stay

positive through some of my tougher days.

To Yuri Ralchenko, thank you for navigating the waters between NIST and UMD. I could not have made things work without you. The support and opportunities I've had with your help have made me a better physicist.

To Steve Rolston and Trey Porto, thank you for helping me navigate the physics program at UMD. Your willingness to give me your time throughout this journey is much appreciated.

To Aung Naing, thank you for being a wonderful office mate and for letting me bounce ideas around with you.

To Joe Reader, Craig Sansonetti, and Albert Henins, thank you for sharing your expertise in the lab with me. Your generosity and skills made this thesis possible.

To my committee members, thank you for helping me on this final step.

To the housemates of 8808, thank you for picking me up when I was down and putting a smile on my face when I needed it most. I will always remember how quickly and brilliantly that house became a home.

Table of Contents

List of Figures

List of Abbreviations

e	Electron Charge
$\hbar$	Reduced Planck Constant
ε_0	Vacuum Permittivity
ASD	Atomic Spectra Database
BF	Branching Fraction
Fe II	Spectrum of Singly Ionized Iron
Fe V	Spectrum of Quadruply Ionized Iron
FTS	Fourier Transform Spectrometer
FUV	Far-ultraviolet
HCL	hollow cathode lamp
NIST	National Institute of Standards and Technology
Ni V	Spectrum of Quadruply Ionized Nickel
NIVS	Normal Incidence Vacuum Spectrograph
NLTE	non-Local Thermodynamic Equilibrium
PMT	Photomultiplier Tube
PTB	Physikalish-Technische Bundesanstalt
UV	Ultraviolet
VUV	Vacuum Ultraviolet
ZOPD	Zero Optical Path Difference

Chapter 1: Introduction

My thesis work, presented here, is intended to aid the astronomy community in interpreting the spectra of astrophysical objects by providing atomic reference data. The development of large sets of atomic data has been ongoing for many decades, as will be shown later, but improvements in astronomical instrumentation for observing astrophysical spectra are also perpetual and often times outpace the improvements of reference data sets. Recently, the need for improved laboratory measurements of atomic features has been cited across the astronomy community as a key element in developing an improved understanding of multiple astrophysical processes and models [1]. It is not uncommon for the laboratory atomic data to be the dominant source of uncertainty in an astrophysical measurement or for the laboratory data to simply not be available to astronomers as it has not yet been measured.

My graduate work is a direct response to these issues and took place in the context of a larger effort by my advisor and our collaborators to greatly improve the availability and quality of atomic data for multiple atomic species. What is presented in the remainder of my thesis, which focuses on three species: singly ionized iron (Fe II), quadruply ionized iron (Fe V), and quadruply ionized nickel (Ni

V), is only a sliver of the work being done and what is left to be done in order to meet the needs of the astronomy community.

The remainder of this chapter will explain the details of the relationship between laboratory measurements of atomic data and astrophysics, particularly in the context of the measurements I carried out in this thesis.

1.1 The Iron-Group

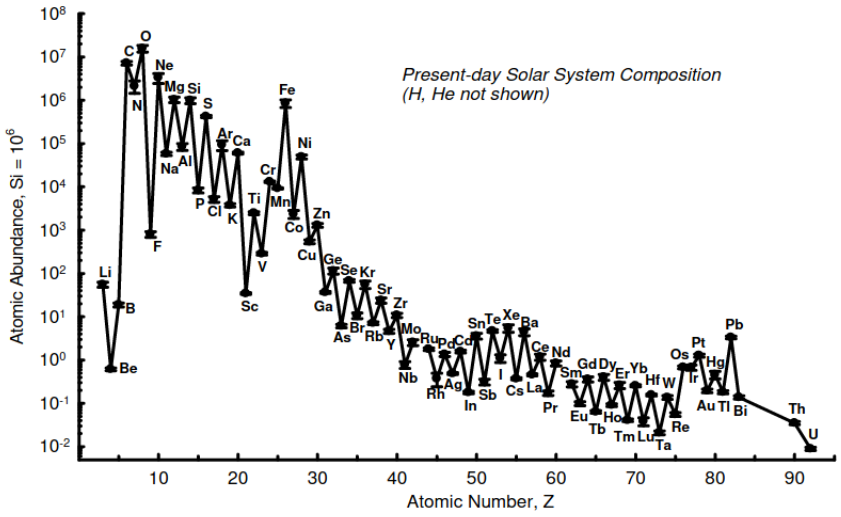

Figure 1.1 Relative solar abundances of the chemical elements from Lodders [2].

As I have noted at the beginning of this chapter, the three species my thesis work is focused on are Fe II, Fe V, and Ni V. All three of these elements are members of what is commonly referred to as the iron-group elements. The iron-group, Sc through Ni, are a part of an abundance peak, shown in Figure 1.1, that is crucial for astrophysics work. Unlike the lighter, most abundant elements, the iron-group elements contribute thousands, not hundreds, of spectral lines in stellar

spectra. For example, the number of lines in the NIST Atomic Spectra Database (ASD) for Fe II is roughly 13000 while O II has only about 1600. The highly dense iron-group spectra, due to the open 3d-shell structure of the iron-group elements, are responsible for the majority of the spectral lines in stellar spectra. Since this group of elements makes up most of the observable lines, they are of critical importance to astrophysicists. While the spectral density makes these elements important, it also increases the need for high quality reference data, since many of the lines are blended in stellar spectra. With many iron-group lines blended in stellar measurements, they require a thorough, accurate, and critically evaluated set of wavelengths, levels, and transition probabilities in order to accurately model the observed stellar spectra.

1.2 Examples of Astrophysics Driving the Need for New Atomic Data

The need for improved atomic reference data spans far too many topics in astronomy for me to provide a comprehensive summary here. I will instead highlight two examples that directly motivated the specific work I pursued during my graduate program. The nature of providing reference data means my work could likely be used for a variety of applications, but what I want to discuss here is what I had in mind when pursing the measurements and analysis that make up my dissertation.

1.2.1 The Search for Variations in Fundamental Constants

The development of unification theories that depend on spatial and temporal variations of physical constants has and continues to be of interest to the physics community. Variations in the fine structure constant, α, contribute to multiple cosmological models and string theories, as discussed by Martins [3], such as the Bekenstein-Sandvik-Barrow-Magueijo theory [4, 5, 6]. The search for variations in α has previously made use of methods involving both measurements based on atomic clocks [7, 8, 9] and on the observations of quasar spectra [10, 11] with the objective being to detect the potential variation of α with ever increasing precision.

In part, α, defined in equation 1.1, is of particular interest in this context because it is a part of a unique class of physical constants that are dimensionless. By studying dimensionless constants, such as α, variability in the constant is less entangled with physical units that might change over space and time in a way that would mask the variation of the constant.

$$\alpha = \frac{e^2}{(4\pi\varepsilon_0)\hbar c} \approx \frac{1}{137} \tag{1.1}$$

Additionally, the particular value of α impacts the interaction strength between matter and electromagnetic radiation, and so a change in α would yield a change in atomic energy levels that would be measurable by studying the spectra of ions in various astronomical conditions.

The motivation behind my work stems from publications that investigate the

possible dependence of α on strong gravitational fields such as the 2013 paper by Berengut et al. [12]. That study makes use of far-UV spectral observations of Fe V and Ni V in the atmosphere of the G191-B2B white dwarf star [13]. G191-B2B provides data for an analysis of the fine structure constant where the ions producing the observed spectrum experience a gravitational potential (relative to laboratory conditions) that is seven orders of magnitude larger than in previous studies based on Earth bound atomic clocks. The proposed relationship between the laboratory wavelengths and those observed near the white dwarf by Berengut et al. [12] is

$$\frac{\lambda - \lambda_0}{\lambda_0} = z - Q_\alpha \frac{\Delta\alpha}{\alpha}(1+z) \tag{1.2}$$

where Q_α is the sensitivity of the transition to variation in α, z is the gravitational redshift, λ_0 is the laboratory wavelength of a transition provided by either Raassen and van Kleff [14] or Ekberg [15], and λ is the wavelength observed near the white dwarf.

The analysis conducted by Berengut et al. [12] resulted in conflicting estimates for $\Delta\alpha/\alpha$. The model described by equation 1.2 was applied to both Ni V and Fe V data with the slope $\Delta\lambda/\lambda$ vs Q_α giving $\Delta\alpha/\alpha$. Figure 1 of Berengut et al. [12], replicated here in Figure 1.2 shows the resulting fitted slopes with the results for Ni V being $\Delta\lambda/\lambda < 0$ and for Fe V $\Delta\lambda/\lambda > 0$. The laboratory wavelength standards for both Fe V and Ni V dominate the uncertainty of the fine structure variation in Berengut et al. [12] and make it difficult to determine what all may underlie the inconsistent results.

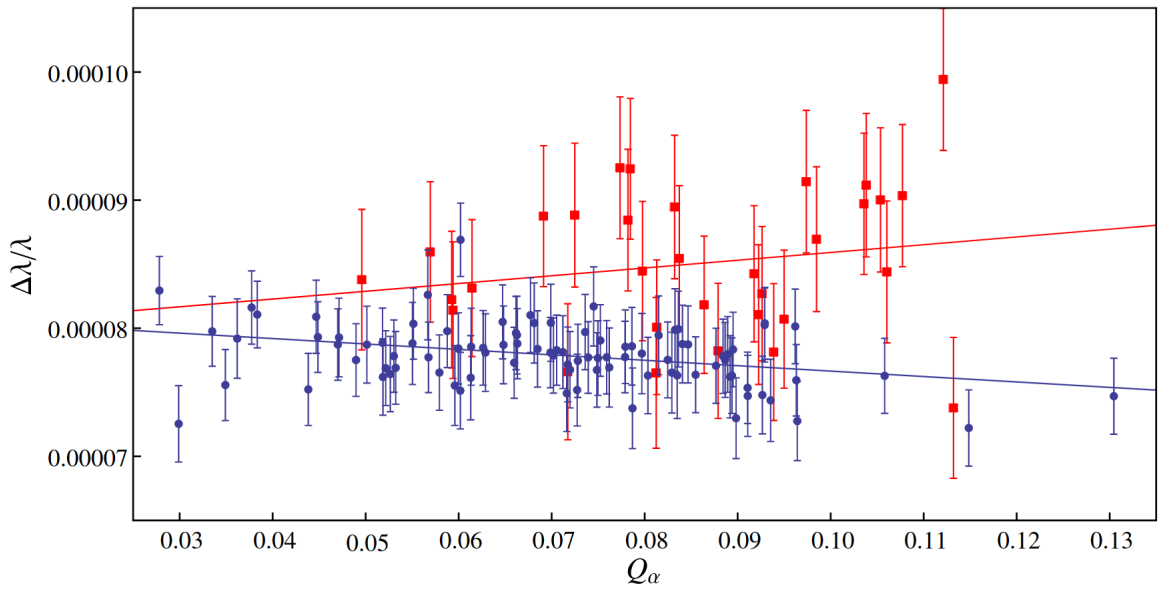

Figure 1.2 Replication of Figure 1 from Berengut et al. [12] with Ni V data shown in red and Fe V shown in blue. The best fit lines through the data provide the value for $\Delta\alpha/\alpha$ and indicate $\Delta\alpha/\alpha > 0$ for Ni V, but $\Delta\alpha/\alpha < 0$ for Fe V.

To help better constrain the potential variation of α, much of my thesis work focused on reevaluating the laboratory wavelength standards for Fe V and Ni V. My approach to this problem is described in chapter 2 and I discuss the results of my efforts in chapter 3. My work on this subject was published in 2019 in the journal contribution Ward et al. [16].

1.2.2 Stellar Atmospheric Models & Chemical Abundances

To determine the stellar abundance of an element, astrophysicists compare laboratory spectra to stellar spectra. This application of laboratory atomic data requires not only transition wavelengths, but also line strength data (oscillator strengths f) to accurately model the stellar spectra and determine abundances. The accuracy of experimental oscillator strengths greatly exceeds the accuracy of

calculated values for all but the strongest transitions. The experimental difficulty and cost of measuring laboratory transition probabilities, which are used to derive oscillator strengths, has meant that astrophysicists often have to supplement the few experimental values available to them with less accurate calculated values.

Having accurate abundance values for a wide variety of stars (with varying metallicity) is an essential prerequisite for understanding the chemical evolution of our universe [2]. The variability in the metallicity of stars is due to the progenerative process by which dying massive stars eject heavier elements into the interstellar medium of their galaxy. The ejected elements are then incorporated into the next generation of stars that will have a higher abundance of metals. Because the chemical evolution of galaxies is tied to the generational changes in the composition of the stars in a galaxy, measuring the abundances of elements in a variety of stars through a galaxy is a primary method of tracing the evolution of elements. While laboratory spectroscopists and astrophysicists have greatly improved our understanding of this topic over many decades, many stellar lines remain unidentified or are without laboratory line strength values. Particularly as astrophysicists are now pushing towards more accurate 3D non-local thermodynamic equilibrium (NLTE) models of stellar atmospheres, the drive to have accurate atomic parameters for all known lines is a priority for multiple applications.

To help address these data needs, I took advantage of the equipment at NIST to measure transition probabilities for Fe II in the UV and VUV. Fe II, a dominate contributor to essentially all stellar spectra, is critically lacking A value data in the VUV and I felt this would be a worthy contribution to tackle. My approach

to this problem is described in chapter 2 and I discuss the results of my efforts in chapter 4. My work on this subject is currently being developed into a manuscript for submission to *The Astrophysical Journal Supplement Series*.

1.3 The Type and Range of Atomic Data Needed

The laboratory atomic data I will be presenting concerns three different parameters: atomic energy levels, transition wavelengths, and transition probabilities that are derived from measuring relative line intensities and level lifetimes. These types of atomic data can be found in a variety of databases that have varying degrees of quality and completeness. One such database is the Atomic Spectra Database (ASD) [17] hosted and supported by the National Institute of Standards and Technology (NIST) Atomic Spectroscopy Group. The NIST ASD contains atomic reference data for: wavelengths, energy levels, ionization energies, relative line intensities, and transition probabilities for a wide range of species. Other databases tend to be more focused, often for a specific set of applications, and so they are less indicative of the general state of available data. For the remainder of my thesis, when it is needed, I will make reference to the values given in the NIST ASD in order to give the reader an understanding of the availability/completeness of a particular type of data for a given ion. Since the NIST ASD is actively managed by NIST staff to keep it up to date with critically evaluated datasets it is a useful metric to point to when trying to understand how much work is left to be done for a specific ion.

1.3.1 Atomic Energy Levels and Wavelengths

Two of the primary atomic parameters most needed by astrophysicists are the discrete energy values that describe the range of states an atom has and the wavelengths of the photons emitted when an atom transitions from one state to another. The lowest possible energy level of a neutral atom or an ion is referred to as the ground level, which is commonly set to zero in atomic spectroscopy work, with states above the ground level having positive energy values. The most common unit for energy level values in atomic spectroscopy is cm^{-1}, but it is also common in astrophysics work to see energy levels given in eV. My thesis will adopt the spectroscopy standard of using cm^{-1} when describing energy level values.

The first step in understanding the energy level structure of a species is determining the hierarchy of interactions (Coulomb, spin-orbit, etc...) within the system of the species. The Coulomb interaction is responsible for the electron-nucleus and electron-electron interactions. The electron-nucleus interaction is described by the principle quantum number n and is usually referred to as the gross structure of the system. The electron- electron Coulomb interaction splits the gross structure of the system with an orbital angular momentum quantum number (l). The quantum numbers n and l describe a system's configurations. The orbital angular momentum and the spin angular momentum (s) of an electron in an atom are magnetically coupled to yield a total angular momentum ($\mathbf{J}$). This spin-orbit interaction produces a fine-structure in the system.

The strength of the various interactions helps to determine the appropriate

way to describe the coupling between the orbital and spin angular momenta. When the relativistic interactions are much smaller than the electron-electron Coulomb interaction, the Russell-Saunders or **LS** coupling scheme is usually valid. In **LS** coupling the orbital angular momenta of the electrons are coupled into a total angular momentum $\mathbf{L} = \sum_i l_i$ and the spin angular momenta of the electrons are coupled into a total spin momentum $\mathbf{S} = \sum_i s_i$. Combining an **L** and an **S** value results in a spectroscopic term ($^{2S+1}\mathbf{L}$). The coupling of the **L** and **S** vectors, such that $\mathbf{J} = \mathbf{L} + \mathbf{S}$, yields a total angular momentum **J** that, along with the term, defines a particular level described by $^{2S+1}\mathbf{L}_J$.

When considering the structure of the excited levels of an atom or ion, the ground configuration of the next higher ion is used. This parent configuration, for complex spectra, results in multiple parent **LS** terms. By adding an electron to each of the parent terms, the **LS** terms of the ion can be determined. Thus, the configuration of the ion is split into subconfigurations by the parent **LS** terms. The common way of denoting this scheme is $nl^N(^M\mathrm{L})n^*l^*$, where nl^N represent the N core electrons that couple to give the parent configuration nl, $M = 2S + 1$ is the multiplicity of the parent term (L), and n^*l^* are the quantum number(s) of the excited electron(s). The coupling of the n^*l^* excited electron to the parent term yields the LS terms and levels of the ion itself. A simple example is that of neutral nitrogen, which has the parent configuration $2p^2$ from the ground configuration of neutral carbon [18]. The $2p^2$ parent configuration splits into three **LS** parent terms: ^{3}P, ^{1}D, ^{1}S. We can now add, for example, a 3p electron to each of the parent terms and determine the **LS** terms of the subconfigurations: $2p^2(^3\mathrm{P})3p$, $2p^2(^1\mathrm{D})3p$,

$2p^2(^1S)3p$. For simplicity we can take just the $2p^2(^3P)3p$ and determine the resulting terms. The 3p electron couples to the three core p electrons of the parent term so that $\mathbf{L} = \mathbf{l} + \mathbf{L}_{core}$ results in $L = 0, 1, 2$. The multiplicity of the parent term is three, so $S_{core} = 1$ and $\mathbf{S} = \mathbf{S}_{core} + \mathbf{s}$ results in $M = 2, 4$. So, we have the terms: ^{4}S, ^{2}S, ^{4}P, ^{2}P, ^{4}D, ^{2}D. A resulting full **LS** term of N I would then be $2p^2(^3P)3p\ ^4S$. Each term then has a corresponding range of total angular momentum values that result in a specific energy level with an energy value.

The energy level values are determined by experimentally measuring the wavelengths of an array of spectral lines that each represent the energy difference between two levels in the species. Because we can only determine the energy level structure of a species by measuring the transition wavelengths which result from the relative energy differences between two energy states, setting the ground state energy to zero, described above, is simply a convenient convention. Each spectral line has an experimentally determined wavenumber, the number of wave oscillations in a given unit of space (cm^{-1}), that is related to the energy difference between the two levels in the transition, E, by $E = (hc)/(\lambda_{vac})$, where h is the Planck constant, c is the speed of light in vacuum, and λ_{vac} is the vacuum wavelength of the emitted photon that registers as the spectral line. The vacuum wavelength, often given in nm or Å (1 Å = 0.1 nm), and the vacuum wavenumber are related by $\lambda_{vac} = (1)/(\sigma_{vac})$, where σ_{vac} is the vacuum wavenumber.

Once an array of spectral line wavelengths is experimentally measured, a combination of theory and computational analysis is used to generate a set of energy levels. The tool used in this thesis to generate energy levels from wavelengths is

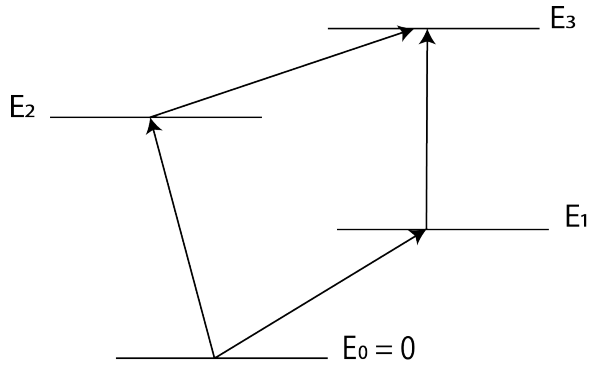

Figure 1.3 Sample four level system with transitions (denoted by arrows) connecting all three levels to demonstrate level optimization.

LOPT [19], a program developed by Alexander Kramida, a member of the NIST Atomic Spectroscopy Group, to optimize the fitting of energy levels to a set of experimentally determined wavelengths using least squares optimization. The general principle behind LOPT and other programs like it is to use matrix inversion to solve the system

$$\sum_N E_N W_{iN} = \Lambda_i \tag{1.3}$$

where E is the energy of the level, W is a matrix of weighting factors related to the inverse of the wavenumber uncertainties used, and Λ is a linear combination of the multiple transition wavenumbers (σ) with weighting factors also connected to the uncertainty of the wavenumbers. The sum is spanned over the range of excited levels (N). In a simple example, such as the one shown in Figure 1.3, the system of

equations for three excited levels is easily understood. In this case, $N = 3$ and so,

$$\mathbf{W} \begin{pmatrix} E_1 \\ E_2 \\ E_3 \end{pmatrix} = \begin{pmatrix} w_{01}\sigma_{01} - w_{13}\sigma_{13} \\ w_{02}\sigma_{02} + w_{23}\sigma_{23} \\ w_{23}\sigma_{23} - w_{13}\sigma_{13} \end{pmatrix} \tag{1.4}$$

where, refering to Figure 1.3, σ_{01} represents a transition from the ground state to the excited state E_1 and σ_{13} represents a transition from the first excited state to the third excited state, both of which help to constrain the E_1 level. By inverting the matrix $\mathbf{W}$ the weighted least-squares approximation to the energy levels is found.

Once a system of optimized energy levels is determined, the energy differences can be used to calculate wavelengths, referred to as Ritz wavelengths, with potentially much lower uncertainties than their experimentally measured counterparts. Provided there are enough measured wavelengths without perturbations increasing their uncertainties, there will be many levels whose energies are determined by more than one transition, thus leading to lower uncertainties in the calculated Ritz wavelengths. There is usually a recursive process where a comparison of Ritz and observed wavelengths can be used to study potential errors in the observed wavelengths. This can yield, in turn, a more sophisticated level optimization with lower energy level uncertainties and Ritz wavelength uncertainties. A more detailed discussion of this process and the particular approach I took is handled in chapter 3.

1.3.1.1 Previous Energy Levels and Wavelengths of Fe V

The vast majority of the atomic data published for Fe V before my thesis work comes from three sources: Ekberg [15], Azarov et al. [20] and the compilation by Kramida [21]. Ekberg [15] published data in 1975 for roughly 1000 lines spanning two spectral regions ($300-530$ Å & $1060-1715$ Å). The shorter region was measured using a grazing incidence spectrograph at NIST and the longer region was measured using a normal incidence spectrograph also located at NIST. Both regions used a sliding spark light source and photographic plates for detectors. The experimental techniques and instrumentation used by Ekberg [15] are very similar to those used in my thesis work. The wavelength uncertainty reported by Ekberg [15] in the grazing incidence region was 0.003 Å and 0.004 Å in the normal incidence region. These reported uncertainties were supported by Berengut et al. [12] who compared the values of Preval et al. [13] to Ekberg [15] and by Kramida [21] who compared the measured wavelengths of Ekberg [15] to wavelengths derived from optimized energy levels. In addition to accurate wavelengths, Ekberg [15] also reported energies for almost all of the levels in the $3d^4$, $3d^34s$, and $3d^34p$ configurations derived from his measured wavelengths. The estimated uncertainties of all level values given by Ekberg [15] are 0.4 cm^{-1}.

The second main source of data, published in 2001 by Azarov et al. [20], added roughly 1000 additional lines in the $647-1185$ Å region. Azarov et al. [20] also used a normal incidence spectrograph, but used a vacuum triggered spark rather than a sliding spark source. They reported uncertainties of 0.003 Å below 950 Å and 0.005

Å above. Kramida [21] also compared the observed wavelengths of Azarov et al. [20] to wavelengths derived using energies and found a consistent standard deviation of 0.006 Å across the entire reported spectral range and so adopted 0.006 Å for the wavelength uncertainties for that dataset. In addition to wavelengths Azarov et al. [20] also reported energies derived from their observations with uncertainties between 0.7 cm^{-1} and 1.0 cm^{-1}.

The final comprehensive source of Fe V data, published in 2014, was a critical compilation and analysis of all reliable sources of data by Kramida [21]. This compilation combined data from Ekberg [15], Azarov et al. [20], and various smaller sources of data and conducted a larger more comprehensive level optimization that resulted in roughly 2000 lines and 300 levels with greatly reduced uncertainties. Kramida [21] reports that 80% of all known Fe V levels had their uncertainties reduced by a factor of three and 65% of all known lines had their calculated Ritz wavelength uncertainties reduced by up to a factor of four compared to the measured wavelength uncertainties.

Other valuable, but significantly less comprehensive, Fe V publications are available [22, 23]. Kramida [21] mentions some of these other datasets, particularly those that focus on "forbidden" M1 and E2 transitions, but my thesis work does not make use of these other sources and so they will not be covered in detail.

1.3.1.2 Previous Energy Levels and Wavelengths of Ni V

The most comprehensive source for laboratory data on Ni V comes from Raassen et al. [24] and Raassen and van Kleff [14], published in 1976 and 1977 respectively. These datasets, which span two spectral regions (200−400 Å & 900−1400 Å), were generated using a grazing incidence spectrograph in the shorter wavelength region and a normal incidence spectrograph in the longer wavelength region. Raassen et al. [24] reported wavelength uncertainties of 0.001 Å (200 − 400 Å), but Raassen and van Kleff [14] did not report wavelength uncertainties. The Ni VI study by Raassen [25], however, which was similarly conducted, reported wavelength uncertainties of 0.006 Å. The estimate of 0.006 Å is plausible as Berengut et al. [12] also suggested an estimate of 0.007 Å when using the values from Raassen and van Kleff [14] after comparing the wavelengths to stellar spectra. In addition to wavelength data, these datasets also report roughly 300 energies from the $3d^6$, $3d^5 4s$, and $3d^5 4p$ configurations with estimated uncertainties of 0.1 cm^{-1}.

1.3.2 Transition Probabilities

Transition probabilities, A_{ik}, defined as the probability per unit time that an atom in an upper energy level (i) spontaneously decays to a lower energy level (k), are another type of essential atomic parameter needed by astrophysicists. If an upper level, i, has j possible decay channels, then the inverse of the sum of the j

transition probabilities is equivalent to that upper level's total lifetime, τ_i,

$$\tau_i = \frac{1}{\sum_j A_{ij}}. \tag{1.5}$$

By defining a second parameter, the transition's branching fraction (BF), as,

$$BF_{ik} = \frac{A_{ik}}{\sum_j A_{ij}} \tag{1.6}$$

and recognizing that the measured intenisty of a spectral line, I_ik, is proportional to,

$$I_{ik} \propto g_i N_i A_{ik} \tag{1.7}$$

where g_i is the statistical weight and N_i is the population of the upper level, equation 1.6 can be redefined as,

$$BF_{ik} = \frac{A_{ik}}{\sum_j A_{ij}} = \frac{I_{ik}}{\sum_j I_{ij}} \tag{1.8}$$

so that measured line intensities can be used to determine a transition's BF. By combining equations 1.5 and 1.6 I can now demonstrate the way that my thesis work approaches the measurement of transition probabilities since we now have an equation,

$$A_{ik} = \frac{BF_{ik}}{\tau_i} \tag{1.9}$$

that relates two measurable or calculable quantities, BFs and lifetimes, to atomic transition probabilities.

With the basic theory laid out, I can highlight a few key challenges to this type

of work. While there are serious considerations to be discussed for measuring both lifetimes and BFs, my thesis is focused on measuring BFs and utilizing theoretically calculated lifetimes from outside sources, so I will only be focusing on some of the experimental difficulties associated with BFs. Noting that equation 1.8 includes a summation over all possible decay channels brings up two challenges. In order to arrive at accurate BFs, the experimental setup needs to have a wide spectral range and the response of the system across that range needs to be well known in order to measure accurate line intensities. This often involves using multiple detectors, sources, and filters to measure various spectral ranges and then joining up the various regions. Additionally, some of the decay channels are likely to produce lines with such low intensities that they are not observed in laboratory spectra. The residual decay channels, not accounted for in the summation in equation 1.8, can severely impact the uncertainty of the resulting BFs. Thus, an ideal setup would have a well known spectral response over a wide spectral range and would be sensitive enough to pick up all but the weakest lines in the spectrum. This is not a trivial goal, but I will show that the equipment used in my thesis approximates this ideal setup, likely in a way that almost no other research groups in the world can currently replicate.

To give some sense as to how difficult this experimental work can be, I would like to point to the current state of available BFs for Fe II in the VUV region, which is the focus of roughly half of my thesis. Of the roughly 3000 spectral lines in the NIST ASD from Fe II in the VUV only 21 have experimentally measured transition probabilities. These 21 values stem from two papers published by my advisor's long time collaborators at Imperial College London [26, 27] who have similar experimental

equipment to that used in my thesis work. These two papers were the first to publish experimental transition probabilities for Fe II in the VUV and they target 7 of the over 100 known levels in the singly excited Fe II system.

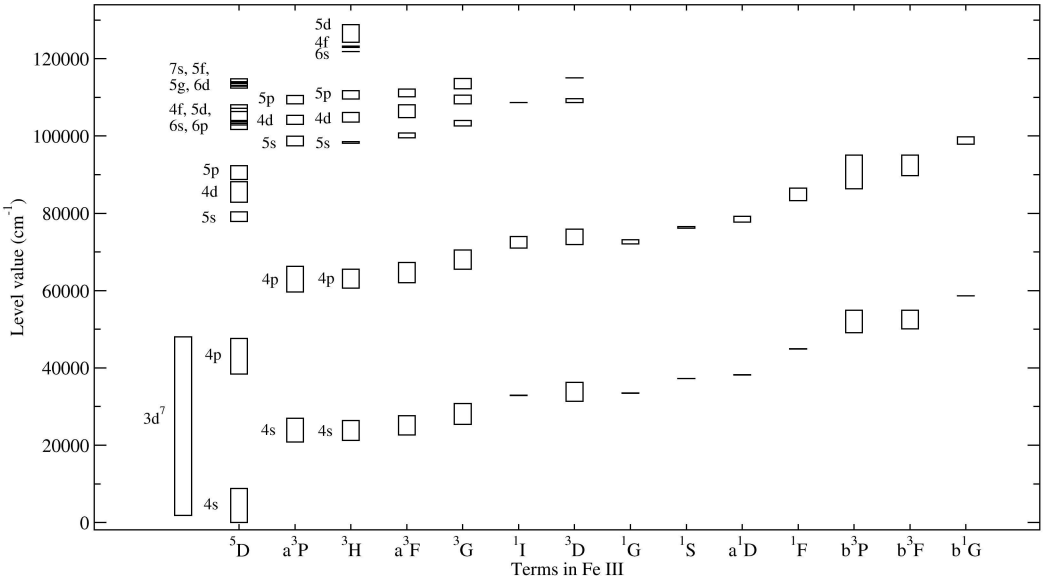

Figure 1.4 Partial energy level diagram of the singly excited system of Fe II. Level values are from Nave and Johansson [28].

To better understand some of the experimental choices I discuss in later chapters, and to get a more general sense of the structure of the Fe II ion, I want to present the makeup of the ion and relate that to the energy level diagram of the singly excited system of Fe II I have included in Figure 1.4. Fe II has seven valence electrons and is based on two parent configurations of Fe III. The singly excited system ($3d^6nl$) is based on the $3d^6$ parent configuration, while the doubly excited system ($3d^54snl$) is based on the $3d^54s$ parent configuration. My work focuses on the singly excited system that is built on the 16 parent **LS** terms of the $3d^6$ ground configuration of Fe III. The ^{5}D term of Fe III sets the ionization limit of Fe II and the 16 parent **LS** terms sit above the ^{5}D term. Figure 1.4 also includes the $3d^7$

configuration whose terms cannot be clearly assigned to a particular parent term.

The energy level diagram highlights a number of features of Fe II that have important implications in experimental measurements of its atomic parameters. The diagram highlights that the bulk of the strongest transitions are all grouped in the ultraviolet (UV) as the separation between the 4s and 4p subconfigurations are relatively constant across the various LS parent terms. Thus, transitions between levels in the 4s and 4p subconfigurations, $3d^6(^M L)4s$-$3d^6(^M L)4p$, where $^M L$ is the parent term, all give lines near 45000 cm^{-1}. Additionally, the Figure illustrates that a variety of vacuum ultraviolet lines (VUV) will be present, coming from the $3d^7$-$3d^6(^M L)4p$ transitions. Recognizing this structure is essential in designing experimental procedures, such as selecting light sources and optics, so that the plasma sufficiently populates the desired 4p levels and the optics support UV and VUV measurements.

While my thesis will present transition probabilities as the final product of chapter 4, astrophysicists usually work in terms of oscillator strengths, f, because astrophysical spectra are absorption spectra rather than emission spectra. In absorption spectroscopy the equivalent width (W_ν) of a line, which is important for determining column densities, can be written as,

$$W_\nu = l \int_0^\infty k_\nu d\nu = \frac{e^2}{4\varepsilon_0 mc} N f l \tag{1.10}$$

for the optically thin case, where l is the length of the absorbing column, k_ν is the opacity, N is the number of absorbing atoms, and f is the oscillator strength of

the transition. This is why, particularly in work related to determining elemental abundances, oscillator strengths are the normal values being discussed. The relation between f and A values for allowed E1 (Electric Dipole) transitions is,

$$f_{ik} = \frac{\varepsilon_0 mc^3}{2\pi e^2 \nu^2} \frac{g_i}{g_j} A_{ik} = 1.499 \times 10^{-16} \frac{g_i}{g_k} \lambda^2 A_{ik} \tag{1.11}$$

where the g values are the statistical weight of the two levels, and λ is the wavelength of the transition given in Å. Traditionally, oscillator strengths are reported as the logarithm of $g_k f$. While an important amount of theoretical work has been done, largely in the UV, to calculate f values, the accuracy of calculated oscillator strengths of weak lines is not sufficient for many modern astrophysics applications. As the strong lines in astrophysical spectra are often saturated, accurate experimental f or A values are critical for determining elemental abundances in dense astrophysical sources.

Chapter 2: Instrumentation and Experimental Methods

A wide variety of equipment and techniques are required for precision spectroscopy. This chapter will detail the experimental setups, and their components, that I used to complete my thesis work.

2.1 Light Sources

2.1.1 Sliding Spark

I obtained the spectra used for the results discussed in chapter 3 with a sliding spark light source. The sliding spark, shown in Figure 2.1, was developed by Vodar and Astoin [29] in 1950 and can produce metal ions from singly ionized up to ten times ionized [30, 31]. The source consists of a glass envelope that encloses a quartz spacer, lined with a thin layer of graphite, and Kovar-to-glass seals surrounding the electrodes. The electrodes, shown in Figure 2.1a, taper down to hold two inner electrodes made of the metal of interest. The two inner electrodes rest in a quartz spacer, shown in Figure 2.1b, with a 5 mm gap. For my work I used electrodes made

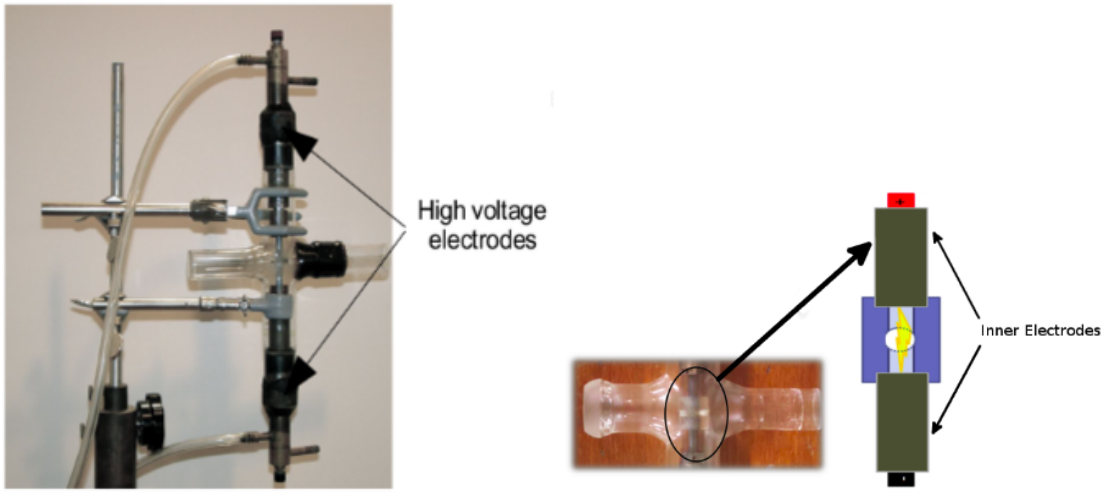

(a) Full view of the sliding spark source. (b) Diagram of the inner components of the sliding spark

Figure 2.1 Sliding spark structure.

of Invar, an iron nickel alloy, so that I could record exposures with Fe V and Ni V simultaneously. By recording spectra with both Fe V and Ni V present at the same time, I could place Fe V and Ni V exposures on the same wavelength scale so that any systematic errors in the calibration would be common to both species. This was a decision largely guided by the application of my work to the search for varying α, where comparisons of Fe V to Ni V data are key. In addition to Invar, I also ran exposures with one yttrium and one nickel inner electrode to help in the analysis of the very dense Invar spectra.

The operation of the sliding spark is based on the circuit shown in Figure 2.2. The circuit is a critically dampened RLC circuit that provides a maximum peak current to the source. The circuit is powered by a high voltage power supply that charges a bank of capacitors for the time it takes for the rotating spark gap to complete a revolution (completing the circuit). When the rotating spark gap

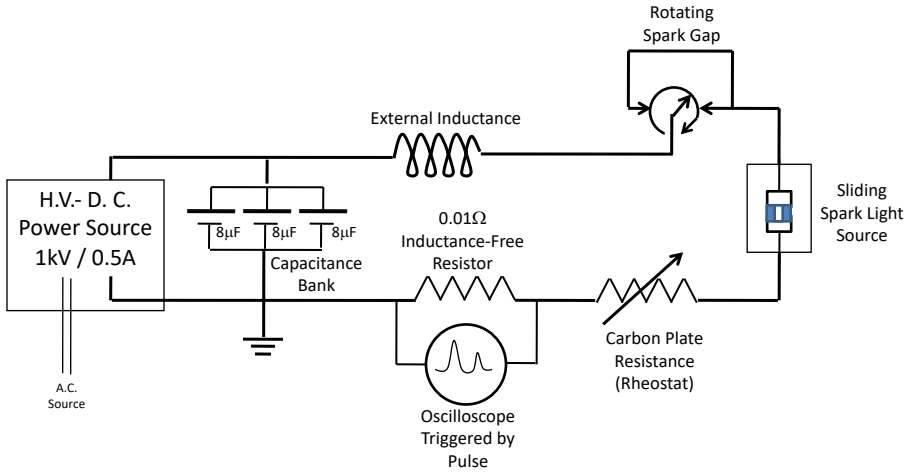

Figure 2.2 A diagram of the circuitry for the sliding spark light source.

triggers the rapid discharge of the capacitors, a voltage pulse is sent to the cathode of the sliding spark that is large enough to ionize the residual gases in the evacuated envelope. The ions and electrons are accelerated in the field between the cathode and anode such that collisions between the accelerated particles and the remaining neutrals further develop a sufficiently energetic plasma capable of stimulating breakdown conditions in the gap. A spark is then generated that slides along the inner lining of the quartz spacer on the thin graphite track, completing the circuit. The now current carrying plasma starts to ablate and ionize the exposed surfaces of the inner electrodes. The ionization of the sputtered surface material, through electron impact ionization of the mostly neutral metals sputtered off the electrodes, eventually becomes the dominant contribution to the plasma. Once these conditions

are reached, spectra can be recorded.

The operation mechanism of the sliding spark is particularly useful for studying dense spectra. The concentration of charge is greatest near the surfaces of the inner electrodes and so the luminosity is greatest at the top and bottom of discharge producing the observed spectral lines. As I mentioned above, exposures with mixed electrodes (yttrium & nickel) were taken so that the luminosity peak of one species was at the top of the observed lines while the other was at the bottom.

As is clear from circuit diagram in Figure 2.2, the discharge in the sliding spark is controlled by a harmonic RLC circuit, whose peak current shape is determined by the resistance, inductance, and capacitance, while the average current is determined by the repetition rate of the rotating spark gap and the peak current shape. The capacitance of the system is essentially fixed, so the peak current shape is modulated by adjusting the tension in a carbon plate resistor and by swapping out wrapped wire inductors with varying numbers of turns to change the impedance of the circuit. I used the sliding spark to get exposures at a range of peak currents from 300 A to 2000 A, with the best spectrum of Ni V and Fe V observed at a peak current of 1500 A. In order to achieve that peak current, the inductor, shown in Figure 2.2, was removed from the spark circuitry. The carbon plate resistor contained thirteen carbon plates (roughly 8 Ω), the supply voltage was approximately $600 - 700$ V depending on the given exposure, the circuit spark gap was run at a repetition rate of 20 ms, and the resulting pulse width was 50 μs. The exposures were run for twenty minutes, and the average current was roughly 0.5 A.

2.1.2 High Current Hollow Cathode

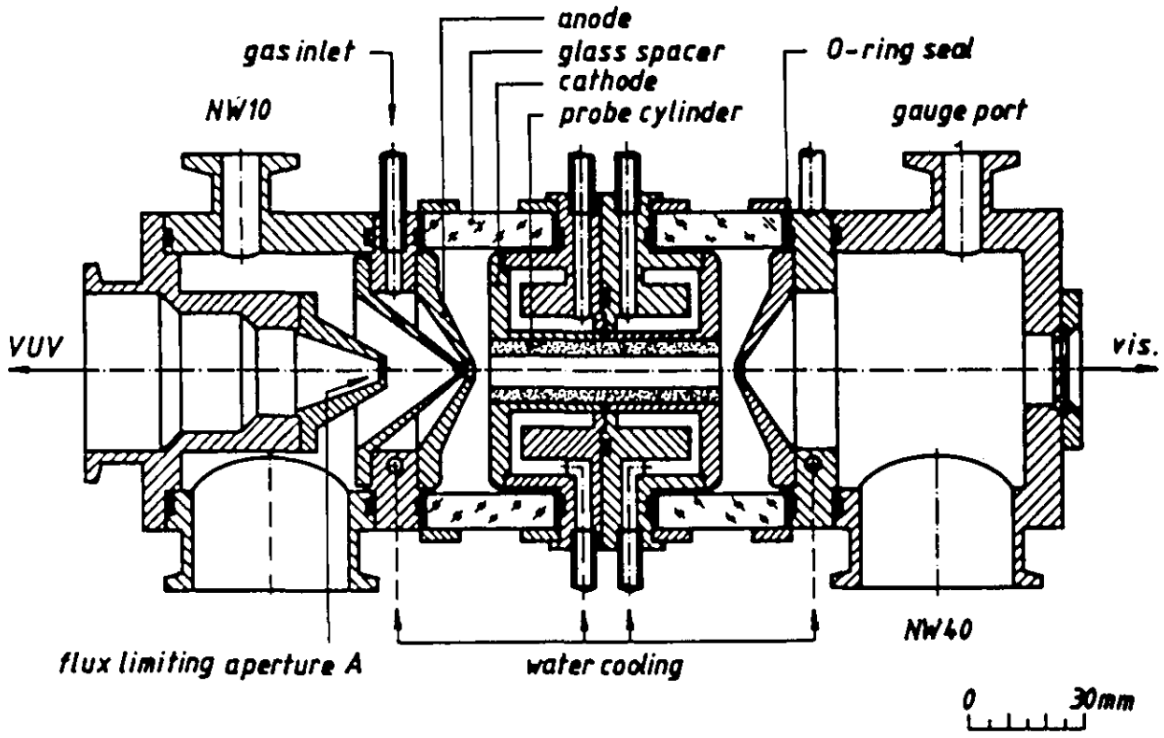

Figure 2.3 Cross section of high current hollow cathode source in its differential pumping configuration. Figure taken from Danzmann et al. [32].

I obtained the spectra used for the results discussed in chapter 4 with a high current hollow cathode lamp (HCL) developed by Danzmann et al. [32]. The HCL, shown in Figure 2.3, consists of two anodes and a central cathode made of water cooled stainless steel blocks. These are connected by insulating glass spacers with Viton O-rings between the blocks and spacers. A hollow metal cylinder, made of the element of interest or an alloy containing the element, is inserted into the cathode block. Although a window can be used to mount the source on to a spectrometer, my work utilized the optional two stage windowless differential pumping configuration

to avoid complications with window absorption in the VUV.

To begin operating the HCL, the inner portion of the HCL is first evacuated along with the chamber the lamp is attached to. Once the HCL is evacuated, a buffer gas such as argon or neon is introduced into the lamp. Neon was used as a carrier gas for all of my work, with a pressure of approximately 3 Torr, as this produced the strongest Fe II spectrum. A voltage is then applied across the HCL electrodes that ionizes the buffer gas and accelerates the resulting ions and electrons through the hollow cathode insert. Collisions between the ions/electrons and the insert material, which was pure iron in my work, cause material from the insert to sputter off into the plasma. The sputtered material is then ionized or excited by subsequent collisions with electrons and ions. The voltage across the electrodes and current traveling through the plasma can be modulated during operation to suit the needs of the experiment. In my work, I mostly ran the HCL at a current of 2 A with a voltage of roughly 480 V as those conditions gave the strongest signal to noise ratio (SNR) of the lines I investigated. I also took some measurements at a lower current of 1.5 A.

The main excitation mechanism in the HCL is collisional excitation with electrons, but charge transfer between the metal atoms and the gas ions is an essential contributor to level populations for the excited levels of Fe II [33]. The charge exchange process is described as

$$Ne^+ + Fe \rightarrow Ne + (Fe^+)^* + \Delta E, \tag{2.1}$$

where $(Fe^{+})^{*}$ represents an excited level of Fe II and ΔE is the energy difference between the ionization potential of the gas and the energy needed to produce the excited state in the metal ion from the state of the metal neutral (the ionization potential of Fe I atom combined with the excitation energy of the excited Fe II state relative to the ground state of Fe II). The charge exchange cross sections are greatest when the final Fe II level has a core configuration with the same parent term as the parent term of the neutral Fe I core configuration and ΔE is small, but cross-sections between configurations with different parent terms are non-zero and are essential in the HCL discharge.

2.1.3 Platinum/Neon Hollow Cathode

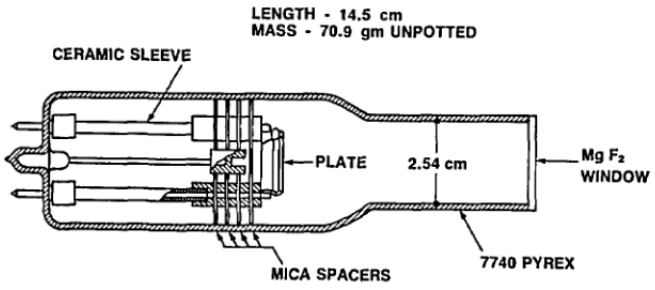

Figure 2.4 Diagram of Pt/Ne HCL taken from Klose et al. [34].

In addition to the sources listed above, I also used a low current platinum/neon hollow cathode lamp run at a current of 20 mA to establish a wavelength scale for calibrating the wavelength results of chapter 3. This lamp, shown in Figure 2.4, unlike those discussed above, is a sealed lamp with a fixed platinum hollow cathode and a filler gas of neon. The principle operation mechanism of the lamp, however, is not dissimilar to the other hollow cathode I discussed.

The Pt II spectrum I recorded using the Pt/Ne HCL provided reference wavelengths [35, 36] that I used to calibrate the Fe V and Ni V wavelengths. The Pt II reference wavelengths were originally measured at NIST for the purpose of calibrating the Goddard High Resolution Spectrograph and Faint Object Spectrograph on the Hubble Space Telescope.

2.1.4 Molecular Deuterium Lamp

The last light source I used in my thesis work is a commercially available Cathodeon V04 molecular deuterium (D_2) lamp [37]. The lamp is a variant of other common, low pressure, hydrogen lamps that emit a UV continuum and have been used for radiometric calibration sources. The lamp consists of a quartz envelope enclosing a coiled cathode and an anode in a low pressure deuterium gas. The cathode coil is heated by a 4 V, 5 A dc power supply to generate free electrons. This generates a discharge and triggers a high voltage supply of 400 V applied across the electrodes, forming an arc. Once the arc is generated, the voltage drops to 100 V and the arc stabilizes with a current of 300 mA. The cathode heating power is turned off once the arc develops. A 1 mm aperture rests in front of the center of the anode where most of the UV radiation is emitted.

The D_2 standard lamp I used in my work was calibrated at the Physikalish-Technische Bundesanstalt (PTB) in the $1160-4000$ Å region [37, 38]. The provided calibration has an uncertainty of 7% across the $1650-3000$ region. Below 1650Å the lamp is no longer a continuum and has line structure and so the calibration provided

has a higher uncertainty of 10% from $1230 - 1650$ Å. In that region, additional care is needed to use the lamp as a radiometric calibration source, but it is still the most reliable and thoroughly studied portable standard source in that region. The D_2 source was used in my line intensity calibration work presented in both chapters 3 and 4 and was an essential part of the procedure discussed in chapter 4 for calculating branching fractions.

2.2 Grating Instrumentation

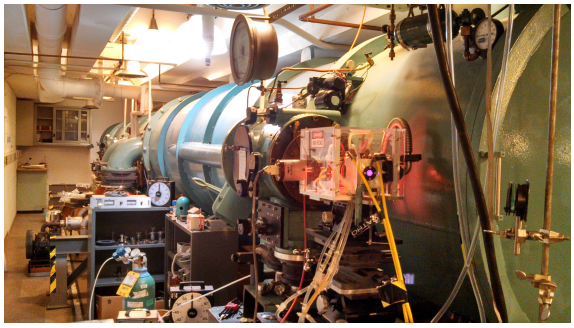

(a) View from Plate Holder end of NIST 10.7 m NIVS

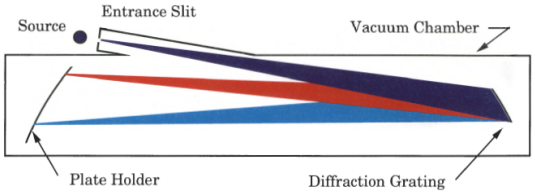

(b) Diagram of NIST 10.7 m NIVS

Figure 2.5 NIST Normal Incidence Vacuum Spectrograph

I used the NIST 10.7 m Normal Incidence Vacuum Spectrograph (NIVS), show in Figure 2.5, to measure all of the results presented in chapter 3. This 12.2 m long grating spectrograph, built by Jarrell-Ash, is one of the largest spectrographs in the world. This spectrograph has a $300 - 5000$ Å spectral range, with a focal length of 10.7 m, and a resolving power of approximately 150000 to first order with photographic plates (discussed below). The spectrograph operates in a Rowland Circle configuration (the entrance slit, grating, and detector holder all lie on the

surface of a circle with a diameter of 10.7 m) and contains a gold-coated, concave grating blazed for 1200 Å with 1200 (grooves) mm^{-1}. This results in a reciprocal linear dispersion, in first order, of 0.78 Å mm^{-1}. The 10.7 m focal length of the spectrograph means that a single exposure can cover a range of roughly 700 Å. The entire spectral region I worked in was covered with only one imaging plate, which greatly simplified the calibration process. This would not have been possible on a more compact instrument, especially while maintaining the resolving power of the NIVS.

The image recorded at the plate holder, shown in Figure 2.5b, is created by a single slit in front of a light source. The NIST NIVS has multiple slits of various widths, but after many trial runs, a width of 21 μm was used for all the exposures in my thesis. Wider slit widths resulted in many lines being not fully resolved, so the 21 μm slit was ultimately the right balance between resolution and signal strength. The NIVS plate holder is constructed such that two masks rest in front of the imaging plate being held. The separation of the two masks determines the amount of the plate width that is exposed to the image coming from the entrance slit. Normally the masks have been set at a fixed separation width and the plate holder itself would be raised or lowered by two motorized leadscrews inside the NIVS between different runs to expose different sections of the plate. Because the two leadscrews are not perfectly synchronized and have some backlash, the plate holder jostles slightly as it is moved up and down. This motion can cause an issue where the position of the plate in the plane of dispersion is shifted between different exposures. This is most clearly seen when comparing the relative position of the same spectral lines on the

same plate across different exposures, as is shown in Figure 2.6.

Figure 2.6 Shown are two exposures from a Pt/Ne HCL on a photographic plate. The wavelength range is approximately $1505 - 1550$ Å with a dispersion of 0.044 Å pixel^{-1}. Note that the bottom track is shifted to the left of the top track due to the plate holder moving between exposures.

As I discussed above, my results in chapter 3 depend on combining two sources: a sliding spark for the Fe V and Ni V spectra and a Pt/Ne hollow cathode as an external calibration source. Thus, I would originally record a Pt II spectrum on one track, move the plate holder, and then record an invar spectrum on a new track. When I attempted to apply a calibration curve derived from Pt II wavelengths onto the invar track, the resulting wavelengths of internal contaminant lines, such as Si IV, were inconsistent and the wavelengths of Fe V and Ni V from different invar tracks were also inconsistent. By measuring the relative change in the position of the same lines in different Pt/Ne HCL exposures, such as the ones shown in Figure 2.6, I determined the shift between different exposures could account for a wavelength shift on the order of 0.25 Å. This was enough to explain the variation.

Because the root of the problem was the shift in the plate holder between the calibration and invar exposures, I instead did not move the plate between the two runs and moved the masks that are held in front of the plate holder. Because the masks have limited travel, this meant that the Pt/Ne HCL and invar sliding spark tracks slightly overlapped, as is shown in Figure 2.7. When I used this method, the calibrated wavelengths of well known contaminant lines in the invar spectrum, such

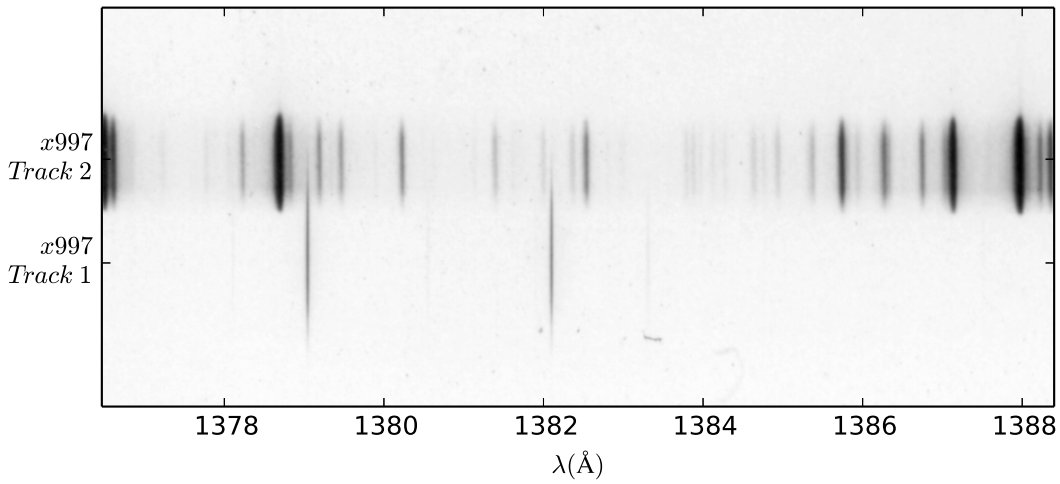

Figure 2.7 A sample section from the photographic plate x997, described in Table 3.1, that was used to measure Fe V and Ni V wavelengths. The top exposure is the spectrum of an invar sliding spark source and the bottom exposure is from a Pt/Ne HCL.

as Si IV [39], and the Fe V wavelengths were in much better agreement. The results of this method are discussed in more detail in chapter 3.

2.2.1 Grating Detectors

I used two types of detectors with the NIST NIVS: Kodak SWR photographic plates and Fuji BAS-TR 2040 phosphor image plates. The 0.5 μm grain size of the Kodak SWR plates [40], in comparison to the 42 μm pixel width of the phosphor image plates, gives the photographic plates a significant advantage over the phosphor plates in terms of resolution and subsequent line width. A detailed study of the phosphor image plates by Nave et al. [41] indicates that the Perkin-Elmer scanner used to scan the image plates actually limits the resolution of the plates further to a resolution of roughly 100 μm. Because the invar exposures were highly dense, with many spectral lines, the high resolution of the photographic plates was essential in

working out the wavelengths for Fe V and Ni V. The positions of the spectral lines present on the photographic plates were measured using the NIST rotating mirror comparator [42]. These line positions were then translated into wavelengths using the Pt II calibration. This process is discussed more in chapter 3. The phosphor image plates do notably scale linearly with intensity [41], so I also ran exposures of an invar sliding spark and a D_2 standard lamp to derive line intensities for Fe V and Ni V in addition to wavelength values.

2.3 Interferometric Instrumentation

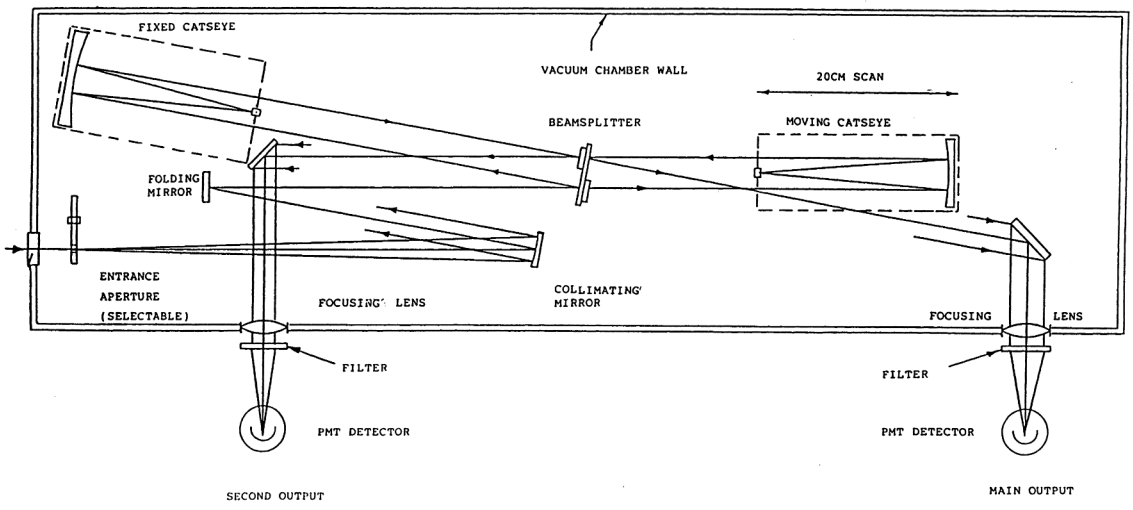

Figure 2.8 Diagram of the NIST FT700 FTS [43]. The Diagram shown was originally created for the FT700's sibling instrument at Imperial College London. Both the NIST FT700 and Imperial College FT500 instruments were manufactured by Chelsea Instruments.

All of the spectra I used for the results presented in chapter 4 were recorded with the NIST FT700 Fourier transform spectrometer (FTS) [44]. This instrument, shown in Figure 2.8, is another world class piece of equipment at NIST. The original instrument was built by Chelsea Instruments and was later improved

upon at NIST by replacing the original silica optics with CaF_2 components to extend the instrument's use further into the VUV. The NIST FT700 FTS now has a CaF_2 input window, CaF_2 output lenses, MgF_2 and Al coated mirrors, and a CaF_2 beam-splitter/combiner. The NIST FT700 is, as is typical of FTSs, based on a Michelson interferometer. The input beam traveling through the aperture hits a collimating mirror and then strikes a folding mirror that sends the beam to the beam-splitter/combiner plate. The path length difference of the two beams is set by the moving "cats-eye" retro-reflector whose position is measured by counting the interference fringes of a He-Ne laser that travels the same optical path as the input beam through the interferometer. The beams from the output of the retro-reflectors then converge on the beam-splitter/combiner plate and the output interference signals are detected using photomultiplier tubes (PMTs). The laser fringes from the He-Ne laser establish a grid of equidistant points for sampling the interferogram. The "cats-eye" retro-reflectors, which consist of a parabolic primary mirror and a flat secondary mirror, are primarily used so that the reflected and transmitted beams from the combiner plate are both measured. The measured interferogram is the Fourier transform of the spectral components of the input source, so running the interferogram through a reverse Fourier transform yields the spectrum. The measured interferograms in my work were all transformed and studied using the spectrum analysis software XGREMLIN [45], which is an updated version of the program developed by Brault and Abrams [46].

Because the FT700 is an amplitude division interferometer, the interference at the beam-splitter is dependent on the alignment of the two beams' wavefronts. The

modulation of the interference signal is critically dependent on the alignment of the internal optics and so great care is taken to align the instrument before use. With the FT700 open to air, a collimated low-power laser is focused onto the entrance aperture of the FT700. Once the laser beam is going through the entrance aperture, the aperture is successively narrowed while making small changes to the tilt and position of the laser so that the beam is centered on a narrow aperture, strikes the center of the collimating mirror and beam-splitter. Once the laser beam is coming through the aperture, a rotating mirror in the main PMT detector box is used to reflect the input laser image at the detector box up through an exit port on the box. The image coming out of the exit port is visible on the ceiling of the room and will show two distinct red laser dots if the instrument is not aligned. Small adjustments to the beam-splitter/combiner plate are then made so that the two dots on the ceiling overlap while moving the non-fixed cats-eye, by hand, through its entire range of motion. This initial geometric alignment is good enough to then move on to aligning the instrument interferometrically.

A germicidal low pressure Hg-arc lamp is then placed in front of the entrance aperture and the exit port of the main PMT detector box is fitted with an eye piece and a filter so that the interference fringes of the 546 nm Hg line can be viewed by eye. The circular fringes viewed through the eye piece should be centered in the image of the aperture. If they are not, adjustments to the angle of the fixed cats-eye or beam-splitter are made until the fringes are centered. This is first done with the mobile cats-eye at roughly the zero optical path difference position (ZOPD). Once the fringes are centered at the ZOPD, the mobile cats-eye should be moved

by hand through its full range while observing the fringes. If the fringes do not stay roughly centered, further adjustments to the beam-splitter/combiner plate or the collimating mirror are needed. The FT700 is at this point interferometrically aligned well enough that the He-Ne laser can be turned on to control the movement of the cats-eye mirror. With the cats-eye now motor controlled, the germicidal lamp is replaced with a higher pressure DC source (Hg(Ar)-Pen-Ray lamp) and the vacuum tank around the optics is closed. The estimated ZOPD can now be checked by taking a sample interferogram of the Hg-Pen-Ray lamp. The programmed ZOPD is changed until the center-burst (maximum amplitude) of the interferogram is at the center of the interferogram. Once the true ZOPD is found and set, the modulation of the interference signal measured by the main PMT detector is observed on an oscilloscope while the mobile cats-eye oscillates at a frequency of a few kHz about the ZOPD over a small spatial interval of about 10000 laser fringes. The angle of the fixed cats-eye is then further adjusted to peak the observed modulation. This essentially completes the alignment of the instrument, but after the FT700 is evacuated the angle of the fixed cats-eye may be further adjusted to maximize the modulation of the VUV signal that was not observed while aligning in air.

With the FT700 aligned, the input sources must be aligned relative to the instrument. To measure accurate BFs I needed to ensure that the response of the FT700 was accurately determined. The response is determined using the standard D_2 lamp discussed above. In order for the measured D_2 spectra to be used for determining an instrument response that was also applicable to the HCL spectra, the two lamps needed to, as much as possible, illuminate the FT700 in the same way.

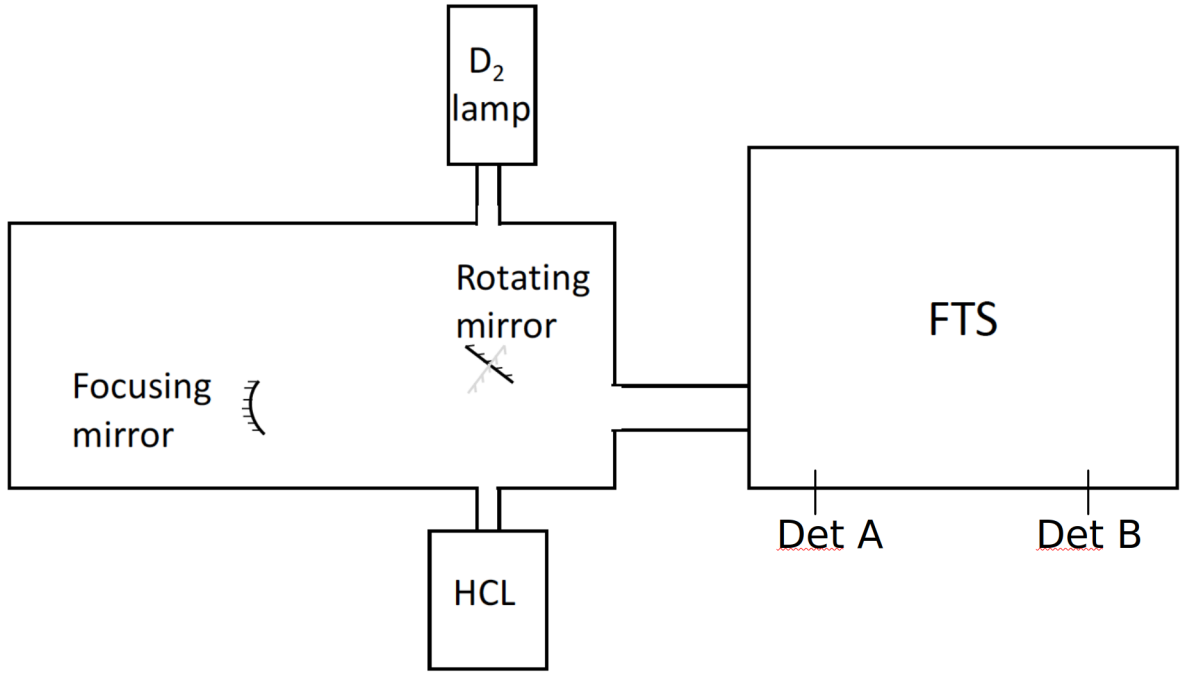

Figure 2.9 Diagram of the experimental setup used for my BF work. The optical path length from the radiometric calibration source (D_2) to the FTS entrance aperture and the HCL lamp to the entrance aperture are the same.

Particularly, the angle between each source and the FTS needed to be the same, as mirror reflectivity is wavelength dependent and I did not want the observed source distributions to be differently affected by mirror reflections. This involved having the light emitting discharge portions of both instruments at the same optical path length from the entrance aperture of the FTS with near identical alignment. To accomplish this, I assembled a fore-optics system in a separate vacuum chamber that was attached to the entrance port of the FT700. This system, shown in Figure 2.9, consists of a focusing mirror that focuses the sources onto the entrance aperture of the FT700 and a rotating mirror that is electronically controlled outside the tank to switch between sources. The optics rest on an optical board that sits on kinematic mounts inside an aluminum tank so that the alignment is not substantially changed

by deformation of the tank during evacuation. The alignment of the fore-optics and sources is critical and was something I took great care in doing.

The alignment was started by sending a low-power laser through the port on the main PMT detector box so that the laser went through the FT700 in reverse light path. The laser and FT700 aperture were adjusted until the beam was exiting the entrance of the FT700 through the center of a narrow aperture. The fore-optics box, which was fixed to its own table, was then vertically adjusted until the beam was centered on the focusing mirror. The heights and angles of the focusing mirror and rotating mirror were recursively adjusted until I could center the beam on the focusing mirror, rotating mirror, D_2 lamp window, and HCL aperture. Once the mirrors were set, the angles of the sources were adjusted so that the light emitting portion of the lamps would be in line with the alignment laser. For the D_2 lamp this was done by observing the reflected laser beam coming of the front window of the lamp. The tilt of the lamp was adjusted until the incoming and outgoing beams overlapped. For the HCL, which has a 1 mm front aperture and a back window, the tilt was adjusted until the beam was going through the front aperture and centered on the back window of the lamp. Particularly for the D_2 lamp, which was affixed to the tank with a flexible metal bellow, there was concern that the alignment would drift during evacuation. A small mirror was placed in the tank so that the reflected beam from the D_2 lamp window could be observed relative to the incoming beam seen on the focusing mirror through a window port on the tank. If the lamp alignment drifted during pump-down there would be two spots observed on the focusing mirror (one from the incoming laser and one from the

window reflection). No observable drift was observed during pump-down.

With the alignments of all components complete and the tanks evacuated, measuring spectra was not a simple process, but a reliable/consistent one. After a range of initial testing, I executed the same procedure for every run of the system. At the start of a set of runs I would begin by turning on the voltage supply to the PMTs with a low applied voltage of roughly 20 V (recommended by the PMT supplier) and start a nitrogen purge of the boxes that held the PMTs to displace VUV absorbing O_2. The PMT warm-up and nitrogen purge were left to run for at least twenty minutes, but often times longer while I prepared the rest of the material. While the above steps were running in the background I would turn on the power to the D_2 lamp, which as described above requires a heating and warm-up period of at least ten minutes. With the D_2 lamp warming-up, I would set up the computer system that operates the FTS and prepare it for the first run of the day. At that point I would move the rotating mirror in the fore-optics box to its programmed point on the center of the D_2 lamp. I would apply a high enough voltage to the main PMT to read an output voltage of 2 V on an oscilloscope connected to the PMT. I would then make small adjustments to the rotating mirror until the output voltage was peaked. I then re-adjusted the PMT voltage so that the output voltage on the oscilloscope was again 2 V and then set the PMT voltage of the second PMT so that it produced 2 V out on the scope. I was then ready to run a scan and record the interferogram. I would first run only one or two scans to ensure everything was working, and then I would run a much longer measurement with at least thirty to forty consecutive scans taking roughly thirty minutes to an hour. Once the D_2

interferogram was recorded I could move on to using the HCL lamp.

To switch to a HCL measurement, I would start by opening up the gas regulator responsible for handling the inflow of neon to the source and turn on the HCL water cooling system. By adjusting an inflow valve and a valve on the HCL vacuum line, I could set an internal pressure of neon of roughly 3 Torr. I would then turn on the power supply to the source and apply a small voltage of around 15 V until a current carrying plasma developed in the HCL and the power-supply switched into a current limited operation. I would then slowly increase the current to the desired point over a period of about ten minutes while adjusting the pressure to avoid excessive arcing in the HCL. Once the lamp was stable at the desired current and pressure, I would make small adjustments to the position of the rotating mirror to peak the observed PMT output on the oscilloscope. I would then set the PMT voltages so that the output signal was an average of 2 V and record an interferogram from the HCL. If desired, I would then change the HCL conditions or PMTs being used and conduct additional scans. After I finished the HCL scans I would switch back to the D_2 lamp, re-peak the signal by adjusting the rotating mirror, and take a final scan. The last D_2 scan was used to compared the instrument response at the start of the set of measurements and the end of the day to ensure that the response had not drifted during measurements. During my thesis work this entire process was conducted many times. For various reasons, such as repairs, I re-aligned the system multiple times and the data I discuss in chapter 4 was taken over the course of many months.

2.3.1 FTS Detectors

While most of the equipment I have talked about was more or less static in my experiments, the day to day choice of which sets of PMTs to use ended up being a key competent of targeting data applicable to BF work.

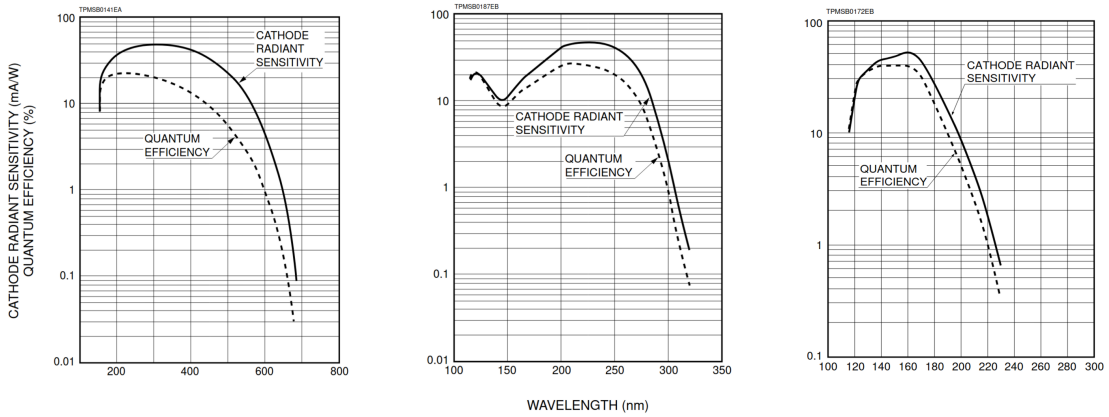

(a) R106 Response Curve (b) R1220 Response Curve (c) R7639 Response Curve

Figure 2.10 PMT Response Curves Provided by Hamamatsu

The product names of the PMTs used in my work, and their sensitivity curves, are shown in Figure 2.10. These PMTs were chosen because they have a history of use with the NIST FT700 (current response curves could be compared to historical data) and, when combined, they adequately cover the spectral region I was interested in. The R106 PMT uses a Sb-Cs cathode, has a Fused Silica window, and works best between 200 nm and 400 nm. The R1220 PMT uses a Te-Cs cathode, has a MgF_2 window, and works best between 180 nm and 300 nm. Finally, the R7639 PMT uses a diamond cathode, has a MgF_2 window, and works best between 160 nm and 220 nm.

Because FT spectrometers sample all spectral features simultaneously, the

dominant contribution to noise in the UV/VUV is photon noise due to the detector seeing all wavelengths in the source, not just the ones in the region of interest. Photon noise from outside the wavelength region of interest can even exceed the local photon noise. To avoid light from outside the UV/VUV contributing to the noise of a spectrum, past BF experiments have opted to use PMTs with narrow spectral sensitivity ranges and/or filters. I, on the other hand, have opted to accept the possible increase in noise (potentially dropping the SNR of the weakest lines below reasonable use) and use PMTs with wide spectral sensitivities and no filters. I have chosen this approach in order to greatly simplify the process of calibrating intensities of lines across a wide spectral range (useful for BF work) without having to stitch together the responses of many different narrow band regions (increasing the potential for systematic errors). Particularly for work in the VUV, which is notoriously difficult and not well established, I think the loss in SNR is acceptable and preferable in order to minimize the chance of errors. Furthermore, the increased photon noise can be mitigated by taking long measurements of broadband spectra rather than taking many short measurements of narrow band spectra.

Chapter 3: Precision Measurements of Wavelengths and Energy Levels

This chapter details the results of my efforts to assist the astronomy community in searching for evidence of fine-structure constant variation in the high gravitational fields of white-dwarf stars. The main goal of my work in this chapter was to provide high quality reference laboratory atomic data that can be used to compare to the observed white-dwarf spectra so that potential fine-structure constant variation can be determined by comparing the laboratory data to the stellar data. The search for varying α that motivated my work was Berengut et al. [12], which used Ni V and Fe V wavelength data to compare to Ni V and Fe V wavelengths observed in the white-dwarf star G191-B2B. The results of Berengut et al. [12] were inconsistent, with $\Delta\alpha/\alpha > 0$ for Ni V and $\Delta\alpha/\alpha < 0$ for Fe V. Because the value for $\Delta\alpha/\alpha$ depends on the relative wavelength differences between the laboratory value and the stellar value, the value of $\Delta\alpha/\alpha$ could be due to systematic errors in the laboratory wavelengths. In fact, the uncertainties of the laboratory values dominate the uncertainty in $\Delta\alpha/\alpha$. To address this data need, specifically for the Ni V and Fe V spectra, I conducted laboratory experiments using grating spectrograph

Table 3.1 Table of Spectra Used for Ni V and Fe V

Plate Number	Exposure Date	Plate Type[a] Type	Track Number	Source[b]	Source Conditions	λ Range (Å)
x988	07/03/2014	PIP	5	D_2	300 mA	1150-1450 Å
x990	07/11/2014	PIP	1	Pt/Ne HCL	20 mA, 340 V	1150-1450 Å
x990	07/11/2014	PIP	4	Invar SS	1000 A Peak, 0.55 A Average, 600 V	1150-1450 Å
x990	07/11/2014	PIP	5	Invar SS	1500 A Peak, 0.65 A Average, 850 V	1150-1450 Å
x997	06/04/2015	KSWR	1	Pt/Ne HCL	20 mA, 310 V	1190-1530 Å
x997	06/04/2015	KSWR	2	Invar SS	1500 A Peak, 0.48 A Average, 530 V	1190-1530 Å
x997	06/04/2015	KSWR	3	Fe/Y SS	1500 A Peak, 0.45 A Average, 750 V	1190-1530 Å
x997	06/04/2015	KSWR	4	Ni/Y SS	1500 A Peak, 0.45 A Average, 750 V	1190-1530 Å
x997	06/04/2015	KSWR	8	Pt/Ne HCL	20 mA, 310 V	1190-1530 Å

[a]PIP: Phosphore Image Plate and KSWR: Kodak SWR Photographic Plate

[b]HCL: Hollow Cathode Lamp and SS: Sliding Spark

equipment at NIST to measure Ni V and Fe V wavelengths and intensity values. I then used those measured values, and the values from past publications, to conduct a critical evaluation of Ni V data across most of the VUV region. This evaluation resulted in a rigorously evaluated set of data that includes measured wavelengths, Ritz wavelengths, line intensities, oscillator strengths, and energy levels.

A detailed explanation of the equipment I used can be found in chapter 2, and a table of the various spectra I used for this work is shown in Table 3.1. Table 3.1 includes: the plate identifier in the first column, the date the measurement was taken in the second column, the type of plate used in the third column, the track number on the plate in the fourth column, the light source in the fifth column, the source conditions in the sixth column, and the wavelength range of the exposure in the seventh column.

The work I present in this chapter is published in *The Astrophysical Journal Supplements Series* [16].

3.1 Analysis

3.1.1 Wavelength Calibration

I carried out the wavelength calibration for Ni V and Fe V using Pt II reference wavelengths [35]. The experimental details of my approach are found in Chapter 2 and are highlighted in Figure 2.7. Of the 93 platinum reference values used in the calibration of the invar spectrum, 59 of the wavelengths have uncertainties of less than 0.002 Å ($0.4 - 1.4$ mÅ), with the remaining values having uncertainties of 0.002 Å.

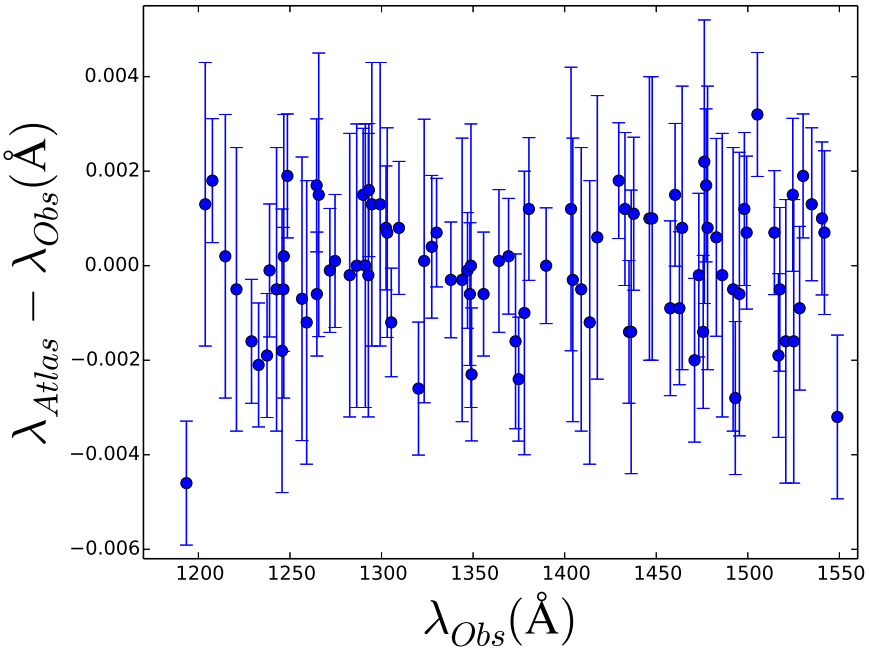

Figure 3.1 Residuals after fitting my observed Pt II wavelengths (λ_{Obs}) with a sixth order polynomial to their Pt II standard reference wavelengths (λ_{Atlas}) [35]. Error bars represent the sum in quadrature of the Pt II reference uncertainty and the calibration uncertainty.

I derived the calibration function by identifying the positions on photographic plates of Pt II lines in the Pt/Ne spectrum that had wavelengths from Sansonetti

et al. [35]. The line positions of both the Pt II lines and the Fe V or Ni V lines were all measured using the NIST comparator discussed in Chapter 2. Repeated measurements of the same set of 83 Pt II lines on the comparator indicated that a measurement uncertainty of 0.002 Å was introduced due to the line position measurement mechanism. The line positions and reference wavelengths were then used to derive a dispersion function that was a weighted sixth order polynomial whose weights were the inverse squares of the Pt II reference uncertainties. The order of the polynomial used to model the dispersion function was determined by testing second through eighth order functions and calculating the standard deviation of the residuals between the model and the standard wavelengths from Sansonetti et al. [35]. Below a sixth order model, the residuals had a systematic behavior and the standard deviation was much larger than the uncertainty of the reference wavelengths, suggesting that the fit was poor due to the order of the model. Above a sixth order model, the standard deviation of the residuals was not meaningfully reduced and so the increased orders did not provide a more accurate model. Once I determined the dispersion function, I measured the line positions of Fe V, Ni V, and contaminant lines and applied the polynomial dispersion function. The contaminant lines, such as Y IV [47] and Si IV [39], were then used to identify and correct illumination shifts between the calibration source and the experimental source.

The standard uncertainty introduced due to the calibration, estimated by the standard deviation of the calibration residuals shown in Figure 3.1, is 0.0013 Å.

3.1.2 Intensity Calibration

I established an intensity scale with the D_2 lamp discussed in chapter 2, and I reported relative intensities for the observed Ni V lines. The D_2 lamp and an invar sliding spark were both imaged onto a phosphor image plate that scales linearly with intensity. The spectra on the image plate were then used to evaluate the Ni V line intensities. The approach to the radiometric calibration follows the same procedure discussed in section IV, subsection A of Nave et al. [41]. The observed lines were fitted with Voigt profiles using the XGREMLIN program [45] and the peak value of the Voigt profile was taken as the line intensity of the spectral line. This observed line intensity was then divided by the instrument response to give the actual line intensity, since,

$$I_{Obs} = I_{Actual} \times Response \tag{3.1}$$

Because the D_2 spectrum below 1660 Å consists of emission lines, the peak intensity of the lines depends on the resolution of the spectrograph. As the resolution of the spectrograph used at PTB to calibrate the D_2 lamp was much lower than the spectrograph I used at NIST, I degraded my measured spectrum by convolving it with two boxcar functions of width 9.2 Å and 4.6 Å to match the resolution of the spectrograph used by PTB. I then interpolated the calibration provided by PTB to the same wavelength scale as my degraded spectra and took the ratio of the two spectra to create an instrument response function. The instrument response function derived from this process was then applied to the invar spectrum by taking

the ratio of the invar spectrum signal and the instrument response function according to Equation 3.1.

The estimated uncertainty of the radiometric calibration is 12% and was derived in a way that is similar to the uncertainty budget described in section IV, subsection B of Nave et al. [41]. This uncertainty is a summation in quadrature of the 10% uncertainty due to variations in the alignment of the source and the 7% uncertainty that comes from the supplied calibration of the D_2 lamp from PTB. Since the line intensities are highly dependent on the source conditions and illumination, they are provided here as only a guide to the spectrum. Caution and great care should be used if the intensities are used for other purposes such as for calculating transition probabilities.

3.2 Wavelength Analysis

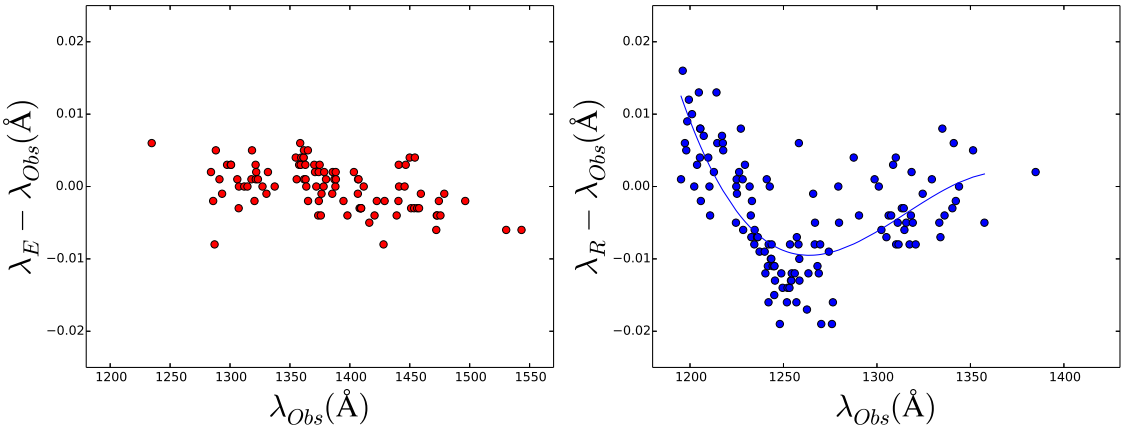

Figure 3.2 A comparison of the newly measured wavelengths (λ_{Obs}) to their previous values as reported by either Ekberg [15] (λ_E) (Fe V) (Left) or Raassen and van Kleff (λ_R) (Ni V) (Right). The uncertainty of each point is 5 mÅ (Left) and 7 mÅ (Right). The Ni V points (Right) are fitted by a third order polynomial shown by the solid line.

Figure 3.2 shows the comparison of the newly measured wavelength values to their previously reported values. Included are 97 of the 164 observed Fe V wavelengths and 123 of the 195 observed Ni V wavelengths. All included values are from unblended and symmetric lines. I excluded lines that were obscured by the calibration spectrum being partially embedded in the invar spectrum, as a sufficiently accurate measurement of the line position was not possible. The excluded values are reported in seperate tables (A.2 and A.1) with an increase in their reported uncertainties reflecting their perturbed measurements. The standard deviation of the difference in wavelengths shown in Figure 3.2 for Fe V is 3 mÅ, and the standard deviation of the difference in wavelengths shown in Figure 3.2 for Ni V is 8 mÅ.

For the observations of both Ni V and Fe V, the reported standard uncertainties, 2.4 mÅ, are the sum in quadrature of the calibration uncertainty discussed above and the line position measurement uncertainty from the NIST comparator instrument used to measure the line positions on the photographic plates. I derived the line position uncertainty by taking multiple measurements of the same set of 83 well measured lines present in the invar spectrum and taking the standard deviation of the calibrated wavelengths that resulted from the line position measurements. The standard uncertainty introduced by the comparator measurements is 2 mÅ for lines without serious perturbations such as an asymmetry or blend. Lines with perturbations such as asymmetry or blending were given an increased measurement uncertainty, ranging from an additional 1 mÅ to 10 mÅ, corresponding to the impact of the perturbation.

An analysis of Figure 3.2 demonstrates the principal improvement coming from

my work in this chapter. The Ni V comparison shown in the figure highlights a systematic difference between the newly measured wavelengths and the previous values from Raassen and van Kleff. This suggests a systematic error in the calibration method used by Raassen and van Kleff. This type of systematic error has been found previously in reports similar to Raassen and van Kleff. For example, in the work on the Co III spectrum by Smillie et al. [48], a similar trend was observed for wavelengths reported by Raassen and Ortin [49].

The impact of correcting this systematic calibration error, concentrated in the 1200-1300 Å range, should be clear, given that the maximum error introduced by the faulty calibration is approximately 10 mÅ, which would contribute significantly to any application requiring Ni V wavelengths. The maximum discrepancy in Figure 2 of Berengut et al. [12], replicated here in Figure 3.3 is roughly 12 mÅ, suggesting that the majority of the discrepancy they observed can by explained by the laboratory wavelengths. Indeed, when my data is used to re-create Figure 2 of Berengut et al. [12], shown in Figure 3.3 the Fe V and Ni V data are inconsistent.

3.3 Results

I have combined my work with the corrected wavelengths from Raassen et al. and Raassen and van Kleff and used them to derive optimized energy levels and Ritz wavelengths. Table A.2 provides the full results of our compilation for Ni V. Columns 1 and 2 give observed wavelengths and their standard uncertainties. Columns 3 and 4 give Ritz wavelengths, derived from the optimized energy levels, and their

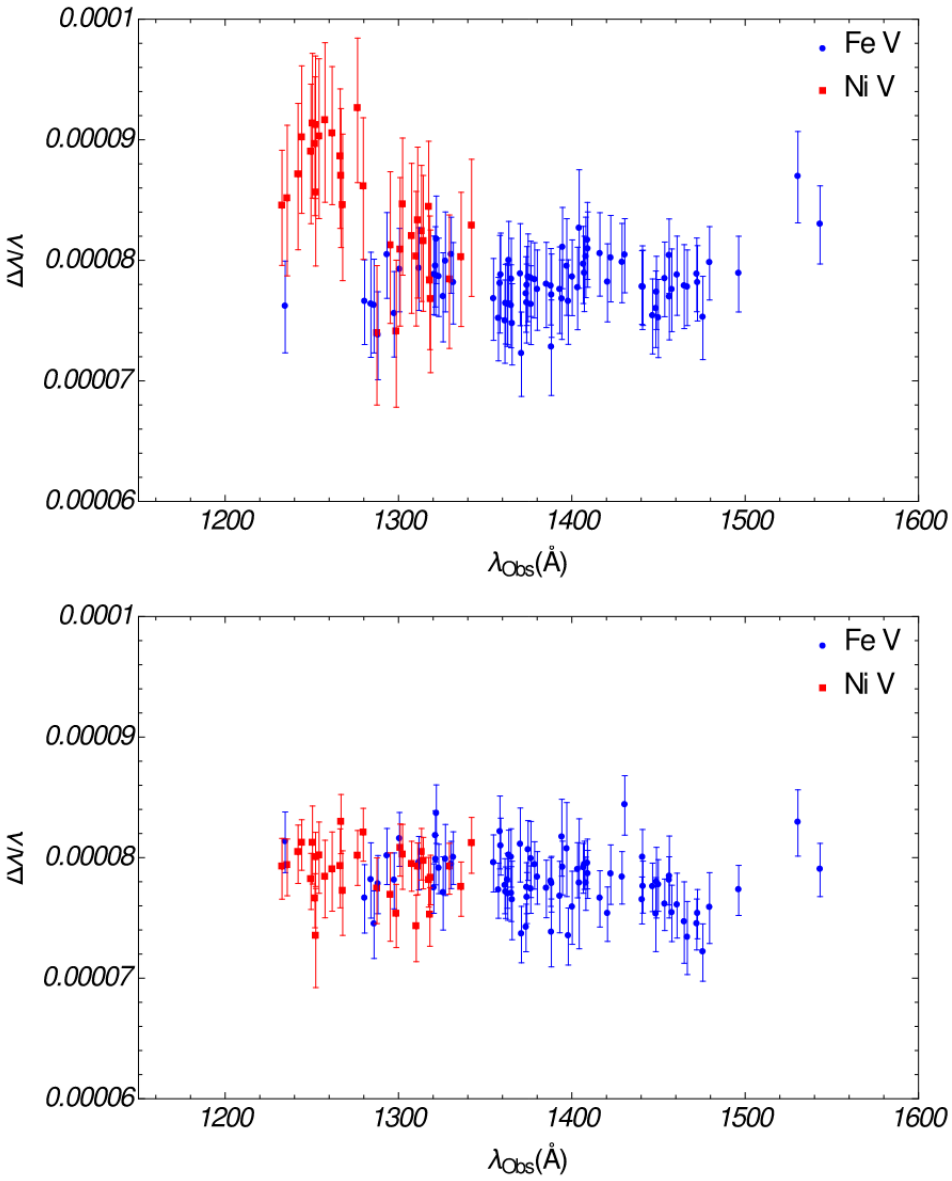

Figure 3.3 Comparison of two versions of Figure 2 from Berengut et al. [12] using two different data sets. The top figure is a recreation of Figure 2 from Berengut et al. [12] using the data used by Berengut et al. [12]. The bottom figure recreates the plot using my new wavelength data. The slope of the best fit line through each set of data is used to evaluate the potential fine-structure constant variation.

standard uncertainties. Column 5 gives the relative intensity of the line. Columns 6 and 7 give the $\log(gf)$ values of each transition as well as the estimated standard uncertainty of each $\log(gf)$ value. Columns 8 and 9 give the lower and upper optimized energy levels for each transition. Columns 10 through 15 give the lower

and upper configuration, term, and J value of each transition. Column 16 provides additional notes for each transition with each note character being described in the footer of Table A.2. An extended explanation of the results compiled in Table A.2 is given below in the following sections.

3.3.1 Wavelengths

3.3.1.1 Fe V

In addition to comparisons with the values from Ekberg [15], I have also compared my results to the Ritz values from Kramida [21]. In almost all cases the two sets of wavelengths agree with each other to within one standard uncertainty. Overall the two reports support each other, which can be clearly seen in figure 3.4, which shows a standard deviation of 7 mÅ in the difference between the two sets. Figure 3.4 does show a small sloping trend in the difference between the two sets of wavelengths towards longer wavelengths. This indicates that there is still a small systematic error in one of the sets of wavelengths, but the sloping trend in figure 3.4 shows that the remaining systematic error is small relative to the wavelength uncertainties.

Figures 3.2 and 3.4 show that no substantial improvements have been made for Fe V as a result of the new measurements reported in this work. The wavelengths I report are in excellent agreement with those from Kramida [21] and my measurement uncertainties are not meaningfully better. The values provided by Kramida [21] cover a wider wavelength range and have been more rigorously evaluated during the

level optimization process. My measurements do, however, validate the wavelengths reported by Ekberg [15] and Kramida [21]. Ultimately, the assessment of Fe V by Kramida [21] stands as the recommended source of reference data for Fe V.

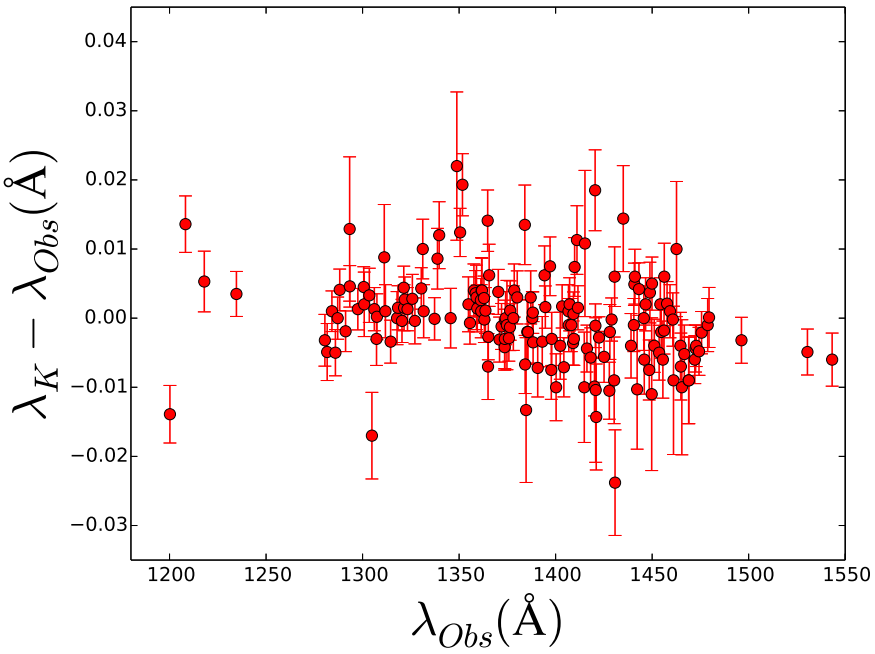

Figure 3.4 A comparison of the new Fe V wavelengths (λ_{Obs}) to the Ritz wavelengths (λ_K) from Kramida [21].

3.3.1.2 Ni V

The reports by Raassen and van Kleff and Raassen et al. span a wavelength range of 400-1400 Å and include approximately 1500 spectral lines (500 of which fall between 1200 Å and 1400 Å). Roughly 300 of the lines that fall between 1200-1400 Å were not remeasured in my work as I targeted the subset of lines used by Berengut et al. [12]. The wavelengths for these lines can be corrected by shifting them to the same wavelength scale as the newly remeasured wavelengths. This was done by fitting the points in Figure 3.2 with a third order polynomial. The order of the

polynomial was determined by increasing the order until the standard deviation of the residuals did not meaningfully change. The standard deviation of the residuals of the third order polynomial fit shown for Ni V in Figure 3.2 is 5 mÅ. This was then applied to the wavelengths reported by Raassen and van Kleff in the 1200-1300 Å region to give wavelengths on my new scale. The wavelengths in Table A.2 that have been corrected in this way are reported as the observed wavelengths with a mark (R1) in the note column.

In the wavelength region that did not overlap with the remeasured wavelengths, the accuracy of the wavelength scale can be examined using Ritz wavelengths. Accurate relative values of the $3d^5 4p$ levels were derived from $3d^5 4s$-$3d^5 4p$ transitions in the 1200-1400 Å range using the level optimization program LOPT described in more detail below and in Chapter 1. The relative values and uncertainties of the $4p$ levels are determined solely by lines in the 1200-1400 Å region. The absolute values are set by fixing the value of one level in the optimization. The $3d^5 4p$ levels combine with each level in the $3d^6$ configuration to give transitions in the 300-400 Å region. The relative Ritz wavelengths and uncertainties of transitions down to a single $3d^6$ level are determined by lines in the longer wavelength region and can be compared to the measured values from Raassen et al. to evaluate the accuracy of their wavelength scale by looking for systematic deviations. For example, the $3d^6\ {}^3P_2$ level at 26152 cm^{-1} combines with $3d^5 4p$ levels to give 25 lines from 329.25-382.37 Å and its value can be derived from roughly 60 lines between 1200-1400 Å. A systematic deviation from a constant value in the difference between the measured and Ritz wavelengths for these lines would suggest a problem in the

relative wavelengths in Raassen et al.. This technique does not validate the absolute wavelength calibration, as the absolute values of the $4p$ levels must be determined by at least one $3d$-$4p$ transition, but it can determine if a wavelength calibration error similar to that shown in figure 3.2 exists in the shorter wavelength region.

In my case, it was necessary to fix the values of two $3d^5 4s$ energy levels in the level optimization in order to provide values for a sufficient number of $4p$ levels to determine Ritz wavelengths across the whole 300-400 Å wavelength range. The $3d^5(^4D)4s\ ^5D_2$ level was set at 216590.519 cm^{-1} and the $3d^5(^2I)4s\ ^1I_6$ level at 233840.023 cm^{-1} using an initial optimization of all lines in the 200-1400 Å wavelength range. Values for 21 levels in the $3d^6$ configuration were then fixed using single $3d$-$4p$ transitions and Ritz wavelengths for $3d$-$4p$ transitions calculated using the fixed $3d^6$ levels and optimized $3d^5 4p$ levels. The results of this comparison, shown in Figure 3.5, indicate no calibration error in the 300-400 Å range since there is no systematic behavior, and the scatter in the difference between the wavelengths is within the estimated measurement uncertainty. From this assessment I have chosen to report the original wavelengths in Table A.2 in the 300-400 Å range given by Raassen et al. with a mark (R2) in the note column.

In the 900-1200 Å range, I took a similar approach. The optimized energy levels used to evaluate the 300-400 Å range were the upper and lower energy levels of most of the transitions in the 900-1200 Å range. I used these levels to calculate Ritz wavelengths to compare to the wavelengths reported by Raassen et al.. The comparison, shown in Figure 3.6, demonstrated that the calibration error trend seen in the 1200-1300 Å range (shown in Figure 3.2) continued down towards 1100 Å. I

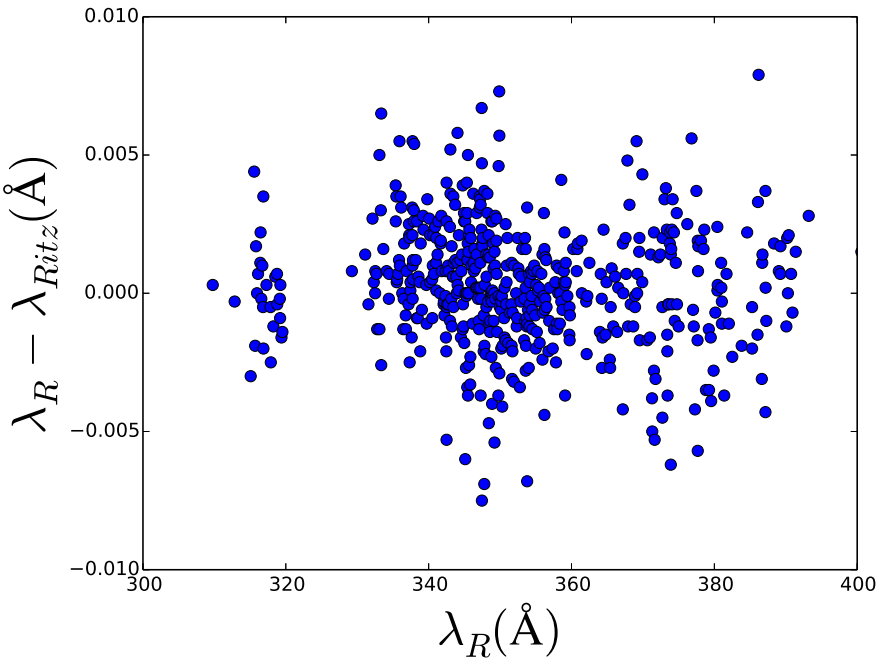

Figure 3.5 A comparison of the wavelengths reported by Raassen et al. (λ_R) to the Ritz wavelengths described above (λ_{Ritz}).

corrected the wavelengths in the 1100-1200 Å range by shifting down the wavelengths reported by Raassen et al. by 11 mÅ (the average of the differences between the Ritz wavelengths and the wavelengths reported by Raassen et al.). I increased the uncertainty of these wavelengths by the standard deviation of the set of differences (12 mÅ). This 12 mÅ correction was added to the original measurement uncertainty of each wavelength as a sum in quadrature. The wavelengths in Table A.2 that have been corrected in this way are reported as the observed wavelengths with a mark (R3) in the note column.

The wavelengths in the 900-1100 Å range and the 1300-1400 Å range, similar to those in the 300-400 Å range, did not demonstrate any systematic errors, so I have given them in Table A.2 as the original values given by Raassen and van Kleff with a mark (R4) in the note column.

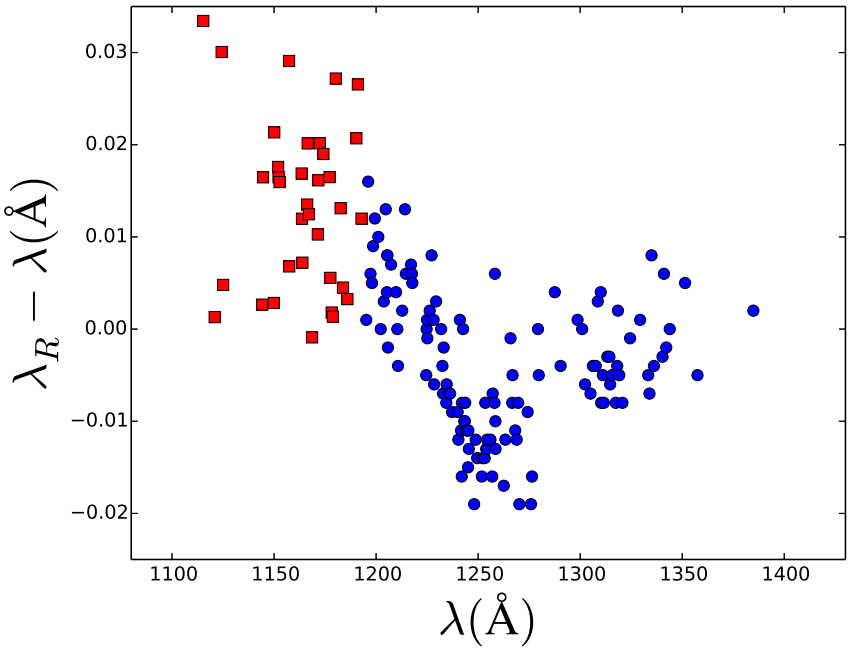

Figure 3.6 A comparison of the wavelengths reported by Raassen and van Kleff (λ_R) to my newly measured wavelengths (λ) (blue circles) and to the Ritz wavelengths (λ) (red squares). The two comparisons, when joined together, show that the calibration error in the 1200-1300 Å range extends into the shorter wavelength region shown with the red squares.

3.3.2 Intensity

The line intensities in column five of Table A.2 were taken from my spectra when available. If an accurate intensity could not be determined from my spectra due to issues with fitting the line profile, which could occur as a result of blending or having a weak line on the shoulder of stronger lines, then the line includes a characteristic mark in Table A.2 indicating an unreliable intensity value.

As not all of the lines reported by Raassen and van Kleff and Raassen et al. were measured in this work, the line intensities reported in Table A.2 are on two scales. Lines that have updated intensity measurements through my work are on the calibrated scale, while lines that were not measured in my work are reported on

the original scale set by Raassen and van Kleff and Raassen and van Kleff. Table A.2 includes a clear marker in the note column on each entry to indicate if the line intensity is from the original (noted as R) or updated scale (noted as W).

3.3.3 $\log(gf)$

The $\log(gf)$ values presented in Table A.2 are the result of detailed calculations carried out by Raassen and Uylings [50]. The accuracy of those $\log(gf)$ values was assessed by comparing them to the $\log(gf)$ values calculated by Kurucz [51]. Figure 3.7 presents the difference of the two sets as a function of the calculated line strength values given in atomic units (a.u.):

$$a_0^2 e^2 = 2.729^{-48} \mathrm{m}^2\mathrm{C}^2, \tag{3.2}$$

where a_0 is the Bohr radius and e is the electric charge. The plot in Figure 3.7 has a standard deviation of 0.3.

Historically, the calculations provided by Raassen and Uylings [50] have been far more accurate than other calculations [52] and so the uncertainties for the $\log(gf)$ values provided by Raassen and Uylings [50] can be roughly estimated by taking the standard deviation of the difference of the two sets of $\log(gf)$ values as a function of the line strengths calculated by Kurucz [51]. This results in a conservative upper limit for the $\log(gf)$ uncertainties reported in Table A.2. Ultimately, the uncertainties for the $\log(gf)$ values were broken down into three levels of quality based on the line strength. The weakest lines ($S \leq 5$ a.u.) have the lowest rating (uncertainty

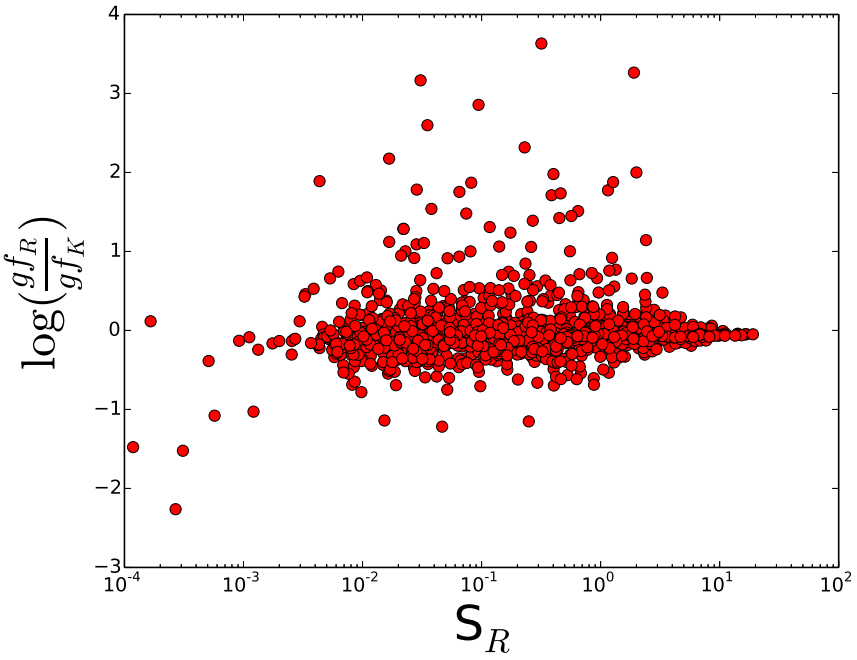

Figure 3.7 Difference between the $\log(gf)$ values reported by Raassen and Uylings [50] ($\log(gf_R)$) and Kurucz [51] ($\log(gf_K)$) as a function of line strengths calculated using values from Raassen and Uylings [50] (S_R). The line strengths are given in atomic units defined by eqautaion 3.2.

$> 50\%$); moderate lines (5 a.u. $< S \leq 10$ a.u.) have the middle rating (uncertainty $\leq 18\%$); and the strongest lines ($S > 10$ a.u.) have the highest rating (uncertainty $\leq 7\%$). These different uncertainty levels are given in column seven of Table A.2.

3.3.4 Level optimization

I have optimized the energy levels of Ni V with the set of critically evaluated wavelengths described above as was done by Kramida [21] for Fe V. The optimization process was done with the Level Optimization program (LOPT) created by Kramida [19]. LOPT was also used to generate Ritz wavelengths. The Ritz wavelengths I have derived have uncertainties that are typically smaller than their experimentally measured counterparts.

In my work, I had LOPT use the inverse square of the wavelength uncertainty (column two of Table A.2) to weight each transition in the optimization. Since many lines in this optimization were multiply classified, the gf values, taken from the $\log(gf)$ values discussed in section 3.3.3, were used as additional weights for multiply classified lines. This was rarely used as almost all levels could be determined by lines that were not multiply classified. In the cases where levels did not depend on multiply classified lines, the weights of those multiply classified lines were decreased by a factor of one over the square root of 20 mÅ in the LOPT input file so that the multiply classified lines would not impact the calculated energy levels, but would be included in the optimization files in order to determine their corresponding Ritz wavelength.

The Ritz wavelengths, along with their estimated standard uncertainties, are reported in Table A.2. The optimized energy levels, their uncertainties, and their classifications are reported in Table A.3. The level uncertainty given in column five of Table A.3 is one standard uncertainty with respect to the ground level. The number of transitions defining a level is included in Table A.3 in addition to the level uncertainty in order to give a full representation of each optimized level.

3.4 Conclusions

The original motivation behind this portion of my thesis work was ultimately to improve the quality of astrophysical assessments of the fine structure constant. The work I presented here supports the wavelength evaluation of Fe V presented

by both Ekberg [15] and Kramida [21]. With the newly established laboratory and Ritz wavelengths for Ni V, the results of Berengut et al. [12] can be revisited and improved upon. The Ni V systematic calibration error that is identified in my work can account for many of the inconsistencies between the iron and nickel data. The comprehensive compilation of data I present here has a wide range of applications in astronomy beyond work related to variations in alpha. For example, in connection to white dwarf stars, it can be used to further develop more accurate models of hot white dwarf atmospheres with non-LTE conditions and to determine relative abundances [53, 54].

Chapter 4: Measurements of Fe II Transition Probabilities

This chapter handles the results of my work regarding branching fractions and transition probabilities for Fe II in the VUV. The spectrum of Fe II has and continues to be one of the astronomy community's most valuable tools. The high relative abundance of iron and the spectral line density of Fe II make the spectrum a key target for understanding a wide variety of astrophysical objects and processes. Particularly for work on elemental abundances, oscillator strengths (related to transition probabilities through Equation 1.11) are essential atomic parameters. The oscillator strengths of weak stellar lines, which can be very difficult to measure, are often the most valuable, because strong lines are often saturated and not useful for abundance calculations. The challenges associated with measuring oscillator strengths across a wide spectral range, with sensitivity sufficient for measuring all but the weakest lines, have made the availability of such data limited.

The availability of oscillator strength data for Fe II, especially in the UV/VUV were the spectrum is dominant in many stellar spectra, is notably lacking. My work in this chapter is a response to this need, which can readily be addressed with the

Table 4.1 Table of Spectra Used for Fe II

Date	Detector A	Detector B	Number of Co-adds	Source	Source Conditions	Resolution (cm^{-1})	σ Range (cm^{-1})
11/25/2019	R106	R7639	39	D_2		1.00	30000-65000
11/25/2019	R106	R7639	39	Fe/Ne HCL	1.5 A, 900 V, 133 Pa (Ne)	0.08	30000-65000
11/25/2019	R106	R7639	36	Fe/Ne HCL	2.0 A, 620 V, 400 Pa (Ne)	0.08	30000-65000
11/25/2019	R106	R7639	25	Fe/Ne HCL	2.0 A, 830 V, 213 Pa (Ne)	0.08	30000-65000
01/17/2020	R1220	R1220	64	D_2		1.00	35000-55000
01/17/2020	R1220	R1220	81	Fe/Ne HCL	2.0 A, 620 V, 400 Pa (Ne)	0.08	35000-55000
03/13/2020	R1220	R7639	120	D_2		1.00	35000-65000
03/13/2020	R1220	R7639	177	Fe/Ne HCL	2.0 A, 620 V, 373 Pa (Ne)	0.08	35000-65000
03/13/2020	R106	R7639	64	D_2		1.00	30000-65000
03/13/2020	R106	R7639	36	Fe/Ne HCL	2.0 A, 670 V, 400 Pa (Ne)	0.08	30000-65000

instrumentation available to me at NIST. As discussed in Chapter 2, I have used high-resolution Fourier transform spectroscopy to measure the branching fractions of Fe II lines in the UV and VUV (see Equations 1.8 and 1.9). The branching fraction measurements I made with the NIST FT700 FTS were combined with calculated level lifetimes to determine transition probabilities. The results of my work are presented in Table B.1, whose content is explained in the sections below.

4.1 Spectra

To measure branching fractions across a wide spectral range, I needed to combine a variety of spectra measured with various equipment over the course of multiple months. The spectra that I eventually used to calculate the branching fractions I present are detailed in Table 4.1. The first column in Table 4.1 is the date the spectrum was measured on. The second column is the PMT detector I used in the secondary detector box of the FT700 FTS. The third column is the PMT detector I used in the main detector box. The combination of detectors sets the spectral region that particular spectrum can be used to evaluate.

I employed a co-adding technique to increase the SNR of the lines in the spectra so that weak lines could be measured and included in the branching fraction calculations. Because the noise in FTS interferogram is random, stacked interferogram measurements, taken back to back over a roughly thirty minute time period, combine the signal constructively and the noise randomly. This co-adding of interferogram measurements improves the SNR by a factor of $\sqrt{N}$ where N is the number of stacked interferogram measurements. Column four of Table 4.1 indicates the number of co-added interferograms for each spectrum.

The fifth column in Table 4.1 is the source used to produce the spectrum. This column has two different options: the high current Fe/Ne HCL used to produce the Fe II spectrum and the standard reference D_2 lamp used to calibrate the intensities of the Fe II lines. The HCL runs include details about the lamp conditions, such as the current, voltage, and Ne pressure. The final column is the resolution at which the spectrum was measured. The resolution impacts the line intensity uncertainty, which I discuss below, and so I have included it in the details of the spectra.

4.1.1 Initial Processing of Spectra

An ideal FTS produces a symmetric interferogram and thus a real spectrum. However, the optics and sampling electronics can introduce phase shift errors in the interferogram that introduce an asymmetry in the interferogram, giving a non-zero imaginary component in the spectrum. The spectral analysis software I used, XGREMLIN, corrects this by fitting a phase shift curve. The center-burst of the

interferogram (see Figure 4.1) is transformed and the strongest lines are used to fit a phase curve function made of Chebychev polynomials to the spectrum. The phase curve correction is then applied to the inteferogram before the entire interferogram is transformed to generate the full spectrum.

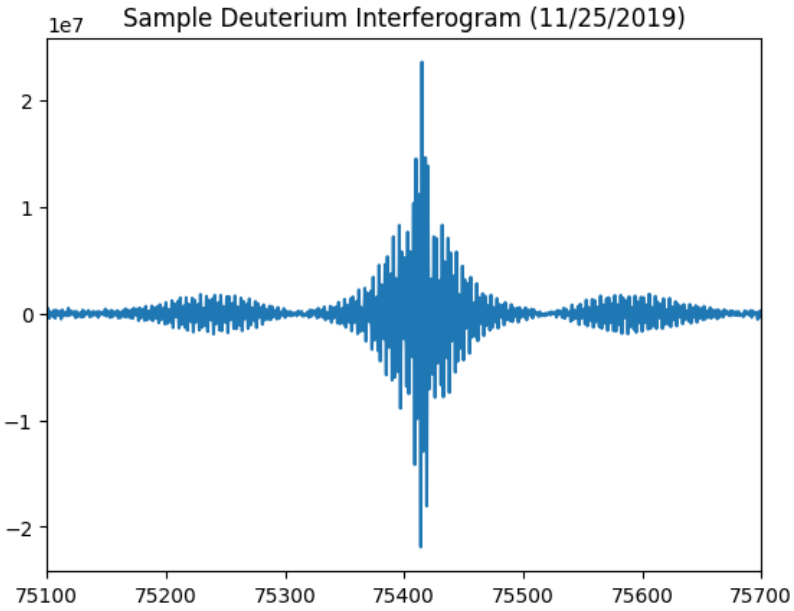

Figure 4.1 Sample interferogram of D_2 lamp taken on 11/25/2019.

Once the Fourier transform is done, the background noise of the spectrum needs to be measured so that the peak intensity values of the lines are set relative to the noise. To do this, I used XGREMLIN to find the root mean square of the deviation of a section of noise in the spectrum where there were no lines. I then used the inverse of this root mean square to the the intensity scale factor of the spectrum. This was done for all spectra cataloged in Table 4.1.

4.1.2 Line Shape and Fitting

In order to understand the process used in XGREMLIN to fit the line profiles of the observed spectral lines, I need to briefly describe the interactions/processes that contribute to the shape of line profiles. The natural line width of a line is due to the finite lifetime of the excited level in the transition and is related to the Heisenberg uncertainty principle ($\Delta E \Delta t \geq \hbar/2$). The longer the level lifetime, the lower the uncertainty in energy and so, there is a narrow spread in the wavelength of the transition. The opposite case, with a very short level lifetime, creates a wider spread in the wavelength of the transition due to the increase in the energy uncertainty. The level lifetime is characterized by the exponential decay of the amplitude of emission over time (decay in level population) whose Fourier transform results in a Lorentz distribution in the frequency domain [55].

In addition to the natural line width, Doppler broadening, due to the motion of the emitting atoms, contributes to the profile of lines. The thermal motion of the atoms in a light source can be reduced by water cooling, as is done in the high current HCL, but is still important in the shape of line profiles. The Doppler broadening of line profiles can be characterized by the velocity distribution of the atoms in the source. The Maxwell-Boltzmann distribution that describes the velocity distribution of the atoms, when combined with the velocity dependent Doppler equation, results in a Gaussian intensity distribution. This effect is proportional to wavenumber and is exaggerated in the UV/VUV.

Lastly, collisional or pressure line width broadening, related to interactions

between the emitting atoms and other particles, should also be considered. This process is also lifetime limited as it depends on the number of excited atoms that have not undergone a collision within the average collision time interval. This population decays exponentially and so the line shape contribution is again a Lorentzian.

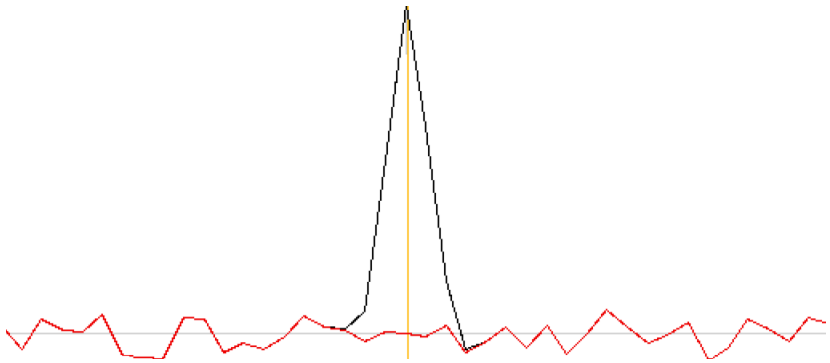

Figure 4.2 Measured Fe II line at 33287.90 cm^{-1}. The black line is the measured data, the red line is residual of the Voigt profile fit, and the yellow line is the center point of the line profile.

The line shapes in my work are a convolution of the Lorentzian and Gaussian components of the processes discussed above. The dominant contributions to the line shapes are the Gaussian Doppler width and the Lorentzian pressure broadening. The convolution of these two distributions results in a Voigt profile whose wings are dominated by the Lorentzian component and whose full width at half max is dominated by the Gaussian component. The validity of the Voigt profile depends on the independence of the Lorentzian and Gaussian components, the argument being that every point on a collision broadened line profile is broadened by a Doppler width. The application of Voigt profiles to the lines observed in my work produces reasonable fits with non-systematic residuals (noise) as is shown Figure 4.2.

Lines in XGREMLIN are fit with the Voigt profiles described above. The initial fit of each line is a least squares fit of a Voigt profile to the line data. This

process works well for unperturbed lines that are symmetric and un-blended with nearby lines. The Fe II spectrum, however, is dense and there can be many blended lines. To treat blended lines, where the intensity of each line in the blend can be obscured by the blending of the other line, I used a more detailed fitting approach and theoretical calculations. To fit a blend with more accuracy than the initial least squares fit, I used the fitting option in XGREMLIN that holds the width and the damping parameters for the initial iterations of the fitting for each line in the blend and checked to see if the line centers had the correct wavelength separation based on the wavelengths provided by Nave and Johansson [28].

4.2 Intensity Calibration

The observed intensity of the Fe/Ne HCL spectrum is not the true emitted intensity of the source, but rather the source distribution having traveled though the spectrometer. The radiative response of the instrument must be taken into account in order to recover the true source distribution. This is done by dividing the observed intensity by the instrument's radiative response function. The D_2 lamp discussed in chapter 2 provides an intensity standard source whose continuum can be used to determine the instrument response.

The observed D_2 spectrum, taken before and after each set of HCL measurements, was first filtered. I needed to apply a filter to the observed D_2 spectrum because below 1660 Å the source is no longer a continuum and has line structure. The calibration of the lamp done by PTB was established with a spectrograph with

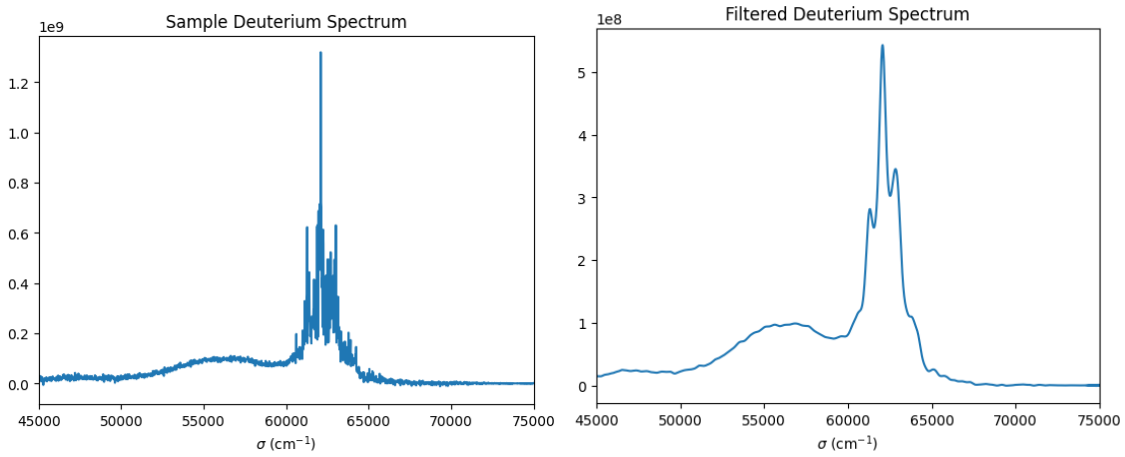

Figure 4.3 Example D_2 spectrum (left) taken on 11/25/2019 and its filtered form (right).

lower resolution than the FTS I used at NIST and so did not resolve the lines below 1660 Å. To address this I degraded my observed spectra by applying two boxcar filters of width 9.2 Å and 4.6 Å to the observed spectrum. The widths of the boxcar filters estimate the widths of the entrance and exit slits of the PTB spectrograph to replicate the resolution of the PTB instrument. One such observed spectrum, and its degraded form, is shown in Figure 4.3.

I then used the low resolution D_2 spectrum with the radiance curve provided by PTB to calculate the instrument's response function. The response is calculated by dividing the observed intensity by the supplied radiance curve. The PTB radiance file needs to be interpolated first because the intensity signal from the FTS is the output of a PMT whose signal is proportional to the number of incident photons, while the PTB radiance curve is given in W/(sr×nm). Thus, the radiance file needs to be converted to (photon flux/cm^{-1}) before the response function can be calculated. The resulting response curve can then be used to calibrate the observed

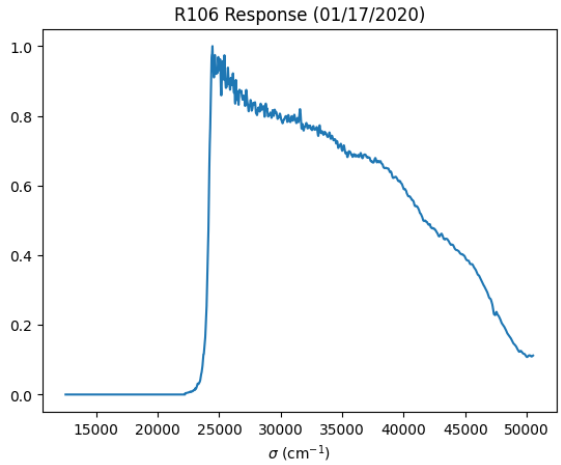

(a) Example R106 Response Curve

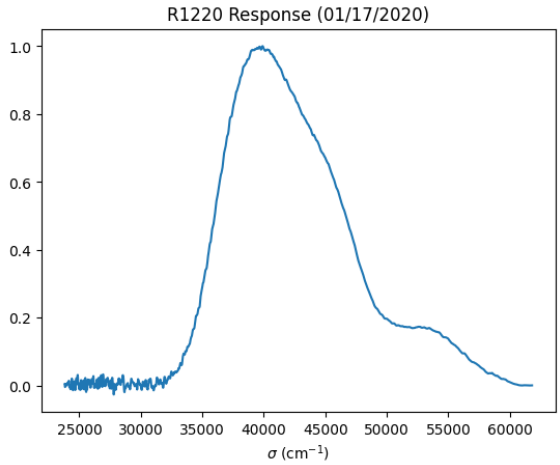

(b) Example R1220 Response Curve

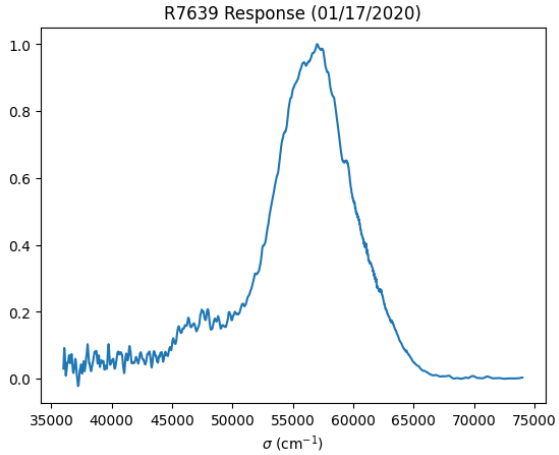

(c) Example R7639 Response Curve

Figure 4.4 Example response curves using each of the PMT detectors used in my work.

intensities of the HCL lines. The interpolation and response curves were developed in XGREMLIN and examples of the response curves I used, from the various sets of measurements, are shown in Figure 4.4.

4.3 Branching Fractions

Once I had calibrated spectra and the fitted line profiles, I used theoretical calculations [50, 56, 57] and the most recent comprehensive study of the Fe II spec-

trum from Nave and Johansson [28], to look for Fe II lines in my measured spectra and catalog the line intensities and line widths of those I could accurately measure. I then organized my line data by common upper level and created individual line files for each spectrum I recorded. These individual line files were read into a custom made python program written by Gillian Nave and updated by Noah Zuckman. The program would read in the line data from all given spectrum files for a specified upper level. The line intensity data could then be normalized by a line common to all the spectra or, when a spectrum did not contain the line used to normalize the other files, a single line could be used to translate one spectrum on to the intensity scale of the other spectra. Additionally, for spectra recorded with both R106 and R7639 PMT detectors simultaneously, as was done on 11/25/2019 and 03/13/2020 (see Table 4.1), I used the region from 45000 cm^{-1} to 48000 cm^{-1} to scale the entire set of R7639 measurements onto the R106 intensity scale. In this region, I used 37 calibrated intensity values from Fe I, Fe II, and Si I lines (unperturbed lines), that were measured on both detectors, to determine a scaling factor that related the intensities between the two detectors. The average standard deviation of the line intensity ratios used to derive the scaling factor was roughly 6% of the weighted mean of the scaling parameter. This approach was used in cases where the R7639 PMT, used for the largest wavenumbers, did not share any overlapping lines with the R1220 spectra for a given level.

For example, the $y^4P_{1/2}$ level of the $3d^6(^3P_2)4p$ configuration, shown in Table B.1, was handled by first scaling the R7639 lines on to the R106 scale. This was needed because the largest wavenumber line at 58494.78 cm^{-1} was only measured

in the R7639 detector and there were no lines for this level that could connect the R7639 lines to the R1220 lines. Once the R7639 line was scaled to the R106 intensity scale, the line at 38922.935 cm^{-1} was used to scale the intensities of all the lines in the spectra such that the 38922.935 cm^{-1} line had an intensity of 1000. This line was chosen to normalize the intensities across different spectra because it was not blended and has a high SNR in all the spectra. Once the intensities were normalized, the intensity for each line was averaged across spectra (weighted by the inverse square of the line intensity uncertainty), and the BFs were calculated according to Equation 1.8.

4.4 Radiative Lifetimes

The level lifetimes I used to combine with branching fraction values were based on the theoretical calculations provided by Raassen and Uylings [56]. The calculated A values from Raassen and Uylings [56] were summed and the inverse of that sum is the level lifetime (see Equation 1.5). Fuhr and Wiese [52] has estimated the uncertainty of these A values to be less than 25% for strong transitions ($\log(gf) > -1$) and up to 70% for weak lines ($\log(gf) < -1.5$). Fuhr and Wiese [52] estimated the A value uncertainties by comparing them to a wide range of experimental values. The lifetimes should have a much smaller uncertainty than the set of A values, however, because the lifetimes are dominated by the strongest transition probabilities, which have the smallest uncertainties.

I compared these theoretical lifetimes to experimental lifetimes [58, 59, 60, 61]

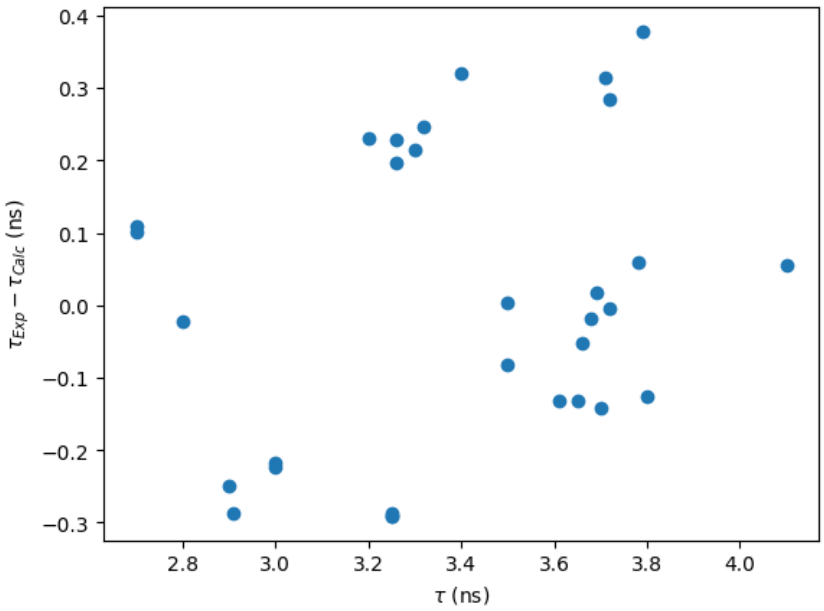

Figure 4.5 Difference between experimental and calculated lifetimes for 31 levels. Standard deviation of the difference shown in this plot is 0.21 ns.

to estimate the uncertainty of the calculated lifetimes. I compared 31 theoretical level lifetimes to their experimentally determined values (see Figure 4.5) and the standard deviation of the differences was 0.21 ns suggesting a lifetime uncertainty of roughly 10%.

4.5 Transition Probability Uncertainties

The uncertainties of the transition probabilities reported in Table B.1 are treated largely in the manner described in Sikström et al. [62] with some modifications. Following Sikström et al. [62], the law of propagation of uncertainty, when applied to Equation 1.9 yields a standard uncertainty $(\mu_c^2(A_k))$ for transition k of

$$\mu_c^2(A_k) = \sum_{n=1}^{j} \left(\frac{\partial A_k}{\partial I_n}\right)^2 \mu^2(I_n) + \left(\frac{\partial A_k}{\partial \tau}\right)^2 \mu^2(\tau) \tag{4.1}$$

where $\mu(\tau)$ is the uncertainty of the level lifetime, $\mu(I_n)$ is the uncertainty of the line intensities, and j is the number of decay channels from the excited level. Using Equations 1.8 and 1.9 to evaluate the partial derivatives of Equation 4.1 results in a relative uncertainty in A_k, $\left(\frac{\mu_c(A_k)}{A_k}\right)^2$, of

$$\left(\frac{\mu_c(A_k)}{A_k}\right)^2 = (1-2(BF)_k)\left(\frac{\mu(I_k)}{I_k}\right)^2 + \sum_{n=1}^{j}(BF)_n^2\left(\frac{\mu(I_n)}{I_n}\right)^2 + \left(\frac{\mu(\tau)}{\tau}\right)^2 \quad (4.2)$$

where the relative uncertainties of the intensity of each line, $\left(\frac{\mu(I)}{I}\right)^2$, is a combination of the uncertainty in the measured intensity, $\mu(I')$, and the uncertainty in the intensity calibration, $\mu(c)$, such that

$$\left(\frac{\mu(I)}{I}\right)^2 = \left(\frac{\mu(I')}{I'}\right)^2 + \left(\frac{\mu(c)}{c}\right)^2. \quad (4.3)$$

The expanded uncertainty of the PTB-provided calibration is 7% with a coverage factor of two ($k = 2$, 95% confidence interval). This results in a standard deviation of 3.5%. This is combined, in quadrature, with the uncertainty with which I can measure the D_2 spectrum. Repeated measurements of the D_2 lamp I used, conducted on the same day, indicate a variation in slope of the measured spectrum of roughly 5%. The combined, absolute measurement uncertainty is then 7%. The calibration uncertainty in Equation 4.3, however, is the relative calibration uncertainty, $\left(\frac{\mu(c)}{c}\right)$, introduced from measuring calibrated line intensities of two lines at different points on the calibration curve (Equation 1.8 shows how BFs are determined by relative intensities). Past authors have taken various approaches to translating the absolute

radiance uncertainty into a relative calibration uncertainty. In my work, I modify the approach taken by Sikström et al. [62] by multiplying the 7% measurement uncertainty by the spectral separation of each line from the dominant decay frequency and divide by the total spectral width of the spectrum. This means that the calibrated line intensity ratio of two lines at very different points in the spectrum will have a larger uncertainty than two lines that are nearer each other, with a maximum relative uncertainty equal to the absolute measurement uncertainty.

The second part of Equation 4.3 to consider, the statistical uncertainty, $\mu(I')$, is described by

$$\left(\frac{\mu(I')}{I'}\right) = \alpha\frac{1}{S\sqrt{n}} = \frac{1.5}{S\sqrt{\frac{FWHM}{\delta x}}} \tag{4.4}$$

where $\alpha = 1.5$, suggested by Sikström et al. [62], was determined by fitting synthetic line profiles [63], S is the signal-to-noise of the line, $FWHM$ is the full width at half maximum of the line, and δx is the resolution at which the spectrum was recorded (shown in Table 4.1). This, combined with the relative calibration uncertainty, describes the dominant components of the relative uncertainty of the intensity measurements. A final consideration needs to be made, however, when two spectral regions need to be joined together using an overlapping line to translate the intensities from one region on to the other region's scale. When this process is used, an additional uncertainty factor needs to be introduced such that

$$\left(\frac{\mu(I)}{I}\right)^2 = \left(\frac{\mu(I')}{I'}\right)^2 + \left(\frac{\mu(c)}{c}\right)^2 + \left(\frac{\mu(nf)}{nf}\right)^2 \tag{4.5}$$

where $\left(\frac{\mu(nf)}{nf}\right)$ is the uncertainty in the normalization factor used to translate the intensity scale across regions. I estimated this uncertainty as the uncertainty of the calibrated intensity of the transfer line. The final result of these considerations transforms Equation 4.2 into

$$\left(\frac{\mu_c(A_k)}{A_k}\right)^2 = (1-2(BF)_k)\left(\frac{\mu(I'_k)}{I'_k}\right)^2 \tag{4.6}$$

$$+ \sum_{(n\neq k)\in B} (BF)_n^2 \left(\left(\frac{\mu(I'_n)}{I'_n}\right)^2 \left(\frac{\mu(c)}{c}\right)^2\right) \tag{4.7}$$

$$+ \sum_{(n\neq k)\in A} (BF)_n^2 \left(\left(\frac{\mu(I'_n)}{I'_n}\right)^2 + \left(\frac{\mu(c)}{c}\right)^2 + \left(\frac{\mu(nf)}{nf}\right)^2\right) \tag{4.8}$$

$$+ \left(\frac{\mu(\tau)}{\tau}\right)^2. \tag{4.9}$$

While Equation 4.6 represents the relative uncertainty of a transition probability when all lines are measured once, my work often includes multiple measurements of the same line and does not include measurements of all decay paths. When multiple measurements of the same line were available, I used a weighted average intensity with the inverse square of the measured line intensity uncertainty for weighting. To prevent the highest SNR measurement from dominating the average when multiple high SNR measurements were available, I implemented a minimum uncertainty such that all lines with a SNR above 24 are given equal weights. When lines from weak transitions were missing from the BF, I added an additional factor of

$$\sum (BF_r)^2 \left(\frac{\mu(I)}{I}\right)^2 = \sum (BF_r)^2 (0.70)^2 \tag{4.10}$$

to Equation 4.6 where the residual BFs, BF_r, are estimated using theoretical calculations by Raassen and Uylings [56], whose uncertainties, $\left(\frac{\mu(I)}{I}\right)$, for weak lines, are estimated to be 70%. Because the BF values of the weak, missing lines are small, the additional uncertainty is small as long as strong lines are not excluded.

The resulting uncertainties, shown in Table B.1 range from 10% to 40% with the majority between 10% and 25%.

4.6 Conclusions

In this chapter I have described my work regarding branching fraction measurements of Fe II lines and the subsequent transition probabilities I derived from combining my branching fractions with theoretical lifetimes. The 105 transition probabilities I report in Table B.1 (16 in the VUV) roughly double the amount of available experimental values in the VUV. The contribution of this data to the astronomy community will assist in a better understanding of a wide variety of astronomical objects and will help to improve the measurement of stellar chemical abundances. This work depended on the combination of high resolution Fourier transform spectroscopy equipment capable of measuring in the VUV and well studied calibration standard sources. This combination of requirements can be difficult to satisfy, which highlights why my contribution to this problem, particularly in the VUV, is not commonly repeated by a wide variety of research groups. The evaluated data I presented helps to fill a critical niche.

Chapter 5: Conclusions

My thesis, through the combination of high-resolution grating and Fourier transform spectroscopy, helped improve the availability and quality of atomic reference data for multiple iron-group elements. Each of my projects has focused on making highly precise and rigorously evaluated measurements that help to meet the needs of modern astrophysics.

I have presented accurate wavelengths and energy levels for Ni V as part of my work in studying the Ni V and Fe V spectra used in the search for fine-structure variation. My correction to previous Ni V wavelengths and my new measurements not only lead to a better understanding of the fine-structure problem, but also provides better reference data for new projects moving forward. Additionally, I presented transition probabilities for UV/VUV lines in the spectrum of Fe II. This important atomic parameter is difficult to measure in the VUV and my thesis work is one of the only modern experimental reports on VUV Fe II transition probabilities.

My work is only a small portion of what is being done and what still needs to be done in the realm of atomic data. Particularly with experimental measurements, the demand for data endlessly outpaces what the community can provide. Future improvements to the data for other iron-group elements and other ionization stages

will be essential for newer generations of astronomy observatories and satellites.

Appendix A: Extended Wavelength and Energy Level Tables

Table A.1 Comparison of Fe V Data

λ_{obs} (Å)[a]	u_{obs} (mÅ)[b]	λ_E (Å)[c]	λ_k (Å)[d]	u_k (mÅ)[b]
1200.1951	0.0038	1200.183	1200.1811	0.0017
1208.2472	0.0038	1208.257	1208.2606	0.0015
1217.9924	0.0038	1217.993	1217.9973	0.0022
1234.6417	0.0024	1234.648	1234.6455	0.0022
1280.4711	0.0031	1280.471	1280.4678	0.0021
1281.6518	0.0038	1281.652	1281.6471	0.0016
1284.1069	0.0024	1284.109	1284.108	0.0017
1285.9205	0.0026	1285.918	1285.915	0.0021
1287.1090	0.0026	1287.101	1287.109	0.0016
1288.1640	0.0024	1288.169	1288.1681	0.0018
1291.1903	0.0024	1291.191	1291.1881	0.0017
1293.29	0.01	1293.305	1293.3059	0.0017
1293.3776	0.0024	1293.377	1293.3826	0.0018
1297.5439	0.0024	1297.547	1297.5453	0.0018
1300.6052	0.0024	1300.608	1300.6095	0.0017
1300.8432	0.0024	1300.846	1300.845	0.004
1303.4815	0.0031	1303.489	1303.4853	0.0024
1304.832	0.006	1304.816	1304.814	0.003
1305.93	0.01	1305.971	1305.9674	0.0018
1306.0792	0.0024	1306.08	1306.0803	0.002
1307.2216	0.0024	1307.219	1307.219	0.003
1307.4237	0.0024	1307.424	1307.4242	0.0023
1311.2293	0.0074	1311.239	1311.2378	0.0019
1311.8278	0.0024	1311.828	1311.829	0.003
1314.5292	0.0026	1314.529	1314.5256	0.0017
1317.8611	0.0024	1317.862	1317.861	0.003
1318.3488	0.0024	1318.354	1318.3505	0.0021
1320.4119	0.0024	1320.41	1320.4116	0.002
1321.3381	0.0024	1321.341	1321.3424	0.002
1321.4887	0.0024	1321.49	1321.4905	0.0023
1321.8476	0.0024	1321.85	1321.8507	0.0022
1323.2685	0.0024	1323.269	1323.2693	0.002
1325.7810	0.0031	1325.781	1325.7838	0.0017
1327.1012	0.0024	1327.101	1327.1006	0.0023
1330.4025	0.0024	1330.401	1330.4063	0.0018
1331.1765	0.0031	1331.185	1331.186	0.003
1331.6376	0.0024	1331.64	1331.639	0.003
1337.2865	0.0024	1337.287	1337.2869	0.0019
1338.7994	0.0038	1338.808	1338.8076	0.0022
1339.6779	0.0038	1339.691	1339.690	0.003
1345.6036	0.0031	1345.611	1345.604	0.003
1348.8203	0.010	1348.838	1348.842	0.003
1350.5250	0.0031	1350.535	1350.5374	0.0016
1351.7366	0.0038	1351.755	1351.7563	0.0024
1354.8432	0.0026	1354.847	1354.845	0.003
1355.6233	0.0024	1355.624	1355.6223	0.0019
1357.6720	0.0024	1357.675	1357.676	0.003
1358.5614	0.0026	1358.567	1358.5646	0.002
1359.0029	0.0024	1359.006	1359.006	0.004
1359.4024	0.0024	1359.406	1359.4034	0.0024
1361.2747	0.0024	1361.279	1361.2776	0.002
1361.4432	0.0024	1361.447	1361.444	0.003
1361.6866	0.0026	1361.692	1361.691	0.004
1361.8239	0.0024	1361.825	1361.828	0.004
1362.8615	0.0024	1362.864	1362.8639	0.0021
1363.0760	0.0024	1363.077	1363.0758	0.0023
1363.6416	0.0024	1363.642	1363.6431	0.0023
1364.8055	0.0038	1364.824	1364.8201	0.0023

Table A.1 (cont'd)

λ_{obs} (Å)[a]	u_{obs} (mÅ)[b]	λ_E (Å)[c]	λ_k (Å)[d]	u_k (mÅ)[b]
1364.9787	0.0026	1364.984	1364.972	0.004
1365.1168	0.0024	1365.115	1365.1143	0.0023
1365.5685	0.0038	1365.571	1365.5742	0.0024
1370.2998	0.0024	1370.303	1370.3038	0.0022
1370.9449	0.0024	1370.947	1370.9419	0.0022
1371.9871	0.0024	1371.987	1371.9858	0.0023
1373.5910	0.0024	1373.587	1373.5868	0.0023
1373.6799	0.0038	1373.674	1373.677	0.002
1373.9654	0.0024	1373.967	1373.9646	0.0018
1374.1175	0.0024	1374.116	1374.118	0.003
1374.7860	0.0024	1374.789	1374.785	0.006
1375.7876	0.0024	1375.784	1375.7851	0.0023
1376.3384	0.0024	1376.337	1376.3367	0.0024
1376.4499	0.0038	1376.455	1376.4511	0.002
1378.0920	0.0024	1378.092	1378.092	0.004
1378.5584	0.0024	1378.56	1378.562	0.003
1380.1107	0.0024	1380.112	1380.114	0.003
1384.045	0.006	1384.055	1384.0585	0.0017
1384.2075	0.0038	1384.201	1384.2003	0.0018
1384.697	0.010	1384.688	1384.6837	0.0019
1385.3136	0.0024	1385.313	1385.312	0.004
1385.6833	0.0024	1385.685	1385.681	0.004
1387.0913	0.0024	1387.092	1387.094	0.003
1387.9376	0.0024	1387.938	1387.938	0.003
1388.1934	0.0024	1388.195	1388.1938	0.0018
1388.3268	0.0024	1388.328	1388.3235	0.0018
1390.7206	0.0038	1390.713	1390.7138	0.0018
1393.0739	0.0031	1393.073	1393.0706	0.0019
1394.2650	0.0038	1394.272	1394.2712	0.0019
1394.6674	0.0024	1394.665	1394.6686	0.0019
1397.1041	0.0038	1397.106	1397.1115	0.0019
1397.7616	0.0038	1397.753	1397.7545	0.0019
1397.9761	0.0024	1397.972	1397.973	0.003
1400.2466	0.0038	1400.243	1400.237	0.003
1402.3946	0.0038	1402.388	1402.391	0.003
1403.3680	0.0024	1403.37	1403.3697	0.002
1404.2665	0.0038	1404.26	1404.2589	0.002
1406.6695	0.0024	1406.669	1406.671	0.003
1406.8232	0.0024	1406.824	1406.822	0.003
1407.2451	0.0024	1407.246	1407.247	0.003
1408.1202	0.0024	1408.117	1408.119	0.003
1409.0288	0.0024	1409.026	1409.0254	0.0021
1409.2230	0.0024	1409.22	1409.2236	0.0021
1409.4539	0.0024	1409.451	1409.451	0.003
1409.8407	0.0038	1409.846	1409.8484	0.0019
1411.059	0.005	1411.069	1411.0703	0.0016
1411.5659	0.0024	1411.566	1411.5675	0.0021
1414.842	0.007	1414.832	1414.832	0.003
1415.19	0.01	1415.196	1415.2028	0.0024
1416.2244	0.0024	1416.219	1416.2196	0.0024
1418.1281	0.0038	1418.123	1418.1223	0.002
1420.1262	0.0038	1420.124	1420.1161	0.0019
1420.458	0.006	1420.465	1420.4765	0.002
1420.6058	0.0026	1420.602	1420.6049	0.0018
1420.76	0.01	1420.749	1420.7486	0.0018
1421.031	0.007	1421.016	1421.0167	0.002
1422.4830	0.0024	1422.481	1422.4802	0.0018
1425.0886	0.0031	1425.088	1425.0834	0.002

Table A.1 (cont'd)

λ_{obs} (Å)[a]	u_{obs} (mÅ)[b]	λ_E (Å)[c]	λ_k (Å)[d]	u_k (mÅ)[b]
1427.8252	0.0038	1427.815	1427.8145	0.0016
1428.0981	0.0026	1428.09	1428.096	0.003
1429.0059	0.0024	1429.004	1429.0058	0.002
1430.322	0.006	1430.309	1430.313	0.003
1430.5672	0.0031	1430.573	1430.573	0.003
1430.779	0.007	1430.751	1430.7552	0.0019
1435.033	0.007	1435.046	1435.0474	0.002
1439.0558	0.0024	1439.052	1439.052	0.004
1440.5297	0.0024	1440.528	1440.529	0.003
1440.7886	0.0024	1440.792	1440.7939	0.0019
1441.0491	0.0026	1441.049	1441.055	0.003
1442.227	0.008	1442.221	1442.2167	0.0021
1443.1616	0.0031	1443.163	1443.1662	0.0022
1445.6859	0.0024	1445.686	1445.686	0.004
1445.917	0.005	1445.91	1445.911	0.0017
1446.6147	0.0024	1446.618	1446.617	0.003
1448.4948	0.0038	1448.494	1448.4875	0.0021
1448.8449	0.0038	1448.846	1448.8487	0.0022
1449.77	0.01	1449.757	1449.758	0.004
1449.9242	0.0024	1449.928	1449.929	0.003
1451.1056	0.0024	1451.103	1451.102	0.003
1453.6212	0.0026	1453.618	1453.616	0.003
1454.2388	0.0024	1454.243	1454.241	0.003
1454.7043	0.0024	1454.701	1454.702	0.003
1455.563	0.005	1455.559	1455.557	0.003
1456.1641	0.0024	1456.161	1456.1622	0.0024
1456.2826	0.0038	1456.285	1456.289	0.003
1457.7299	0.0024	1457.727	1457.7321	0.0021
1459.2552	0.0024	1459.254	1459.256	0.003
1460.7297	0.0031	1460.726	1460.7298	0.0023
1461.06	0.01	1461.05	1461.054	0.003
1462.625	0.009	1462.631	1462.635	0.003
1464.6886	0.0038	1464.683	1464.685	0.003
1464.8805	0.0038	1464.876	1464.873	0.003
1465.389	0.009	1465.383	1465.379	0.003
1466.6552	0.0038	1466.649	1466.6498	0.0018
1468.917	0.006	1468.911	1468.908	0.003
1469.009	0.006	1469.000	1469.000	0.003
1472.1041	0.0026	1472.098	1472.098	0.0023
1472.5158	0.0024	1472.512	1472.5116	0.0024
1472.8090	0.0024	1472.805	1472.805	0.0018
1474.2773	0.0026	1474.275	1474.2722	0.0023
1475.6083	0.0024	1475.604	1475.6059	0.0019
1478.7865	0.0024	1478.785	1478.785	0.003
1479.4765	0.0038	1479.471	1479.4771	0.0021
1496.2679	0.0024	1496.266	1496.2648	0.0023
1530.4446	0.0024	1530.439	1530.4401	0.0023
1543.2397	0.0024	1543.234	1543.234	0.003

[a]Wavelengths measured in this report.

[b]One standard uncertainty of the wavelength value in the previous column.

[c]Wavelengths as reported by Ekberg [15]

[d]Wavelengths as reported by Kramida [21]

Table A.2 Compilation of Ni V Data

λ_{obs} [a] (Å)	u_{obs} [b] (Å)	λ_{Ritz} [c] (Å)	u_{Ritz} [d] (Å)	I [e]	$\log(gf_R)$ [f]	$\log(gf_R)$ [g]	E_i [h] (cm^{-1})	E_k [i] (cm^{-1})	Lower Level Configuration	Term	J	Upper Level Configuration	Term [k]	J	Notes [j]
199.1540	0.0019	199.1540	0.0019	41			0.00	502124.0	$3d^6$	^5D	4	$3d^5(^6S)5f$	$^5F°$	5	R2
199.5040	0.0019	199.5040	0.0019	37			889.61	502132.7	$3d^6$	^5D	3	$3d^5(^6S)5f$	$^5F°$	4	R2
199.7415	0.0019	199.7415	0.0019	23			1489.82	502136.9	$3d^6$	^5D	2	$3d^5(^6S)5f$	$^5F°$	3	R2
199.890	0.004	199.8897	0.0040	12			1871.38	502150.	$3d^6$	^5D	1	$3d^5(^6S)5f$	$^5F°$	2	d,R2
199.9660	0.0019	199.9660	0.0019	25			2057.52	502142.5	$3d^6$	^5D	0	$3d^5(^6S)5f$	$^5F°$	1	R2
227.5655	0.0019	227.5655	0.0019	82			0.00	439433.9	$3d^6$	^5D	4	$3d^5(^6S)4f$	$^5F°$	5	R2
228.0309	0.0019	228.0309	0.0019	78			889.61	439426.7	$3d^6$	^5D	3	$3d^5(^6S)4f$	$^5F°$	4	R2
228.3454	0.0019	228.3454	0.0019	66			1489.82	439422.9	$3d^6$	^5D	2	$3d^5(^6S)4f$	$^5F°$	3	R2
228.5464	0.0019	228.5464	0.0019	58			1871.38	439419.3	$3d^6$	^5D	1	$3d^5(^6S)4f$	$^5F°$	2	R2
228.6435	0.0019	228.6435	0.0019	30			2057.52	439419.6	$3d^6$	^5D	0	$3d^5(^6S)4f$	$^5F°$	1	R2
236.1097	0.0019	236.1092	0.0013	42			0.00	423532.8	$3d^6$	^5D	4	$3d^5(^6S)5p$	$^5P°$	3	R2
236.4670	0.0019	236.4667	0.0013	29			889.61	423782.2	$3d^6$	^5D	3	$3d^5(^6S)5p$	$^5P°$	2	R2
236.6057	0.0019	236.6062	0.0013	20			889.61	423532.8	$3d^6$	^5D	3	$3d^5(^6S)5p$	$^5P°$	3	R2
236.7161	0.0019	236.7170	0.0013	23			1489.82	423935.1	$3d^6$	^5D	2	$3d^5(^6S)5p$	$^5P°$	1	R2
236.8024	0.0019	236.8028	0.0013	12			1489.82	423782.2	$3d^6$	^5D	2	$3d^5(^6S)5p$	$^5P°$	2	R2
236.9320	0.0019	236.9310	0.0013	10			1871.38	423935.1	$3d^6$	^5D	1	$3d^5(^6S)5p$	$^5P°$	1	R2
304.0177	0.0010	304.02069	0.0004	29			27111.40	356036.38	$3d^6$	^3H	6	$3d^5(^2G_1)4p$	$^3G°$	5	R2
304.7020	0.0010	304.70401	0.00030	21	-1.057	E	27578.61	355765.96	$3d^6$	^3H	5	$3d^5(^2G_1)4p$	$^3G°$	4	R2
304.854	0.003	304.85775	0.00070	2	-1.887	E	41627.23	369649.07	$3d^6$	^3D	2	$3d^5(^2P)4p$	$^3P°$	2	H,R2
304.991	0.003	304.9910	0.0029	13	-1.319	E	27111.40	354989.9	$3d^6$	^3H	6	$3d^5(^2G_1)4p$	$^3H°$	6	s,R2
305.1290	0.0010	305.13059	0.00066	10	-1.241	E	41920.54	369649.07	$3d^6$	^3D	3	$3d^5(^2P)4p$	$^3P°$	2	R2
305.3049	0.0010	305.30602	0.00030	8	-1.410	E	27858.94	355399.16	$3d^6$	^3H	4	$3d^5(^2G_1)4p$	$^3G°$	3	R2
305.891	0.003	305.89227	0.00035	3	-2.076	E	29123.90	356036.38	$3d^6$	$^3F_2$	4	$3d^5(^2G_1)4p$	$^3G°$	5	d,R2
306.054	0.003	306.05429	0.00093	2	-1.803	E	41700.99	368440.41	$3d^6$	^3D	1	$3d^5(^2P)4p$	$^3P°$	0	d,R2
306.338	0.003	306.33668	0.00031	7	-1.772	E	27111.40	353549.6	$3d^6$	^3H	6	$3d^5(^2G_1)4p$	$^3H°$	5	G,R2
306.488	0.003	306.48968	0.00030	2	-1.870	E	29123.90	355399.16	$3d^6$	$^3F_2$	4	$3d^5(^2G_1)4p$	$^3G°$	3	d,R2
306.565	0.003	306.56492	0.00031	2	-2.151	E	29570.78	355765.96	$3d^6$	$^3F_2$	3	$3d^5(^2G_1)4p$	$^3G°$	4	d,R2
306.6687	0.0010	306.66772	0.00039	12	-1.352	E	27858.94	353944.78	$3d^6$	^3H	4	$3d^5(^2G_1)4p$	$^3F°$	3	R2
306.7763	0.0010	306.77575	0.00029	16	-1.302	E	27578.61	353549.6	$3d^6$	^3H	5	$3d^5(^2G_1)4p$	$^3H°$	5	R2
307.225	0.003	307.22668	0.00030	18	-1.743	E	27578.61	353071.17	$3d^6$	^3H	5	$3d^5(^2G_1)4p$	$^3H°$	4	H,R2*
307.225	0.003	307.23063	0.00031	18	-2.177	E	27858.94	353347.32	$3d^6$	^3H	4	$3d^5(^2G_1)4p$	$^3F°$	4	H,R2*
307.4923	0.0010	307.49151	0.00030	13	-1.477	E	27858.94	353071.17	$3d^6$	^3H	4	$3d^5(^2G_1)4p$	$^3H°$	4	R2
309.351	0.004	309.35053	0.00079	3	-1.378	E	69156.49	392414.38	$3d^6$	$^3P_1$	2	$3d^5(^2D_1)4p$	$^3P°$	2	d,R2
309.769	0.003	309.76854	0.00026	2	-2.330	E	0.00	322821.68	$3d^6$	^5D	4	$3d^5(^4F)4p$	$^3F°$	4	H,R2
309.8106	0.0010	309.80864	0.00034	21	-0.990	E	33256.49	356036.38	$3d^6$	^3G	5	$3d^5(^2G_1)4p$	$^3G°$	5	R2
310.0705	0.0010	310.06841	0.00030	13	-1.318	E	33256.49	355765.96	$3d^6$	^3G	5	$3d^5(^2G_1)4p$	$^3G°$	4	R2

Table A.2 (cont'd)

λ_{obs} [a] (Å)	u_{obs} [b] (Å)	λ_{Ritz} [c] (Å)	u_{Ritz} [d] (Å)	I [e]	$\log(gf_R)$ [f]	$\log(gf_R)$ [g]	E_i [h] (cm^{-1})	E_k [i] (cm^{-1})	Lower Level Configuration	Term	J	Upper Level Configuration	Term [k]	J	Notes [j]
310.538	0.003	310.5360	0.0013	7	-1.397	E	67548.05	389572.0	$3d^6$	$^3P_1$	1	$3d^5(^2D_1)4p$	$^3D°$	2	d,R2
310.7911	0.0010	310.79055	0.00068	23	-0.691	E	68719.26	390479.36	$3d^6$	$^3F_1$	4	$3d^5(^2D_1)4p$	$^3D°$	3	R2
310.8465	0.0010	310.84478	0.00030	16	-1.197	E	34061.99	355765.96	$3d^6$	^3G	4	$3d^5(^2G_1)4p$	$^3G°$	4	R2
311.0236	0.0010	311.02363	0.00081	1	-1.906	E	69156.49	390675.47	$3d^6$	$^3P_1$	2	$3d^5(^2D_1)4p$	$^1D°$	2	R2
311.201	0.003	311.19960	0.00030	24	-1.170	E	34061.99	355399.16	$3d^6$	^3G	4	$3d^5(^2G_1)4p$	$^3G°$	3	l,R2
311.5473	0.0010	311.54311	0.00033	17	-1.537	E	34416.29	355399.16	$3d^6$	^3G	3	$3d^5(^2G_1)4p$	$^3G°$	3	R2
311.788	0.003	311.78619	0.00037	26	-1.231	E	34416.29	355148.90	$3d^6$	^3G	3	$3d^5(^2G_1)4p$	$^3F°$	2	p,R2
311.800	0.003	311.8015	0.0013	25	-0.803	E	68855.07	389572.0	$3d^6$	$^3F_1$	3	$3d^5(^2D_1)4p$	$^3D°$	2	p,R2
312.217	0.003	312.21401	0.00028	10	-2.057	E	33256.49	353549.6	$3d^6$	^3G	5	$3d^5(^2G_1)4p$	$^3H°$	5	H,R2
312.388	0.004	312.3888	0.0017	22	-0.927	E	68632.25	388746.2	$3d^6$	$^3F_1$	2	$3d^5(^2D_1)4p$	$^3D°$	1	l,R2
312.4123	0.0010	312.41132	0.00030	24	-1.280	E	33256.49	353347.32	$3d^6$	^3G	5	$3d^5(^2G_1)4p$	$^3F°$	4	R2
312.5195	0.0019	312.51950	0.00078	16	-1.125	E	68719.26	388699.29	$3d^6$	$^3F_1$	4	$3d^5(^2D_1)4p$	$^3F°$	4	R2
312.615	0.003	312.61450	0.00041	12	-1.734	E	34061.99	353944.78	$3d^6$	^3G	4	$3d^5(^2G_1)4p$	$^3F°$	3	H,R2
312.6800	0.0010	312.68108	0.00029	13	-2.015	E	33256.49	353071.17	$3d^6$	^3G	5	$3d^5(^2G_1)4p$	$^3H°$	4	R2
312.8389	0.0010	312.83910	0.00027	9	-2.089	E	0.00	319653.14	$3d^6$	^5D	4	$3d^5(^4F)4p$	$^3G°$	5	R2
312.9622	0.0010	312.96114	0.00042	17	-1.235	E	34416.29	353944.78	$3d^6$	^3G	3	$3d^5(^2G_1)4p$	$^3F°$	3	R2
313.000	0.003	313.00117	0.00029	10	-2.352	E	34061.99	353549.6	$3d^6$	^3G	4	$3d^5(^2G_1)4p$	$^3H°$	5	d,R2
313.9927	0.0019	313.9943	0.0012	12	-1.202	E	68855.07	387332.2	$3d^6$	$^3F_1$	3	$3d^5(^2D_1)4p$	$^3F°$	3	R2
314.132	0.004	314.1334	0.0017	11	-1.288	E	68632.25	386968.3	$3d^6$	$^3F_1$	2	$3d^5(^2D_1)4p$	$^3F°$	2	d,R2
315.0824	0.0010	315.08396	0.00035	13	-1.857	E	0.00	317375.72	$3d^6$	^5D	4	$3d^5(^2H)4p$	$^3G°$	3	R2
315.235	0.003	315.23563	0.00049	55	-0.390	E	41252.65	358475.67	$3d^6$	^1I	6	$3d^5(^2G_1)4p$	$^1H°$	5	s,R2*
315.235	0.003	315.22654	0.00031	55	-1.572	E	0.00	317232.17	$3d^6$	^5D	4	$3d^5(^4F)4p$	$^5D°$	3	s,R2*
315.573	0.003	315.56822	0.00028	24	-1.753	E	0.00	316888.69	$3d^6$	^5D	4	$3d^5(^2H)4p$	$^3G°$	4	G,R2*
315.573	0.004	315.5764	0.0015	24	-1.086	E	57924.12	374804.6	$3d^6$	^1F	3	$3d^5(^2P)4p$	$^3D°$	2	G,R2*
315.7121	0.0010	315.71309	0.00028	56	-0.662	E	0.00	316743.28	$3d^6$	^5D	4	$3d^5(^4F)4p$	$^5D°$	4	R2
315.8290	0.0010	315.82815	0.00033	38	-1.221	E	889.61	317517.50	$3d^6$	^5D	3	$3d^5(^4F)4p$	$^5D°$	2	R2
315.9054	0.0010	315.90364	0.00037	21	-2.378	E	42208.47	358760.69	$3d^6$	$^1G_2$	4	$3d^5(^2G_1)4p$	$^1G°$	4	R2
315.9686	0.0010	315.96963	0.00035	30	-1.324	E	889.61	317375.72	$3d^6$	^5D	3	$3d^5(^2H)4p$	$^3G°$	3	R2
316.1126	0.0010	316.11301	0.00028	42	-1.013	E	889.61	317232.17	$3d^6$	^5D	3	$3d^5(^4F)4p$	$^5D°$	3	R2
316.189	0.003	316.18834	0.00043	21	-1.386	E	42208.47	358475.67	$3d^6$	$^1G_2$	4	$3d^5(^2G_1)4p$	$^1H°$	5	H,R2
316.4279	0.0010	316.42798	0.00036	31	-1.207	E	1489.82	317517.50	$3d^6$	^5D	2	$3d^5(^4F)4p$	$^5D°$	2	R2
316.4676	0.0010	316.46734	0.00050	33	-1.182	E	1489.82	317478.19	$3d^6$	^5D	2	$3d^5(^4F)4p$	$^5D°$	1	R2
316.569	0.003	316.57000	0.00038	6	-2.084	E	1489.82	317375.72	$3d^6$	^5D	2	$3d^5(^2H)4p$	$^3G°$	3	d,R2
316.668	0.003	316.66888	0.00042	6	-1.764	E	29123.90	344911.17	$3d^6$	$^3F_2$	4	$3d^5(^2D_2)4p$	$^3F°$	4	d,R2
316.714	0.003	316.71393	0.00032	9	-1.907	E	1489.82	317232.17	$3d^6$	^5D	2	$3d^5(^4F)4p$	$^5D°$	3	d,R2
316.776	0.003	316.77495	0.00036	14	-1.488	E	29123.90	344805.43	$3d^6$	$^3F_2$	4	$3d^5(^2D_2)4p$	$^3D°$	3	s,R2

Table A.2 (cont'd)

λ_{obs} [a] (Å)	u_{obs} [b] (Å)	λ_{Ritz} [c] (Å)	u_{Ritz} [d] (Å)	I [e]	$\log(gf_R)$ [f]	$\log(gf_R)$ [g]	E_i [h] (cm^{-1})	E_k [i] (cm^{-1})	Lower Level Configuration	Term	J	Upper Level Configuration	Term [k]	J	Notes [j]
316.8102	0.0010	316.81048	0.00037	21	-1.504	E	1871.38	317517.50	$3d^6$	^5D	1	$3d^5(^4F)4p$	$^5D^\circ$	2	R2
316.853	0.003	316.84994	0.00053	24	-1.761	E	1871.38	317478.19	$3d^6$	^5D	1	$3d^5(^4F)4p$	$^5D^\circ$	1	p,R2
316.8660	0.0010	316.86742	0.00052	27	-1.381	E	1871.38	317460.78	$3d^6$	^5D	1	$3d^5(^4F)4p$	$^5D^\circ$	0	R2
317.0373	0.0010	317.03693	0.00056	19	-1.566	E	2057.52	317478.19	$3d^6$	^5D	0	$3d^5(^4F)4p$	$^5D^\circ$	1	R2
317.2910	0.0010	317.29042	0.00030	41	-1.043	E	0.00	315168.67	$3d^6$	^5D	4	$3d^5(^4F)4p$	$^5F^\circ$	5	R2
317.4019	0.0010	317.40159	0.00076	29	-0.433	E	77900.04	392958.32	$3d^6$	$^1G_1$	4	$3d^5(^2D_1)4p$	$^1F^\circ$	3	R2
317.8648	0.0010	317.86478	0.00026	16	-1.543	E	0.00	314599.18	$3d^6$	^5D	4	$3d^5(^4F)4p$	$^5F^\circ$	4	R2
317.901	0.003	317.90265	0.00028	2	-2.084	E	0.00	314561.71	$3d^6$	^5D	4	$3d^5(^4F)4p$	$^5F^\circ$	3	d,R2
318.2595	0.0010	318.26045	0.00026	8	-1.789	E	0.00	314208.06	$3d^6$	^5D	4	$3d^5(^2F_1)4p$	$^3F^\circ$	4	R2
318.5280	0.0010	318.52798	0.00036	4	-1.973	E	889.61	314833.77	$3d^6$	^5D	3	$3d^5(^4F)4p$	$^5F^\circ$	2	R2
318.7032	0.0010	318.70282	0.00037	2	-1.506	E	41627.23	355399.16	$3d^6$	^3D	2	$3d^5(^2G_1)4p$	$^3G^\circ$	3	R2
318.7657	0.0010	318.76618	0.00025	39	-0.988	E	889.61	314599.18	$3d^6$	^5D	3	$3d^5(^4F)4p$	$^5F^\circ$	4	R2
318.803	0.003	318.80425	0.00027	2	-2.258	E	889.61	314561.71	$3d^6$	^5D	3	$3d^5(^4F)4p$	$^5F^\circ$	3	d,R2
318.900	0.003	318.89848	0.00084	8	-1.552	E	29898.79	343478.21	$3d^6$	$^3F_2$	2	$3d^5(^2D_2)4p$	$^3D^\circ$	1	d,R2
319.0153	0.0010	319.01457	0.00032	11	-1.921	E	0.00	313465.31	$3d^6$	^5D	4	$3d^5(^4F)4p$	$^5G^\circ$	5	R2
319.0307	0.0010	319.03228	0.00043	9	-1.282	E	41700.99	355148.90	$3d^6$	^3D	1	$3d^5(^2G_1)4p$	$^3F^\circ$	2	R2
319.1625	0.0010	319.16410	0.00025	20	-1.450	E	889.61	314208.06	$3d^6$	^5D	3	$3d^5(^2F_1)4p$	$^3F^\circ$	4	R2
319.202	0.003	319.20285	0.00040	2	-2.177	E	1871.38	315151.79	$3d^6$	^5D	1	$3d^5(^4F)4p$	$^5F^\circ$	1	d,R2
319.241	0.003	319.24004	0.00057	2	-2.184	E	2057.52	315301.44	$3d^6$	^5D	0	$3d^5(^2F_1)4p$	$^3D^\circ$	1	H,R2
319.392	0.003	319.39262	0.00051	26	-1.555	E	2057.52	315151.79	$3d^6$	^5D	0	$3d^5(^4F)4p$	$^5F^\circ$	1	p,R2
319.4144	0.0010	319.41545	0.00030	48	-0.908	E	1489.82	314561.71	$3d^6$	^5D	2	$3d^5(^4F)4p$	$^5F^\circ$	3	R2
319.5256	0.0010	319.52721	0.00040	36	-1.105	E	1871.38	314833.77	$3d^6$	^5D	1	$3d^5(^4F)4p$	$^5F^\circ$	2	R2
320.1106	0.0019	320.11145	0.00027	5	-2.029	E	889.61	313280.81	$3d^6$	^5D	3	$3d^5(^4F)4p$	$^5G^\circ$	4	R2
320.185	0.003	320.18694	0.00047	22	-1.305	E	41627.23	353944.78	$3d^6$	^3D	2	$3d^5(^2G_1)4p$	$^3F^\circ$	3	p,R2
320.208	0.003	320.20805	0.00040	11	-1.563	E	41252.65	353549.6	$3d^6$	^1I	6	$3d^5(^2G_1)4p$	$^3H^\circ$	5	d,R2
320.702	0.003	320.70041	0.00094	3	-1.658	E	66738.13	378555.63	$3d^6$	$^3P_1$	0	$3d^5(^2P)4p$	$^3S^\circ$	1	d,R2
320.815	0.003	320.81520	0.00052	2	-2.352	E	1871.38	313577.31	$3d^6$	^5D	1	$3d^5(^2D_3)4p$	$^3P^\circ$	0	G,R2
320.868	0.003	320.86796	0.00043	29	-1.025	E	33256.49	344911.17	$3d^6$	^3G	5	$3d^5(^2D_2)4p$	$^3F^\circ$	4	G,R2
321.1020	0.0010	321.10276	0.00033	17	-1.053	E	41920.54	353347.32	$3d^6$	^3D	3	$3d^5(^2G_1)4p$	$^3F^\circ$	4	R2
321.3854	0.0010	321.38775	0.00032	8	-1.473	E	41920.54	353071.17	$3d^6$	^3D	3	$3d^5(^2G_1)4p$	$^3H^\circ$	4	R2
321.5348	0.0010	321.53557	0.00073	6	-1.097	E	67548.05	378555.63	$3d^6$	$^3P_1$	1	$3d^5(^2P)4p$	$^3S^\circ$	1	R2
321.809	0.003	321.80889	0.00036	10	-1.437	E	34061.99	344805.43	$3d^6$	^3G	4	$3d^5(^2D_2)4p$	$^3D^\circ$	3	G,R2
323.1126	0.0010	323.11305	0.00043	5	-1.745	E	34416.29	343905.49	$3d^6$	^3G	3	$3d^5(^2D_2)4p$	$^3D^\circ$	2	R2
323.167	0.004	323.1726	0.0013	4	-1.926	E	77900.04	387332.2	$3d^6$	$^1G_1$	4	$3d^5(^2D_1)4p$	$^3F^\circ$	3	d,R2
323.2077	0.0010	323.20710	0.00073	18	-0.732	E	69156.49	378555.63	$3d^6$	$^3P_1$	2	$3d^5(^2P)4p$	$^3S^\circ$	1	R2
323.3937	0.0010	323.39374	0.00035	16	-1.383	E	34061.99	343282.57	$3d^6$	^3G	4	$3d^5(^2D_2)4p$	$^3F^\circ$	3	R2

Table A.2 (cont'd)

λ_{obs} [a] (Å)	u_{obs} [b] (Å)	λ_{Ritz} [c] (Å)	u_{Ritz} [d] (Å)	I [e]	$\log(gf_R)$ [f]	$\log(gf_R)$ [g]	E_i [h] (cm^{-1})	E_k [i] (cm^{-1})	Lower Level Configuration	Term	J	Upper Level Configuration	Term [k]	J	Notes [j]
324.1720	0.0010	324.17264	0.00047	13	-1.348	E	34416.29	342893.90	$3d^6$	^3G	3	$3d^5(^2D_2)4p$	$^3F^\circ$	2	R2
324.4600	0.0010	324.4600	0.0010	12	-0.964	E	68855.07	377060.	$3d^6$	$^3F_1$	3	$3d^5(^2P)4p$	$^1D^\circ$	2	R2
324.9359	0.0010	324.93617	0.00095	34	-0.400	E	68719.26	376472.01	$3d^6$	$^3F_1$	4	$3d^5(^2P)4p$	$^3D^\circ$	3	R2
325.082	0.003	325.0796	0.0010	2	-1.495	E	68855.07	376472.01	$3d^6$	$^3F_1$	3	$3d^5(^2P)4p$	$^3D^\circ$	3	d,R2
326.5882	0.0019	326.5882	0.0019	28	-0.768	E	68632.25	374829.	$3d^6$	$^3F_1$	2	$3d^5(^2P)4p$	$^3D^\circ$	1	R2
326.613	0.004	326.6134	0.0017	1	-1.747	E	68632.25	374804.6	$3d^6$	$^3F_1$	2	$3d^5(^2P)4p$	$^3D^\circ$	2	G,R2
326.8519	0.0019	326.8513	0.0016	22	-0.814	E	68855.07	374804.6	$3d^6$	$^3F_1$	3	$3d^5(^2P)4p$	$^3D^\circ$	2	R2
327.510	0.003	327.51145	0.00052	2	-1.858	E	41627.23	346960.07	$3d^6$	^3D	2	$3d^5(^2D_2)4p$	$^3P^\circ$	1	d,R2
327.876	0.003	327.87688	0.00038	2	-1.727	E	41920.54	346913.07	$3d^6$	^3D	3	$3d^5(^2D_2)4p$	$^3P^\circ$	2	H,R2
328.612	0.004	328.61255	0.00060	4	-2.017	E	41627.23	345936.97	$3d^6$	^3D	2	$3d^5(^2D_2)4p$	$^1F^\circ$	3	d,R2
329.251	0.003	329.25030	0.00047	2	-1.957	E	26152.49	329872.79	$3d^6$	$^3P_2$	2	$3d^5(^2F_2)4p$	$^3D^\circ$	3	d,R2
330.0432	0.0010	330.04321	0.00044	18	-1.217	E	41920.54	344911.17	$3d^6$	^3D	3	$3d^5(^2D_2)4p$	$^3F^\circ$	4	R2
330.1582	0.0010	330.15843	0.00038	21	-1.082	E	41920.54	344805.43	$3d^6$	^3D	3	$3d^5(^2D_2)4p$	$^3D^\circ$	3	R2
330.8204	0.0010	330.82101	0.00046	16	-1.250	E	41627.23	343905.49	$3d^6$	^3D	2	$3d^5(^2D_2)4p$	$^3D^\circ$	2	R2
331.0167	0.0010	331.01510	0.00076	15	-1.102	E	67548.05	369649.07	$3d^6$	$^3P_1$	1	$3d^5(^2P)4p$	$^3P^\circ$	2	R2
331.113	0.003	331.1162	0.0025	12	-1.167	E	66738.13	368746.9	$3d^6$	$^3P_1$	0	$3d^5(^2P)4p$	$^3P^\circ$	1	R2*
331.113	0.003	331.11064	0.00039	12	-2.112	E	27858.94	329872.79	$3d^6$	^3H	4	$3d^5(^2F_2)4p$	$^3D^\circ$	3	R2*
331.141	0.003	331.14233	0.00044	4	-2.166	E	41920.54	343905.49	$3d^6$	^3D	3	$3d^5(^2D_2)4p$	$^3D^\circ$	2	H,R2
331.3704	0.0010	331.37027	0.00085	11	-1.462	E	41700.99	343478.21	$3d^6$	^3D	1	$3d^5(^2D_2)4p$	$^3D^\circ$	1	R2
331.5067	0.0010	331.50416	0.00041	20	-1.289	E	41627.23	343282.57	$3d^6$	^3D	2	$3d^5(^2D_2)4p$	$^3F^\circ$	3	R2
331.5711	0.0010	331.57096	0.00026	16	-1.432	E	29123.90	330718.47	$3d^6$	$^3F_2$	4	$3d^5(^2F_2)4p$	$^3G^\circ$	5	R2
332.012	0.003	332.01313	0.00056	20	-1.318	E	41700.99	342893.90	$3d^6$	^3D	1	$3d^5(^2D_2)4p$	$^3F^\circ$	2	s,R2*
332.012	0.003	332.0066	0.0026	20	-1.273	E	67548.05	368746.9	$3d^6$	$^3P_1$	1	$3d^5(^2P)4p$	$^3P^\circ$	1	s,R2*
332.140	0.003	332.13866	0.00054	4	-1.857	E	28697.33	329776.40	$3d^6$	$^3P_2$	1	$3d^5(^2F_2)4p$	$^3D^\circ$	2	d,R2
332.2928	0.0010	332.29318	0.00065	23	-0.900	E	48607.12	349546.19	$3d^6$	$^1D_2$	2	$3d^5(^2D_2)4p$	$^1D^\circ$	2	R2
332.3163	0.0010	332.31569	0.00031	20	-1.652	E	0.00	300918.68	$3d^6$	^5D	4	$3d^5(^4D)4p$	$^3F^\circ$	4	R2
332.3448	0.0010	332.34476	0.00096	7	-1.275	E	67548.05	368440.41	$3d^6$	$^3P_1$	1	$3d^5(^2P)4p$	$^3P^\circ$	0	R2
332.410	0.003	332.40640	0.00045	2	-2.133	E	57924.12	358760.69	$3d^6$	^1F	3	$3d^5(^2G_1)4p$	$^1G^\circ$	4	G,R2
332.4711	0.0010	332.47091	0.00095	22	-1.029	E	47699.96	348478.15	$3d^6$	$^1S_2$	0	$3d^5(^2D_2)4p$	$^1P^\circ$	1	R2
332.504	0.003	332.50331	0.00038	15	-1.613	E	29123.90	329872.79	$3d^6$	$^3F_2$	4	$3d^5(^2F_2)4p$	$^3D^\circ$	3	d,R2
332.5277	0.0010	332.52787	0.00042	22	-1.298	E	29570.78	330297.45	$3d^6$	$^3F_2$	3	$3d^5(^2F_2)4p$	$^3G^\circ$	4	R2
332.689	0.003	332.69014	0.00042	6	-2.173	E	889.61	301469.60	$3d^6$	^5D	3	$3d^5(^4D)4p$	$^3F^\circ$	3	d,R2
332.788	0.003	332.78692	0.00082	29	-0.691	E	69156.49	369649.07	$3d^6$	$^3P_1$	2	$3d^5(^2P)4p$	$^3P^\circ$	2	R2*
332.788	0.003	332.78897	0.00028	29	-1.461	E	29123.90	329614.63	$3d^6$	$^3F_2$	4	$3d^5(^2F_2)4p$	$^3G^\circ$	3	R2*
333.109	0.003	333.11023	0.00029	33	-2.074	E	0.00	300200.93	$3d^6$	^5D	4	$3d^5(^4D)4p$	$^5P^\circ$	3	p,R2*
333.109	0.003	333.10502	0.00045	33	-1.380	E	29570.78	329776.40	$3d^6$	$^3F_2$	3	$3d^5(^2F_2)4p$	$^3D^\circ$	2	p,R2*

Table A.2 (cont'd)

λ_{obs} [a] (Å)	u_{obs} [b] (Å)	λ_{Ritz} [c] (Å)	u_{Ritz} [d] (Å)	I [e]	$\log(gf_R)$ [f]	$\log(gf_R)$ [g]	E_i [h] (cm^{-1})	E_k [i] (cm^{-1})	Lower Level Configuration	Term	J	Upper Level Configuration	Term [k]	J	Notes [j]
333.302	0.003	333.30104	0.00030	11	-1.916	E	889.61	300918.68	$3d^6$	^5D	3	$3d^5(^4D)4p$	$^3F°$	4	d,R2
333.360	0.003	333.36222	0.00043	15	-1.606	E	29898.79	329872.79	$3d^6$	$^3F_2$	2	$3d^5(^2F_2)4p$	$^3D°$	3	d,R2*
333.360	0.003	333.35580	0.00044	15	-2.064	E	1489.82	301469.60	$3d^6$	^5D	2	$3d^5(^4D)4p$	$^3F°$	3	d,R2*
333.475	0.003	333.4767	0.0011	4	-2.064	E	48607.12	348478.15	$3d^6$	$^1D_2$	2	$3d^5(^2D_2)4p$	$^1P°$	1	H,R2
333.651	0.003	333.64937	0.00034	14	-1.570	E	29898.79	329614.63	$3d^6$	$^3F_2$	2	$3d^5(^2F_2)4p$	$^3G°$	3	H,R2
334.1164	0.0010	334.11515	0.00033	18	-1.173	E	27578.61	326876.62	$3d^6$	^3H	5	$3d^5(^2F_2)4p$	$^3F°$	4	R2
334.429	0.003	334.42839	0.00034	2	-2.011	E	27858.94	326876.62	$3d^6$	^3H	4	$3d^5(^2F_2)4p$	$^3F°$	4	R2
334.4791	0.0010	334.47869	0.00038	15	-1.639	E	0.00	298972.71	$3d^6$	^5D	4	$3d^5(^4D)4p$	$^3D°$	3	R2
335.382	0.003	335.37768	0.00035	42	-0.999	E	27858.94	326030.24	$3d^6$	^3H	4	$3d^5(^2F_2)4p$	$^3F°$	3	p,R2
335.3951	0.0010	335.39465	0.00030	42	-1.167	E	889.61	299045.83	$3d^6$	^5D	3	$3d^5(^4D)4p$	$^5P°$	2	R2
335.4777	0.0010	335.47692	0.00036	39	-1.162	E	889.61	298972.71	$3d^6$	^5D	3	$3d^5(^4D)4p$	$^3D°$	3	R2
335.5293	0.0010	335.52864	0.00029	24	-1.281	E	27111.40	325148.55	$3d^6$	^3H	6	$3d^5(^2G_2)4p$	$^3H°$	6	R2
335.5933	0.0010	335.59263	0.00032	24	-1.130	E	27578.61	325558.93	$3d^6$	^3H	5	$3d^5(^2F_2)4p$	$^1G°$	4	R2
335.7182	0.0010	335.71758	0.00028	57	-0.218	E	27111.40	324980.8	$3d^6$	^3H	6	$3d^5(^2G_2)4p$	$^3G°$	5	R2
335.8508	0.0010	335.84916	0.00032	22	-1.164	E	29123.90	326876.62	$3d^6$	$^3F_2$	4	$3d^5(^2F_2)4p$	$^3F°$	4	R2
335.911	0.003	335.90644	0.00050	9	-3.824	E	26152.49	323854.43	$3d^6$	$^3P_2$	2	$3d^5(^4F)4p$	$^3F°$	2	d,R2
335.971	0.003	335.97044	0.00040	51	-0.436	E	27578.61	325223.84	$3d^6$	^3H	5	$3d^5(^2G_2)4p$	$^3G°$	4	s,R2
336.0715	0.0010	336.07118	0.00032	16	-1.844	E	1489.82	299045.83	$3d^6$	^5D	2	$3d^5(^4D)4p$	$^5P°$	2	R2
336.1540	0.0010	336.15379	0.00038	28	-1.474	E	1489.82	298972.71	$3d^6$	^5D	2	$3d^5(^4D)4p$	$^3D°$	3	R2
336.3006	0.0010	336.30033	0.00038	46	-0.524	E	27858.94	325212.20	$3d^6$	^3H	4	$3d^5(^2G_2)4p$	$^3G°$	3	R2
336.446	0.003	336.44713	0.00044	9	-1.830	E	29898.79	327122.31	$3d^6$	$^3F_2$	2	$3d^5(^2F_2)4p$	$^1D°$	2	d,R2
336.5043	0.0010	336.50268	0.00035	29	-1.528	E	1871.38	299045.83	$3d^6$	^5D	1	$3d^5(^4D)4p$	$^5P°$	2	R2
336.5755	0.0010	336.57528	0.00049	36	-1.233	E	1489.82	298600.17	$3d^6$	^5D	2	$3d^5(^4P)4p$	$^3D°$	1	R2
336.7917	0.0010	336.79164	0.00038	63	-0.500	E	0.00	296919.48	$3d^6$	^5D	4	$3d^5(^4D)4p$	$^5D°$	4	R2
336.8181	0.0019	336.81776	0.00034	57	-0.683	E	0.00	296896.46	$3d^6$	^5D	4	$3d^5(^4G)4p$	$^3G°$	4	R2
336.9304	0.0010	336.92947	0.00028	32	-0.982	E	27111.40	323909.42	$3d^6$	^3H	6	$3d^5(^2G_2)4p$	$^3H°$	5	R2
337.1840	0.0010	337.18387	0.00042	38	-1.153	E	0.00	296574.09	$3d^6$	^5D	4	$3d^5(^4D)4p$	$^5D°$	3	R2
337.2358	0.0010	337.23513	0.00035	23	-1.629	E	889.61	297418.62	$3d^6$	^5D	3	$3d^5(^4P)4p$	$^3D°$	3	R2
337.2764	0.0010	337.27634	0.00041	25	-1.558	E	1489.82	297982.60	$3d^6$	^5D	2	$3d^5(^4D)4p$	$^5P°$	1	R2
337.3152	0.0010	337.31425	0.00033	22	-1.183	E	29570.78	326030.24	$3d^6$	$^3F_2$	3	$3d^5(^2F_2)4p$	$^3F°$	3	R2
337.340	0.003	337.34205	0.00031	10	-1.891	E	29123.90	325558.93	$3d^6$	$^3F_2$	4	$3d^5(^2F_2)4p$	$^1G°$	4	d,R2
337.441	0.003	337.44103	0.00028	23	-1.633	E	27578.61	323926.69	$3d^6$	^3H	5	$3d^5(^2H)4p$	$^3H°$	4	p,R2
337.4606	0.0010	337.46069	0.00027	34	-0.992	E	27578.61	323909.42	$3d^6$	^3H	5	$3d^5(^2G_2)4p$	$^3H°$	5	R2
337.6227	0.0019	337.62282	0.00047	31	-1.230	E	1871.38	298059.89	$3d^6$	^5D	1	$3d^5(^4D)4p$	$^5D°$	0	R2
337.6965	0.0010	337.69585	0.00028	36	-1.191	E	889.61	297014.07	$3d^6$	^5D	3	$3d^5(^4D)4p$	$^5D°$	2	R2
337.726	0.003	337.72381	0.00039	24	-1.464	E	29123.90	325223.84	$3d^6$	$^3F_2$	4	$3d^5(^2G_2)4p$	$^3G°$	4	H,R2

Table A.2 (cont'd)

λ_{obs} [a] (Å)	u_{obs} [b] (Å)	λ_{Ritz} [c] (Å)	u_{Ritz} [d] (Å)	I [e]	$\log(gf_R)$ [f]	$\log(gf_R)$ [g]	E_i [h] (cm^{-1})	E_k [i] (cm^{-1})	Lower Level Configuration	Term	J	Upper Level Configuration	Term [k]	J	Notes [j]
337.743	0.003	337.73709	0.00039	33	-1.631	E	29123.90	325212.20	$3d^6$	$^3F_2$	4	$3d^5(^2G_2)4p$	$^3G°$	3	d,R2*
337.743	0.003	337.74222	0.00042	33	-1.216	E	29898.79	325982.59	$3d^6$	$^3F_2$	2	$3d^5(^2F_2)4p$	$^3F°$	2	d,R2*
337.7612	0.0010	337.76053	0.00027	35	-1.053	E	27858.94	323926.69	$3d^6$	^3H	4	$3d^5(^2H)4p$	$^3H°$	4	R2
337.8042	0.0010	337.80375	0.00037	37	-1.085	E	889.61	296919.48	$3d^6$	^5D	3	$3d^5(^4D)4p$	$^5D°$	4	R2
337.830	0.003	337.83002	0.00033	16	-1.733	E	889.61	296896.46	$3d^6$	^5D	3	$3d^5(^4G)4p$	$^3G°$	4	d,R2
337.920	0.003	337.92001	0.00033	25	-1.496	E	1489.82	297417.84	$3d^6$	^5D	2	$3d^5(^4D)4p$	$^5D°$	1	R2*
337.920	0.003	337.91912	0.00039	25	-2.229	E	1489.82	297418.62	$3d^6$	^5D	2	$3d^5(^4P)4$ p	$^3D°$	3	R2*
337.978	0.003	337.97353	0.00048	2	-2.208	E	34416.29	330297.45	$3d^6$	^3G	3	$3d^5(^2F_2)4p$	$^3G°$	4	d,R2
338.1983	0.0010	338.19834	0.00041	49	-0.832	E	889.61	296574.09	$3d^6$	^5D	3	$3d^5(^4D)4p$	$^5D°$	3	R2
338.3569	0.0010	338.35628	0.00036	23	-1.633	E	1871.38	297417.84	$3d^6$	^5D	1	$3d^5(^4D)4p$	$^5D°$	1	R2
338.3821	0.0010	338.38171	0.00031	35	-1.184	E	1489.82	297014.07	$3d^6$	^5D	2	$3d^5(^4D)4p$	$^5D°$	2	R2
338.4733	0.0010	338.47320	0.00038	55	-0.827	E	0.00	295444.37	$3d^6$	^5D	4	$3d^5(^4D)4p$	$^5F°$	5	R2
338.5693	0.0010	338.56951	0.00050	30	-1.296	E	2057.52	297417.84	$3d^6$	^5D	0	$3d^5(^4D)4p$	$^5D°$	1	R2
338.7381	0.0010	338.73790	0.00037	9	-1.728	E	27111.40	322324.90	$3d^6$	^3H	6	$3d^5(^2H)4p$	$^1I°$	6	R2
338.8193	0.0010	338.81917	0.00035	41	-1.045	E	1871.38	297014.07	$3d^6$	^5D	1	$3d^5(^4D)4p$	$^5D°$	2	R2
338.8864	0.0010	338.88624	0.00043	44	-0.966	E	1489.82	296574.09	$3d^6$	^5D	2	$3d^5(^4D)4p$	$^5D°$	3	R2
339.0521	0.0010	339.05241	0.00031	22	-1.683	E	0.00	294939.65	$3d^6$	^5D	4	$3d^5(^4D)4p$	$^5F°$	4	R2
339.213	0.003	339.20982	0.00026	4	-1.979	E	29123.90	323926.69	$3d^6$	$^3F_2$	4	$3d^5(^2H)4p$	$^3H°$	4	G,R2
339.2767	0.0010	339.27484	0.00036	4	-2.002	E	27578.61	322324.90	$3d^6$	^3H	5	$3d^5(^2H)4p$	$^1I°$	6	R2
339.6743	0.0010	339.67358	0.00036	6	-1.599	E	29123.90	323524.19	$3d^6$	$^3F_2$	4	$3d^5(^4F)4p$	$^3F°$	3	R2
339.716	0.003	339.71796	0.00047	2	-2.219	E	26152.49	320514.32	$3d^6$	$^3P_2$	2	$3d^5(^2G_2)4p$	$^3F°$	3	H,R2
339.810	0.003	339.80821	0.00042	6	-1.743	E	29570.78	323854.43	$3d^6$	$^3F_2$	3	$3d^5(^4F)4p$	$^3F°$	2	d,R2
340.0786	0.0010	340.07817	0.00029	49	-0.929	E	889.61	294939.65	$3d^6$	^5D	3	$3d^5(^4D)4p$	$^5F°$	4	R2
340.189	0.003	340.18996	0.00037	16	-1.611	E	29570.78	323524.19	$3d^6$	$^3F_2$	3	$3d^5(^4F)4p$	$^3F°$	3	R2*
340.189	0.003	340.18738	0.00046	16	-1.597	E	29898.79	323854.43	$3d^6$	$^3F_2$	2	$3d^5(^4F)4p$	$^3F°$	2	R2*
340.4868	0.0010	340.48606	0.00026	29	-1.110	E	29123.90	322821.68	$3d^6$	$^3F_2$	4	$3d^5(^4F)4p$	$^3F°$	4	R2
340.5161	0.0010	340.51672	0.00044	46	-0.784	E	27111.40	320782.74	$3d^6$	^3H	6	$3d^5(^2H)4p$	$^3I°$	7	R2
340.577	0.003	340.57610	0.00034	9	-1.548	E	33256.49	326876.62	$3d^6$	^3G	5	$3d^5(^2F_2)4p$	$^3F°$	4	d,R2
340.6533	0.0010	340.65313	0.00045	36	-1.233	E	889.61	294443.35	$3d^6$	^5D	3	$3d^5(^4D)4p$	$^5F°$	3	R2
340.742	0.003	340.74110	0.00035	14	-1.499	E	27578.61	321056.56	$3d^6$	^3H	5	$3d^5(^2G_2)4p$	$^3F°$	4	H,R2
340.897	0.003	340.89615	0.00078	3	-2.086	E	29640.25	322984.72	$3d^6$	$^3P_2$	0	$3d^5(^4F)4p$	$^3D°$	1	H,R2
341.039	0.003	341.03675	0.00050	6	-2.124	E	27858.94	321082.47	$3d^6$	^3H	4	$3d^5(^2F_1)4p$	$^1F°$	3	d,R2
341.068	0.003	341.06821	0.00031	9	-2.313	E	889.61	294086.09	$3d^6$	^5D	3	$3d^5(^4D)4p$	$^5F°$	2	R2*
341.068	0.003	341.06689	0.00036	9	-1.879	E	27858.94	321056.56	$3d^6$	^3H	4	$3d^5(^2G_2)4p$	$^3F°$	4	R2*
341.242	0.003	341.24169	0.00038	3	-2.071	E	29570.78	322618.21	$3d^6$	$^3F_2$	3	$3d^5(^4F)4p$	$^3D°$	3	H,R2
341.3511	0.0010	341.35107	0.00046	43	-1.109	E	1489.82	294443.35	$3d^6$	^5D	2	$3d^5(^4D)4p$	$^5F°$	3	R2

Table A.2 (cont'd)

λ_{obs} [a] (Å)	u_{obs} [b] (Å)	λ_{Ritz} [c] (Å)	u_{Ritz} [d] (Å)	I [e]	$\log(gf_R)$ [f]	$\log(gf_R)$ [g]	E_i [h] (cm^{-1})	E_k [i] (cm^{-1})	Lower Level Configuration	Term	J	Upper Level Configuration	Term [k]	J	Notes [j]
341.5890	0.0010	341.58913	0.00030	27	-1.197	E	27111.40	319860.76	$3d^6$	^3H	6	$3d^5(^2H)4p$	$^3I^\circ$	6	R2
341.6738	0.0010	341.67300	0.00028	18	-1.165	E	34061.99	326739.49	$3d^6$	^3G	4	$3d^5(^2G_2)4p$	$^1F^\circ$	3	R2
341.7008	0.0010	341.69883	0.00037	38	-0.975	E	27858.94	320514.32	$3d^6$	^3H	4	$3d^5(^2G_2)4p$	$^3F^\circ$	3	R2
341.7681	0.0010	341.76786	0.00032	36	-1.251	E	1489.82	294086.09	$3d^6$	^5D	2	$3d^5(^4D)4p$	$^5F^\circ$	2	R2
341.8320	0.0010	341.83156	0.00031	50	-0.634	E	27111.40	319653.14	$3d^6$	^3H	6	$3d^5(^4F)4p$	$^3G^\circ$	5	R2
341.8583	0.0010	341.85741	0.00039	32	-0.791	E	42208.47	334728.09	$3d^6$	$^1G_2$	4	$3d^5(^2F_2)4p$	$^1F^\circ$	3	R2
342.0900	0.0010	342.08988	0.00051	44	-0.781	E	27578.61	319899.45	$3d^6$	^3H	5	$3d^5(^4F)4p$	$^3G^\circ$	4	R2
342.1355	0.0010	342.13516	0.00030	35	-1.048	E	27578.61	319860.76	$3d^6$	^3H	5	$3d^5(^2H)4p$	$^3I^\circ$	6	R2
342.2146	0.0010	342.21412	0.00036	37	-1.200	E	1871.38	294086.09	$3d^6$	^5D	1	$3d^5(^4D)4p$	$^5F^\circ$	2	R2
342.355	0.003	342.35703	0.00042	10	-2.255	E	889.61	292982.34	$3d^6$	^5D	3	$3d^5(^4P)4p$	$^3P^\circ$	2	d,R2
342.379	0.003	342.37836	0.00030	22	-1.341	E	27578.61	319653.14	$3d^6$	^3H	5	$3d^5(^4F)4p$	$^3G^\circ$	5	d,R2
342.418	0.003	342.41825	0.00054	18	-1.417	E	27858.94	319899.45	$3d^6$	^3H	4	$3d^5(^4F)4p$	$^3G^\circ$	4	d,R2
342.472	0.003	342.47087	0.00091	11	-2.064	E	1871.38	293867.02	$3d^6$	^5D	1	$3d^5(^4P)4p$	$^3P^\circ$	0	d,R2
342.506	0.003	342.50299	0.00034	50	-1.430	E	34061.99	326030.24	$3d^6$	^3G	4	$3d^5(^2F_2)4p$	$^3F^\circ$	3	R2
342.506	0.004	342.5096	0.0015	50	-1.478	E	1871.38	293834.0	$3d^6$	^5D	1	$3d^5(^4D)4p$	$^5F^\circ$	1	R2
342.506	0.003	342.50405	0.00040	50	-0.679	E	33256.49	325223.84	$3d^6$	^3G	5	$3d^5(^2G_2)4p$	$^3G^\circ$	4	R2
342.5454	0.0010	342.54475	0.00034	36	-0.846	E	29123.90	321056.56	$3d^6$	$^3F_2$	4	$3d^5(^2G_2)4p$	$^3F^\circ$	4	R2
342.5923	0.0010	342.59240	0.00028	50	-0.599	E	33256.49	325148.55	$3d^6$	^3G	5	$3d^5(^2G_2)4p$	$^3H^\circ$	6	R2
342.7284	0.0019	342.7281	0.0014	34	-1.325	E	2057.52	293834.0	$3d^6$	^5D	0	$3d^5(^4D)4p$	$^5F^\circ$	1	R2
342.747	0.003	342.74637	0.00039	20	-1.740	E	27858.94	319619.87	$3d^6$	^3H	4	$3d^5(^4F)4p$	$^3G^\circ$	3	H,R2
342.7901	0.0010	342.78937	0.00026	40	-0.698	E	33256.49	324980.8	$3d^6$	^3G	5	$3d^5(^2G_2)4p$	$^3G^\circ$	5	R2
342.9105	0.0010	342.90957	0.00068	42	-0.465	E	57924.12	349546.19	$3d^6$	^1F	3	$3d^5(^2D_2)4p$	$^1D^\circ$	2	R2
342.9760	0.0010	342.97517	0.00041	42	-0.720	E	34416.29	325982.59	$3d^6$	^3G	3	$3d^5(^2F_2)4p$	$^3F^\circ$	2	R2
342.9960	0.0010	342.99558	0.00045	35	-1.386	E	1871.38	293420.33	$3d^6$	^5D	1	$3d^5(^4P)4p$	$^3P^\circ$	1	R2
343.044	0.003	343.03942	0.00049	44	-1.075	E	29570.78	321082.47	$3d^6$	$^3F_2$	3	$3d^5(^2F_1)4p$	$^1F^\circ$	3	p,R2
343.0566	0.0010	343.05402	0.00038	51	-1.222	E	27578.61	319077.89	$3d^6$	^3H	5	$3d^5(^2H)4p$	$^3I^\circ$	5	R2
343.182	0.003	343.18218	0.00037	9	-1.717	E	29123.90	320514.32	$3d^6$	$^3F_2$	4	$3d^5(^2G_2)4p$	$^3F^\circ$	3	d,R2
343.2153	0.0010	343.21470	0.00055	14	-1.837	E	2057.52	293420.33	$3d^6$	^5D	0	$3d^5(^4P)4p$	$^3P^\circ$	1	R2
343.2562	0.0010	343.25565	0.00035	18	-1.716	E	0.00	291328.05	$3d^6$	^5D	4	$3d^5(^4G)4p$	$^3F^\circ$	3	R2
343.3850	0.0010	343.38425	0.00038	34	-1.082	E	27858.94	319077.89	$3d^6$	^3H	4	$3d^5(^2H)4p$	$^3I^\circ$	5	R2
343.427	0.003	343.42584	0.00052	14	-1.623	E	29898.79	321082.47	$3d^6$	$^3F_2$	2	$3d^5(^2F_1)4p$	$^1F^\circ$	3	d,R2
343.4541	0.0010	343.45159	0.00038	46	-0.824	E	34061.99	325223.84	$3d^6$	^3G	4	$3d^5(^2G_2)4p$	$^3G^\circ$	4	R2
343.464	0.003	343.46532	0.00039	43	-0.870	E	34061.99	325212.20	$3d^6$	^3G	4	$3d^5(^2G_2)4p$	$^3G^\circ$	3	p,R2
343.5030	0.0010	343.50185	0.00036	39	-0.831	E	29898.79	321018.04	$3d^6$	$^3F_2$	2	$3d^5(^2G_2)4p$	$^3F^\circ$	2	R2
343.7108	0.0010	343.70930	0.00037	38	-0.826	E	29570.78	320514.32	$3d^6$	$^3F_2$	3	$3d^5(^2G_2)4p$	$^3F^\circ$	3	R2
343.7391	0.0010	343.73849	0.00026	31	-0.934	E	34061.99	324980.8	$3d^6$	^3G	4	$3d^5(^2G_2)4p$	$^3G^\circ$	5	R2

Table A.2 (cont'd)

λ_{obs} [a] (Å)	u_{obs} [b] (Å)	λ_{Ritz} [c] (Å)	u_{Ritz} [d] (Å)	I [e]	$\log(gf_R)$ [f]	$\log(gf_R)$ [g]	E_i [h] (cm^{-1})	E_k [i] (cm^{-1})	Lower Level Configuration	Term	J	Upper Level Configuration	Term [k]	J	Notes [j]
343.869	0.003	343.87003	0.00044	36	-1.227	E	34416.29	325223.84	$3d^6$	^3G	3	$3d^5(^2G_2)4p$	$^3G^\circ$	4	p,R2
343.8831	0.0010	343.88379	0.00042	45	-0.745	E	34416.29	325212.20	$3d^6$	^3G	3	$3d^5(^2G_2)4p$	$^3G^\circ$	3	R2
343.930	0.003	343.92934	0.00032	68	-0.284	E	0.00	290757.40	$3d^6$	^5D	4	$3d^5(^4P)4p$	$^5P^\circ$	3	s,R2
344.038	0.003	344.03252	0.00026	32	-1.584	E	33256.49	323926.69	$3d^6$	^3G	5	$3d^5(^2H)4p$	$^3H^\circ$	4	p,R2*
344.038	0.003	344.03779	0.00034	32	-2.041	E	889.61	291555.35	$3d^6$	^5D	3	$3d^5(^4G)4p$	$^3F^\circ$	4	p,R2*
344.0535	0.0010	344.05296	0.00025	37	-0.959	E	33256.49	323909.42	$3d^6$	^3G	5	$3d^5(^2G_2)4p$	$^3H^\circ$	5	R2
344.2001	0.0010	344.19943	0.00028	36	-1.024	E	29123.90	319653.14	$3d^6$	$^3F_2$	4	$3d^5(^4F)4p$	$^3G^\circ$	5	R2
344.2336	0.0010	344.23344	0.00038	59	-0.489	E	889.61	291390.15	$3d^6$	^5D	3	$3d^5(^4P)4p$	$^5P^\circ$	2	R2
344.4381	0.0010	344.43722	0.00051	25	-1.192	E	29570.78	319899.45	$3d^6$	$^3F_2$	3	$3d^5(^4F)4p$	$^3G^\circ$	4	R2
344.516	0.003	344.51718	0.00030	6	-2.583	E	0.00	290261.29	$3d^6$	^5D	4	$3d^5(^4P)4p$	$^5D^\circ$	4	H,R2
344.5711	0.0010	344.57033	0.00031	60	-0.551	E	27111.40	317327.91	$3d^6$	^3H	6	$3d^5(^2H)4p$	$^3H^\circ$	6	R2
344.676	0.003	344.67517	0.00061	6	-2.051	E	26152.49	316280.73	$3d^6$	$^3P_2$	2	$3d^5(^2F_1)4p$	$^3F^\circ$	3	d,R2
344.767	0.003	344.76603	0.00093	53	-0.888	E	1489.82	291541.60	$3d^6$	^5D	2	$3d^5(^4P)4p$	$^5P^\circ$	1	R2*
344.767	0.003	344.76706	0.00082	53	-0.865	E	41627.23	331678.14	$3d^6$	^3D	2	$3d^5(^2S)4p$	$^3P^\circ$	2	R2*
344.8102	0.0010	344.80969	0.00028	33	-1.006	E	29123.90	319138.95	$3d^6$	$^3F_2$	4	$3d^5(^2G_2)4p$	$^1G^\circ$	4	R2
344.881	0.003	344.88230	0.00038	13	-1.890	E	29123.90	319077.89	$3d^6$	$^3F_2$	4	$3d^5(^2H)4p$	$^3I^\circ$	5	d,R2
344.9465	0.0010	344.94614	0.00040	49	-0.835	E	1489.82	291390.15	$3d^6$	^5D	2	$3d^5(^4P)4p$	$^5P^\circ$	2	R2
344.986	0.003	344.98486	0.00030	50	-1.000	E	889.61	290757.40	$3d^6$	^5D	3	$3d^5(^4P)4p$	$^5P^\circ$	3	R2*
344.986	0.003	344.98854	0.00026	50	-1.486	E	34061.99	323926.69	$3d^6$	^3G	4	$3d^5(^2H)4p$	$^3H^\circ$	4	R2*
345.0106	0.0010	345.00910	0.00025	46	-0.887	E	34061.99	323909.42	$3d^6$	^3G	4	$3d^5(^2G_2)4p$	$^3H^\circ$	5	R2
345.120	0.003	345.11606	0.00080	54	-0.523	E	41920.54	331678.14	$3d^6$	^3D	3	$3d^5(^2S)4p$	$^3P^\circ$	2	R2*
345.120	0.003	345.12594	0.00030	54	-1.111	E	27578.61	317327.91	$3d^6$	^3H	5	$3d^5(^2H)4p$	$^3H^\circ$	6	R2*
345.1600	0.0010	345.15956	0.00041	28	-1.166	E	29898.79	319619.87	$3d^6$	$^3F_2$	2	$3d^5(^4F)4p$	$^3G^\circ$	3	R2
345.2195	0.0010	345.22016	0.00087	46	-0.929	E	1871.38	291541.60	$3d^6$	^5D	1	$3d^5(^4P)4p$	$^5P^\circ$	1	R2
345.2869	0.0010	345.28675	0.00036	33	-1.089	E	27111.40	316725.76	$3d^6$	^3H	6	$3d^5(^2H)4p$	$^3G^\circ$	5	R2
345.345	0.003	345.34182	0.00029	50	-1.337	E	29570.78	319138.95	$3d^6$	$^3F_2$	3	$3d^5(^2G_2)4p$	$^1G^\circ$	4	R2*
345.345	0.003	345.34538	0.00026	50	-0.686	E	33256.49	322821.68	$3d^6$	^3G	5	$3d^5(^4F)4p$	$^3F^\circ$	4	R2*
345.406	0.003	345.40075	0.00045	55	-1.268	E	1871.38	291390.15	$3d^6$	^5D	1	$3d^5(^4P)4p$	$^5P^\circ$	2	R2*
345.406	0.003	345.40312	0.00043	55	-1.144	E	27858.94	317375.72	$3d^6$	^3H	4	$3d^5(^2H)4p$	$^3G^\circ$	3	R2*
345.406	0.003	345.41073	0.00033	55	-0.895	E	34416.29	323926.69	$3d^6$	^3G	3	$3d^5(^2H)4p$	$^3H^\circ$	4	R2*
345.442	0.003	345.44214	0.00100	36	-1.259	E	2057.52	291541.60	$3d^6$	^5D	0	$3d^5(^4P)4p$	$^5P^\circ$	1	H,R2
345.4692	0.0010	345.46825	0.00036	38	-0.923	E	34061.99	323524.19	$3d^6$	^3G	4	$3d^5(^4F)4p$	$^3F^\circ$	3	R2
345.500	0.003	345.50324	0.00065	38	-1.274	E	29640.25	319073.14	$3d^6$	$^3P_2$	0	$3d^5(^2D_3)4p$	$^1P^\circ$	1	d,R2*
345.500	0.003	345.49697	0.00047	38	-1.138	E	34416.29	323854.43	$3d^6$	^3G	3	$3d^5(^4F)4p$	$^3F^\circ$	2	d,R2*
345.576	0.003	345.57447	0.00036	59	-1.528	E	27858.94	317232.17	$3d^6$	^3H	4	$3d^5(^4F)4p$	$^5D^\circ$	3	R2*
345.576	0.003	345.57632	0.00027	59	-0.860	E	889.61	290261.29	$3d^6$	^5D	3	$3d^5(^4P)4p$	$^5D^\circ$	4	R2*

Table A.2 (cont'd)

λ_{obs} [a] (Å)	u_{obs} [b] (Å)	λ_{Ritz} [c] (Å)	u_{Ritz} [d] (Å)	I [e]	$\log(gf_R)$ [f]	$\log(gf_R)$ [g]	E_i [h] (cm^{-1})	E_k [i] (cm^{-1})	Lower Level Configuration	Term	J	Upper Level Configuration	Term [k]	J	Notes [j]
345.652	0.003	345.64990	0.00031	52	-0.880	E	27578.61	316888.69	$3d^6$	^3H	5	$3d^5(^2H)4p$	$^3G°$	4	p,R2
345.662	0.003	345.66408	0.00040	51	-1.274	E	0.00	289298.21	$3d^6$	^5D	4	$3d^5(^4P)4p$	$^5D°$	3	p,R2
345.7014	0.0010	345.70068	0.00033	34	-1.294	E	1489.82	290757.40	$3d^6$	^5D	2	$3d^5(^4P)4p$	$^5P°$	3	R2
345.821	0.003	345.82371	0.00033	29	-1.514	E	27578.61	316743.28	$3d^6$	^3H	5	$3d^5(^4F)4p$	$^5D°$	4	d,R2
345.8431	0.0010	345.84467	0.00035	28	-1.254	E	27578.61	316725.76	$3d^6$	^3H	5	$3d^5(^2H)4p$	$^3G°$	5	R2
345.892	0.003	345.89162	0.00041	16	-1.534	E	34416.29	323524.19	$3d^6$	^3G	3	$3d^5(^4F)4p$	$^3F°$	3	d,R2
345.9385	0.0010	345.93887	0.00036	20	-1.439	E	33256.49	322324.90	$3d^6$	^3G	5	$3d^5(^2H)4p$	$^1I°$	6	R2
345.987	0.003	345.98515	0.00031	9	-2.006	E	27858.94	316888.69	$3d^6$	^3H	4	$3d^5(^2H)4p$	$^3G°$	4	d,R2
346.036	0.003	346.03399	0.00048	8	-2.143	E	57924.12	346913.07	$3d^6$	^1F	3	$3d^5(^2D_2)4p$	$^3P°$	2	H,R2
346.1653	0.0010	346.16621	0.00031	32	-1.169	E	27111.40	315989.97	$3d^6$	^3H	6	$3d^5(^2H)4p$	$^3H°$	5	R2
346.239	0.003	346.23621	0.00051	16	-1.488	E	28697.33	317517.50	$3d^6$	$^3P_2$	1	$3d^5(^4F)4p$	$^5D°$	2	d,R2
346.3093	0.0010	346.30872	0.00026	30	-1.168	E	34061.99	322821.68	$3d^6$	^3G	4	$3d^5(^4F)4p$	$^3F°$	4	R2
346.3273	0.0010	346.32775	0.00067	25	-1.190	E	41627.23	330371.06	$3d^6$	^3D	2	$3d^5(^2S)4p$	$^3P°$	1	R2
346.4172	0.0010	346.41624	0.00068	34	-0.712	E	41700.99	330371.06	$3d^6$	^3D	1	$3d^5(^2S)4p$	$^3P°$	1	R2
346.5528	0.0010	346.55292	0.00037	24	-1.116	E	34061.99	322618.21	$3d^6$	^3G	4	$3d^5(^4F)4p$	$^3D°$	3	R2
346.577	0.003	346.5768	0.0012	13	-0.952	E	104421.97	392958.32	$3d^6$	$^1D_1$	2	$3d^5(^2D_1)4p$	$^1F°$	3	R2
346.6325	0.0010	346.63147	0.00029	13	-1.715	E	27578.61	316069.44	$3d^6$	^3H	5	$3d^5(^2F_1)4p$	$^3G°$	4	R2
346.730	0.003	346.72955	0.00042	63	-1.697	E	26152.49	314561.71	$3d^6$	$^3P_2$	2	$3d^5(^4F)4p$	$^5F°$	3	s,R2*
346.730	0.003	346.73030	0.00037	63	-0.736	E	889.61	289298.21	$3d^6$	^5D	3	$3d^5(^4P)4p$	$^5D°$	3	s,R2*
346.730	0.003	346.72698	0.00031	63	-0.630	E	27578.61	315989.97	$3d^6$	^3H	5	$3d^5(^2H)4p$	$^3H°$	5	s,R2*
346.925	0.003	346.92642	0.00048	11	-1.698	E	41627.23	329872.79	$3d^6$	^3D	2	$3d^5(^2F_2)4p$	$^3D°$	3	d,R2
346.970	0.003	346.96862	0.00030	27	-1.315	E	27858.94	316069.44	$3d^6$	^3H	4	$3d^5(^2F_1)4p$	$^3G°$	4	d,R2
347.028	0.003	347.04247	0.00054	60	-0.747	E	41627.23	329776.40	$3d^6$	^3D	2	$3d^5(^2F_2)4p$	$^3D°$	2	l,R2*
347.028	0.003	347.02826	0.00035	60	-0.822	E	0.00	288160.97	$3d^6$	^5D	4	$3d^5(^4G)4p$	$^5F°$	4	l,R2*
347.0641	0.0010	347.06432	0.00031	40	-1.046	E	27858.94	315989.97	$3d^6$	^3H	4	$3d^5(^2H)4p$	$^3H°$	5	R2
347.134	0.003	347.13133	0.00057	26	-1.373	E	41700.99	329776.40	$3d^6$	^3D	1	$3d^5(^2F_2)4p$	$^3D°$	2	p,R2
347.156	0.003	347.15319	0.00034	41	-1.044	E	27111.40	315168.67	$3d^6$	^3H	6	$3d^5(^4F)4p$	$^5F°$	5	d,R2
347.200	0.004	347.20673	0.00068	19	-1.614	E	57924.12	345936.97	$3d^6$	^1F	3	$3d^5(^2D_2)4p$	$^1F°$	3	G,R2*
347.200	0.003	347.19776	0.00052	19	-1.690	E	34416.29	322436.58	$3d^6$	^3G	3	$3d^5(^4F)4p$	$^3D°$	2	G,R2*
347.236	0.003	347.23741	0.00040	24	-1.513	E	41627.23	329614.63	$3d^6$	^3D	2	$3d^5(^2F_2)4p$	$^3G°$	3	d,R2*
347.236	0.004	347.2314	0.0012	24	-1.230	E	104421.97	392414.38	$3d^6$	$^1D_1$	2	$3d^5(^2D_1)4p$	$^3P°$	2	d,R2*
347.236	0.004	347.23658	0.00031	24	-3.301	E	889.61	288877.70	$3d^6$	^5D	3	$3d^5(^4P)4p$	$^5S°$	2	d,R2*
347.275	0.003	347.27120	0.00033	62	-1.111	E	0.00	287959.38	$3d^6$	^5D	4	$3d^5(^4G)4p$	$^5F°$	3	R2*
347.275	0.003	347.27980	0.00043	62	-0.635	E	41920.54	329872.79	$3d^6$	^3D	3	$3d^5(^2F_2)4p$	$^3D°$	3	R2*
347.335	0.003	347.3346	0.0013	78	-0.079	E	0.00	287906.8	$3d^6$	^5D	4	$3d^5(^4G)4p$	$^5F°$	5	s,R2*
347.335	0.004	347.3219	0.0033	78	-1.031	E	41700.99	329618.3	$3d^6$	^3D	1	$3d^5(^2S)4p$	$^3P°$	0	s,R2*

Table A.2 (cont'd)

λ_{obs} [a] (Å)	u_{obs} [b] (Å)	λ_{Ritz} [c] (Å)	u_{Ritz} [d] (Å)	I [e]	$\log(gf_R)$ [f]	$\log(gf_R)$ [g]	E_i [h] (cm^{-1})	E_k [i] (cm^{-1})	Lower Level Configuration	Term	J	Upper Level Configuration	Term [k]	J	Notes [j]
347.3970	0.0010	347.39609	0.00048	41	-0.842	E	41920.54	329776.40	$3d^6$	^3D	3	$3d^5(^2F_2)4p$	$^3D^\circ$	2	R2
347.4215	0.0010	347.42077	0.00088	49	-0.690	E	41627.23	329462.64	$3d^6$	^3D	2	$3d^5(^2F_2)4p$	$^3D^\circ$	1	R2
347.456	0.003	347.46343	0.00035	70	-0.688	E	33256.49	321056.56	$3d^6$	^3G	5	$3d^5(^2G_2)4p$	$^3F^\circ$	4	R2*
347.456	0.003	347.45339	0.00040	70	-0.712	E	1489.82	289298.21	$3d^6$	^5D	2	$3d^5(^4P)4p$	$^5D^\circ$	3	R2*
347.505	0.003	347.50224	0.00058	63	-0.658	E	26152.49	313920.42	$3d^6$	$^3P_2$	2	$3d^5(^2D_3)4p$	$^3D^\circ$	3	p,R2
347.515	0.003	347.51581	0.00051	61	-0.835	E	1489.82	289246.51	$3d^6$	^5D	2	$3d^5(^4G)4p$	$^5F^\circ$	2	p,R2
347.5921	0.0010	347.59143	0.00032	45	-0.642	E	41920.54	329614.63	$3d^6$	^3D	3	$3d^5(^2F_2)4p$	$^3G^\circ$	3	R2
347.702	0.003	347.70290	0.00035	64	-0.480	E	29123.90	316725.76	$3d^6$	$^3F_2$	4	$3d^5(^2H)4p$	$^3G^\circ$	5	s,R2
347.716	0.003	347.71649	0.00050	67	-0.853	E	27111.40	314702.02	$3d^6$	^3H	6	$3d^5(^2F_1)4p$	$^3G^\circ$	5	p,R2
347.788	0.003	347.79450	0.00050	46	-1.473	E	26152.49	313678.60	$3d^6$	$^3P_2$	2	$3d^5(^2D_3)4p$	$^3D^\circ$	1	p,R2*
347.788	0.003	347.78447	0.00061	46	-1.190	E	26152.49	313686.89	$3d^6$	$^3P_2$	2	$3d^5(^2D_3)4p$	$^3D^\circ$	2	p,R2*
347.8114	0.0010	347.81210	0.00031	63	-0.514	E	27858.94	315370.50	$3d^6$	^3H	4	$3d^5(^2G_2)4p$	$^3H^\circ$	4	R2
347.865	0.003	347.86533	0.00050	53	-0.759	E	28697.33	316164.90	$3d^6$	$^3P_2$	1	$3d^5(^2F_1)4p$	$^3F^\circ$	2	s,R2*
347.865	0.003	347.85400	0.00046	53	-1.225	E	29898.79	317375.72	$3d^6$	$^3F_2$	2	$3d^5(^2H)4p$	$^3G^\circ$	3	s,R2*
347.977	0.003	347.97722	0.00056	61	-0.846	E	1871.38	289246.51	$3d^6$	^5D	1	$3d^5(^4G)4p$	$^5F^\circ$	2	s,R2
348.047	0.003	348.04652	0.00030	61	-0.792	E	29570.78	316888.69	$3d^6$	$^3F_2$	3	$3d^5(^2H)4p$	$^3G^\circ$	4	s,R2*
348.047	0.003	348.04748	0.00047	61	-0.604	E	68719.26	356036.38	$3d^6$	$^3F_1$	4	$3d^5(^2G_1)4p$	$^3G^\circ$	5	s,R2*
348.080	0.003	348.07810	0.00050	63	-0.982	E	1871.38	289163.23	$3d^6$	^5D	1	$3d^5(^4G)4p$	$^5F^\circ$	1	p,R2
348.1023	0.0010	348.10292	0.00033	71	-0.346	E	889.61	288160.97	$3d^6$	^5D	3	$3d^5(^4G)4p$	$^5F^\circ$	4	R2
348.226	0.003	348.22276	0.00031	22	-1.790	E	29570.78	316743.28	$3d^6$	$^3F_2$	3	$3d^5(^4F)4p$	$^5D^\circ$	4	H,R2
348.245	0.003	348.24176	0.00055	23	-1.648	E	29123.90	316280.73	$3d^6$	$^3F_2$	4	$3d^5(^2F_1)4p$	$^3F^\circ$	3	H,R2
348.2777	0.0010	348.27704	0.00037	62	-0.986	E	0.00	287127.74	$3d^6$	^5D	4	$3d^5(^4G)4p$	$^5H^\circ$	5	R2
348.303	0.003	348.30377	0.00062	53	-1.051	E	2057.52	289163.23	$3d^6$	^5D	0	$3d^5(^4G)4p$	$^5F^\circ$	1	p,R2
348.3469	0.0010	348.34737	0.00030	42	-1.319	E	889.61	287959.38	$3d^6$	^5D	3	$3d^5(^4G)4p$	$^5F^\circ$	3	R2
348.3750	0.0010	348.37537	0.00041	31	-0.859	E	68719.26	355765.96	$3d^6$	$^3F_1$	4	$3d^5(^2G_1)4p$	$^3G^\circ$	4	R2
348.409	0.003	348.40708	0.00031	41	-1.368	E	27578.61	314599.18	$3d^6$	^3H	5	$3d^5(^4F)4p$	$^5F^\circ$	4	R2*
348.409	0.003	348.40719	0.00050	41	-1.437	E	34061.99	321082.47	$3d^6$	^3G	4	$3d^5(^2F_1)4p$	$^1F^\circ$	3	R2*
348.421	0.004	348.42438	0.00039	37	-1.821	E	1871.38	288877.70	$3d^6$	^5D	1	$3d^5(^4P)4p$	$^5S^\circ$	2	p,R2
348.4982	0.0010	348.49819	0.00027	45	-0.874	E	29123.90	316069.44	$3d^6$	$^3F_2$	4	$3d^5(^2F_1)4p$	$^3G^\circ$	4	R2
348.5412	0.0010	348.54027	0.00040	33	-0.854	E	68855.07	355765.96	$3d^6$	$^3F_1$	3	$3d^5(^2G_1)4p$	$^3G^\circ$	4	R2
348.5633	0.0010	348.56330	0.00040	40	-1.389	E	889.61	287781.55	$3d^6$	^5D	3	$3d^5(^4P)4p$	$^5D^\circ$	2	R2
348.594	0.003	348.59473	0.00030	14	-1.714	E	29123.90	315989.97	$3d^6$	$^3F_2$	4	$3d^5(^2H)4p$	$^3H^\circ$	5	d,R2
348.623	0.003	348.62267	0.00050	5	-2.066	E	27858.94	314702.02	$3d^6$	^3H	4	$3d^5(^2F_1)4p$	$^3G^\circ$	5	H,R2
348.6739	0.0010	348.67389	0.00042	50	-0.468	E	26152.49	312953.43	$3d^6$	$^3P_2$	2	$3d^5(^2F_1)4p$	$^3D^\circ$	3	R2
348.716	0.003	348.71527	0.00049	7	-1.409	E	68632.25	355399.16	$3d^6$	$^3F_1$	2	$3d^5(^2G_1)4p$	$^3G^\circ$	3	d,R2
348.7524	0.0019	348.75197	0.00041	28	-1.246	E	26152.49	312889.22	$3d^6$	$^3P_2$	2	$3d^5(^4F)4p$	$^5G^\circ$	3	R2

Table A.2 (cont'd)

λ_{obs} [a] (Å)	u_{obs} [b] (Å)	λ_{Ritz} [c] (Å)	u_{Ritz} [d] (Å)	I [e]	$\log(gf_R)$ [f]	$\log(gf_R)$ [g]	E_i [h] (cm^{-1})	E_k [i] (cm^{-1})	Lower Level Configuration	Term	J	Upper Level Configuration	Term [k]	J	Notes [j]
348.786	0.004	348.78455	0.00055	32	-1.079	E	29570.78	316280.73	$3d^6$	$^3F_2$	3	$3d^5(^2F_1)4p$	$^3F°$	3	R2*
348.786	0.003	348.7887	0.0030	32	-2.336	E	0.00	286706.5	$3d^6$	^5D	4	$3d^5(^4G)4p$	$^5H°$	4	R2*
348.8362	0.0010	348.83621	0.00075	41	-0.675	E	28697.33	315364.82	$3d^6$	$^3P_2$	1	$3d^5(^2F_1)4p$	$^3D°$	2	R2
348.883	0.003	348.88250	0.00030	31	-1.181	E	27578.61	314208.06	$3d^6$	^3H	5	$3d^5(^2F_1)4p$	$^3F°$	4	R2
348.883	0.004	348.88685	0.00053	31	-3.569	E	26152.49	312778.37	$3d^6$	$^3P_2$	2	$3d^5(^4F)4p$	$^5G°$	2	R2
348.915	0.003	348.91622	0.00037	41	-0.900	E	34416.29	321018.04	$3d^6$	^3G	3	$3d^5(^2G_2)4p$	$^3F°$	2	R2*
348.915	0.003	348.91335	0.00062	41	-1.372	E	28697.33	315301.44	$3d^6$	$^3P_2$	1	$3d^5(^2F_1)4p$	$^3D°$	1	R2*
348.9868	0.0010	348.98643	0.00039	32	-0.546	E	68855.07	355399.16	$3d^6$	$^3F_1$	3	$3d^5(^2G_1)4p$	$^3G°$	3	R2
349.0191	0.0010	349.01986	0.00051	38	-0.444	E	68632.25	355148.90	$3d^6$	$^3F_1$	2	$3d^5(^2G_1)4p$	$^3F°$	2	R2
349.0426	0.0010	349.04177	0.00027	34	-1.101	E	29570.78	316069.44	$3d^6$	$^3F_2$	3	$3d^5(^2F_1)4p$	$^3G°$	4	R2
349.0764	0.0010	349.07723	0.00033	55	-0.889	E	1489.82	287959.38	$3d^6$	^5D	2	$3d^5(^4G)4p$	$^5F°$	3	R2
349.096	0.003	349.09823	0.00038	39	-0.992	E	34061.99	320514.32	$3d^6$	^3G	4	$3d^5(^2G_2)4p$	$^3F°$	3	p,R2
349.1843	0.0010	349.18403	0.00055	16	-1.333	E	29898.79	316280.73	$3d^6$	$^3F_2$	2	$3d^5(^2F_1)4p$	$^3F°$	3	R2
349.220	0.003	349.21821	0.00039	6	-1.948	E	27111.40	313465.31	$3d^6$	^3H	6	$3d^5(^4F)4p$	$^5G°$	5	R2*
349.220	0.003	349.22405	0.00031	6	-2.541	E	27858.94	314208.06	$3d^6$	^3H	4	$3d^5(^2F_1)4p$	$^3F°$	4	R2*
349.293	0.003	349.29406	0.00044	18	-1.914	E	1489.82	287781.55	$3d^6$	^5D	2	$3d^5(^4P)4p$	$^5D°$	2	d,R2*
349.293	0.003	349.29150	0.00045	18	-1.328	E	68855.07	355148.90	$3d^6$	$^3F_1$	3	$3d^5(^2G_1)4p$	$^3F°$	2	d,R2*
349.326	0.004	349.32537	0.00055	36	-1.902	E	1489.82	287755.89	$3d^6$	^5D	2	$3d^5(^4P)4p$	$^5D°$	1	R2*
349.326	0.003	349.32532	0.00043	36	-1.210	E	29898.79	316164.90	$3d^6$	$^3F_2$	2	$3d^5(^2F_1)4p$	$^3F°$	2	R2*
349.339	0.003	349.3407	0.0013	33	-0.590	E	104421.97	390675.47	$3d^6$	$^1D_1$	2	$3d^5(^2D_1)4p$	$^1D°$	2	p,R2
349.403	0.003	349.40411	0.00044	12	-1.504	E	29123.90	315325.46	$3d^6$	$^3F_2$	4	$3d^5(^2D_3)4p$	$^1F°$	3	d,R2
349.485	0.003	349.48169	0.00059	21	-1.474	E	26152.49	312290.51	$3d^6$	$^3P_2$	2	$3d^5(^2D_3)4p$	$^3P°$	1	d,R2*
349.485	0.003	349.48362	0.00054	21	-2.409	E	28697.33	314833.77	$3d^6$	$^3P_2$	1	$3d^5(^4F)4p$	$^5F°$	2	d,R2*
349.500	0.003	349.50252	0.00049	23	-1.474	E	48607.12	334728.09	$3d^6$	$^1D_2$	2	$3d^5(^2F_2)4p$	$^1F°$	3	p,R2
349.5223	0.0010	349.52237	0.00041	24	-1.154	E	41252.65	327357.37	$3d^6$	^1I	6	$3d^5(^2H)4p$	$^1H°$	5	R2
349.576	0.003	349.57520	0.00053	4	-1.833	E	27858.94	313920.42	$3d^6$	^3H	4	$3d^5(^2D_3)4p$	$^3D°$	3	d,R2
349.7593	0.0010	349.76021	0.00045	31	-1.516	E	1871.38	287781.55	$3d^6$	^5D	1	$3d^5(^4P)4p$	$^5D°$	2	R2
349.794	0.003	349.79411	0.00029	49	-1.143	E	33256.49	319138.95	$3d^6$	^3G	5	$3d^5(^2G_2)4p$	$^1G°$	4	p,R2*
349.794	0.003	349.78892	0.00038	49	-1.461	E	27578.61	313465.31	$3d^6$	^3H	5	$3d^5(^4F)4p$	$^5G°$	5	p,R2*
349.794	0.004	349.79160	0.00058	49	-2.636	E	1871.38	287755.89	$3d^6$	^5D	1	$3d^5(^4P)4p$	$^5D°$	1	p,R2*
349.8089	0.0010	349.80890	0.00100	49	-0.408	E	48607.12	334477.49	$3d^6$	$^1D_2$	2	$3d^5(^2S)4p$	$^1P°$	1	R2
349.879	0.003	349.87853	0.00055	57	-0.529	E	26152.49	311965.97	$3d^6$	$^3P_2$	2	$3d^5(^2D_3)4p$	$^3P°$	2	R2
349.879	0.004	349.8744	0.0030	57	-1.814	E	889.61	286706.5	$3d^6$	^5D	3	$3d^5(^4G)4p$	$^5H°$	4	R2
349.900	0.003	349.89537	0.00030	27	-1.256	E	29570.78	315370.50	$3d^6$	$^3F_2$	3	$3d^5(^2G_2)4p$	$^3H°$	4	R2*
349.900	0.003	349.90233	0.00079	27	-2.472	E	29570.78	315364.82	$3d^6$	$^3F_2$	3	$3d^5(^2F_1)4p$	$^3D°$	2	R2*
349.9504	0.0010	349.95052	0.00043	19	-1.346	E	29570.78	315325.46	$3d^6$	$^3F_2$	3	$3d^5(^2D_3)4p$	$^1F°$	3	R2

Table A.2 (cont'd)

λ_{obs} [a] (Å)	u_{obs} [b] (Å)	λ_{Ritz} [c] (Å)	u_{Ritz} [d] (Å)	I [e]	$\log(gf_R)$ [f]	$\log(gf_R)$ [g]	E_i [h] (cm^{-1})	E_k [i] (cm^{-1})	Lower Level Configuration	Term	J	Upper Level Configuration	Term [k]	J	Notes [j]
350.019	0.004	350.01950	0.00068	24	-2.282	E	2057.52	287755.89	$3d^6$	^5D	0	$3d^5(^4P)4p$	$^5D^\circ$	1	d,R2
350.0653	0.0010	350.06505	0.00064	31	-0.880	E	29640.25	315301.44	$3d^6$	$^3P_2$	0	$3d^5(^2F_1)4p$	$^3D^\circ$	1	R2
350.133	0.003	350.13225	0.00038	8	-1.980	E	27858.94	313465.31	$3d^6$	^3H	4	$3d^5(^4F)4p$	$^5G^\circ$	5	d,R2
350.1664	0.0010	350.16688	0.00047	29	-1.102	E	29123.90	314702.02	$3d^6$	$^3F_2$	4	$3d^5(^2F_1)4p$	$^3G^\circ$	5	R2
350.1907	0.0010	350.19170	0.00038	16	-1.436	E	34061.99	319619.87	$3d^6$	^3G	4	$3d^5(^4F)4p$	$^3G^\circ$	3	R2
350.249	0.003	350.24854	0.00064	26	-1.629	E	29640.25	315151.79	$3d^6$	$^3P_2$	0	$3d^5(^4F)4p$	$^5F^\circ$	1	d,R2*
350.249	0.003	350.24993	0.00035	26	-1.221	E	34416.29	319926.70	$3d^6$	^3G	3	$3d^5(^2F_1)4p$	$^1D^\circ$	2	d,R2*
350.302	0.003	350.30438	0.00081	47	-0.799	E	29898.79	315364.82	$3d^6$	$^3F_2$	2	$3d^5(^2F_1)4p$	$^3D^\circ$	2	s,R2*
350.302	0.003	350.29303	0.00029	47	-1.158	E	29123.90	314599.18	$3d^6$	$^3F_2$	4	$3d^5(^4F)4p$	$^5F^\circ$	4	s,R2*
350.352	0.003	350.35268	0.00048	35	-1.059	E	29898.79	315325.46	$3d^6$	$^3F_2$	2	$3d^5(^2D_3)4p$	$^1F^\circ$	3	d,R2*
350.352	0.004	350.35858	0.00033	35	-1.834	E	27858.94	313280.81	$3d^6$	^3H	4	$3d^5(^4F)4p$	$^5G^\circ$	4	d,R2*
350.439	0.003	350.43644	0.00048	2	-1.824	E	57924.12	343282.57	$3d^6$	^1F	3	$3d^5(^2D_2)4p$	$^3F^\circ$	3	H,R2
350.4928	0.0010	350.49284	0.00056	22	-0.757	E	68632.25	353944.78	$3d^6$	$^3F_1$	2	$3d^5(^2G_1)4p$	$^3F^\circ$	3	R2
350.566	0.003	350.56599	0.00046	39	-1.481	E	29898.79	315151.79	$3d^6$	$^3F_2$	2	$3d^5(^4F)4p$	$^5F^\circ$	1	p,R2
350.600	0.003	350.59976	0.00054	21	-1.541	E	68719.26	353944.78	$3d^6$	$^3F_1$	4	$3d^5(^2G_1)4p$	$^3F^\circ$	3	d,R2
350.626	0.003	350.62673	0.00044	15	-1.507	E	34416.29	319619.87	$3d^6$	^3G	3	$3d^5(^4F)4p$	$^3G^\circ$	3	d,R2*
350.626	0.003	350.62896	0.00044	15	-1.916	E	41920.54	327122.31	$3d^6$	^3D	3	$3d^5(^2F_2)4p$	$^1D^\circ$	2	d,R2*
350.6941	0.0010	350.69397	0.00031	46	-0.627	E	42208.47	327357.37	$3d^6$	$^1G_2$	4	$3d^5(^2H)4p$	$^1H^\circ$	5	R2
350.773	0.003	350.78247	0.00028	69	-1.028	E	34061.99	319138.95	$3d^6$	^3G	4	$3d^5(^2G_2)4p$	$^1G^\circ$	4	R2*
350.773	0.003	350.77167	0.00041	69	0.261	E	41252.65	326338.39	$3d^6$	^1I	6	$3d^5(^2G_2)4p$	$^1H^\circ$	5	R2*
350.773	0.003	350.77361	0.00028	69	-0.979	E	29123.90	314208.06	$3d^6$	$^3F_2$	4	$3d^5(^2F_1)4p$	$^3F^\circ$	4	R2*
350.8406	0.0019	350.83992	0.00032	31	-1.609	E	27858.94	312889.22	$3d^6$	^3H	4	$3d^5(^4F)4p$	$^5G^\circ$	3	R2
350.900	0.003	350.90025	0.00051	32	-1.014	E	28697.33	313678.60	$3d^6$	$^3P_2$	1	$3d^5(^2D_3)4p$	$^3D^\circ$	1	s,R2*
350.900	0.003	350.89005	0.00062	32	-1.600	E	28697.33	313686.89	$3d^6$	$^3P_2$	1	$3d^5(^2D_3)4p$	$^3D^\circ$	2	s,R2*
350.9312	0.0010	350.93127	0.00036	22	-1.104	E	41920.54	326876.62	$3d^6$	^3D	3	$3d^5(^2F_2)4p$	$^3F^\circ$	4	R2
351.0256	0.0010	351.02502	0.00059	27	-1.134	E	28697.33	313577.31	$3d^6$	$^3P_2$	1	$3d^5(^2D_3)4p$	$^3P^\circ$	0	R2
351.085	0.003	351.08618	0.00040	22	-1.272	E	68719.26	353549.6	$3d^6$	$^3F_1$	4	$3d^5(^2G_1)4p$	$^3H^\circ$	5	d,R2
351.128	0.003	351.12789	0.00052	35	-1.063	E	29123.90	313920.42	$3d^6$	$^3F_2$	4	$3d^5(^2D_3)4p$	$^3D^\circ$	3	R2*
351.128	0.004	351.11770	0.00050	35	-2.656	E	1489.82	286294.60	$3d^6$	^5D	2	$3d^5(^4G)4p$	$^5H^\circ$	3	R2*
351.2862	0.0010	351.28623	0.00036	32	-0.811	E	42208.47	326876.62	$3d^6$	$^1G_2$	4	$3d^5(^2F_2)4p$	$^3F^\circ$	4	R2
351.3350	0.0010	351.33570	0.00041	43	-0.345	E	68719.26	353347.32	$3d^6$	$^3F_1$	4	$3d^5(^2G_1)4p$	$^3F^\circ$	4	R2
351.3647	0.0010	351.36439	0.00041	40	-1.010	E	27858.94	312463.76	$3d^6$	^3H	4	$3d^5(^2F_1)4p$	$^3G^\circ$	3	R2
351.4554	0.0010	351.45553	0.00031	45	-0.358	E	42208.47	326739.49	$3d^6$	$^1G_2$	4	$3d^5(^2G_2)4p$	$^1F^\circ$	3	R2
351.503	0.003	351.50342	0.00041	6	-1.351	E	68855.07	353347.32	$3d^6$	$^3F_1$	3	$3d^5(^2G_1)4p$	$^3F^\circ$	4	d,R2
351.581	0.003	351.58113	0.00037	6	-2.199	E	27578.61	312007.98	$3d^6$	^3H	5	$3d^5(^2F_1)4p$	$^1G^\circ$	4	G,R2
351.613	0.003	351.61372	0.00045	30	-1.274	E	41627.23	326030.24	$3d^6$	^3D	2	$3d^5(^2F_2)4p$	$^3F^\circ$	3	R2*

Table A.2 (cont'd)

λ_{obs} [a] (Å)	u_{obs} [b] (Å)	λ_{Ritz} [c] (Å)	u_{Ritz} [d] (Å)	I [e]	log(gf_R) [f]	log(gf_R) [g]	E_i [h] (cm^{-1})	E_k [i] (cm^{-1})	Lower Level Configuration	Term	J	Upper Level Configuration	Term [k]	J	Notes [j]
351.613	0.004	351.61415	0.00079	30	-1.782	E	0.00	284402.66	$3d^6$	^5D	4	$3d^5(^4G)4p$	$^5G°$	5	R2*
351.6769	0.0010	351.67971	0.00050	33	-2.073	E	29570.78	313920.42	$3d^6$	$^3F_2$	3	$3d^5(^2D_3)4p$	$^3D°$	3	R2
351.691	0.003	351.68989	0.00036	20	-1.882	E	29123.90	313465.31	$3d^6$	$^3F_2$	4	$3d^5(^4F)4p$	$^5G°$	5	p,R2
351.729	0.004	351.73149	0.00045	4	-2.629	E	0.00	284307.78	$3d^6$	^5D	4	$3d^5(^4G)4p$	$^5G°$	4	d,R2
351.762	0.003	351.76388	0.00051	12	-1.702	E	41700.99	325982.59	$3d^6$	^3D	1	$3d^5(^2F_2)4p$	$^3F°$	2	H,R2
351.8438	0.0010	351.84495	0.00039	20	-1.042	E	68855.07	353071.17	$3d^6$	$^3F_1$	3	$3d^5(^2G_1)4p$	$^3H°$	4	R2
351.9264	0.0010	351.92799	0.00036	27	-1.498	E	27858.94	312007.98	$3d^6$	^3H	4	$3d^5(^2F_1)4p$	$^1G°$	4	R2
351.9692	0.0010	351.96878	0.00053	50	-0.433	E	29570.78	313686.89	$3d^6$	$^3F_2$	3	$3d^5(^2D_3)4p$	$^3D°$	2	R2
352.2408	0.0010	352.24179	0.00041	13	-1.411	E	41252.65	325148.55	$3d^6$	^1I	6	$3d^5(^2G_2)4p$	$^3H°$	6	R2
352.3238	0.0010	352.32416	0.00030	53	-0.360	E	29123.90	312953.43	$3d^6$	$^3F_2$	4	$3d^5(^2F_1)4p$	$^3D°$	3	R2
352.3859	0.0010	352.38589	0.00043	38	-0.782	E	29898.79	313678.60	$3d^6$	$^3F_2$	2	$3d^5(^2D_3)4p$	$^3D°$	1	R2
352.451	0.003	352.45002	0.00040	6	-2.130	E	41252.65	324980.8	$3d^6$	^1I	6	$3d^5(^2G_2)4p$	$^3G°$	5	G,R2
352.561	0.003	352.56158	0.00036	14	-1.323	E	41920.54	325558.93	$3d^6$	^3D	3	$3d^5(^2F_2)4p$	$^1G°$	4	s,R2
352.6175	0.0010	352.61779	0.00056	21	-1.254	E	28697.33	312290.51	$3d^6$	$^3P_2$	1	$3d^5(^2D_3)4p$	$^3P°$	1	R2
352.7694	0.0010	352.77192	0.00035	57	-0.217	E	33256.49	316725.76	$3d^6$	^3G	5	$3d^5(^2H)4p$	$^3G°$	5	R2
352.8339	0.0019	352.83553	0.00043	21	-2.029	E	889.61	284307.78	$3d^6$	^5D	3	$3d^5(^4G)4p$	$^5G°$	4	R2
352.8788	0.0010	352.87975	0.00030	7	-1.657	E	29570.78	312953.43	$3d^6$	$^3F_2$	3	$3d^5(^2F_1)4p$	$^3D°$	3	R2
352.9192	0.0010	352.91984	0.00034	40	-0.654	E	42208.47	325558.93	$3d^6$	$^1G_2$	4	$3d^5(^2F_2)4p$	$^1G°$	4	R2
352.959	0.004	352.95973	0.00029	12	-2.028	E	29570.78	312889.22	$3d^6$	$^3F_2$	3	$3d^5(^4F)4p$	$^5G°$	3	d,R2
353.0991	0.0019	353.09788	0.00046	26	-1.472	E	29570.78	312778.37	$3d^6$	$^3F_2$	3	$3d^5(^4F)4p$	$^5G°$	2	R2
353.368	0.004	353.36884	0.00036	16	-1.862	E	29898.79	312889.22	$3d^6$	$^3F_2$	2	$3d^5(^4F)4p$	$^5G°$	3	d,R2
353.4067	0.0010	353.40755	0.00044	41	-0.650	E	34416.29	317375.72	$3d^6$	^3G	3	$3d^5(^2H)4p$	$^3G°$	3	R2
353.4915	0.0010	353.49057	0.00040	33	-1.343	E	29570.78	312463.76	$3d^6$	$^3F_2$	3	$3d^5(^2F_1)4p$	$^3G°$	3	R2
353.507	0.004	353.50731	0.00050	20	-2.167	E	29898.79	312778.37	$3d^6$	$^3F_2$	2	$3d^5(^4F)4p$	$^5G°$	2	p,R2
353.573	0.003	353.57341	0.00030	62	-0.350	E	34061.99	316888.69	$3d^6$	^3G	4	$3d^5(^2H)4p$	$^3G°$	4	p,R2
353.588	0.003	353.58693	0.00040	69	-0.869	E	34416.29	317232.17	$3d^6$	^3G	3	$3d^5(^4F)4p$	$^5D°$	3	p,R2*
353.588	0.003	353.59060	0.00028	69	-0.907	E	33256.49	316069.44	$3d^6$	^3G	5	$3d^5(^2F_1)4p$	$^3G°$	4	p,R2*
353.6193	0.0010	353.62066	0.00047	28	-1.626	E	26152.49	308941.40	$3d^6$	$^3P_2$	2	$3d^5(^2D_3)4p$	$^1D°$	2	R2
353.6549	0.0019	353.6550	0.0019	17	-2.391	E	1489.82	284251.3	$3d^6$	^5D	2	$3d^5(^4G)4p$	$^5G°$	3	R2
353.6886	0.0010	353.68998	0.00029	23	-1.233	E	33256.49	315989.97	$3d^6$	^3G	5	$3d^5(^2H)4p$	$^3H°$	5	R2
353.7544	0.0010	353.75528	0.00031	17	-1.385	E	34061.99	316743.28	$3d^6$	^3G	4	$3d^5(^4F)4p$	$^5D°$	4	R2
353.788	0.003	353.78597	0.00040	41	-1.149	E	41252.65	323909.42	$3d^6$	^1I	6	$3d^5(^2G_2)4p$	$^3H°$	5	R2*
353.788	0.003	353.79412	0.00072	41	-1.477	E	29640.25	312290.51	$3d^6$	$^3P_2$	0	$3d^5(^2D_3)4p$	$^3P°$	1	R2*
353.8147	0.0010	353.81560	0.00033	16	-1.785	E	27578.61	310211.71	$3d^6$	^3H	5	$3d^5(^2D_3)4p$	$^3F°$	4	R2
353.901	0.003	353.90091	0.00046	3	-1.962	E	29898.79	312463.76	$3d^6$	$^3F_2$	2	$3d^5(^2F_1)4p$	$^3G°$	3	H,R2
354.013	0.003	354.01689	0.00037	2	-2.290	E	34416.29	316888.69	$3d^6$	^3G	3	$3d^5(^2H)4p$	$^3G°$	4	G,R2

Table A.2 (cont'd)

λ_{obs} [a] (Å)	u_{obs} [b] (Å)	λ_{Ritz} [c] (Å)	u_{Ritz} [d] (Å)	I [e]	$\log(gf_R)$ [f]	$\log(gf_R)$ [g]	E_i [h] (cm^{-1})	E_k [i] (cm^{-1})	Lower Level Configuration	Term	J	Upper Level Configuration	Term [k]	J	Notes [j]
354.061	0.003	354.06101	0.00038	22	-1.483	E	29570.78	312007.98	$3d^6$	$^3F_2$	3	$3d^5(^2F_1)4p$	$^1G°$	4	d,R2
354.1182	0.0010	354.11803	0.00053	44	-0.970	E	29898.79	312290.51	$3d^6$	$^3F_2$	2	$3d^5(^2D_3)4p$	$^3P°$	1	R2
354.1399	0.0010	354.14049	0.00037	40	-1.086	E	27578.61	309952.42	$3d^6$	^3H	5	$3d^5(^2I)4p$	$^3H°$	4	R2
354.181	0.003	354.18136	0.00040	72	-0.139	E	27578.61	309919.84	$3d^6$	^3H	5	$3d^5(^2I)4p$	$^3H°$	5	s,R2*
354.181	0.004	354.1774	0.0032	72	-2.943	E	1871.38	284215.8	$3d^6$	^5D	1	$3d^5(^4G)4p$	$^5G°$	2	s,R2*
354.3349	0.0010	354.33508	0.00055	41	-0.968	E	34061.99	316280.73	$3d^6$	^3G	4	$3d^5(^2F_1)4p$	$^3F°$	3	R2
354.418	0.003	354.41827	0.00042	76	0.030	E	27111.40	309263.90	$3d^6$	^3H	6	$3d^5(^2I)4p$	$^3H°$	6	s,R2*
354.418	0.003	354.40782	0.00070	76	-0.152	E	77900.04	360060.86	$3d^6$	$^1G_1$	4	$3d^5(^2G_1)4p$	$^1F°$	3	s,R2*
354.4671	0.0010	354.46662	0.00029	36	-1.348	E	33256.49	315370.50	$3d^6$	^3G	5	$3d^5(^2G_2)4p$	$^3H°$	4	R2
354.4925	0.0010	354.49242	0.00036	68	-0.335	E	27858.94	309952.42	$3d^6$	^3H	4	$3d^5(^2I)4p$	$^3H°$	4	R2
354.533	0.003	354.53336	0.00039	18	-1.542	E	27858.94	309919.84	$3d^6$	^3H	4	$3d^5(^2I)4p$	$^3H°$	5	d,R2
354.7206	0.0010	354.72040	0.00032	37	-1.228	E	33256.49	315168.67	$3d^6$	^3G	5	$3d^5(^4F)4p$	$^5F°$	5	R2
354.780	0.003	354.78048	0.00060	29	-1.201	E	34416.29	316280.73	$3d^6$	^3G	3	$3d^5(^2F_1)4p$	$^3F°$	3	l,R2
354.9251	0.0010	354.92633	0.00042	25	-1.232	E	34416.29	316164.90	$3d^6$	^3G	3	$3d^5(^2F_1)4p$	$^3F°$	2	R2
354.9640	0.0010	354.96462	0.00030	35	-0.966	E	42208.47	323926.69	$3d^6$	$^1G_2$	4	$3d^5(^2H)4p$	$^3H°$	4	R2
354.994	0.003	354.99617	0.00038	0	-1.844	E	27111.40	308804.58	$3d^6$	^3H	6	$3d^5(^2I)4p$	$^1H°$	5	H,R2
355.046	0.003	355.04662	0.00034	7	-1.666	E	34416.29	316069.44	$3d^6$	^3G	3	$3d^5(^2F_1)4p$	$^3G°$	4	d,R2
355.140	0.003	355.14109	0.00046	25	-1.564	E	26152.49	307730.72	$3d^6$	$^3P_2$	2	$3d^5(^2D_3)4p$	$^3F°$	2	s,R2
355.2397	0.0010	355.23936	0.00034	12	-1.609	E	33256.49	314756.83	$3d^6$	^3G	5	$3d^5(^4F)4p$	$^5G°$	6	R2
355.309	0.003	355.30854	0.00050	22	-1.473	E	33256.49	314702.02	$3d^6$	^3G	5	$3d^5(^2F_1)4p$	$^3G°$	5	H,R2
355.4385	0.0010	355.43842	0.00029	9	-1.865	E	33256.49	314599.18	$3d^6$	^3G	5	$3d^5(^4F)4p$	$^5F°$	4	R2
355.471	0.003	355.47249	0.00041	5	-2.341	E	42208.47	323524.19	$3d^6$	$^1G_2$	4	$3d^5(^4F)4p$	$^3F°$	3	d,R2
355.5371	0.0010	355.53853	0.00044	42	-0.996	E	34061.99	315325.46	$3d^6$	^3G	4	$3d^5(^2D_3)4p$	$^1F°$	3	R2
355.586	0.003	355.58594	0.00036	40	-1.260	E	27578.61	308804.58	$3d^6$	^3H	5	$3d^5(^2I)4p$	$^1H°$	5	p,R2
355.6111	0.0010	355.61147	0.00052	68	-0.517	E	27111.40	308317.18	$3d^6$	^3H	6	$3d^5(^2I)4p$	$^3I°$	7	R2
355.780	0.003	355.78041	0.00049	70	-0.224	E	41252.65	322324.90	$3d^6$	^1I	6	$3d^5(^2H)4p$	$^1I°$	6	s,R2
355.935	0.003	355.93323	0.00029	58	-0.933	E	33256.49	314208.06	$3d^6$	^3G	5	$3d^5(^2F_1)4p$	$^3F°$	4	R2*
355.935	0.003	355.93708	0.00084	58	-1.096	E	34416.29	315364.82	$3d^6$	^3G	3	$3d^5(^2F_1)4p$	$^3D°$	2	R2*
355.986	0.003	355.98695	0.00049	14	-1.625	E	34416.29	315325.46	$3d^6$	^3G	3	$3d^5(^2D_3)4p$	$^1F°$	3	H,R2
356.0467	0.0010	356.04845	0.00051	58	-0.073	E	77900.04	358760.69	$3d^6$	$^1G_1$	4	$3d^5(^2G_1)4p$	$^1G°$	4	R2
356.0896	0.0010	356.08919	0.00036	16	-1.428	E	29123.90	309952.42	$3d^6$	$^3F_2$	4	$3d^5(^2I)4p$	$^3H°$	4	R2
356.134	0.003	356.13051	0.00039	2	-2.025	E	29123.90	309919.84	$3d^6$	$^3F_2$	4	$3d^5(^2I)4p$	$^3H°$	5	H,R2
356.208	0.003	356.20706	0.00061	13	-2.036	E	41700.99	322436.58	$3d^6$	^3D	1	$3d^5(^4F)4p$	$^3D°$	2	R2*
356.208	0.003	356.21001	0.00076	13	-1.935	E	27858.94	308592.21	$3d^6$	^3H	4	$3d^5(^2D_3)4p$	$^3F°$	3	R2*
356.253	0.003	356.25518	0.00042	4	-2.134	E	41920.54	322618.21	$3d^6$	^3D	3	$3d^5(^4F)4p$	$^3D°$	3	H,R2
356.328	0.003	356.32835	0.00050	22	-2.024	E	34061.99	314702.02	$3d^6$	^3G	4	$3d^5(^2F1)4p$	$^3G°$	5	R2*

Table A.2 (cont'd)

λ_{obs} [a] (Å)	u_{obs} [b] (Å)	λ_{Ritz} [c] (Å)	u_{Ritz} [d] (Å)	I [e]	$\log(gf_R)$ [f]	$\log(gf_R)$ [g]	E_i [h] (cm^{-1})	E_k [i] (cm^{-1})	Lower Level Configuration	Term	J	Upper Level Configuration	Term [k]	J	Notes [j]
356.328	0.003	356.32721	0.00032	22	-1.585	E	29570.78	310211.71	$3d^6$	$^3F_2$	3	$3d^5(^2D3)4p$	$^3F^\circ$	4	R2*
356.359	0.003	356.36241	0.00030	2	-2.186	E	42208.47	322821.68	$3d^6$	$^1G_2$	4	$3d^5(^4F)4p$	$^3F^\circ$	4	G,R2
356.4095	0.0010	356.41014	0.00055	25	-0.862	E	77900.04	358475.67	$3d^6$	$^1G_1$	4	$3d^5(^2G_1)4p$	$^1H^\circ$	5	R2
356.460	0.003	356.45898	0.00029	6	-1.931	E	34061.99	314599.18	$3d^6$	^3G	4	$3d^5(^4F)4p$	$^5F^\circ$	4	d,R2
356.506	0.003	356.50659	0.00031	7	-1.884	E	34061.99	314561.71	$3d^6$	^3G	4	$3d^5(^4F)4p$	$^5F^\circ$	3	d,R2
356.6209	0.0010	356.62099	0.00041	39	-0.859	E	42208.47	322618.21	$3d^6$	$^1G_2$	4	$3d^5(^4F)4p$	$^3D^\circ$	3	R2
356.7753	0.0010	356.77524	0.00060	49	-0.970	E	27111.40	307399.91	$3d^6$	^3H	6	$3d^5(^2I)4p$	$^3I^\circ$	6	R2
356.831	0.003	356.83181	0.00050	7	-2.104	E	28697.33	308941.40	$3d^6$	$^3P_2$	1	$3d^5(^2D_3)4p$	$^1D^\circ$	2	d,R2
356.860	0.003	356.85999	0.00094	17	-1.534	E	66738.13	346960.07	$3d^6$	$^3P_1$	0	$3d^5(^2D_2)4p$	$^3P^\circ$	1	p,R2
356.8761	0.0010	356.87670	0.00036	33	-1.314	E	33256.49	313465.31	$3d^6$	^3G	5	$3d^5(^4F)4p$	$^5G^\circ$	5	R2
356.957	0.003	356.95747	0.00037	3	-2.333	E	34416.29	314561.71	$3d^6$	^3G	3	$3d^5(^4F)4p$	$^5F^\circ$	3	H,R2
357.3707	0.0010	357.37094	0.00060	65	-0.489	E	27578.61	307399.91	$3d^6$	^3H	5	$3d^5(^2I)4p$	$^3I^\circ$	6	R2
357.5500	0.0010	357.55062	0.00034	23	-1.376	E	29123.90	308804.58	$3d^6$	$^3F_2$	4	$3d^5(^2I)4p$	$^1H^\circ$	5	R2
357.743	0.003	357.74324	0.00056	2	-2.087	E	41252.65	320782.74	$3d^6$	^1I	6	$3d^5(^2H)4p$	$^3I^\circ$	7	H,R2
357.8218	0.0010	357.82232	0.00072	40	-1.149	E	29123.90	308592.21	$3d^6$	$^3F_2$	4	$3d^5(^2D_3)4p$	$^3F^\circ$	3	R2
357.897	0.003	357.89441	0.00073	11	-1.297	E	67548.05	346960.07	$3d^6$	$^3P_1$	1	$3d^5(^2D_2)4p$	$^3P^\circ$	1	d,R2
357.921	0.003	357.92158	0.00043	13	-1.483	E	41627.23	321018.04	$3d^6$	^3D	2	$3d^5(^2G_2)4p$	$^3F^\circ$	2	d,R2
357.946	0.003	357.94745	0.00038	16	-2.987	E	29570.78	308941.40	$3d^6$	$^3F_2$	3	$3d^5(^2D_3)4p$	$^1D^\circ$	2	d,R2*
357.946	0.004	357.94403	0.00095	16	-1.308	E	67548.05	346921.34	$3d^6$	$^3P_1$	1	$3d^5(^2D_2)4p$	$^3P^\circ$	0	d,R2*
357.946	0.004	357.95462	0.00064	16	-1.724	E	67548.05	346913.07	$3d^6$	$^3P_1$	1	$3d^5(^2D_2)4p$	$^3P^\circ$	2	d,R2*
358.0144	0.0010	358.01610	0.00045	36	-0.877	E	41700.99	321018.04	$3d^6$	^3D	1	$3d^5(^2G_2)4p$	$^3F^\circ$	2	R2
358.141	0.004	358.14205	0.00031	5	-1.994	E	34061.99	313280.81	$3d^6$	^3G	4	$3d^5(^4F)4p$	$^5G^\circ$	4	d,bl,R2
358.2475	0.0010	358.24828	0.00038	37	-0.809	E	41920.54	321056.56	$3d^6$	^3D	3	$3d^5(^2G_2)4p$	$^3F^\circ$	4	R2
358.368	0.003	358.36821	0.00043	10	-1.923	E	29898.79	308941.40	$3d^6$	$^3F_2$	2	$3d^5(^2D_3)4p$	$^1D^\circ$	2	d,R2
358.396	0.003	358.39541	0.00076	14	-1.722	E	29570.78	308592.21	$3d^6$	$^3F_2$	3	$3d^5(^2D_3)4p$	$^3F^\circ$	3	d,R2
358.503	0.003	358.50322	0.00039	7	-1.967	E	27111.40	306048.92	$3d^6$	^3H	6	$3d^5(^2I)4p$	$^3I^\circ$	5	H,R2
358.570	0.003	358.56805	0.00049	69	-0.846	E	41627.23	320514.32	$3d^6$	^3D	2	$3d^5(^2G_2)4p$	$^3F^\circ$	3	p,R2*
358.570	0.004	358.57043	0.00049	69	-0.733	E	27111.40	305996.64	$3d^6$	^3H	6	$3d^5(^2I)4p$	$^3K^\circ$	7	p,R2*
358.583	0.003	358.58488	0.00055	68	-0.264	E	42208.47	321082.47	$3d^6$	$^1G_2$	4	$3d^5(^2F_1)4p$	$^1F^\circ$	3	p,R2
358.6178	0.0010	358.61820	0.00038	53	-0.585	E	42208.47	321056.56	$3d^6$	$^1G_2$	4	$3d^5(^2G_2)4p$	$^3F^\circ$	4	R2
358.7422	0.0010	358.74248	0.00036	26	-1.384	E	33256.49	312007.98	$3d^6$	^3G	5	$3d^5(^2F_1)4p$	$^1G^\circ$	4	R2
358.819	0.003	358.81723	0.00078	6	-2.010	E	29898.79	308592.21	$3d^6$	$^3F_2$	2	$3d^5(^2D_3)4p$	$^3F^\circ$	3	l,R2
358.9269	0.0010	358.92710	0.00042	26	-1.366	E	41252.65	319860.76	$3d^6$	^1I	6	$3d^5(^2H)4p$	$^3I^\circ$	6	R2
358.944	0.003	358.94556	0.00043	12	-1.585	E	41920.54	320514.32	$3d^6$	^3D	3	$3d^5(^2G_2)4p$	$^3F^\circ$	3	p,R2
359.0196	0.0010	359.01855	0.00037	24	-4.000	E	34416.29	312953.43	$3d^6$	^3G	3	$3d^5(^2F_1)4p$	$^3D^\circ$	3	R2
359.0472	0.0010	359.04684	0.00050	38	-0.859	E	48607.12	327122.31	$3d^6$	$^1D_2$	2	$3d^5(^2F_2)4p$	$^1D^\circ$	2	R2

Table A.2 (cont'd)

λ_{obs} [a] (Å)	u_{obs} [b] (Å)	λ_{Ritz} [c] (Å)	u_{Ritz} [d] (Å)	I [e]	$\log(gf_R)$ [f]	$\log(gf_R)$ [g]	E_i [h] (cm^{-1})	E_k [i] (cm^{-1})	Lower Level Configuration	Term	J	Upper Level Configuration	Term [k]	J	Notes [j]
359.101	0.004	359.10133	0.00036	19	-1.666	E	34416.29	312889.22	$3d^6$	^3G	3	$3d^5(^4F)4p$	$^5G°$	3	R2*
359.101	0.003	359.10471	0.00038	19	-2.093	E	27578.61	306048.92	$3d^6$	^3H	5	$3d^5(^2I)4p$	$^3I°$	5	R2*
359.194	0.003	359.19312	0.00042	15	-1.711	E	34061.99	312463.76	$3d^6$	^3G	4	$3d^5(^2F_1)4p$	$^3G°$	3	R2*
359.194	0.003	359.19477	0.00043	15	-2.132	E	41252.65	319653.14	$3d^6$	^1I	6	$3d^5(^4F)4p$	$^3G°$	5	R2*
359.3163	0.0010	359.31692	0.00041	15	-1.404	E	42208.47	320514.32	$3d^6$	$^1G_2$	4	$3d^5(^2G_2)4p$	$^3F°$	3	R2
359.420	0.003	359.42041	0.00045	7	-1.803	E	41700.99	319926.70	$3d^6$	^3D	1	$3d^5(^2F_1)4p$	$^1D°$	2	G,R2
359.4675	0.0010	359.46658	0.00037	66	-0.520	E	27858.94	306048.92	$3d^6$	^3H	4	$3d^5(^2I)4p$	$^3I°$	5	R2
359.505	0.003	359.50540	0.00035	33	-1.347	E	29570.78	307730.72	$3d^6$	$^3F_2$	3	$3d^5(^2D_3)4p$	$^3F°$	2	d,R2
359.5418	0.0010	359.54103	0.00043	33	-0.867	E	48607.12	326739.49	$3d^6$	$^1D_2$	2	$3d^5(^2G_2)4p$	$^1F°$	3	R2
359.6959	0.0010	359.69590	0.00100	58	-0.900	E	27578.61	305591.23	$3d^6$	^3H	5	$3d^5(^2I)4p$	$^3K°$	6	R2
359.720	0.003	359.72175	0.00050	26	-1.432	E	41627.23	319619.87	$3d^6$	^3D	2	$3d^5(^4F)4p$	$^3G°$	3	H,R2
359.737	0.003	359.73952	0.00059	17	-1.689	E	41920.54	319899.45	$3d^6$	^3D	3	$3d^5(^4F)4p$	$^3G°$	4	p,R2
359.781	0.003	359.78213	0.00037	35	-1.249	E	34061.99	312007.98	$3d^6$	^3G	4	$3d^5(^2F_1)4p$	$^1G°$	4	d,R2
359.967	0.003	359.96656	0.00060	14	-1.239	E	69156.49	346960.07	$3d^6$	$^3P_1$	2	$3d^5(^2D_2)4p$	$^3P°$	1	d,R2
360.0278	0.0010	360.02747	0.00046	35	-0.708	E	69156.49	346913.07	$3d^6$	$^3P_1$	2	$3d^5(^2D_2)4p$	$^3P°$	2	R2
360.1119	0.0010	360.11253	0.00056	22	-1.367	E	42208.47	319899.45	$3d^6$	$^1G_2$	4	$3d^5(^4F)4p$	$^3G°$	4	R2
360.242	0.003	360.24133	0.00042	6	-1.865	E	34416.29	312007.98	$3d^6$	^3G	3	$3d^5(^2F_1)4p$	$^1G°$	4	d,R2
360.474	0.003	360.47545	0.00043	41	-1.002	E	42208.47	319619.87	$3d^6$	$^1G_2$	4	$3d^5(^4F)4p$	$^3G°$	3	s,R2
360.726	0.004	360.72731	0.00074	27	-2.099	E	68719.26	345936.97	$3d^6$	$^3F_1$	4	$3d^5(^2D_2)4p$	$^1F°$	3	R2
360.726	0.003	360.72640	0.00033	27	-1.130	E	41920.54	319138.95	$3d^6$	^3D	3	$3d^5(^2G_2)4p$	$^1G°$	4	R2
360.827	0.003	360.82660	0.00063	9	-1.718	E	28697.33	305838.76	$3d^6$	$^3P_2$	1	$3d^5(^4D)4p$	$^3P°$	1	d,R2
360.8856	0.0010	360.88464	0.00045	55	-0.560	E	26152.49	303249.35	$3d^6$	$^3P_2$	2	$3d^5(^4P)4p$	$^3S°$	1	R2
361.1013	0.0010	361.10146	0.00032	55	-0.552	E	42208.47	319138.95	$3d^6$	$^1G_2$	4	$3d^5(^2G_2)4p$	$^1G°$	4	R2
361.2665	0.0010	361.26649	0.00044	58	-0.152	E	57924.12	334728.09	$3d^6$	^1F	3	$3d^5(^2F_2)4p$	$^1F°$	3	R2
361.349	0.003	361.3499	0.0013	8	-1.412	E	66738.13	343478.21	$3d^6$	$^3P_1$	0	$3d^5(^2D_2)4p$	$^3D°$	1	d,R2
361.415	0.004	361.41554	0.00078	7	-1.979	E	28697.33	305387.15	$3d^6$	$^3P_2$	1	$3d^5(^4D)4p$	$^3P°$	0	H,R2
361.450	0.003	361.45012	0.00039	14	-1.454	E	33256.49	309919.84	$3d^6$	^3G	5	$3d^5(^2I)4p$	$^3H°$	5	d,R2
361.526	0.003	361.52626	0.00054	11	-1.341	E	48607.12	325212.20	$3d^6$	$^1D_2$	2	$3d^5(^2G_2)4p$	$^3G°$	3	d,R2
361.851	0.003	361.85022	0.00070	17	-1.115	E	67548.05	343905.49	$3d^6$	$^3P_1$	1	$3d^5(^2D_2)4p$	$^3D°$	2	d,R2
362.058	0.003	362.05843	0.00075	7	-1.852	E	29640.25	305838.76	$3d^6$	$^3P_2$	0	$3d^5(^4D)4p$	$^3P°$	1	H,R2
362.120	0.003	362.12240	0.00033	13	-1.752	E	34061.99	310211.71	$3d^6$	^3G	4	$3d^5(^2D_3)4p$	$^3F°$	4	d,R2
362.219	0.003	362.22007	0.00044	55	-0.664	E	41252.65	317327.91	$3d^6$	^1I	6	$3d^5(^2H)4p$	$^3H°$	6	s,R2
362.3090	0.0010	362.30911	0.00040	59	-0.468	E	33256.49	309263.90	$3d^6$	^3G	5	$3d^5(^2I)4p$	$^3H°$	6	R2
362.5056	0.0010	362.50554	0.00039	56	-0.541	E	34061.99	309919.84	$3d^6$	^3G	4	$3d^5(^2I)4p$	$^3H°$	5	R2
362.6538	0.0010	362.6538	0.0010	28	-0.242	E	104421.97	380167.	$3d^6$	$^1D_1$	2	$3d^5(^2P)4p$	$^1P°$	1	R2
362.7789	0.0010	362.78028	0.00046	22	-1.049	E	69156.49	344805.43	$3d^6$	$^3P_1$	2	$3d^5(^2D_2)4p$	$^3D°$	3	R2

Table A.2 (cont'd)

λ_{obs} [a] (Å)	u_{obs} [b] (Å)	λ_{Ritz} [c] (Å)	u_{Ritz} [d] (Å)	I [e]	$\log(gf_R)$ [f]	$\log(gf_R)$ [g]	E_i [h] (cm^{-1})	E_k [i] (cm^{-1})	Lower Level Configuration	Term	J	Upper Level Configuration	Term [k]	J	Notes [j]
362.9278	0.0010	362.92881	0.00042	53	-0.599	E	34416.29	309952.42	$3d^6$	^3G	3	$3d^5(^2I)4p$	$^3H^\circ$	4	R2
363.043	0.003	363.04588	0.00051	4	-1.693	E	77900.04	353347.32	$3d^6$	$^1G_1$	4	$3d^5(^2G_1)4p$	$^3F^\circ$	4	H,R2
363.182	0.003	363.17962	0.00073	2	-1.807	E	67548.05	342893.90	$3d^6$	$^3P_1$	1	$3d^5(^2D_2)4p$	$^3F^\circ$	2	H,R2
363.309	0.003	363.30964	0.00057	5	-1.644	E	48607.12	323854.43	$3d^6$	$^1D_2$	2	$3d^5(^4F)4p$	$^3F^\circ$	2	d,R2
363.5405	0.0010	363.54143	0.00059	34	-0.835	E	57924.12	332995.93	$3d^6$	^1F	3	$3d^5(^2H)4p$	$^1G^\circ$	4	R2
363.568	0.003	363.56970	0.00058	6	-1.573	E	68855.07	343905.49	$3d^6$	$^3F_1$	3	$3d^5(^2D_2)4p$	$^3D^\circ$	2	G,R2
363.839	0.003	363.8402	0.0011	2	-1.617	E	68632.25	343478.21	$3d^6$	$^3F_1$	2	$3d^5(^2D_2)4p$	$^3D^\circ$	1	d,R2
363.975	0.003	363.97706	0.00035	6	-1.858	E	34061.99	308804.58	$3d^6$	^3G	4	$3d^5(^2I)4p$	$^1H^\circ$	5	d,R2
364.059	0.003	364.05971	0.00035	8	-1.600	E	42208.47	316888.69	$3d^6$	$^1G_2$	4	$3d^5(^2H)4p$	$^3G^\circ$	4	d,R2
364.094	0.003	364.09512	0.00066	2	-2.233	E	41627.23	316280.73	$3d^6$	^3D	2	$3d^5(^2F_1)4p$	$^3F^\circ$	3	G,R2
364.2291	0.0010	364.22970	0.00048	36	-0.954	E	28697.33	303249.35	$3d^6$	$^3P_2$	1	$3d^5(^4P)4p$	$^3S^\circ$	1	R2
364.262	0.003	364.26540	0.00045	16	-1.842	E	34416.29	308941.40	$3d^6$	^3G	3	$3d^5(^2D_3)4p$	$^1D^\circ$	2	d,R2
364.345	0.003	364.34663	0.00053	2	-2.039	E	41700.99	316164.90	$3d^6$	^3D	1	$3d^5(^2F_1)4p$	$^3F^\circ$	2	H,R2
364.485	0.003	364.48437	0.00061	5	-1.861	E	41920.54	316280.73	$3d^6$	^3D	3	$3d^5(^2F_1)4p$	$^3F^\circ$	3	H,R2
364.7726	0.0010	364.77257	0.00061	24	-1.400	E	33256.49	307399.91	$3d^6$	^3G	5	$3d^5(^2I)4p$	$^3I^\circ$	6	R2
364.797	0.003	364.79564	0.00046	12	-1.440	E	69156.49	343282.57	$3d^6$	$^3P_1$	2	$3d^5(^2D_2)4p$	$^3F^\circ$	3	d,R2
364.867	0.003	364.86728	0.00062	11	-1.729	E	42208.47	316280.73	$3d^6$	$^1G_2$	4	$3d^5(^2F_1)4p$	$^3F^\circ$	3	d,R2
364.8986	0.0010	364.89899	0.00044	34	-1.229	E	26152.49	300200.93	$3d^6$	$^3P_2$	2	$3d^5(^4D)4p$	$^5P^\circ$	3	R2
365.148	0.003	365.14878	0.00033	5	-1.997	E	42208.47	316069.44	$3d^6$	$^1G_2$	4	$3d^5(^2F_1)4p$	$^3G^\circ$	4	d,R2
365.189	0.003	365.19080	0.00063	10	-1.638	E	48607.12	322436.58	$3d^6$	$^1D_2$	2	$3d^5(^4F)4p$	$^3D^\circ$	2	d,R2
365.363	0.003	365.36590	0.00055	6	-2.024	E	41627.23	315325.46	$3d^6$	^3D	2	$3d^5(^2D_3)4p$	$^1F^\circ$	3	d,R2
365.410	0.003	365.41183	0.00091	8	-1.933	E	41700.99	315364.82	$3d^6$	^3D	1	$3d^5(^2F_1)4p$	$^3D^\circ$	2	d,R2
365.4849	0.0010	365.48492	0.00060	19	-1.415	E	29640.25	303249.35	$3d^6$	$^3P_2$	0	$3d^5(^4P)4p$	$^3S^\circ$	1	R2
365.6252	0.0010	365.62512	0.00043	69	-0.000	E	41252.65	314756.83	$3d^6$	^1I	6	$3d^5(^4F)4p$	$^5G^\circ$	6	R2
365.844	0.003	365.84464	0.00039	14	-1.805	E	27578.61	300918.68	$3d^6$	^3H	5	$3d^5(^4D)4p$	$^3F^\circ$	4	d,R2
366.085	0.003	366.08309	0.00034	18	-1.661	E	42208.47	315370.50	$3d^6$	$^1G_2$	4	$3d^5(^2G_2)4p$	$^3H^\circ$	4	p,R2
366.1129	0.0010	366.11291	0.00100	62	-0.518	E	41252.65	314392.43	$3d^6$	^1I	6	$3d^5(^2I)4p$	$^1I^\circ$	6	R2
366.386	0.003	366.38830	0.00044	8	-2.020	E	41627.23	314561.71	$3d^6$	^3D	2	$3d^5(^4F)4p$	$^5F^\circ$	3	d,R2
366.541	0.003	366.54175	0.00055	14	-1.566	E	26152.49	298972.71	$3d^6$	$^3P_2$	2	$3d^5(^4D)4p$	$^3D^\circ$	3	d,R2
367.0052	0.0010	367.00568	0.00058	41	-0.615	E	48607.12	321082.47	$3d^6$	$^1D_2$	2	$3d^5(^2F_1)4p$	$^1F^\circ$	3	R2
367.093	0.003	367.09248	0.00048	3	-1.649	E	48607.12	321018.04	$3d^6$	$^1D_2$	2	$3d^5(^2G_2)4p$	$^3F^\circ$	2	d,R2
367.182	0.003	367.18539	0.00037	15	-1.832	E	27858.94	300200.93	$3d^6$	^3H	4	$3d^5(^4D)4p$	$^5P^\circ$	3	H,R2*
367.182	0.003	367.18039	0.00050	15	-1.997	E	29123.90	301469.60	$3d^6$	$^3F_2$	4	$3d^5(^4D)4p$	$^3F^\circ$	3	H,R2*
367.2575	0.0010	367.25884	0.00033	28	-1.177	E	41920.54	314208.06	$3d^6$	^3D	3	$3d^5(^2F_1)4p$	$^3F^\circ$	4	R2
367.567	0.003	367.56644	0.00066	11	-1.513	E	41627.23	313686.89	$3d^6$	^3D	2	$3d^5(^2D_3)4p$	$^3D^\circ$	2	H,R2
367.648	0.003	367.64722	0.00058	13	-1.793	E	41920.54	313920.42	$3d^6$	^3D	3	$3d^5(^2D_3)4p$	$^3D^\circ$	3	H,R2*

Table A.2 (cont'd)

λ_{obs} [a] (Å)	u_{obs} [b] (Å)	λ_{Ritz} [c] (Å)	u_{Ritz} [d] (Å)	I [e]	$\log(gf_R)$ [f]	$\log(gf_R)$ [g]	E_i [h] (cm^{-1})	E_k [i] (cm^{-1})	Lower Level Configuration	Term	J	Upper Level Configuration	Term [k]	J	Notes [j]
367.648	0.003	367.64761	0.00034	13	-2.380	E	42208.47	314208.06	$3d^6$	$^1G_2$	4	$3d^5(^2F_1)4p$	$^3F^\circ$	4	H,R2*
367.664	0.003	367.66473	0.00037	12	-1.914	E	34061.99	306048.92	$3d^6$	^3G	4	$3d^5(^2I)4p$	$^3I^\circ$	5	H,R2
367.778	0.003	367.77253	0.00054	9	-1.899	E	48607.12	320514.32	$3d^6$	$^1D_2$	2	$3d^5(^2G_2)4p$	$^3F^\circ$	3	H,R2
367.826	0.003	367.82823	0.00095	5	-2.095	E	28697.33	300563.36	$3d^6$	$^3P_2$	1	$3d^5(^4D)4p$	$^3D^\circ$	1	H,R2
367.9231	0.0010	367.92465	0.00036	13	-1.696	E	29123.90	300918.68	$3d^6$	$^3F_2$	4	$3d^5(^4D)4p$	$^3F^\circ$	4	R2
368.037	0.003	368.03681	0.00059	5	-2.303	E	42208.47	313920.42	$3d^6$	$^1G_2$	4	$3d^5(^2D_3)4p$	$^3D^\circ$	3	H,R2
368.115	0.003	368.11542	0.00070	2	-2.159	E	29898.79	301552.72	$3d^6$	$^3F_2$	2	$3d^5(^4D)4p$	$^3F^\circ$	2	H,R2
368.2864	0.0010	368.28703	0.00052	32	-1.218	E	28697.33	300224.68	$3d^6$	$^3P_2$	1	$3d^5(^4D)4p$	$^3D^\circ$	2	R2
368.4958	0.0010	368.49625	0.00076	42	-0.688	E	47699.96	319073.14	$3d^6$	$^1S_2$	0	$3d^5(^2D_3)4p$	$^1P^\circ$	1	R2
368.5689	0.0010	368.56905	0.00045	58	-0.337	E	48607.12	319926.70	$3d^6$	$^1D_2$	2	$3d^5(^2F_1)4p$	$^1D^\circ$	2	R2
368.641	0.003	368.64273	0.00051	4	-2.182	E	26152.49	297417.84	$3d^6$	$^3P_2$	2	$3d^5(^4D)4p$	$^5D^\circ$	1	H,R2
368.898	0.003	368.89883	0.00033	51	-0.871	E	29123.90	300200.93	$3d^6$	$^3F_2$	4	$3d^5(^4D)4p$	$^5P^\circ$	3	R2
368.898	0.004	368.90522	0.00037	51	-2.572	E	42208.47	313280.81	$3d^6$	$^1G_2$	4	$3d^5(^4F)4p$	$^5G^\circ$	4	R2*
368.898	0.004	368.89836	0.00061	51	-1.981	E	41700.99	312778.37	$3d^6$	^3D	1	$3d^5(^4F)4p$	$^5G^\circ$	2	R2*
368.958	0.003	368.95891	0.00036	9	-1.578	E	41920.54	312953.43	$3d^6$	^3D	3	$3d^5(^2F_1)4p$	$^3D^\circ$	3	R2
368.9859	0.0010	368.98633	0.00051	23	-1.179	E	48607.12	319619.87	$3d^6$	$^1D_2$	2	$3d^5(^4F)4p$	$^3G^\circ$	3	R2
369.108	0.003	369.1084	0.0010	15	-1.657	E	29640.25	300563.36	$3d^6$	$^3P_2$	0	$3d^5(^4D)4p$	$^3D^\circ$	1	d,R2
369.192	0.003	369.19226	0.00047	8	-1.951	E	26152.49	297014.07	$3d^6$	$^3P_2$	2	$3d^5(^4D)4p$	$^5D^\circ$	2	d,R2
369.2258	0.0010	369.22641	0.00050	15	-1.524	E	41627.23	312463.76	$3d^6$	^3D	2	$3d^5(^2F_1)4p$	$^3G^\circ$	3	R2
369.4746	0.0010	369.47556	0.00042	21	-1.455	E	29570.78	300224.68	$3d^6$	$^3F_2$	3	$3d^5(^4D)4p$	$^3D^\circ$	2	R2
369.5082	0.0010	369.50798	0.00032	12	-1.670	E	29570.78	300200.93	$3d^6$	$^3F_2$	3	$3d^5(^4D)4p$	$^5P^\circ$	3	R2
369.562	0.003	369.56346	0.00066	8	-1.600	E	41700.99	312290.51	$3d^6$	^3D	1	$3d^5(^2D_3)4p$	$^3P^\circ$	1	d,R2
369.733	0.003	369.73221	0.00058	12	-1.434	E	48607.12	319073.14	$3d^6$	$^1D_2$	2	$3d^5(^2D_3)4p$	$^1P^\circ$	1	H,R2
369.906	0.003	369.90629	0.00059	7	-1.928	E	41627.23	311965.97	$3d^6$	^3D	2	$3d^5(^2D_3)4p$	$^3P^\circ$	2	H,R2
369.925	0.003	369.92387	0.00048	4	-2.126	E	29898.79	300224.68	$3d^6$	$^3F_2$	2	$3d^5(^4D)4p$	$^3D^\circ$	2	H,R2
370.021	0.003	370.02051	0.00048	6	-1.980	E	42208.47	312463.76	$3d^6$	$^1G_2$	4	$3d^5(^2F_1)4p$	$^3G^\circ$	3	d,R2
370.6159	0.0010	370.61612	0.00041	70	-0.078	E	27111.40	296932.37	$3d^6$	^3H	6	$3d^5(^4G)4p$	$^3G^\circ$	5	R2
370.975	0.003	370.97536	0.00047	22	-1.505	E	27858.94	297418.62	$3d^6$	^3H	4	$3d^5(^4P)4p$	$^3D^\circ$	3	d,R2
371.0910	0.0010	371.09187	0.00037	29	-1.357	E	29570.78	299045.83	$3d^6$	$^3F_2$	3	$3d^5(^4D)4p$	$^5P^\circ$	2	R2
371.2752	0.0019	371.27674	0.00048	59	-0.657	E	27578.61	296919.48	$3d^6$	^3H	5	$3d^5(^4D)4p$	$^5D^\circ$	4	R2
371.3065	0.0010	371.30847	0.00040	67	-0.344	E	27578.61	296896.46	$3d^6$	^3H	5	$3d^5(^4G)4p$	$^3G^\circ$	4	R2
371.4725	0.0010	371.47352	0.00048	33	-0.936	E	57924.12	327122.31	$3d^6$	^1F	3	$3d^5(^2F_2)4p$	$^1D^\circ$	2	R2
371.543	0.003	371.54633	0.00052	10	-2.342	E	28697.33	297842.77	$3d^6$	$^3P_2$	1	$3d^5(^4P)4p$	$^3D^\circ$	2	d,R2*
371.543	0.003	371.54412	0.00043	10	-2.179	E	29898.79	299045.83	$3d^6$	$^3F_2$	2	$3d^5(^4D)4p$	$^5P^\circ$	2	d,R2*
371.6432	0.0010	371.64576	0.00040	12	-1.753	E	27858.94	296932.37	$3d^6$	^3H	4	$3d^5(^4G)4p$	$^3G^\circ$	5	R2
371.7630	0.0010	371.76366	0.00062	68	-0.293	E	27858.94	296847.04	$3d^6$	^3H	4	$3d^5(^4G)4p$	$^3G^\circ$	3	R2

Table A.2 (cont'd)

λ_{obs} [a] (Å)	u_{obs} [b] (Å)	λ_{Ritz} [c] (Å)	u_{Ritz} [d] (Å)	I [e]	$\log(gf_R)$ [f]	$\log(gf_R)$ [g]	E_i [h] (cm^{-1})	E_k [i] (cm^{-1})	Lower Level Configuration	Term	J	Upper Level Configuration	Term [k]	J	Notes [j]
371.8120	0.0010	371.81287	0.00044	25	-1.070	E	57924.12	326876.62	$3d^6$	^1F	3	$3d^5(^2F_2)4p$	$^3F^\circ$	4	R2
372.0019	0.0010	372.00254	0.00039	43	-0.528	E	57924.12	326739.49	$3d^6$	^1F	3	$3d^5(^2G_2)4p$	$^1F^\circ$	3	R2
372.1592	0.0010	372.16035	0.00059	39	-1.091	E	29898.79	298600.17	$3d^6$	$^3F_2$	2	$3d^5(^4P)4p$	$^3D^\circ$	1	R2
372.4514	0.0010	372.45069	0.00044	61	-0.564	E	41252.65	309744.57	$3d^6$	^1I	6	$3d^5(^2I)4p$	$^1K^\circ$	7	R2
372.724	0.003	372.72444	0.00045	62	-0.676	E	29123.90	297418.62	$3d^6$	$^3F_2$	4	$3d^5(^4P)4p$	$^3D^\circ$	3	R2*
372.724	0.003	372.72937	0.00037	62	-1.525	E	41920.54	310211.71	$3d^6$	^3D	3	$3d^5(^2D_3)4p$	$^3F^\circ$	4	R2*
372.7560	0.0010	372.75602	0.00039	56	-0.777	E	29570.78	297842.77	$3d^6$	$^3F_2$	3	$3d^5(^4P)4p$	$^3D^\circ$	2	R2
372.9872	0.0010	372.98664	0.00044	30	-0.873	E	57924.12	326030.24	$3d^6$	^1F	3	$3d^5(^2F_2)4p$	$^3F^\circ$	3	R2
373.0176	0.0010	373.01768	0.00050	41	-1.072	E	29898.79	297982.60	$3d^6$	$^3F_2$	2	$3d^5(^4D)4p$	$^5P^\circ$	1	R2
373.0832	0.0019	373.08292	0.00082	23	-1.086	E	77900.04	345936.97	$3d^6$	$^1G_1$	4	$3d^5(^2D_2)4p$	$^1F^\circ$	3	R2
373.2134	0.0010	373.21234	0.00044	17	-1.651	E	29898.79	297842.77	$3d^6$	$^3F_2$	2	$3d^5(^4P)4p$	$^3D^\circ$	2	R2
373.347	0.003	373.34630	0.00044	14	-1.766	E	29570.78	297418.62	$3d^6$	$^3F_2$	3	$3d^5(^4P)4p$	$^3D^\circ$	3	H,R2
373.4007	0.0010	373.40118	0.00038	54	-0.681	E	29123.90	296932.37	$3d^6$	$^3F_2$	4	$3d^5(^4G)4p$	$^3G^\circ$	5	R2
373.417	0.004	373.41916	0.00047	27	-1.634	E	29123.90	296919.48	$3d^6$	$^3F_2$	4	$3d^5(^4D)4p$	$^5D^\circ$	4	p,R2
373.449	0.003	373.45126	0.00039	14	-1.637	E	29123.90	296896.46	$3d^6$	$^3F_2$	4	$3d^5(^4G)4p$	$^3G^\circ$	4	d,R2
373.5211	0.0010	373.52020	0.00062	22	-1.526	E	29123.90	296847.04	$3d^6$	$^3F_2$	4	$3d^5(^4G)4p$	$^3G^\circ$	3	R2
373.536	0.003	373.53662	0.00044	23	-1.286	E	42208.47	309919.84	$3d^6$	$^1G_2$	4	$3d^5(^2I)4p$	$^3H^\circ$	5	d,R2
373.6052	0.0010	373.60525	0.00037	67	-0.392	E	33256.49	300918.68	$3d^6$	^3G	5	$3d^5(^4D)4p$	$^3F^\circ$	4	R2
373.6436	0.0010	373.64347	0.00041	40	-0.714	E	57924.12	325558.93	$3d^6$	^1F	3	$3d^5(^2F_2)4p$	$^1G^\circ$	4	R2
373.6903	0.0010	373.69001	0.00078	18	-1.349	E	47699.96	315301.44	$3d^6$	$^1S_2$	0	$3d^5(^2F_1)4p$	$^3D^\circ$	1	R2
373.7598	0.0010	373.75922	0.00044	39	-1.082	E	41252.65	308804.58	$3d^6$	^1I	6	$3d^5(^2I)4p$	$^1H^\circ$	5	R2
373.804	0.003	373.80516	0.00045	40	-1.884	E	29898.79	297417.84	$3d^6$	$^3F_2$	2	$3d^5(^4D)4p$	$^5D^\circ$	1	H,R2
373.903	0.003	373.90140	0.00053	37	-1.438	E	29123.90	296574.09	$3d^6$	$^3F_2$	4	$3d^5(^4D)4p$	$^5D^\circ$	3	d,R2*
373.903	0.003	373.91104	0.00035	37	-1.540	E	29570.78	297014.07	$3d^6$	$^3F_2$	3	$3d^5(^4D)4p$	$^5D^\circ$	2	d,R2*
373.9597	0.0010	373.96094	0.00049	64	-0.526	E	34061.99	301469.60	$3d^6$	^3G	4	$3d^5(^4D)4p$	$^3F^\circ$	3	R2
374.0450	0.0019	374.04334	0.00046	39	-1.219	E	29570.78	296919.48	$3d^6$	$^3F_2$	3	$3d^5(^4D)4p$	$^5D^\circ$	4	R2
374.0748	0.0010	374.07555	0.00038	64	-0.938	E	29570.78	296896.46	$3d^6$	$^3F_2$	3	$3d^5(^4G)4p$	$^3G^\circ$	4	R2
374.159	0.003	374.15650	0.00059	50	-1.181	E	26152.49	293420.33	$3d^6$	$^3P_2$	2	$3d^5(^4P)4p$	$^3P^\circ$	1	s,R2
374.340	0.003	374.34056	0.00072	62	-0.649	E	34416.29	301552.72	$3d^6$	^3G	3	$3d^5(^4D)4p$	$^3F^\circ$	2	s,R2
374.454	0.003	374.45707	0.00056	21	-1.685	E	34416.29	301469.60	$3d^6$	^3G	3	$3d^5(^4D)4p$	$^3F^\circ$	3	p,R2
374.581	0.003	374.58097	0.00087	24	-1.501	E	41627.23	308592.21	$3d^6$	^3D	2	$3d^5(^2D_3)4p$	$^3F^\circ$	3	p,R2
374.6042	0.0010	374.60444	0.00064	48	-0.810	E	29898.79	296847.04	$3d^6$	$^3F_2$	2	$3d^5(^4G)4p$	$^3G^\circ$	3	R2
374.733	0.003	374.73297	0.00037	13	-1.755	E	34061.99	300918.68	$3d^6$	^3G	4	$3d^5(^4D)4p$	$^3F^\circ$	4	d,R2
374.7699	0.0010	374.77066	0.00053	59	-0.694	E	26152.49	292982.34	$3d^6$	$^3P_2$	2	$3d^5(^4P)4p$	$^3P^\circ$	2	R2
374.963	0.003	374.96112	0.00070	5	-1.976	E	48607.12	315301.44	$3d^6$	$^1D_2$	2	$3d^5(^2F_1)4p$	$^3D^\circ$	1	G,R2
374.992	0.003	374.99296	0.00084	4	-2.288	E	41920.54	308592.21	$3d^6$	^3D	3	$3d^5(^2D_3)4p$	$^3F^\circ$	3	G,R2

Table A.2 (cont'd)

λ_{obs} [a] (Å)	u_{obs} [b] (Å)	λ_{Ritz} [c] (Å)	u_{Ritz} [d] (Å)	I [e]	$\log(gf_R)$ [f]	$\log(gf_R)$ [g]	E_i [h] (cm^{-1})	E_k [i] (cm^{-1})	Lower Level Configuration	Term	J	Upper Level Configuration	Term [k]	J	Notes [j]
375.1000	0.0010	375.09925	0.00038	58	-0.537	E	42208.47	308804.58	$3d^6$	$^1G_2$	4	$3d^5(^2I)4p$	$^1H^\circ$	5	R2
375.733	0.003	375.73184	0.00075	2	-2.069	E	41252.65	307399.91	$3d^6$	^1I	6	$3d^5(^2I)4p$	$^3I^\circ$	6	H,R2
375.8977	0.0010	375.89784	0.00050	16	-1.478	E	41700.99	307730.72	$3d^6$	^3D	1	$3d^5(^2D_3)4p$	$^3F^\circ$	2	R2
376.119	0.003	376.11940	0.00052	2	-1.532	E	68855.07	334728.09	$3d^6$	$^3F_1$	3	$3d^5(^2F_2)4p$	$^1F^\circ$	3	H,R2
376.211	0.003	376.21085	0.00050	7	-1.791	E	34416.29	300224.68	$3d^6$	^3G	3	$3d^5(^4D)4p$	$^3D^\circ$	2	d,R2
376.509	0.003	376.50592	0.00050	2	-2.253	E	57924.12	323524.19	$3d^6$	^1F	3	$3d^5(^4F)4p$	$^3F^\circ$	3	G,R2
376.810	0.003	376.8052	0.0011	11	-1.914	E	26152.49	291541.60	$3d^6$	$^3P_2$	2	$3d^5(^4P)4p$	$^5P^\circ$	1	H,R2
377.015	0.003	377.01384	0.00046	11	-1.919	E	27111.40	292353.65	$3d^6$	^3H	6	$3d^5(^4G)4p$	$^3H^\circ$	5	d,R2
377.1169	0.0010	377.11701	0.00096	24	-1.346	E	28697.33	293867.02	$3d^6$	$^3P_2$	1	$3d^5(^4P)4p$	$^3P^\circ$	0	R2
377.251	0.003	377.25673	0.00059	2	-3.387	E	48607.12	313678.60	$3d^6$	$^1D_2$	2	$3d^5(^2D_3)4p$	$^3D^\circ$	1	H,R2*
377.251	0.003	377.24493	0.00072	2	-3.131	E	48607.12	313686.89	$3d^6$	$^1D_2$	2	$3d^5(^2D_3)4p$	$^3D^\circ$	2	H,R2*
377.283	0.003	377.28343	0.00091	6	-1.912	E	27578.61	292631.33	$3d^6$	^3H	5	$3d^5(^4G)4p$	$^3H^\circ$	4	d,R2
377.4858	0.0010	377.48567	0.00045	10	-1.698	E	34061.99	298972.71	$3d^6$	^3G	4	$3d^5(^4D)4p$	$^3D^\circ$	3	R2
377.646	0.003	377.64882	0.00046	29	-1.683	E	41252.65	306048.92	$3d^6$	^1I	6	$3d^5(^2I)4p$	$^3I^\circ$	5	p,R2
377.676	0.003	377.67260	0.00044	72	-0.475	E	27111.40	291891.00	$3d^6$	^3H	6	$3d^5(^4G)4p$	$^3H^\circ$	6	w,R2*
377.676	0.003	377.67910	0.00045	72	-0.553	E	27578.61	292353.65	$3d^6$	^3H	5	$3d^5(^4G)4p$	$^3H^\circ$	5	w,R2*
377.676	0.003	377.68288	0.00091	72	-0.653	E	27858.94	292631.33	$3d^6$	^3H	4	$3d^5(^4G)4p$	$^3H^\circ$	4	w,R2*
377.713	0.003	377.71270	0.00047	32	-1.366	E	41627.23	306378.72	$3d^6$	^3D	2	$3d^5(^4D)4p$	$^3P^\circ$	2	R2*
377.713	0.004	377.72340	0.00061	32	-1.807	E	41252.65	305996.64	$3d^6$	^1I	6	$3d^5(^2I)4p$	$^3K^\circ$	7	R2*
377.7543	0.0010	377.75335	0.00056	22	-1.468	E	28697.33	293420.33	$3d^6$	$^3P_2$	1	$3d^5(^4P)4p$	$^3P^\circ$	1	R2
377.7953	0.0010	377.79461	0.00048	5	-1.526	E	57924.12	322618.21	$3d^6$	^1F	3	$3d^5(^4F)4p$	$^3D^\circ$	3	R2
378.054	0.003	378.05402	0.00062	7	-1.528	E	57924.12	322436.58	$3d^6$	^1F	3	$3d^5(^4F)4p$	$^3D^\circ$	2	d,R2
378.133	0.003	378.13162	0.00039	52	-0.598	E	41920.54	306378.72	$3d^6$	^3D	3	$3d^5(^4D)4p$	$^3P^\circ$	2	d,R2
378.379	0.003	378.37939	0.00059	19	-1.458	E	28697.33	292982.34	$3d^6$	$^3P_2$	1	$3d^5(^4P)4p$	$^3P^\circ$	2	H,R2
378.4848	0.0010	378.48462	0.00059	37	-0.887	E	41627.23	305838.76	$3d^6$	^3D	2	$3d^5(^4D)4p$	$^3P^\circ$	1	R2
378.591	0.003	378.59031	0.00070	15	-1.380	E	41700.99	305838.76	$3d^6$	^3D	1	$3d^5(^4D)4p$	$^3P^\circ$	1	d,R2
378.820	0.003	378.82126	0.00043	4	-1.922	E	27578.61	291555.35	$3d^6$	^3H	5	$3d^5(^4G)4p$	$^3F^\circ$	4	d,R2
379.0179	0.0010	379.01694	0.00040	31	-1.087	E	42208.47	306048.92	$3d^6$	$^1G_2$	4	$3d^5(^2I)4p$	$^3I^\circ$	5	R2
379.1038	0.0010	379.10368	0.00066	16	-1.539	E	29640.25	293420.33	$3d^6$	$^3P_2$	0	$3d^5(^4P)4p$	$^3P^\circ$	1	R2
379.225	0.003	379.22397	0.00042	19	-1.847	E	27858.94	291555.35	$3d^6$	^3H	4	$3d^5(^4G)4p$	$^3F^\circ$	4	p,R2
379.252	0.003	379.25350	0.00040	56	-0.536	E	33256.49	296932.37	$3d^6$	^3G	5	$3d^5(^4G)4p$	$^3G^\circ$	5	s,R2*
379.252	0.004	379.23871	0.00088	56	-1.241	E	41700.99	305387.15	$3d^6$	^3D	1	$3d^5(^4D)4p$	$^3P^\circ$	0	s,R2*
379.497	0.003	379.49594	0.00091	8	-1.923	E	29123.90	292631.33	$3d^6$	$^3F_2$	4	$3d^5(^4G)4p$	$^3H^\circ$	4	d,R2
379.550	0.003	379.55114	0.00044	7	-1.794	E	27858.94	291328.05	$3d^6$	^3H	4	$3d^5(^4G)4p$	$^3F^\circ$	3	d,R2
379.895	0.003	379.89627	0.00042	4	-2.032	E	29123.90	292353.65	$3d^6$	$^3F_2$	4	$3d^5(^4G)4p$	$^3H^\circ$	5	d,R2
380.037	0.003	380.03676	0.00049	3	-1.533	E	57924.12	321056.56	$3d^6$	^1F	3	$3d^5(^2G_2)4p$	$^3F^\circ$	4	d,R2

Table A.2 (cont'd)

λ_{obs} [a] (Å)	u_{obs} [b] (Å)	λ_{Ritz} [c] (Å)	u_{Ritz} [d] (Å)	I [e]	$\log(gf_R)$ [f]	$\log(gf_R)$ [g]	E_i [h] (cm^{-1})	E_k [i] (cm^{-1})	Lower Level Configuration	Term	J	Upper Level Configuration	Term [k]	J	Notes [j]
380.141	0.003	380.14062	0.00091	2	-2.331	E	29570.78	292631.33	$3d^6$	$^3F_2$	3	$3d^5(^4G)4p$	$^3H^\circ$	4	d,R2
380.417	0.003	380.41563	0.00038	27	-1.349	E	34061.99	296932.37	$3d^6$	^3G	4	$3d^5(^4G)4p$	$^3G^\circ$	5	p,R2
380.4331	0.0019	380.43428	0.00047	33	-1.123	E	34061.99	296919.48	$3d^6$	^3G	4	$3d^5(^4D)4p$	$^5D^\circ$	4	R2
380.4670	0.0010	380.46760	0.00038	37	-0.967	E	34061.99	296896.46	$3d^6$	^3G	4	$3d^5(^4G)4p$	$^3G^\circ$	4	R2
380.626	0.003	380.6268	0.0013	22	-1.190	E	66738.13	329462.64	$3d^6$	$^3P_1$	0	$3d^5(^2F_2)4p$	$^3D^\circ$	1	R2*
380.626	0.004	380.62583	0.00052	22	-1.830	E	26152.49	288877.70	$3d^6$	$^3P_2$	2	$3d^5(^4P)4p$	$^5S^\circ$	2	R2*
380.9202	0.0010	380.92096	0.00089	14	-1.031	E	69156.49	331678.14	$3d^6$	$^3P_1$	2	$3d^5(^2S)4p$	$^3P^\circ$	2	R2
380.947	0.004	380.94775	0.00054	6	-1.875	E	34416.29	296919.48	$3d^6$	^3G	3	$3d^5(^4D)4p$	$^5D^\circ$	4	d,R2
380.981	0.003	380.98116	0.00047	8	-1.673	E	34416.29	296896.46	$3d^6$	^3G	3	$3d^5(^4G)4p$	$^3G^\circ$	4	d,R2
381.052	0.003	381.05189	0.00040	62	-0.601	E	29123.90	291555.35	$3d^6$	$^3F_2$	4	$3d^5(^4G)4p$	$^3F^\circ$	4	R2*
381.052	0.003	381.05291	0.00071	62	-0.888	E	34416.29	296847.04	$3d^6$	^3G	3	$3d^5(^4G)4p$	$^3G^\circ$	3	R2*
381.3459	0.0010	381.34702	0.00067	21	-0.858	E	67548.05	329776.40	$3d^6$	$^3P_1$	1	$3d^5(^2F_2)4p$	$^3D^\circ$	2	R2
381.3801	0.0010	381.38222	0.00040	13	-1.593	E	29123.90	291328.05	$3d^6$	$^3F_2$	4	$3d^5(^4G)4p$	$^3F^\circ$	3	R2
381.576	0.004	381.5771	0.0039	2	-1.817	E	67548.05	329618.3	$3d^6$	$^3P_1$	1	$3d^5(^2S)4p$	$^3P^\circ$	0	G,R2
381.678	0.003	381.67563	0.00043	40	-1.053	E	57924.12	319926.70	$3d^6$	^1F	3	$3d^5(^2F_1)4p$	$^1D^\circ$	2	R2*
381.678	0.003	381.68054	0.00041	40	-0.870	E	68719.26	330718.47	$3d^6$	$^3F_1$	4	$3d^5(^2F_2)4p$	$^3G^\circ$	5	R2*
381.702	0.003	381.70187	0.00041	13	-1.718	E	29570.78	291555.35	$3d^6$	$^3F_2$	3	$3d^5(^4G)4p$	$^3F^\circ$	4	p,R2
382.0324	0.0010	382.03332	0.00040	50	-0.780	E	29570.78	291328.05	$3d^6$	$^3F_2$	3	$3d^5(^4G)4p$	$^3F^\circ$	3	R2
382.142	0.003	382.14152	0.00039	3	-2.120	E	33256.49	294939.65	$3d^6$	^3G	5	$3d^5(^4D)4p$	$^5F^\circ$	4	H,R2
382.294	0.003	382.29487	0.00060	2	-1.918	E	68719.26	330297.45	$3d^6$	$^3F_1$	4	$3d^5(^2F_2)4p$	$^3G^\circ$	4	H,R2
382.3700	0.0010	382.37009	0.00058	17	-1.479	E	29570.78	291097.51	$3d^6$	$^3F_2$	3	$3d^5(^4G)4p$	$^3F^\circ$	2	R2
382.4927	0.0010	382.49346	0.00056	31	-0.916	E	68855.07	330297.45	$3d^6$	$^3F_1$	3	$3d^5(^2F_2)4p$	$^3G^\circ$	4	R2
382.509	0.003	382.51265	0.00048	16	-1.789	E	29898.79	291328.05	$3d^6$	$^3F_2$	2	$3d^5(^4G)4p$	$^3F^\circ$	3	p,R2
382.788	0.003	382.78898	0.00066	12	-1.288	E	68632.25	329872.79	$3d^6$	$^3F_1$	2	$3d^5(^2F_2)4p$	$^3D^\circ$	3	d,R2
382.827	0.003	382.82666	0.00042	24	-1.271	E	57924.12	319138.95	$3d^6$	^1F	3	$3d^5(^2G_2)4p$	$^1G^\circ$	4	p,R2
382.8490	0.0010	382.85027	0.00060	48	-0.875	E	29898.79	291097.51	$3d^6$	$^3F_2$	2	$3d^5(^4G)4p$	$^3F^\circ$	2	R2
382.914	0.003	382.91652	0.00055	9	-1.362	E	68719.26	329872.79	$3d^6$	$^3F_1$	4	$3d^5(^2F_2)4p$	$^3D^\circ$	3	H,R2
383.167	0.003	383.16763	0.00058	8	-1.276	E	68632.25	329614.63	$3d^6$	$^3F_1$	2	$3d^5(^2F_2)4p$	$^3G^\circ$	3	d,R2
383.255	0.003	383.25728	0.00062	3	-1.460	E	68855.07	329776.40	$3d^6$	$^3F_1$	3	$3d^5(^2F_2)4p$	$^3D^\circ$	2	d,R2
383.293	0.003	383.29542	0.00043	5	-1.387	E	68719.26	329614.63	$3d^6$	$^3F_1$	4	$3d^5(^2F_2)4p$	$^3G^\circ$	3	H,R2
383.496	0.003	383.49505	0.00042	2	-1.802	E	68855.07	329614.63	$3d^6$	$^3F_1$	3	$3d^5(^2F_2)4p$	$^3G^\circ$	3	H,R2
383.5571	0.0010	383.55868	0.00053	23	-0.888	E	69156.49	329872.79	$3d^6$	$^3P_1$	2	$3d^5(^2F_2)4p$	$^3D^\circ$	3	R2
383.826	0.004	383.82727	0.00059	7	-2.120	E	27111.40	287645.26	$3d^6$	^3H	6	$3d^5(^4G)4p$	$^5H^\circ$	6	d,R2
383.9385	0.0010	383.93885	0.00044	22	-0.859	E	69156.49	329614.63	$3d^6$	$^3P_1$	2	$3d^5(^2F_2)4p$	$^3G^\circ$	3	R2
384.594	0.003	384.59121	0.00049	7	-2.268	E	27111.40	287127.74	$3d^6$	^3H	6	$3d^5(^4G)4p$	$^5H^\circ$	5	d,R2
385.245	0.003	385.24621	0.00074	2	-1.879	E	67548.05	327122.31	$3d^6$	$^3P_1$	1	$3d^5(^2F_2)4p$	$^1D^\circ$	2	H,R2

Table A.2 (cont'd)

λ_{obs} [a] (Å)	u_{obs} [b] (Å)	λ_{Ritz} [c] (Å)	u_{Ritz} [d] (Å)	I [e]	$\log(gf_R)$ [f]	$\log(gf_R)$ [g]	E_i [h] (cm^{-1})	E_k [i] (cm^{-1})	Lower Level Configuration	Term	J	Upper Level Configuration	Term [k]	J	Notes [j]
385.283	0.003	385.28361	0.00056	7	-2.165	E	41920.54	301469.60	$3d^6$	^3D	3	$3d^5(^4D)4p$	$^3F^\circ$	3	d,R2*
385.283	0.003	385.28351	0.00047	7	-2.348	E	27578.61	287127.74	$3d^6$	^3H	5	$3d^5(^4G)4p$	$^5H^\circ$	5	d,R2*
385.910	0.004	385.9098	0.0036	2	-2.325	E	27578.61	286706.5	$3d^6$	^3H	5	$3d^5(^4G)4p$	$^5H^\circ$	4	d,R2
386.044	0.003	386.04513	0.00043	2	-2.240	E	29123.90	288160.97	$3d^6$	$^3F_2$	4	$3d^5(^4G)4p$	$^5F^\circ$	4	H,R2
386.106	0.003	386.10316	0.00040	2	-2.024	E	41920.54	300918.68	$3d^6$	^3D	3	$3d^5(^4D)4p$	$^3F^\circ$	4	d,R2
386.196	0.003	386.1956	0.0010	9	-1.775	E	41627.23	300563.36	$3d^6$	^3D	2	$3d^5(^4D)4p$	$^3D^\circ$	1	d,R2
386.3059	0.0010	386.30567	0.00089	23	-1.335	E	41700.99	300563.36	$3d^6$	^3D	1	$3d^5(^4D)4p$	$^3D^\circ$	1	R2
386.6454	0.0010	386.64600	0.00042	48	-0.916	E	33256.49	291891.00	$3d^6$	^3G	5	$3d^5(^4G)4p$	$^3H^\circ$	6	R2
386.7019	0.0010	386.70142	0.00050	40	-0.939	E	41627.23	300224.68	$3d^6$	^3D	2	$3d^5(^4D)4p$	$^3D^\circ$	2	R2
386.738	0.003	386.73693	0.00047	12	-1.687	E	41627.23	300200.93	$3d^6$	^3D	2	$3d^5(^4D)4p$	$^5P^\circ$	3	d,R2
386.945	0.003	386.94518	0.00072	9	-1.872	E	67548.05	325982.59	$3d^6$	$^3P_1$	1	$3d^5(^2F_2)4p$	$^3F^\circ$	2	H,R2*
386.945	0.004	386.94350	0.00063	9	-2.483	E	27858.94	286294.60	$3d^6$	^3H	4	$3d^5(^4G)4p$	$^5H^\circ$	3	H,R2*
387.154	0.003	387.14844	0.00041	58	-0.959	E	33256.49	291555.35	$3d^6$	^3G	5	$3d^5(^4G)4p$	$^3F^\circ$	4	R2*
387.154	0.003	387.15923	0.00042	58	-1.057	E	34061.99	292353.65	$3d^6$	^3G	4	$3d^5(^4G)4p$	$^3H^\circ$	5	R2*
387.1761	0.0010	387.17612	0.00037	53	-0.716	E	41920.54	300200.93	$3d^6$	^3D	3	$3d^5(^4D)4p$	$^5P^\circ$	3	R2
387.2742	0.0010	387.27411	0.00087	34	-1.174	E	34416.29	292631.33	$3d^6$	^3G	3	$3d^5(^4G)4p$	$^3H^\circ$	4	R2
387.3595	0.0010	387.36064	0.00046	31	-0.758	E	68719.26	326876.62	$3d^6$	$^3F_1$	4	$3d^5(^2F_2)4p$	$^3F^\circ$	4	R2
387.5631	0.0010	387.56453	0.00046	13	-1.301	E	68855.07	326876.62	$3d^6$	$^3F_1$	3	$3d^5(^2F_2)4p$	$^3F^\circ$	4	R2
387.7711	0.0010	387.77061	0.00042	16	-0.999	E	68855.07	326739.49	$3d^6$	$^3F_1$	3	$3d^5(^2G_2)4p$	$^1F^\circ$	3	R2
388.224	0.003	388.22438	0.00046	2	-1.856	E	69156.49	326739.49	$3d^6$	$^3P_1$	2	$3d^5(^2G_2)4p$	$^1F^\circ$	3	H,R2*
388.224	0.004	388.2250	0.0037	2	-2.863	E	29123.90	286706.5	$3d^6$	$^3F_2$	4	$3d^5(^4G)4p$	$^5H^\circ$	4	H,R2*
388.3598	0.0010	388.35953	0.00040	13	-1.639	E	34061.99	291555.35	$3d^6$	^3G	4	$3d^5(^4G)4p$	$^3F^\circ$	4	R2
388.397	0.004	388.3964	0.0019	6	-2.318	E	27111.40	284580.3	$3d^6$	^3H	6	$3d^5(^4G)4p$	$^5G^\circ$	6	d,R2
388.503	0.003	388.50342	0.00063	12	-1.207	E	68632.25	326030.24	$3d^6$	$^3F_1$	2	$3d^5(^2F_2)4p$	$^3F^\circ$	3	d,R2
388.5756	0.0010	388.57536	0.00060	36	-0.606	E	68632.25	325982.59	$3d^6$	$^3F_1$	2	$3d^5(^2F_2)4p$	$^3F^\circ$	2	R2
388.7017	0.0010	388.70265	0.00040	28	-1.203	E	34061.99	291328.05	$3d^6$	^3G	4	$3d^5(^4G)4p$	$^3F^\circ$	3	R2
388.841	0.003	388.84003	0.00048	21	-0.935	E	68855.07	326030.24	$3d^6$	$^3F_1$	3	$3d^5(^2F_2)4p$	$^3F^\circ$	3	d,R2
389.0265	0.0010	389.02609	0.00049	24	-1.270	E	41920.54	298972.71	$3d^6$	^3D	3	$3d^5(^4D)4p$	$^3D^\circ$	3	R2
389.239	0.003	389.23870	0.00050	10	-1.788	E	34416.29	291328.05	$3d^6$	^3G	3	$3d^5(^4G)4p$	$^3F^\circ$	3	H,R2
389.259	0.003	389.25776	0.00077	8	-1.702	E	41700.99	298600.17	$3d^6$	^3D	1	$3d^5(^4P)4p$	$^3D^\circ$	1	H,R2
389.350	0.003	389.34795	0.00047	23	-1.043	E	68719.26	325558.93	$3d^6$	$^3F_1$	4	$3d^5(^2F_2)4p$	$^1G^\circ$	4	p,R2
389.365	0.003	389.36557	0.00065	26	-0.726	E	77900.04	334728.09	$3d^6$	$^1G_1$	4	$3d^5(^2F_2)4p$	$^1F^\circ$	3	d,R2*
389.365	0.004	389.37163	0.00098	26	-2.703	E	27578.61	284402.66	$3d^6$	^3H	5	$3d^5(^4G)4p$	$^5G^\circ$	5	d,R2*
389.554	0.003	389.55394	0.00047	6	-1.592	E	68855.07	325558.93	$3d^6$	$^3F_1$	3	$3d^5(^2F_2)4p$	$^1G^\circ$	4	d,R2
389.588	0.003	389.58830	0.00068	25	-1.307	E	34416.29	291097.51	$3d^6$	^3G	3	$3d^5(^4G)4p$	$^3F^\circ$	2	d,R2
389.855	0.003	389.85659	0.00056	16	-1.033	E	68719.26	325223.84	$3d^6$	$^3F_1$	4	$3d^5(^2G_2)4p$	$^3G^\circ$	4	l,R2

Table A.2 (cont'd)

λ_{obs} [a] (Å)	u_{obs} [b] (Å)	λ_{Ritz} [c] (Å)	u_{Ritz} [d] (Å)	I [e]	$\log(gf_R)$ [f]	$\log(gf_R)$ [g]	E_i [h] (cm^{-1})	E_k [i] (cm^{-1})	Lower Level Configuration	Term	J	Upper Level Configuration	Term [k]	J	Notes [j]
390.082	0.003	390.08350	0.00065	13	-2.043	E	41627.23	297982.60	$3d^6$	^3D	2	$3d^5(^4D)4p$	$^5P°$	1	s,R2*
390.082	0.003	390.08082	0.00055	13	-1.422	E	68855.07	325212.20	$3d^6$	$^3F_1$	3	$3d^5(^2G_2)4p$	$^3G°$	3	s,R2*
390.158	0.003	390.15806	0.00077	9	-1.494	E	67548.05	323854.43	$3d^6$	$^3P_1$	1	$3d^5(^4F)4p$	$^3F°$	2	d,R2
390.197	0.003	390.19577	0.00068	9	-1.775	E	41700.99	297982.60	$3d^6$	^3D	1	$3d^5(^4D)4p$	$^5P°$	1	d,R2
390.2259	0.0010	390.22630	0.00040	18	-1.077	E	68719.26	324980.8	$3d^6$	$^3F_1$	4	$3d^5(^2G_2)4p$	$^3G°$	5	R2
390.2492	0.0010	390.24910	0.00085	15	-1.164	E	66738.13	322984.72	$3d^6$	$^3P_1$	0	$3d^5(^4F)4p$	$^3D°$	1	R2
390.296	0.003	390.29639	0.00054	9	-1.656	E	41627.23	297842.77	$3d^6$	^3D	2	$3d^5(^4P)4p$	$^3D°$	2	H,R2
390.410	0.003	390.40878	0.00059	3	-2.178	E	41700.99	297842.77	$3d^6$	^3D	1	$3d^5(^4P)4p$	$^3D°$	2	G,R2
390.744	0.003	390.74370	0.00046	5	-1.977	E	41920.54	297842.77	$3d^6$	^3D	3	$3d^5(^4P)4p$	$^3D°$	2	d,R2
390.943	0.003	390.94357	0.00058	3	-2.075	E	41627.23	297418.62	$3d^6$	^3D	2	$3d^5(^4P)4p$	$^3D°$	3	H,R2
391.1772	0.0010	391.17679	0.00090	30	-0.284	E	104421.97	360060.86	$3d^6$	$^1D_1$	2	$3d^5(^2G_1)4p$	$^1F°$	3	R2
391.3937	0.0010	391.39237	0.00048	12	-1.563	E	41920.54	297418.62	$3d^6$	^3D	3	$3d^5(^4P)4p$	$^3D°$	3	R2
391.487	0.003	391.48647	0.00097	13	-1.265	E	67548.05	322984.72	$3d^6$	$^3P_1$	1	$3d^5(^4F)4p$	$^3D°$	1	H,R2
391.816	0.003	391.81548	0.00070	23	-0.983	E	68632.25	323854.43	$3d^6$	$^3F_1$	2	$3d^5(^4F)4p$	$^3F°$	2	d,R2
392.0104	0.0010	392.00945	0.00070	48	-0.406	E	77900.04	332995.93	$3d^6$	$^1G_1$	4	$3d^5(^2H)4p$	$^1G°$	4	R2
392.1593	0.0010	392.15785	0.00055	25	-0.988	E	68855.07	323854.43	$3d^6$	$^3F_1$	3	$3d^5(^4F)4p$	$^3F°$	2	R2
392.328	0.003	392.32836	0.00082	25	-1.084	E	67548.05	322436.58	$3d^6$	$^3P_1$	1	$3d^5(^4F)4p$	$^3D°$	2	d,R2
392.4576	0.0010	392.45708	0.00050	31	-0.842	E	68719.26	323524.19	$3d^6$	$^3F_1$	4	$3d^5(^4F)4p$	$^3F°$	3	R2
392.623	0.003	392.62194	0.00061	8	-1.832	E	69156.49	323854.43	$3d^6$	$^3P_1$	2	$3d^5(^4F)4p$	$^3F°$	2	G,R2
392.669	0.003	392.66637	0.00052	37	-0.785	E	68855.07	323524.19	$3d^6$	$^3F_1$	3	$3d^5(^4F)4p$	$^3F°$	3	p,R2
393.134	0.003	393.13168	0.00056	19	-1.193	E	69156.49	323524.19	$3d^6$	$^3P_1$	2	$3d^5(^4F)4p$	$^3F°$	3	d,R2
393.1550	0.0010	393.15521	0.00078	25	-0.955	E	68632.25	322984.72	$3d^6$	$^3F_1$	2	$3d^5(^4F)4p$	$^3D°$	1	R2
393.210	0.004	393.2100	0.0039	10	-2.478	E	29898.79	284215.8	$3d^6$	$^3F_2$	2	$3d^5(^4G)4p$	$^5G°$	2	G,R2
393.5429	0.0010	393.54210	0.00040	44	-0.495	E	68719.26	322821.68	$3d^6$	$^3F_1$	4	$3d^5(^4F)4p$	$^3F°$	4	R2
393.573	0.003	393.57085	0.00053	14	-1.525	E	57924.12	312007.98	$3d^6$	^1F	3	$3d^5(^2F_1)4p$	$^1G°$	4	d,R2
393.8582	0.0010	393.85748	0.00051	24	-1.045	E	68719.26	322618.21	$3d^6$	$^3F_1$	4	$3d^5(^4F)4p$	$^3D°$	3	R2
393.9137	0.0010	393.91366	0.00054	70	-0.313	E	0.00	253862.74	$3d^6$	^5D	4	$3d^5(^6S)4p$	$^5P°$	3	R2
394.005	0.003	394.00431	0.00077	13	-1.348	E	68632.25	322436.58	$3d^6$	$^3F_1$	2	$3d^5(^4F)4p$	$^3D°$	2	d,R2
394.070	0.003	394.06826	0.00055	18	-1.100	E	68855.07	322618.21	$3d^6$	$^3F_1$	3	$3d^5(^4F)4p$	$^3D°$	3	d,R2
394.3126	0.0010	394.31236	0.00049	66	-0.606	E	889.61	254495.66	$3d^6$	^5D	3	$3d^5(^6S)4p$	$^5P°$	2	R2
394.3502	0.0010	394.35052	0.00061	26	-1.053	E	68855.07	322436.58	$3d^6$	$^3F_1$	3	$3d^5(^4F)4p$	$^3D°$	2	R2
394.5372	0.0010	394.53689	0.00053	27	-0.933	E	69156.49	322618.21	$3d^6$	$^3P_1$	2	$3d^5(^4F)4p$	$^3D°$	3	R2
394.6406	0.0010	394.64097	0.00053	52	-1.035	E	1489.82	254884.70	$3d^6$	^5D	2	$3d^5(^6S)4p$	$^5P°$	1	R2
394.819	0.003	394.81982	0.00069	9	-1.433	E	69156.49	322436.58	$3d^6$	$^3P_1$	2	$3d^5(^4F)4p$	$^3D°$	2	d,R2
395.242	0.003	395.23611	0.00057	66	-0.927	E	1871.38	254884.70	$3d^6$	^5D	1	$3d^5(^6S)4p$	$^5P°$	1	w,R2*
395.242	0.003	395.24779	0.00054	66	-0.813	E	1489.82	54495.66	$3d^6$	^5D	2	$3d^5(^6S)4p$	$^5P°$	2	w,R2*

Table A.2 (cont'd)

λ_{obs} [a] (Å)	u_{obs} [b] (Å)	λ_{Ritz} [c] (Å)	u_{Ritz} [d] (Å)	I [e]	$\log(gf_R)$ [f]	$\log(gf_R)$ [g]	E_i [h] (cm^{-1})	E_k [i] (cm^{-1})	Lower Level Configuration	Term	J	Upper Level Configuration	Term [k]	J	Notes [j]
395.2991	0.0010	395.29890	0.00049	58	-0.905	E	889.61	53862.74	$3d^6$	^5D	3	$3d^5(^6S)4p$	$^5P°$	3	R2
395.5266	0.0010	395.52709	0.00068	42	-1.280	E	2057.52	254884.70	$3d^6$	^5D	0	$3d^5(^6S)4p$	$^5P°$	1	R2
395.8451	0.0010	395.84477	0.00056	34	-1.405	E	1871.38	254495.66	$3d^6$	^5D	1	$3d^5(^6S)4p$	$^5P°$	2	R2
396.239	0.003	396.23903	0.00054	21	-1.754	E	1489.82	253862.74	$3d^6$	^5D	2	$3d^5(^6S)4p$	$^5P°$	3	w,R2
396.256	0.003	396.25427	0.00069	7	-1.562	E	68719.26	321082.47	$3d^6$	$^3F_1$	4	$3d^5(^2F_1)4p$	$^1F°$	3	p,R2
397.015	0.003	397.01119	0.00069	3	-1.884	E	68632.25	320514.32	$3d^6$	$^3F_1$	2	$3d^5(^2G_2)4p$	$^3F°$	3	G,R2
398.336	0.003	398.33594	0.00075	10	-1.528	E	68855.07	319899.45	$3d^6$	$^3F_1$	3	$3d^5(^4F)4p$	$^3G°$	4	p,R2
398.514	0.003	398.51135	0.00044	23	-1.324	E	68719.26	319653.14	$3d^6$	$^3F_1$	4	$3d^5(^4F)4p$	$^3G°$	5	d,R2
400.481	0.003	400.47926	0.00057	31	-1.003	E	41627.23	291328.05	$3d^6$	^3D	2	$3d^5(^4G)4p$	$^3F°$	3	s,R2
400.5876	0.0010	400.58516	0.00045	41	-0.829	E	41920.54	291555.35	$3d^6$	^3D	3	$3d^5(^4G)4p$	$^3F°$	4	R2
400.871	0.003	400.87016	0.00059	25	-0.786	E	77900.04	327357.37	$3d^6$	$^1G_1$	4	$3d^5(^2H)4p$	$^1H°$	5	s,R2
400.952	0.003	400.95024	0.00048	12	-1.921	E	41920.54	291328.05	$3d^6$	^3D	3	$3d^5(^4G)4p$	$^3F°$	3	p,R2
400.9692	0.0010	400.96790	0.00067	26	-1.157	E	41700.99	291097.51	$3d^6$	^3D	1	$3d^5(^4G)4p$	$^3F°$	2	R2
401.644	0.003	401.64420	0.00064	2	-1.545	E	77900.04	326876.62	$3d^6$	$^1G_1$	4	$3d^5(^2F_2)4p$	$^3F°$	4	H,R2
402.024	0.003	402.02060	0.00074	2	-1.770	E	68632.25	317375.72	$3d^6$	$^3F_1$	2	$3d^5(^2H)4p$	$^3G°$	3	d,R2
402.5152	0.0010	402.51435	0.00058	21	-0.607	E	77900.04	326338.39	$3d^6$	$^1G_1$	4	$3d^5(^2G_2)4p$	$^1H°$	5	R2
403.172	0.003	403.17115	0.00048	6	-1.575	E	68855.07	316888.69	$3d^6$	$^3F_1$	3	$3d^5(^2H)4p$	$^3G°$	4	d,R2
403.211	0.003	403.21524	0.00053	5	-1.462	E	68719.26	316725.76	$3d^6$	$^3F_1$	4	$3d^5(^2H)4p$	$^3G°$	5	d,R2
403.781	0.003	403.78118	0.00063	6	-1.355	E	77900.04	325558.93	$3d^6$	$^1G_1$	4	$3d^5(^2F_2)4p$	$^1G°$	4	d,R2
404.954	0.003	404.9559	0.0011	2	-2.558	E	66738.13	313678.60	$3d^6$	$^3P_1$	0	$3d^5(^2D_3)4p$	$^3D°$	1	d,bl,R2
407.953	0.003	407.9564	0.0014	11	-0.983	E	104421.97	349546.19	$3d^6$	$^1D_1$	2	$3d^5(^2D_2)4p$	$^1D°$	2	d,R2
408.443	0.003	408.44364	0.00079	8	-2.398	E	68855.07	313686.89	$3d^6$	$^3F_1$	3	$3d^5(^2D_3)4p$	$^3D°$	2	d,bl,R2
409.127	0.003	409.13530	0.00087	2	-2.121	E	67548.05	311965.97	$3d^6$	$^3P_1$	1	$3d^5(^2D_3)4p$	$^3P°$	2	H,R2
409.451	0.003	409.44312	0.00050	8	-1.817	E	68719.26	312953.43	$3d^6$	$^3F_1$	4	$3d^5(^2F_1)4p$	$^3D°$	3	H,R2
410.494	0.004	410.4942	0.0039	18	-2.238	E	0.00	243608.8	$3d^6$	^5D	4	$3d^5(^6S)4p$	$^7P°$	3	d,R2
413.320	0.004	413.3163	0.0022	22	-2.833	E	889.61	242835.05	$3d^6$	^5D	3	$3d^5(^6S)4p$	$^7P°$	2	d,bl,R2
414.343	0.004	414.3442	0.0022	2	-3.086	E	1489.82	242835.05	$3d^6$	^5D	2	$3d^5(^6S)4p$	$^7P°$	2	G,R2
418.237	0.003	418.2339	0.0012	7	-1.713	E	66738.13	305838.76	$3d^6$	$^3P_1$	0	$3d^5(^4D)4p$	$^3P°$	1	H,bl,R2
418.704	0.003	418.70669	0.00079	12	-1.457	E	67548.05	306378.72	$3d^6$	$^3P_1$	1	$3d^5(^4D)4p$	$^3P°$	2	w,R2
420.455	0.004	420.4523	0.0012	5	-1.615	E	67548.05	305387.15	$3d^6$	$^3P_1$	1	$3d^5(^4D)4p$	$^3P°$	0	d,R2
421.5473	0.0010	421.54565	0.00055	12	-1.123	E	69156.49	306378.72	$3d^6$	$^3P_1$	2	$3d^5(^4D)4p$	$^3P°$	2	R2
422.510	0.003	422.50736	0.00082	5	-1.375	E	69156.49	305838.76	$3d^6$	$^3P_1$	2	$3d^5(^4D)4p$	$^3P°$	1	d,R2
424.273	0.003	424.26580	0.00085	2	-1.410	E	67548.05	303249.35	$3d^6$	$^3P_1$	1	$3d^5(^4P)4p$	$^3S°$	1	H,R2
990.816	0.022	990.8156	0.0033	3	-1.606	E	216590.56	317517.50	$3d^5(^4D)4s$	^5D	2	$3d^5(^4F)4p$	$^5D°$	2	d,R4
990.867	0.022	990.8713	0.0031	9	-1.557	E	216596.2	317517.50	$3d^5(^4D)4s$	^5D	3	$3d^5(^4F)4p$	$^5D°$	2	R4
993.683	0.022	993.6806	0.0025	11	-1.361	E	216596.2	317232.17	$3d^5(^4D)4s$	^5D	3	$3d^5(^4F)4p$	$^5D°$	3	d,R4

Table A.2 (cont'd)

λ_{obs} [a] (Å)	u_{obs} [b] (Å)	λ_{Ritz} [c] (Å)	u_{Ritz} [d] (Å)	I [e]	$\log(gf_R)$ [f]	$\log(gf_R)$ [g]	E_i [h] (cm^{-1})	E_k [i] (cm^{-1})	Lower Level Configuration	Term	J	Upper Level Configuration	Term [k]	J	Notes [j]
1002.410	0.022	1002.4196	0.0027	18	-1.161	E	217130.07	316888.69	$3d^5(^4G)4s$	^3G	4	$3d^5(^2H)4p$	$^3G°$	4	R4
1003.233	0.022	1003.2499	0.0031	27	-1.057	E	217049.7	316725.76	$3d^5(^4G)4s$	^3G	5	$3d^5(^2H)4p$	$^3G°$	5	R4
1008.269	0.022	1008.2699	0.0056	14	-1.317	E	217100.94	316280.73	$3d^5(^4G)4s$	^3G	3	$3d^5(^2F_1)4p$	$^3F°$	3	d,R4
1010.338	0.022	1010.3184	0.0027	54	-0.931	E	216189.97	315168.67	$3d^5(^4D)4s$	^5D	4	$3d^5(^4F)4p$	$^5F°$	5	R4
1020.382	0.022	1020.3773	0.0022	34	-0.979	E	216596.2	314599.18	$3d^5(^4D)4s$	^5D	3	$3d^5(^4F)4p$	$^5F°$	4	R4
1020.707	0.022	1020.7085	0.0027	32	-0.977	E	216590.56	314561.71	$3d^5(^4D)4s$	^5D	2	$3d^5(^4F)4p$	$^5F°$	3	R4
1021.536	0.022	1021.5524	0.0064	14	-1.023	E	251655.96	349546.19	$3d^5(^2F_2)4s$	^1F	3	$3d^5(^2D_2)4p$	$^1D°$	2	R4
1024.462	0.022	1024.4658	0.0022	5	-1.453	E	216596.2	314208.06	$3d^5(^4D)4s$	^5D	3	$3d^5(^2F_1)4p$	$^3F°$	4	R4
1026.306	0.022	1026.2829	0.0070	28	-1.168	E	225545.70	322984.72	$3d^5(^4D)4s$	^3D	1	$3d^5(^4F)4p$	$^3D°$	1	R4
1026.504	0.022	1026.5245	0.0033	22	-0.940	E	225202.1	322618.21	$3d^5(^4D)4s$	^3D	3	$3d^5(^4F)4p$	$^3D°$	3	R4
1043.230	0.022	1043.2485	0.0032	15	-1.020	E	225202.1	321056.56	$3d^5(^4D)4s$	^3D	3	$3d^5(^2G_2)4p$	$^3F°$	4	R4
1044.633	0.022	1044.6252	0.0050	2	-1.567	E	247165.79	342893.90	$3d^5(^2F_2)4s$	^3F	2	$3d^5(^2D_2)4p$	$^3F°$	2	G,R4
1047.429	0.022	1047.4238	0.0053	55	-1.025	E	225545.70	321018.04	$3d^5(^4D)4s$	^3D	1	$3d^5(^2G_2)4p$	$^3F°$	2	R4
1058.190	0.022	1058.2045	0.0029	11	-1.262	E	229409.73	323909.42	$3d^5(^2I)4s$	^3I	6	$3d^5(^2G_2)4p$	$^3H°$	5	d,R4
1064.534	0.022	1064.5452	0.0026	10	-1.145	E	225202.1	319138.95	$3d^5(^4D)4s$	^3D	3	$3d^5(^2G_2)4p$	$^1G°$	4	R4
1074.646	0.022	1074.634	0.010	15	-0.846	E	253905.16	346960.07	$3d^5(^2S)4s$	^3S	1	$3d^5(^2D_2)4p$	$^3P°$	1	R4
1075.182	0.022	1075.1774	0.0097	30	-0.577	E	253905.16	346913.07	$3d^5(^2S)4s$	^3S	1	$3d^5(^2D_2)4p$	$^3P°$	2	G,R4
1081.097	0.022	1081.1005	0.0029	64	-0.357	E	233840.06	326338.39	$3d^5(^2I)4s$	^1I	6	$3d^5(^2G_2)4p$	$^1H°$	5	p,R4
1089.481	0.022	1089.4848	0.0087	17	-0.656	E	268274.36	360060.86	$3d^5(^2D_2)4s$	^1D	2	$3d^5(^2G_1)4p$	$^1F°$	3	R4
1094.767	0.022	1094.7911	0.0054	23	-0.881	E	229441.11	320782.74	$3d^5(^2I)4s$	^3I	7	$3d^5(^2H)4p$	$^3I°$	7	R4
1105.561	0.022	1105.5706	0.0034	60	-1.012	E	229409.73	319860.76	$3d^5(^2I)4s$	^3I	6	$3d^5(^2H)4p$	$^3I°$	6	d,bl,R4
1115.387	0.013	1115.2740	0.0040	42	-0.948	E	229413.82	319077.89	$3d^5(^2I)4s$	^3I	5	$3d^5(^2H)4p$	$^3I°$	5	R3
1119.334	0.025	1119.325	0.017	58	-1.449	E	164523.18	253862.74	$3d^5(^6S)4s$	^7S	3	$3d^5(^6S)4p$	$^5P°$	3	s,R3
1120.883	0.013	1120.8905	0.0045	82	-0.208	E	241082.67	330297.45	$3d^5(^2H)4s$	^3H	5	$3d^5(^2F_2)4p$	$^3G°$	4	R3
1124.300	0.013	1124.2842	0.0030	82	-0.037	E	241772.99	330718.47	$3d^5(^2H)4s$	^3H	6	$3d^5(^2F_2)4p$	$^3G°$	5	R3
1125.042	0.013	1125.0396	0.0067	54	-1.312	E	208046.61	296932.37	$3d^5(^4G)4s$	^5G	6	$3d^5(^4G)4p$	$^3G°$	5	R3
1135.009	0.025	1135.0045	0.0022	44	-1.056	E	212095.56	300200.93	$3d^5(^4P)4s$	^5P	3	$3d^5(^4D)4p$	$^5P°$	3	s,R3
1137.818	0.025	1137.8273	0.0045	18	-1.514	E	229441.11	317327.91	$3d^5(^2I)4s$	^3I	7	$3d^5(^2H)4p$	$^3H°$	6	p,R3
1139.044	0.025	1139.0454	0.0046	53	-0.698	E	242504.64	330297.45	$3d^5(^2G_2)4s$	^3G	4	$3d^5(^2F_2)4p$	$^3G°$	4	s,R3
1141.129	0.025	1141.1403	0.0040	9	-1.197	E	239107.85	326739.49	$3d^5(^2D_3)4s$	^1D	2	$3d^5(^2G_2)4p$	$^1F°$	3	d,R3
1141.747	0.025	1141.7843	0.0041	2	-0.987	E	242290.58	329872.79	$3d^5(^2G_2)4s$	^3G	3	$3d^5(^2F_2)4p$	$^3D°$	3	d,R3
1143.565	0.025	1143.5643	0.0039	5	-1.053	E	247282.20	334728.09	$3d^5(^2F_2)4s$	^3F	4	$3d^5(^2F_2)4p$	$^1F°$	3	d,R3
1144.186	0.013	1144.1941	0.0073	69	-0.733	E	208046.61	295444.37	$3d^5(^4G)4s$	^5G	6	$3d^5(^4D)4p$	$^5F°$	5	R3
1144.591	0.013	1144.5819	0.0040	45	-0.606	E	242504.64	329872.79	$3d^5(^2G_2)4s$	^3G	4	$3d^5(^2F_2)4p$	$^3D°$	3	R3
1145.307	0.025	1145.3006	0.0040	45	-1.355	E	208131.05	295444.37	$3d^5(^4G)4s$	^5G	5	$3d^5(^4D)4p$	$^5F°$	5	l,R3
1149.878	0.013	1149.8819	0.0047	31	-0.941	E	243332.00	330297.45	$3d^5(^4F)4s$	^3F	4	$3d^5(^2F_2)4p$	$^3G°$	4	R3

Table A.2 (cont'd)

λ_{obs} [a] (Å)	u_{obs} [b] (Å)	λ_{Ritz} [c] (Å)	u_{Ritz} [d] (Å)	I [e]	$\log(gf_R)$ [f]	$\log(gf_R)$ [g]	E_i [h] (cm^{-1})	E_k [i] (cm^{-1})	Lower Level Configuration	Term	J	Upper Level Configuration	Term [k]	J	Notes [j]
1150.085	0.013	1150.0826	0.0031	54	-0.853	E	212095.56	299045.83	$3d^5(^4P)4s$	^5P	3	$3d^5(^4D)4p$	$^5P^\circ$	2	R3
1150.471	0.025	1150.4516	0.0046	17	-1.499	E	239107.85	326030.24	$3d^5(^2D_3)4s$	^1D	2	$3d^5(^2F_2)4p$	$^3F^\circ$	3	d,R3
1151.055	0.025	1151.0826	0.0050	69	-1.062	E	239107.85	325982.59	$3d^5(^2D_3)4s$	^1D	2	$3d^5(^2F_2)4p$	$^3F^\circ$	2	z,R3*
1151.055	0.025	1151.0505	0.0040	69	-0.720	E	212095.56	298972.71	$3d^5(^4P)4s$	^5P	3	$3d^5(^4D)4p$	$^3D^\circ$	3	z,R3*
1151.961	0.013	1151.9596	0.0033	66	-0.752	E	208131.05	294939.65	$3d^5(^4G)4s$	^5G	5	$3d^5(^4D)4p$	$^5F^\circ$	4	R3
1152.168	0.013	1152.1718	0.0036	31	-1.267	E	212253.22	299045.83	$3d^5(^4P)4s$	^5P	2	$3d^5(^4D)4p$	$^5P^\circ$	2	R3
1152.392	0.025	1152.3978	0.0041	46	-1.202	E	208164.06	294939.65	$3d^5(^4G)4s$	^5G	4	$3d^5(^4D)4p$	$^5F^\circ$	4	p,R3
1152.522	0.025	1152.5538	0.0049	49	-1.334	E	225202.1	311965.97	$3d^5(^4D)4s$	^3D	3	$3d^5(^2D_3)4p$	$^3P^\circ$	2	G,R3
1152.676	0.013	1152.6815	0.0058	78	-0.022	E	246241.70	332995.93	$3d^5(^2H)4s$	^1H	5	$3d^5(^2H)4p$	$^1G^\circ$	4	R3
1153.983	0.025	1153.9933	0.0032	7	-1.342	E	229413.82	316069.44	$3d^5(^2I)4s$	^3I	5	$3d^5(^2F_1)4p$	$^3G^\circ$	4	d,R3
1154.877	0.025	1154.8579	0.0045	28	-1.853	E	212455.09	299045.83	$3d^5(^4P)4s$	^5P	1	$3d^5(^4D)4p$	$^5P^\circ$	2	H,R3
1155.460	0.025	1155.4646	0.0026	4	-1.309	E	240194.22	326739.49	$3d^5(^2F_1)4s$	^1F	3	$3d^5(^2G_2)4p$	$^1F^\circ$	3	d,R3
1155.918	0.025	1155.9400	0.0062	3	-1.493	E	243266.72	329776.40	$3d^5(^4F)4s$	^3F	2	$3d^5(^2F_2)4p$	$^3D^\circ$	2	w,R3
1157.332	0.013	1157.3151	0.0056	15	-0.930	E	243369.51	329776.40	$3d^5(^4F)4s$	^3F	3	$3d^5(^2F_2)4p$	$^3D^\circ$	2	R3
1157.439	0.013	1157.4432	0.0027	26	-1.662	E	240960.04	327357.37	$3d^5(^2H)4s$	^3H	4	$3d^5(^2H)4p$	$^1H^\circ$	5	R3
1158.116	0.025	1158.0976	0.0056	42	-1.349	E	225617.46	311965.97	$3d^5(^4D)4s$	^3D	2	$3d^5(^2D_3)4p$	$^3P^\circ$	2	z,R3*
1158.116	0.025	1158.1185	0.0061	42	-1.136	E	212253.22	298600.17	$3d^5(^4P)4s$	^5P	2	$3d^5(^4P)4p$	$^3D^\circ$	1	z,R3*
1158.116	0.025	1158.1056	0.0047	42	-1.271	E	243266.72	329614.63	$3d^5(^4F)4s$	^3F	2	$3d^5(^2F_2)4p$	$^3G^\circ$	3	z,R3*
1159.010	0.025	1159.041	0.010	79	-1.152	E	208165.11	294443.35	$3d^5(^4G)4s$	^5G	3	$3d^5(^4D)4p$	$^5F^\circ$	3	s,z,R3*
1159.010	0.025	1159.0267	0.0061	79	-0.750	E	208164.06	294443.35	$3d^5(^4G)4s$	^5G	4	$3d^5(^4D)4p$	$^5F^\circ$	3	s,z,R3*
1159.510	0.013	1159.4859	0.0041	19	-1.087	E	243369.51	329614.63	$3d^5(^4F)4s$	^3F	3	$3d^5(^2F_2)4p$	$^3G^\circ$	3	R3
1160.109	0.025	1160.148	0.011	32	-1.009	E	243266.72	329462.64	$3d^5(^4F)4s$	^3F	2	$3d^5(^2F_2)4p$	$^3D^\circ$	1	d,bl,R3
1163.351	0.025	1163.3767	0.0035	13	-1.426	E	229413.82	315370.50	$3d^5(^2I)4s$	^3I	5	$3d^5(^2G_2)4p$	$^3H^\circ$	4	d,R3
1163.512	0.013	1163.5169	0.0058	45	-0.505	E	247049.61	332995.93	$3d^5(^2G_2)4s$	^1G	4	$3d^5(^2H)4p$	$^1G^\circ$	4	R3
1163.677	0.013	1163.6836	0.0049	26	-1.237	E	208152.08	294086.09	$3d^5(^4G)4s$	^5G	2	$3d^5(^4D)4p$	$^5F^\circ$	2	R3
1163.854	0.013	1163.8601	0.0095	63	-0.726	E	208165.11	294086.09	$3d^5(^4G)4s$	^5G	3	$3d^5(^4D)4p$	$^5F^\circ$	2	R3
1165.585	0.025	1165.5833	0.0034	7	-1.284	E	241082.67	326876.62	$3d^5(^2H)4s$	^3H	5	$3d^5(^2F_2)4p$	$^3F^\circ$	4	d,R3
1165.850	0.025	1165.8601	0.0058	18	-1.120	E	234125.87	319899.45	$3d^5(^4F)4s$	^5F	4	$3d^5(^4F)4p$	$^3G^\circ$	4	d,R3
1166.215	0.025	1166.2186	0.0034	24	-1.178	E	212095.56	297842.77	$3d^5(^4P)4s$	^5P	3	$3d^5(^4P)4p$	$^3D^\circ$	2	R3
1166.464	0.025	1166.4613	0.0050	32	-1.003	E	212253.22	297982.60	$3d^5(^4P)4s$	^5P	2	$3d^5(^4D)4p$	$^5P^\circ$	1	R3
1166.672	0.025	1166.6742	0.0058	37	-0.569	E	247282.20	332995.93	$3d^5(^2F_2)4s$	^3F	4	$3d^5(^2H)4p$	$^1G^\circ$	4	s,R3
1167.102	0.025	1167.107	0.017	65	-0.749	E	208152.08	293834.0	$3d^5(^4G)4s$	^5G	2	$3d^5(^4D)4p$	$^5F^\circ$	1	R3
1167.882	0.025	1167.8948	0.0061	2	-1.852	E	234275.30	319899.45	$3d^5(^4F)4s$	^5F	3	$3d^5(^4F)4p$	$^3G^\circ$	4	d,R3
1168.155	0.025	1168.1588	0.0059	5	-1.614	E	212455.09	298059.89	$3d^5(^4P)4s$	^5P	1	$3d^5(^4D)4p$	$^5D^\circ$	0	d,R3
1168.615	0.013	1168.6340	0.0027	39	-0.759	E	234083.15	319653.14	$3d^5(^4F)4s$	^5F	5	$3d^5(^4F)4p$	$^3G^\circ$	5	R3
1170.243	0.013	1170.255	0.010	29	-0.192	E	306962.95	392414.38	$3d^5(^2D_1)4s$	^3D	3	$3d^5(^2D_1)4p$	$^3P^\circ$	2	R3

Table A.2 (cont'd)

λ_{obs} [a] (Å)	u_{obs} [b] (Å)	λ_{Ritz} [c] (Å)	u_{Ritz} [d] (Å)	I [e]	$\log(gf_R)$ [f]	$\log(gf_R)$ [g]	E_i [h] (cm^{-1})	E_k [i] (cm^{-1})	Lower Level Configuration	Term	J	Upper Level Configuration	Term [k]	J	Notes [j]
1171.127	0.025	1171.1291	0.0049	45	-0.923	E	212455.09	297842.77	$3d^5(^4P)4s$	^5P	1	$3d^5(^4P)4p$	$^3D^\circ$	2	z,R3*
1171.127	0.025	1171.117	0.019	45	-0.736	E	307025.84	392414.38	$3d^5(^2D_1)4s$	^3D	2	$3d^5(^2D_1)4p$	$^3P^\circ$	2	z,R3*
1171.439	0.013	1171.4443	0.0032	35	-1.073	E	240194.22	325558.93	$3d^5(^2F_1)4s$	^1F	3	$3d^5(^2F_2)4p$	$^1G^\circ$	4	R3
1171.701	0.013	1171.6994	0.0056	24	-1.413	E	235736.35	321082.47	$3d^5(^2F_1)4s$	^3F	2	$3d^5(^2F_1)4p$	$^1F^\circ$	3	R3
1172.117	0.025	1172.1169	0.0045	15	-1.261	E	229441.11	314756.83	$3d^5(^2I)4s$	^3I	7	$3d^5(^4F)4p$	$^5G^\circ$	6	l,R3
1172.457	0.013	1172.4501	0.0036	42	-0.795	E	221087.24	306378.72	$3d^5(^4P)4s$	^3P	2	$3d^5(^4D)4p$	$^3P^\circ$	2	R3
1174.191	0.013	1174.1858	0.0039	80	-0.623	E	212253.22	297418.62	$3d^5(^4P)4s$	^5P	2	$3d^5(^4P)4p$	$^3D^\circ$	3	R3
1176.975	0.025	1176.9864	0.0048	76	-0.726	E	212455.09	297417.84	$3d^5(^4P)4s$	^5P	1	$3d^5(^4D)4p$	$^5D^\circ$	1	p,R3
1177.167	0.013	1177.1611	0.0047	18	-1.120	E	221428.58	306378.72	$3d^5(^4P)4s$	^3P	1	$3d^5(^4D)4p$	$^3P^\circ$	2	R3
1177.590	0.013	1177.5994	0.0024	16	-1.204	E	212095.56	297014.07	$3d^5(^4P)4s$	^5P	3	$3d^5(^4D)4p$	$^5D^\circ$	2	R3
1178.216	0.013	1178.2257	0.0047	61	-1.059	E	216596.2	301469.60	$3d^5(^4D)4s$	^5D	3	$3d^5(^4D)4p$	$^3F^\circ$	3	R3
1178.371	0.025	1178.3879	0.0051	17	-1.461	E	232655.80	317517.50	$3d^5(^2D_3)4s$	^3D	2	$3d^5(^4F)4p$	$^5D^\circ$	2	d,R3
1178.795	0.013	1178.8041	0.0044	2	-1.556	E	242290.58	327122.31	$3d^5(^2G_2)4s$	^3G	3	$3d^5(^2F_2)4p$	$^1D^\circ$	2	R3
1178.903	0.013	1178.9126	0.0041	71	-0.269	E	212095.56	296919.48	$3d^5(^4P)4s$	^5P	3	$3d^5(^4D)4p$	$^5D^\circ$	4	R3
1179.223	0.013	1179.2326	0.0034	56	-0.527	E	212095.56	296896.46	$3d^5(^4P)4s$	^5P	3	$3d^5(^4G)4p$	$^3G^\circ$	4	R3
1179.959	0.025	1179.9198	0.0060	70	-1.058	E	221087.24	305838.76	$3d^5(^4P)4s$	^3P	2	$3d^5(^4D)4p$	$^3P^\circ$	1	s,R3
1180.245	0.013	1180.2374	0.0032	57	-0.994	E	216189.97	300918.68	$3d^5(^4D)4s$	^5D	4	$3d^5(^4D)4p$	$^3F^\circ$	4	R3
1182.495	0.025	1182.4895	0.0073	7	-1.290	E	232910.84	317478.19	$3d^5(^2D_3)4s$	^3D	1	$3d^5(^4F)4p$	$^5D^\circ$	1	d,R3
1182.604	0.013	1182.6065	0.0044	62	-0.556	E	212455.09	297014.07	$3d^5(^4P)4s$	^5P	1	$3d^5(^4D)4p$	$^5D^\circ$	2	R3
1182.713	0.025	1182.7330	0.0072	2	-1.501	E	232910.84	317460.78	$3d^5(^2D_3)4s$	^3D	1	$3d^5(^4F)4p$	$^5D^\circ$	0	d,R3
1183.756	0.013	1183.7645	0.0032	26	-0.869	E	241082.67	325558.93	$3d^5(^2H)4s$	^3H	5	$3d^5(^2F_2)4p$	$^1G^\circ$	4	R3
1185.225	0.025	1185.2276	0.0034	3	-1.455	E	242504.64	326876.62	$3d^5(^2G_2)4s$	^3G	4	$3d^5(^2F_2)4p$	$^3F^\circ$	4	d,R3
1185.937	0.013	1185.9460	0.0049	77	-0.288	E	212253.22	296574.09	$3d^5(^4P)4s$	^5P	2	$3d^5(^4D)4p$	$^5D^\circ$	3	R3
1187.168	0.025	1187.2012	0.0029	2	-1.496	E	235421.42	319653.14	$3d^5(^2F_1)4s$	^3F	4	$3d^5(^4F)4p$	$^3G^\circ$	5	d,R3
1187.310	0.013	1187.3298	0.0039	20	-1.487	E	208131.05	292353.65	$3d^5(^4G)4s$	^5G	5	$3d^5(^4G)4p$	$^3H^\circ$	5	R3
1187.770	0.025	1187.7953	0.0048	35	-1.249	E	208164.06	292353.65	$3d^5(^4G)4s$	^5G	4	$3d^5(^4G)4p$	$^3H^\circ$	5	p,R3
1189.533	0.013	1189.5432	0.0025	55	-0.347	E	241082.67	325148.55	$3d^5(^2H)4s$	^3H	5	$3d^5(^2G_2)4p$	$^3H^\circ$	6	R3
1189.676	0.013	1189.6890	0.0044	2	-1.530	E	229409.73	313465.31	$3d^5(^2I)4s$	^3I	6	$3d^5(^4F)4p$	$^5G^\circ$	5	R3
1190.323	0.013	1190.3208	0.0028	55	-0.563	E	216189.97	300200.93	$3d^5(^4D)4s$	^5D	4	$3d^5(^4D)4p$	$^5P^\circ$	3	R3
1191.071	0.013	1191.0636	0.0079	22	-0.921	E	221428.58	305387.15	$3d^5(^4P)4s$	^3P	1	$3d^5(^4D)4p$	$^3P^\circ$	0	R3
1192.676	0.013	1192.6856	0.0075	33	-1.103	E	208046.61	291891.00	$3d^5(^4G)4s$	^5G	6	$3d^5(^4G)4p$	$^3H^\circ$	6	R3
1192.838	0.013	1192.8370	0.0024	2	-1.291	E	242504.64	326338.39	$3d^5(^2G_2)4s$	^3G	4	$3d^5(^2G_2)4p$	$^1H^\circ$	5	R3
1193.583	0.01	1193.6148	0.0054	180	-0.816	E	274696.55	358475.67	$3d^5(^2G_1)4s$	^3G	5	$3d^5(^2G_1)4p$	$^1H^\circ$	5	d,W
1193.884	0.007	1193.8880	0.0036	44	-1.111	E	208131.05	291891.00	$3d^5(^4G)4s$	^5G	5	$3d^5(^4G)4p$	$^3H^\circ$	6	R1
1194.279	0.022	1194.2798	0.0026	55	-0.701	E	240194.22	323926.69	$3d^5(^2F_1)4s$	^1F	3	$3d^5(^2H)4p$	$^3H^\circ$	4	s,z,R1*
1194.279	0.022	1194.2495	0.0062	55	-1.096	E	232546.14	316280.73	$3d^5(^2D_3)4s$	^3D	3	$3d^5(^2F_1)4p$	$^3F^\circ$	3	s,z,R1*

Table A.2 (cont'd)

λ_{obs} [a] (Å)	u_{obs} [b] (Å)	λ_{Ritz} [c] (Å)	u_{Ritz} [d] (Å)	I [e]	log(gf_R) [f]	log(gf_R) [g]	E_i [h] (cm^{-1})	E_k [i] (cm^{-1})	Lower Level Configuration	Term	J	Upper Level Configuration	Term [k]	J	Notes [j]
1194.495	0.022	1194.4930	0.0028	3	-1.614	E	235421.42	319138.95	$3d^5(^2F_1)4s$	^3F	4	$3d^5(^2G_2)4p$	$^1G°$	4	d,R1
1194.573	0.022	1194.564	0.014	2	-1.053	E	306962.95	390675.47	$3d^5(^2D_1)4s$	^3D	3	$3d^5(^2D_1)4p$	$^1D°$	2	d,R1
1194.859	0.007	1194.8571	0.0040	39	-0.852	E	242290.58	325982.59	$3d^5(^2G_2)4s$	^3G	3	$3d^5(^2F_2)4p$	$^3F°$	2	R1
1195.191	0.002	1195.1878	0.0017	210	-0.032	E	247049.61	330718.47	$3d^5(^2G_2)4s$	^1G	4	$3d^5(^2F_2)4p$	$^3G°$	5	W
1195.815	0.022	1195.8156	0.0069	12	-1.310	E	232655.80	316280.73	$3d^5(^2D_3)4s$	^3D	2	$3d^5(^2F_1)4p$	$^3F°$	3	H,R1
1196.026	0.022	1196.0237	0.0031	10	-1.452	E	216590.56	300200.93	$3d^5(^4D)4s$	^5D	2	$3d^5(^4D)4p$	$^5P°$	3	d,R1
1196.102	0.002	1196.1048	0.0018	170	-0.637	E	216596.2	300200.93	$3d^5(^4D)4s$	^5D	3	$3d^5(^4D)4p$	$^5P°$	3	W
1196.965	0.007	1196.9652	0.0034	30	-0.664	E	243332.00	326876.62	$3d^5(^4F)4s$	^3F	4	$3d^5(^2F_2)4p$	$^3F°$	4	R1
1197.268	0.002	1197.2706	0.0016	400	-0.790	E	232546.14	316069.44	$3d^5(^2D_3)4s$	^3D	3	$3d^5(^2F_1)4p$	$^3G°$	4	W
1197.368	0.007	1197.3695	0.0066	37	0.032	E	306962.95	390479.36	$3d^5(^2D_1)4s$	^3D	3	$3d^5(^2D_1)4p$	$^3D°$	3	R1
1197.966	0.022	1197.9516	0.0025	23	-0.984	E	242862.56	326338.39	$3d^5(^2G_2)4s$	^3G	5	$3d^5(^2G_2)4p$	$^1H°$	5	p,z,R1*
1197.966	0.022	1197.9955	0.0051	23	-1.450	E	243266.72	326739.49	$3d^5(^4F)4s$	^3F	2	$3d^5(^2G_2)4p$	$^1F°$	3	p,z,R1*
1197.993	0.002	1197.9972	0.0018	110	-1.399	E	236454.05	319926.70	$3d^5(^2F_1)4s$	^3F	3	$3d^5(^2F_1)4p$	$^1D°$	2	I,W
1198.269	0.022	1198.272	0.017	41	-0.123	E	307025.84	390479.36	$3d^5(^2D_1)4s$	^3D	2	$3d^5(^2D_1)4p$	$^3D°$	3	s,R1
1198.516	0.002	1198.5195	0.0017	240	-0.008	E	247282.20	330718.47	$3d^5(^2F_2)4s$	^3F	4	$3d^5(^2F_2)4p$	$^3G°$	5	W
1198.690	0.007	1198.6915	0.0035	21	-1.315	E	208131.05	291555.35	$3d^5(^4G)4s$	^5G	5	$3d^5(^4G)4p$	$^3F°$	4	R1
1198.889	0.022	1198.9331	0.0026	27	-1.291	E	243332.00	326739.49	$3d^5(^4F)4s$	^3F	4	$3d^5(^2G_2)4p$	$^1F°$	3	l,R1
1199.390	0.002	1199.3922	0.0019	450	0.160	C+	241772.99	325148.55	$3d^5(^2H)4s$	^3H	6	$3d^5(^2G_2)4p$	$^3H°$	6	W
1200.939	0.007	1200.9364	0.0033	23	-0.786	E	242290.58	325558.93	$3d^5(^2G_2)4s$	^3G	3	$3d^5(^2F_2)4p$	$^1G°$	4	R1
1201.077	0.002	1201.0773	0.0020	40	-0.479	E	263701.48	346960.07	$3d^5(^2D_2)4s$	^3D	1	$3d^5(^2D_2)4p$	$^3P°$	1	W
1201.189	0.022	1201.2033	0.0045	44	-0.856	E	234125.87	317375.72	$3d^5(^4F)4s$	^5F	4	$3d^5(^2H)4p$	$^3G°$	3	H,R1
1201.316	0.007	1201.3138	0.0042	46	-0.638	E	234275.30	317517.50	$3d^5(^4F)4s$	^5F	3	$3d^5(^4F)4p$	$^5D°$	2	R1
1201.586	0.007	1201.5821	0.0052	34	-0.448	E	263736.46	346960.07	$3d^5(^2D_2)4s$	^3D	2	$3d^5(^2D_2)4p$	$^3P°$	1	R1
1201.636	0.007	1201.6362	0.0069	24	-0.625	E	263701.48	346921.34	$3d^5(^2D_2)4s$	^3D	1	$3d^5(^2D_2)4p$	$^3P°$	0	R1
1201.752	0.022	1201.7557	0.0056	46	-1.043	E	263701.48	346913.07	$3d^5(^2D_2)4s$	^3D	1	$3d^5(^2D_2)4p$	$^3P°$	2	d,bl,R1
1201.826	0.022	1201.8100	0.0029	35	-0.835	E	241772.99	324980.8	$3d^5(^2H)4s$	^3H	6	$3d^5(^2G_2)4p$	$^3G°$	5	p,R1
1201.849	0.022	1201.8470	0.0084	29	-0.784	E	247165.79	330371.06	$3d^5(^2F_2)4s$	^3F	2	$3d^5(^2S)4p$	$^3P°$	1	p,R1
1202.032	0.007	1202.0278	0.0052	75	0.093	C+	247104.70	330297.45	$3d^5(^2F_2)4s$	^3F	3	$3d^5(^2F_2)4p$	$^3G°$	4	R1
1202.261	0.002	1202.2611	0.0020	50	-0.367	E	263736.46	346913.07	$3d^5(^2D_2)4s$	^3D	2	$3d^5(^2D_2)4p$	$^3P°$	2	W
1202.406	0.007	1202.4435	0.0049	340	-1.077	E	208164.06	291328.05	$3d^5(^4G)4s$	^5G	4	$3d^5(^4G)4p$	$^3F°$	3	d,z,W
1203.278	0.022	1203.2707	0.0029	78	-0.213	E	263806.25	346913.07	$3d^5(^2D_2)4s$	^3D	3	$3d^5(^2D_2)4p$	$^3P°$	2	p,z,R1*
1203.278	0.022	1203.2782	0.0030	78	-0.581	E	234125.87	317232.17	$3d^5(^4F)4s$	^5F	4	$3d^5(^4F)4p$	$^5D°$	3	p,z,R1*
1203.307	0.022	1203.2963	0.0043	79	-0.373	E	234412.45	317517.50	$3d^5(^4F)4s$	^5F	2	$3d^5(^4F)4p$	$^5D°$	2	p,R1
1203.354	0.022	1203.3634	0.0049	63	-0.517	E	234275.30	317375.72	$3d^5(^4F)4s$	^5F	3	$3d^5(^2H)4p$	$^3G°$	3	p,R1
1203.773	0.002	1203.7732	0.0019	120	0.216	C+	251655.96	334728.09	$3d^5(^2F_2)4s$	^1F	3	$3d^5(^2F_2)4p$	$^1F°$	3	W
1203.851	0.01	1203.8658	0.0068	140	-0.809	E	234412.45	317478.19	$3d^5(^4F)4s$	^5F	2	$3d^5(^4F)4p$	$^5D°$	1	W

Table A.2 (cont'd)

λ_{obs} [a] (Å)	u_{obs} [b] (Å)	λ_{Ritz} [c] (Å)	u_{Ritz} [d] (Å)	I [e]	$\log(gf_R)$ [f]	$\log(gf_R)$ [g]	E_i [h] (cm^{-1})	E_k [i] (cm^{-1})	Lower Level Configuration	Term	J	Upper Level Configuration	Term [k]	J	Notes [j]
1204.725	0.002	1204.7265	0.0018	100	-0.921	E	243332.00	326338.39	$3d^5(^4F)4s$	^3F	4	$3d^5(^2G_2)4p$	$^1H°$	5	W
1205.306	0.002	1205.3036	0.0016	90	-0.058	E	240960.04	323926.69	$3d^5(^2H)4s$	^3H	4	$3d^5(^2H)4p$	$^3H°$	4	I,W
1205.445	0.002	1205.4457	0.0019	230	-0.269	E	234275.30	317232.17	$3d^5(^4F)4s$	^5F	3	$3d^5(^4F)4p$	$^5D°$	3	I,W
1205.551	0.002	1205.5545	0.0016	1	-0.216	E	240960.04	323909.42	$3d^5(^2H)4s$	^3H	4	$3d^5(^2G_2)4p$	$^3H°$	5	I,W
1205.796	0.002	1205.7888	0.0045	30	-1.609	E	242290.58	325223.84	$3d^5(^2G_2)4s$	^3G	3	$3d^5(^2G_2)4p$	$^3G°$	4	I,z,W*
1205.796	0.002	1205.801	0.012	30	-1.290	E	208165.11	291097.51	$3d^5(^4G)4s$	^5G	3	$3d^5(^4G)4p$	$^3F°$	2	I,z,W*
1205.951	0.007	1205.9580	0.0042	53	-0.284	E	242290.58	325212.20	$3d^5(^2G_2)4s$	^3G	3	$3d^5(^2G_2)4p$	$^3G°$	3	R1
1207.338	0.002	1207.3394	0.0016	350	0.060	E	241082.67	323909.42	$3d^5(^2H)4s$	^3H	5	$3d^5(^2G_2)4p$	$^3H°$	5	W
1207.389	0.022	1207.3915	0.0045	67	-0.466	E	247049.61	329872.79	$3d^5(^2G_2)4s$	^1G	4	$3d^5(^2F_2)4p$	$^3D°$	3	p,z,R1*
1207.389	0.022	1207.3741	0.0029	67	-0.928	E	232546.14	315370.50	$3d^5(^2D_3)4s$	^3D	3	$3d^5(^2G_2)4p$	$^3H°$	4	p,z,R1*
1207.447	0.007	1207.4419	0.0031	49	-0.653	E	234412.45	317232.17	$3d^5(^4F)4s$	^5F	2	$3d^5(^4F)4p$	$^5D°$	3	R1
1207.675	0.01	1207.6487	0.0029	300	-1.238	E	234083.15	316888.69	$3d^5(^4F)4s$	^5F	5	$3d^5(^2H)4p$	$^3G°$	4	d,W
1207.984	0.022	1208.0310	0.0048	21	-1.512	E	232546.14	315325.46	$3d^5(^2D_3)4s$	^3D	3	$3d^5(^2D_3)4p$	$^1F°$	3	z,R1*
1207.984	0.022	1207.9812	0.0045	21	-1.173	E	216189.97	298972.71	$3d^5(^4D)4s$	^5D	4	$3d^5(^4D)4p$	$^3D°$	3	z,R1*
1208.205	0.022	1208.1951	0.0057	13	-1.131	E	247104.70	329872.79	$3d^5(^2F_2)4s$	^3F	3	$3d^5(^2F_2)4p$	$^3D°$	3	d,R1
1208.261	0.022	1208.2720	0.0029	2	-1.566	E	234125.87	316888.69	$3d^5(^4F)4s$	^5F	4	$3d^5(^2H)4p$	$^3G°$	4	G,R1
1208.903	0.007	1208.9092	0.0042	65	-0.170	E	242504.64	325223.84	$3d^5(^2G_2)4s$	^3G	4	$3d^5(^2G_2)4p$	$^3G°$	4	R1
1208.961	0.007	1208.9578	0.0049	48	-0.485	E	243266.72	325982.59	$3d^5(^4F)4s$	^3F	2	$3d^5(^2F_2)4p$	$^3F°$	2	R1
1209.094	0.007	1209.0875	0.0045	53	-0.320	E	247165.79	329872.79	$3d^5(^2F_2)4s$	^3F	2	$3d^5(^2F_2)4p$	$^3D°$	3	R1
1209.221	0.007	1209.2156	0.0035	30	-0.617	E	243332.00	326030.24	$3d^5(^4F)4s$	^3F	4	$3d^5(^2F_2)4p$	$^3F°$	3	R1
1209.456	0.01	1209.4107	0.0026	120	-1.586	E	236454.05	319138.95	$3d^5(^2F_1)4s$	^3F	3	$3d^5(^2G_2)4p$	$^1G°$	4	d,W
1209.603	0.007	1209.6038	0.0053	70	-0.075	E	247104.70	329776.40	$3d^5(^2F_2)4s$	^3F	3	$3d^5(^2F_2)4p$	$^3D°$	2	R1
1209.767	0.002	1209.7731	0.0026	180	-0.152	E	234083.15	316743.28	$3d^5(^4F)4s$	^5F	5	$3d^5(^4F)4p$	$^5D°$	4	z,W*
1209.767	0.002	1209.7643	0.0050	180	-0.339	E	243369.51	326030.24	$3d^5(^4F)4s$	^3F	3	$3d^5(^2F_2)4p$	$^3F°$	3	z,W*
1210.399	0.002	1210.3986	0.0019	250	0.024	E	234125.87	316743.28	$3d^5(^4F)4s$	^5F	4	$3d^5(^4F)4p$	$^5D°$	4	W
1210.505	0.022	1210.4575	0.0036	85	-0.843	E	234275.30	316888.69	$3d^5(^4F)4s$	^5F	3	$3d^5(^2H)4p$	$^3G°$	4	w,z,R1*
1210.505	0.022	1210.4983	0.0060	85	-0.802	E	247165.79	329776.40	$3d^5(^2F_2)4s$	^3F	2	$3d^5(^2F_2)4p$	$^3D°$	2	w,z,R1*
1210.505	0.022	1210.522	0.020	85	-0.574	E	306962.95	389572.0	$3d^5(^2D_1)4s$	^3D	3	$3d^5(^2D_1)4p$	$^3D°$	2	w,z,R1*
1210.505	0.022	1210.4621	0.0052	85	-0.474	E	243369.51	325982.59	$3d^5(^4F)4s$	^3F	3	$3d^5(^2F_2)4p$	$^3F°$	2	w,z,R1*
1210.505	0.022	1210.4916	0.0048	85	-0.506	E	216434.77	299045.83	$3d^5(^4D)4s$	^5D	1	$3d^5(^4D)4p$	$^5P°$	2	w,z,R1*
1210.634	0.007	1210.6553	0.0036	19	-1.008	E	234125.87	316725.76	$3d^5(^4F)4s$	^5F	4	$3d^5(^2H)4p$	$^3G°$	5	R1
1210.740	0.002	1210.7394	0.0019	160	-0.816	E	229413.82	312007.98	$3d^5(^2I)4s$	^3I	5	$3d^5(^2F_1)4p$	$^1G°$	4	W
1210.795	0.007	1210.7917	0.0043	42	-0.531	E	247282.20	329872.79	$3d^5(^2F_2)4s$	^3F	4	$3d^5(^2F_2)4p$	$^3D°$	3	R1
1211.444	0.01	1211.4443	0.0097	600	-0.299	E	307025.84	389572.0	$3d^5(^2D_1)4s$	^3D	2	$3d^5(^2D_1)4p$	$^3D°$	2	d,W
1211.912	0.01	1211.9753	0.0046	180	-0.790	E	247104.70	329614.63	$3d^5(^2F_2)4s$	^3F	3	$3d^5(^2F_2)4p$	$^3G°$	3	d,W
1212.438	0.01	1212.4713	0.0020	990	-1.100	E	242504.64	324980.8	$3d^5(^2G_2)4s$	^3G	4	$3d^5(^2G_2)4p$	$^3G°$	5	d,W

Table A.2 (cont'd)

λ_{obs} [a] (Å)	u_{obs} [b] (Å)	λ_{Ritz} [c] (Å)	u_{Ritz} [d] (Å)	I [e]	$\log(gf_R)$ [f]	$\log(gf_R)$ [g]	E_i [h] (cm^{-1})	E_k [i] (cm^{-1})	Lower Level Configuration	Term	J	Upper Level Configuration	Term [k]	J	Notes [j]
1212.573	0.01	1212.5918	0.0032	280	-0.574	E	234275.30	316743.28	$3d^5(^4F)4s$	^5F	3	$3d^5(^4F)4p$	$^5D^\circ$	4	d,z,W*
1212.573	0.01	1212.612	0.023	280	-0.312	E	307105.32	389572.0	$3d^5(^2D_1)4s$	^3D	1	$3d^5(^2D_1)4p$	$^3D^\circ$	2	d,z,W*
1212.778	0.002	1212.7786	0.0019	140	-0.264	E	216590.56	299045.83	$3d^5(^4D)4s$	^5D	2	$3d^5(^4D)4p$	$^5P^\circ$	2	W
1212.886	0.007	1212.8733	0.0036	46	-0.579	E	247165.79	329614.63	$3d^5(^2F_2)4s$	^3F	2	$3d^5(^2F_2)4p$	$^3G^\circ$	3	R1
1213.234	0.007	1213.2390	0.0040	20	-0.906	E	240194.22	322618.21	$3d^5(^2F_1)4s$	^1F	3	$3d^5(^4F)4p$	$^3D^\circ$	3	R1
1213.525	0.01	1213.5663	0.0052	140	-0.910	E	235115.74	317517.50	$3d^5(^4F)4s$	^5F	1	$3d^5(^4F)4p$	$^5D^\circ$	2	H,W
1213.857	0.007	1213.8550	0.0043	66	-0.570	E	216590.56	298972.71	$3d^5(^4D)4s$	^5D	2	$3d^5(^4D)4p$	$^3D^\circ$	3	R1
1213.919	0.01	1213.9385	0.0042	700	-0.260	E	216596.2	298972.71	$3d^5(^4D)4s$	^5D	3	$3d^5(^4D)4p$	$^3D^\circ$	3	d,W
1214.161	0.002	1214.1455	0.0078	65	-0.354	E	235115.74	317478.19	$3d^5(^4F)4s$	^5F	1	$3d^5(^4F)4p$	$^5D^\circ$	1	z,W*
1214.161	0.002	1214.1628	0.0044	65	-0.975	E	242862.56	325223.84	$3d^5(^2G_2)4s$	^3G	5	$3d^5(^2G_2)4p$	$^3G^\circ$	4	z,W*
1214.408	0.007	1214.4022	0.0062	70	-0.630	E	235115.74	317460.78	$3d^5(^4F)4s$	^5F	1	$3d^5(^4F)4p$	$^5D^\circ$	0	R1
1214.589	0.002	1214.5882	0.0019	50	-0.301	E	247282.20	329614.63	$3d^5(^2F_2)4s$	^3F	4	$3d^5(^2F_2)4p$	$^3G^\circ$	3	W
1215.071	0.01	1215.113	0.012	630	-0.378	E	247165.79	329462.64	$3d^5(^2F_2)4s$	^3F	2	$3d^5(^2F_2)4p$	$^3D^\circ$	1	z,W*
1215.071	0.01	1215.1491	0.0090	630	-0.832	E	216305.74	298600.17	$3d^5(^4D)4s$	^5D	0	$3d^5(^4P)4p$	$^3D^\circ$	1	z,W*
1215.276	0.002	1215.2737	0.0018	230	-0.086	E	242862.56	325148.55	$3d^5(^2G_2)4s$	^3G	5	$3d^5(^2G_2)4p$	$^3H^\circ$	6	W
1216.150	0.007	1216.1466	0.0031	67	-0.214	E	243332.00	325558.93	$3d^5(^4F)4s$	^3F	4	$3d^5(^2F_2)4p$	$^1G^\circ$	4	R1
1216.538	0.007	1216.5375	0.0066	28	-1.164	E	263736.46	345936.97	$3d^5(^2D_2)4s$	^3D	2	$3d^5(^2D_2)4p$	$^1F^\circ$	3	R1
1217.061	0.007	1217.0572	0.0056	64	-0.779	E	216434.77	298600.17	$3d^5(^4D)4s$	^5D	1	$3d^5(^4P)4p$	$^3D^\circ$	1	R1
1217.105	0.002	1217.1060	0.0019	80	-0.235	E	221087.24	303249.35	$3d^5(^4P)4s$	^3P	2	$3d^5(^4P)4p$	$^3S^\circ$	1	W
1217.501	0.007	1217.4866	0.0030	32	-0.926	E	241772.99	323909.42	$3d^5(^2H)4s$	^3H	6	$3d^5(^2G_2)4p$	$^3H^\circ$	5	R1
1217.570	0.002	1217.5712	0.0069	240	-0.739	E	263806.25	345936.97	$3d^5(^2D_2)4s$	^3D	3	$3d^5(^2D_2)4p$	$^1F^\circ$	3	z,W*
1217.570	0.002	1217.5783	0.0033	240	-0.615	E	208131.05	290261.29	$3d^5(^4G)4s$	^5G	5	$3d^5(^4P)4p$	$^5D^\circ$	4	z,W*
1217.756	0.002	1217.7560	0.0017	210	0.200	C+	242862.56	324980.8	$3d^5(^2G_2)4s$	^3G	5	$3d^5(^2G_2)4p$	$^3G^\circ$	5	W
1218.060	0.007	1218.0679	0.0042	41	-1.166	E	208164.06	290261.29	$3d^5(^4G)4s$	^5G	4	$3d^5(^4P)4p$	$^5D^\circ$	4	R1
1218.726	0.007	1218.7237	0.0021	16	-1.067	E	232546.14	314599.18	$3d^5(^2D_3)4s$	^3D	3	$3d^5(^4F)4p$	$^5F^\circ$	4	R1
1219.886	0.007	1219.8898	0.0054	25	-1.086	E	239107.85	321082.47	$3d^5(^2D_3)4s$	^1D	2	$3d^5(^2F_1)4p$	$^1F^\circ$	3	R1
1220.317	0.007	1220.3236	0.0049	36	-0.680	E	243266.72	325212.20	$3d^5(^4F)4s$	^3F	2	$3d^5(^2G_2)4p$	$^3G^\circ$	3	R1
1220.837	0.022	1220.8493	0.0048	25	-1.167	E	239107.85	321018.04	$3d^5(^2D_3)4s$	^1D	2	$3d^5(^2G_2)4p$	$^3F^\circ$	2	H,R1
1220.880	0.022	1220.8996	0.0030	30	-1.046	E	234083.15	315989.97	$3d^5(^4F)4s$	^5F	5	$3d^5(^2H)4p$	$^3H^\circ$	5	H,R1
1221.114	0.007	1221.1229	0.0043	64	-0.662	E	243332.00	325223.84	$3d^5(^4F)4s$	^3F	4	$3d^5(^2G_2)4p$	$^3G^\circ$	4	R1
1221.692	0.01	1221.6825	0.0053	100	-0.512	E	243369.51	325223.84	$3d^5(^4F)4s$	^3F	3	$3d^5(^2G_2)4p$	$^3G^\circ$	4	d,bl,W
1221.871	0.007	1221.8562	0.0046	32	-0.997	E	243369.51	325212.20	$3d^5(^4F)4s$	^3F	3	$3d^5(^2G_2)4p$	$^3G^\circ$	3	R1
1222.190	0.007	1222.1836	0.0046	54	-0.728	E	221428.58	303249.35	$3d^5(^4P)4s$	^3P	1	$3d^5(^4P)4p$	$^3S^\circ$	1	R1
1222.789	0.007	1222.7757	0.0044	51	-0.560	E	235736.35	317517.50	$3d^5(^2F_1)4s$	^3F	2	$3d^5(^4F)4p$	$^5D^\circ$	2	R1
1223.206	0.007	1223.2049	0.0040	38	-0.660	E	234412.45	316164.90	$3d^5(^4F)4s$	^5F	2	$3d^5(^2F_1)4p$	$^3F^\circ$	2	R1
1223.392	0.022	1223.3637	0.0074	52	-0.949	E	235736.35	317478.19	$3d^5(^2F_1)4s$	^3F	2	$3d^5(^4F)4p$	$^5D^\circ$	1	p,R1

Table A.2 (cont'd)

λ_{obs} [a] (Å)	u_{obs} [b] (Å)	λ_{Ritz} [c] (Å)	u_{Ritz} [d] (Å)	I [e]	$\log(gf_R)$ [f]	$\log(gf_R)$ [g]	E_i [h] (cm^{-1})	E_k [i] (cm^{-1})	Lower Level Configuration	Term	J	Upper Level Configuration	Term [k]	J	Notes [j]
1223.446	0.007	1223.4460	0.0068	76	0.373	C+	306962.95	388699.29	$3d^5(^2D_1)4s$	^3D	3	$3d^5(^2D_1)4p$	$^3F°$	4	R1
1223.687	0.022	1223.686	0.021	6	-0.679	E	307025.84	388746.2	$3d^5(^2D_1)4s$	^3D	2	$3d^5(^2D_1)4p$	$^3D°$	1	d,R1
1224.337	0.007	1224.3370	0.0070	50	-0.783	E	216305.74	297982.60	$3d^5(^4D)4s$	^5D	0	$3d^5(^4D)4p$	$^5P°$	1	R1
1224.563	0.002	1224.5608	0.0017	90	-0.285	E	232546.14	314208.06	$3d^5(^2D_3)4s$	^3D	3	$3d^5(^2F_1)4p$	$^3F°$	4	W
1224.758	0.002	1224.7574	0.0017	60	-0.416	E	243332.00	324980.8	$3d^5(^4F)4s$	^3F	4	$3d^5(^2G_2)4p$	$^3G°$	5	W
1224.877	0.007	1224.8770	0.0070	51	-0.278	E	307105.32	388746.2	$3d^5(^2D_1)4s$	^3D	1	$3d^5(^2D_1)4p$	$^3D°$	1	R1
1224.947	0.002	1224.9480	0.0018	200	-0.093	E	242290.58	323926.69	$3d^5(^2G_2)4s$	^3G	3	$3d^5(^2H)4p$	$^3H°$	4	W
1225.113	0.002	1225.1130	0.0020	40	-0.700	E	216434.77	298059.89	$3d^5(^4D)4s$	^5D	1	$3d^5(^4D)4p$	$^5D°$	0	W
1226.274	0.002	1226.2741	0.0020	40	-0.860	E	216434.77	297982.60	$3d^5(^4D)4s$	^5D	1	$3d^5(^4D)4p$	$^5P°$	1	W
1227.060	0.007	1227.0568	0.0037	24	-0.852	E	235736.35	317232.17	$3d^5(^2F_1)4s$	^3F	2	$3d^5(^4F)4p$	$^5D°$	3	R1
1227.188	0.002	1227.1881	0.0020	70	0.246	C+	311471.22	392958.32	$3d^5(^2D_1)4s$	^1D	2	$3d^5(^2D_1)4p$	$^1F°$	3	W
1227.420	0.01	1227.4868	0.0030	210	-1.330	E	235421.42	316888.69	$3d^5(^2F_1)4s$	^3F	4	$3d^5(^2H)4p$	$^3G°$	4	d,W
1228.167	0.002	1228.1685	0.0016	100	-0.810	E	242504.64	323926.69	$3d^5(^2G_2)4s$	^3G	4	$3d^5(^2H)4p$	$^3H°$	4	I,W
1228.432	0.002	1228.4291	0.0015	20	-0.129	E	242504.64	323909.42	$3d^5(^2G_2)4s$	^3G	4	$3d^5(^2G_2)4p$	$^3H°$	5	I,W
1229.397	0.003	1229.4100	0.0043	320	0.273	C+	274696.55	356036.38	$3d^5(^2G_1)4s$	^3G	5	$3d^5(^2G_1)4p$	$^3G°$	5	s,z,W*
1229.397	0.003	1229.4079	0.0073	320	-0.029	E	251655.96	332995.93	$3d^5(^2F_2)4s$	^1F	3	$3d^5(^2H)4p$	$^1G°$	4	s,z,W*
1229.684	0.007	1229.6817	0.0029	20	-0.972	E	235421.42	316743.28	$3d^5(^2F_1)4s$	^3F	4	$3d^5(^4F)4p$	$^5D°$	4	R1
1230.070	0.004	1230.0689	0.0038	80	0.025	E	274740.12	356036.38	$3d^5(^2G_1)4s$	^3G	4	$3d^5(^2G_1)4p$	$^3G°$	5	q,W
1230.439	0.004	1230.4386	0.0040	80	0.093	C+	268274.36	349546.19	$3d^5(^2D_2)4s$	^1D	2	$3d^5(^2D_2)4p$	$^1D°$	2	q,W
1230.736	0.007	1230.7356	0.0039	32	-1.029	E	216590.56	297842.77	$3d^5(^4D)4s$	^5D	2	$3d^5(^4P)4p$	$^3D°$	2	R1
1230.826	0.007	1230.8214	0.0035	58	-0.864	E	216596.2	297842.77	$3d^5(^4D)4s$	^5D	3	$3d^5(^4P)4p$	$^3D°$	2	R1
1230.885	0.004	1230.8869	0.0036	180	-0.096	E	241082.67	322324.90	$3d^5(^2H)4s$	^3H	5	$3d^5(^2H)4p$	$^1I°$	6	q,W
1231.035	0.022	1231.0175	0.0042	60	-0.773	E	242290.58	323524.19	$3d^5(^2G_2)4s$	^3G	3	$3d^5(^4F)4p$	$^3F°$	3	p,R1
1231.089	0.004	1231.0927	0.0035	140	-0.456	E	216189.97	297418.62	$3d^5(^4D)4s$	^5D	4	$3d^5(^4P)4p$	$^3D°$	3	q,W
1231.881	0.002	1231.8821	0.0019	150	-0.134	E	225202.1	306378.72	$3d^5(^4D)4s$	^3D	3	$3d^5(^4D)4p$	$^3P°$	2	W
1232.346	0.007	1232.3446	0.0049	18	-1.573	E	208152.08	289298.21	$3d^5(^4G)4s$	^5G	2	$3d^5(^4P)4p$	$^5D°$	3	R1
1232.521	0.002	1232.5266	0.0054	300	-0.197	E	208164.06	289298.21	$3d^5(^4G)4s$	^5G	4	$3d^5(^4P)4p$	$^5D°$	3	z,W*
1232.521	0.002	1232.543	0.011	300	-0.632	E	208165.11	289298.21	$3d^5(^4G)4s$	^5G	3	$3d^5(^4P)4p$	$^5D°$	3	z,W*
1232.808	0.002	1232.8074	0.0019	310	0.326	C+	246241.70	327357.37	$3d^5(^2H)4s$	^1H	5	$3d^5(^2H)4p$	$^1H°$	5	W
1232.971	0.004	1232.9708	0.0038	290	0.354	C+	263806.25	344911.17	$3d^5(^2D_2)4s$	^3D	3	$3d^5(^2D_2)4p$	$^3F°$	4	q,W
1233.124	0.002	1233.1186	0.0038	50	-1.200	E	234275.30	315370.50	$3d^5(^4F)4s$	^5F	3	$3d^5(^2G_2)4p$	$^3H°$	4	z,W*
1233.124	0.002	1233.1303	0.0076	50	-0.710	E	208152.08	289246.51	$3d^5(^4G)4s$	^5G	2	$3d^5(^4G)4p$	$^5F°$	2	z,W*
1233.273	0.022	1233.2658	0.0035	86	0.205	C+	234083.15	315168.67	$3d^5(^4F)4s$	^5F	5	$3d^5(^4F)4p$	$^5F°$	5	p,R1
1233.329	0.022	1233.328	0.011	81	-0.223	E	208165.11	289246.51	$3d^5(^4G)4s$	^5G	3	$3d^5(^4G)4p$	$^5F°$	2	p,R1
1233.501	0.004	1233.5176	0.0025	200	0.045	E	263736.46	344805.43	$3d^5(^2D_2)4s$	^3D	2	$3d^5(^2D_2)4p$	$^3D°$	3	p,W
1233.601	0.004	1233.6016	0.0049	130	-0.878	E	236454.05	317517.50	$3d^5(^2F_1)4s$	^3F	3	$3d^5(^4F)4p$	$^5D°$	2	p,z,W*

Table A.2 (cont'd)

λ_{obs} [a] (Å)	u_{obs} [b] (Å)	λ_{Ritz} [c] (Å)	u_{Ritz} [d] (Å)	I [e]	$\log(gf_R)$ [f]	$\log(gf_R)$ [g]	E_i [h] (cm^{-1})	E_k [i] (cm^{-1})	Lower Level Configuration	Term	J	Upper Level Configuration	Term [k]	J	Notes [j]
1233.601	0.004	1233.5912	0.0024	130	-1.225	E	242862.56	323926.69	$3d^5(^2G_2)4s$	^3G	5	$3d^5(^2H)4p$	$^3H°$	4	p,z,W*
1233.856	0.022	1233.8191	0.0054	44	-0.707	E	235115.74	316164.90	$3d^5(^4F)4s$	^5F	1	$3d^5(^2F_1)4p$	$^3F°$	2	G,R1
1233.940	0.01	1233.9159	0.0034	310	0.020	E	234125.87	315168.67	$3d^5(^4F)4s$	^5F	4	$3d^5(^4F)4p$	$^5F°$	5	d,bl,W
1234.172	0.004	1234.1742	0.0033	190	0.256	C+	274740.12	355765.96	$3d^5(^2G_1)4s$	^3G	4	$3d^5(^2G_1)4p$	$^3G°$	4	p,W
1234.294	0.01	1234.2700	0.0040	1	-1.095	E	242504.64	323524.19	$3d^5(^2G_2)4s$	^3G	4	$3d^5(^4F)4p$	$^3F°$	3	I,d,W
1234.398	0.002	1234.3979	0.0020	200	-0.236	E	208152.08	289163.23	$3d^5(^4G)4s$	^5G	2	$3d^5(^4G)4p$	$^5F°$	1	W
1234.585	0.002	1234.5804	0.0018	280	-0.159	E	263806.25	344805.43	$3d^5(^2D_2)4s$	^3D	3	$3d^5(^2D_2)4p$	$^3D°$	3	W
1234.703	0.007	1234.7040	0.0041	44	-0.242	E	274774.89	355765.96	$3d^5(^2G_1)4s$	^3G	3	$3d^5(^2G_1)4p$	$^3G°$	4	R1
1235.311	0.022	1235.2943	0.0096	27	-1.461	E	234412.45	315364.82	$3d^5(^4F)4s$	^5F	2	$3d^5(^2F_1)4p$	$^3D°$	2	s,R1
1235.436	0.007	1235.4348	0.0067	16	-0.631	E	311471.22	392414.38	$3d^5(^2D_1)4s$	^1D	2	$3d^5(^2D_1)4p$	$^3P°$	2	R1
1235.770	0.007	1235.7629	0.0044	68	-0.513	E	236454.05	317375.72	$3d^5(^2F_1)4s$	^3F	3	$3d^5(^2H)4p$	$^3G°$	3	R1
1235.838	0.002	1235.8376	0.0019	330	0.386	B+	233840.06	314756.83	$3d^5(^2I)4s$	^1I	6	$3d^5(^4F)4p$	$^5G°$	6	W
1236.274	0.002	1236.2735	0.0059	170	-0.090	E	240194.22	321082.47	$3d^5(^2F_1)4s$	^1F	3	$3d^5(^2F_1)4p$	$^1F°$	3	z,W*
1236.274	0.002	1236.2622	0.0063	170	-0.399	E	234412.45	315301.44	$3d^5(^4F)4s$	^5F	2	$3d^5(^2F_1)4p$	$^3D°$	1	z,W*
1236.274	0.002	1236.2958	0.0050	170	-1.126	E	212095.56	292982.34	$3d^5(^4P)4s$	^5P	3	$3d^5(^4P)4p$	$^3P°$	2	z,W*
1236.671	0.022	1236.6696	0.0040	62	-0.753	E	240194.22	321056.56	$3d^5(^2F_1)4s$	^1F	3	$3d^5(^2G_2)4p$	$^3F°$	4	p,R1
1236.703	0.007	1236.7056	0.0065	69	0.177	C+	279200.87	360060.86	$3d^5(^2G_1)4s$	^1G	4	$3d^5(^2G_1)4p$	$^1F°$	3	R1
1237.126	0.022	1237.1182	0.0071	27	-1.600	E	225545.70	306378.72	$3d^5(^4D)4s$	^3D	1	$3d^5(^4D)4p$	$^3P°$	2	H,R1
1237.206	0.002	1237.2059	0.0019	110	-0.389	E	216590.56	297417.84	$3d^5(^4D)4s$	^5D	2	$3d^5(^4D)4p$	$^5D°$	1	W
1237.335	0.007	1237.3351	0.0041	56	-0.370	E	239107.85	319926.70	$3d^5(^2D_3)4s$	^1D	2	$3d^5(^2F_1)4p$	$^1D°$	2	R1
1237.980	0.007	1237.9907	0.0058	38	-0.661	E	232910.84	313686.89	$3d^5(^2D_3)4s$	^3D	1	$3d^5(^2D_3)4p$	$^3D°$	2	R1
1238.118	0.007	1238.1178	0.0048	64	-0.228	E	232910.84	313678.60	$3d^5(^2D_3)4s$	^3D	1	$3d^5(^2D_3)4p$	$^3D°$	1	R1
1238.216	0.007	1238.2174	0.0043	49	-0.641	E	225617.46	306378.72	$3d^5(^4D)4s$	^3D	2	$3d^5(^4D)4p$	$^3P°$	2	R1
1238.555	0.007	1238.5536	0.0045	38	-0.753	E	234412.45	315151.79	$3d^5(^4F)4s$	^5F	2	$3d^5(^4F)4p$	$^5F°$	1	R1
1238.644	0.022	1238.6251	0.0027	60	-1.137	E	232546.14	313280.81	$3d^5(^2D_3)4s$	^3D	3	$3d^5(^4F)4p$	$^5G°$	4	p,R1
1238.705	0.007	1238.7044	0.0043	83	-0.011	E	216189.97	296919.48	$3d^5(^4D)4s$	^5D	4	$3d^5(^4D)4p$	$^5D°$	4	R1
1238.969	0.022	1238.964	0.011	69	-1.189	E	208165.11	288877.70	$3d^5(^4G)4s$	^5G	3	$3d^5(^4P)4p$	$^5S°$	2	l,R1
1239.058	0.007	1239.0577	0.0036	70	-0.483	E	216189.97	296896.46	$3d^5(^4D)4s$	^5D	4	$3d^5(^4G)4p$	$^3G°$	4	R1
1239.556	0.007	1239.5617	0.0037	78	-0.028	E	234083.15	314756.83	$3d^5(^4F)4s$	^5F	5	$3d^5(^4F)4p$	$^5G°$	6	R1
1239.671	0.007	1239.6724	0.0060	40	-0.655	E	232910.84	313577.31	$3d^5(^2D_3)4s$	^3D	1	$3d^5(^2D_3)4p$	$^3P°$	0	R1
1239.777	0.007	1239.7866	0.0038	24	-0.552	E	274740.12	355399.16	$3d^5(^2G_1)4s$	^3G	4	$3d^5(^2G_1)4p$	$^3G°$	3	R1
1239.959	0.002	1239.9560	0.0017	10	-0.388	E	235421.42	316069.44	$3d^5(^2F_1)4s$	^3F	4	$3d^5(^2F_1)4p$	$^3G°$	4	I,W
1240.160	0.007	1240.1575	0.0039	21	-0.769	E	246241.70	326876.62	$3d^5(^2H)4s$	^1H	5	$3d^5(^2F_2)4p$	$^3F°$	4	R1
1240.321	0.002	1240.3213	0.0019	10	0.183	C+	274774.89	355399.16	$3d^5(^2G_1)4s$	^3G	3	$3d^5(^2G_1)4p$	$^3G°$	3	I,W
1241.043	0.002	1241.0425	0.0022	100	-0.770	E	243332.00	323909.42	$3d^5(^4F)4s$	^3F	4	$3d^5(^2G_2)4p$	$^3H°$	5	z,W*
1241.043	0.002	1241.0620	0.0056	100	-0.720	E	234125.87	314702.02	$3d^5(^4F)4s$	^5F	4	$3d^5(^2F_1)4p$	$^3G°$	5	z,W*

Table A.2 (cont'd)

λ_{obs} [a] (Å)	u_{obs} [b] (Å)	λ_{Ritz} [c] (Å)	u_{Ritz} [d] (Å)	I [e]	$\log(gf_R)$ [f]	$\log(gf_R)$ [g]	E_i [h] (cm^{-1})	E_k [i] (cm^{-1})	Lower Level Configuration	Term	J	Upper Level Configuration	Term [k]	J	Notes [j]
1241.043	0.002	1241.0134	0.0053	100	-1.068	E	216434.77	297014.07	$3d^5(^4D)4s$	^5D	1	$3d^5(^4D)4p$	$^5D°$	2	z,W*
1241.174	0.022	1241.121	0.019	12	-1.876	E	253905.16	334477.49	$3d^5(^2S)4s$	^3S	1	$3d^5(^2S)4p$	$^1P°$	1	d,z,R1*
1241.174	0.022	1241.1791	0.0031	12	-1.340	E	235421.42	315989.97	$3d^5(^2F_1)4s$	^3F	4	$3d^5(^2H)4p$	$^3H°$	5	d,z,R1*
1241.338	0.006	1241.3344	0.0045	160	-0.081	E	234275.30	314833.77	$3d^5(^4F)4s$	^5F	3	$3d^5(^4F)4p$	$^5F°$	2	p,W
1241.429	0.006	1241.4355	0.0047	220	-0.601	E	241772.99	322324.90	$3d^5(^2H)4s$	^3H	6	$3d^5(^2H)4p$	$^1I°$	6	p,z,W*
1241.429	0.006	1241.428	0.012	220	-0.092	E	233840.06	314392.43	$3d^5(^2I)4s$	^1I	6	$3d^5(^2I)4p$	$^1I°$	6	p,z,W*
1241.641	0.002	1241.6407	0.0019	270	0.278	C+	229413.82	309952.42	$3d^5(^2I)4s$	^3I	5	$3d^5(^2I)4p$	$^3H°$	4	W
1241.991	0.002	1241.9887	0.0017	220	-0.016	E	234083.15	314599.18	$3d^5(^4F)4s$	^5F	5	$3d^5(^4F)4p$	$^5F°$	4	W
1242.080	0.002	1242.0800	0.0019	390	0.349	C+	229409.73	309919.84	$3d^5(^2I)4s$	^3I	6	$3d^5(^2I)4p$	$^3H°$	5	W
1242.142	0.007	1242.1432	0.0038	70	-0.589	E	229413.82	309919.84	$3d^5(^2I)4s$	^3I	5	$3d^5(^2I)4p$	$^3H°$	5	R1
1242.645	0.002	1242.6480	0.0017	80	-0.538	E	234125.87	314599.18	$3d^5(^4F)4s$	^5F	4	$3d^5(^4F)4p$	$^5F°$	4	W
1243.228	0.002	1243.2269	0.0018	210	-0.008	E	234125.87	314561.71	$3d^5(^4F)4s$	^5F	4	$3d^5(^4F)4p$	$^5F°$	3	W
1243.334	0.007	1243.3396	0.0044	56	-0.548	E	235736.35	316164.90	$3d^5(^2F_1)4s$	^3F	2	$3d^5(^2F_1)4p$	$^3F°$	2	R1
1243.415	0.007	1243.4173	0.0034	53	-1.152	E	216590.56	297014.07	$3d^5(^4D)4s$	^5D	2	$3d^5(^4D)4p$	$^5D°$	2	R1
1243.505	0.002	1243.5050	0.0019	180	-0.256	E	216596.2	297014.07	$3d^5(^4D)4s$	^5D	3	$3d^5(^4D)4p$	$^5D°$	2	W
1243.668	0.002	1243.6682	0.0019	130	-0.215	E	232546.14	312953.43	$3d^5(^2D_3)4s$	^3D	3	$3d^5(^2F_1)4p$	$^3D°$	3	W
1244.024	0.007	1244.0268	0.0049	75	-0.356	E	216189.97	296574.09	$3d^5(^4D)4s$	^5D	4	$3d^5(^4D)4p$	$^5D°$	3	R1
1244.185	0.002	1244.1833	0.0033	4560	0.093	C+	274774.89	355148.90	$3d^5(^2G_1)4s$	^3G	3	$3d^5(^2G_1)4p$	$^3F°$	2	W*
1244.185	0.002	1244.1850	0.0025	4560	0.391	B+	164523.18	244897.1	$3d^5(^6S)4s$	^7S	3	$3d^5(^6S)4p$	$^7P°$	4	W*
1244.281	0.022	1244.257	0.018	52	-0.179	E	306962.95	387332.2	$3d^5(^2D_1)4s$	^3D	3	$3d^5(^2D_1)4p$	$^3F°$	3	p,R1
1244.659	0.007	1244.6621	0.0024	17	-1.110	E	232546.14	312889.22	$3d^5(^2D_3)4s$	^3D	3	$3d^5(^4F)4p$	$^5G°$	3	R1
1244.792	0.004	1244.7899	0.0032	110	-0.548	E	229409.73	309744.57	$3d^5(^2I)4s$	^3I	6	$3d^5(^2I)4p$	$^1K°$	7	l,W
1244.966	0.002	1245.0184	0.0045	150	-1.216	E	240194.22	320514.32	$3d^5(^2F_1)4s$	^1F	3	$3d^5(^2G_2)4p$	$^3F°$	3	I,z,W*
1244.966	0.002	1244.9598	0.0031	150	-0.172	E	234275.30	314599.18	$3d^5(^4F)4s$	^5F	3	$3d^5(^4F)4p$	$^5F°$	4	I,z,W*
1244.966	0.002	1244.9693	0.0045	150	-0.925	E	216596.2	296919.48	$3d^5(^4D)4s$	^5D	3	$3d^5(^4D)4p$	$^5D°$	4	I,z,W*
1245.069	0.002	1245.0658	0.0016	150	-0.242	E	242504.64	322821.68	$3d^5(^2G_2)4s$	^3G	4	$3d^5(^4F)4p$	$^3F°$	4	I,W
1245.187	0.002	1245.2097	0.0027	670	-0.469	E	247049.61	327357.37	$3d^5(^2G_2)4s$	^1G	4	$3d^5(^2H)4p$	$^1H°$	5	z,W*
1245.187	0.002	1245.231	0.025	670	0.024	E	307025.84	387332.2	$3d^5(^2D_1)4s$	^3D	2	$3d^5(^2D_1)4p$	$^3F°$	3	z,W*
1245.187	0.002	1245.186	0.013	670	0.391	B+	234083.15	314392.43	$3d^5(^4F)4s$	^5F	5	$3d^5(^2I)4p$	$^1I°$	6	z,W*
1245.272	0.022	1245.2764	0.0049	53	-1.105	E	229441.11	309744.57	$3d^5(^2I)4s$	^3I	7	$3d^5(^2I)4p$	$^1K°$	7	d,R1
1245.362	0.022	1245.3668	0.0043	69	-0.420	E	232655.80	312953.43	$3d^5(^2D_3)4s$	^3D	2	$3d^5(^2F_1)4p$	$^3D°$	3	s,R1
1245.452	0.002	1245.433	0.049	480	0.539	B+	274696.55	354989.9	$3d^5(^2G_1)4s$	^3G	5	$3d^5(^2G_1)4p$	$^3H°$	6	z,W*
1245.452	0.002	1245.4377	0.0085	480	-0.751	E	225545.70	305838.76	$3d^5(^4D)4s$	^3D	1	$3d^5(^4D)4p$	$^3P°$	1	z,W*
1245.531	0.007	1245.5408	0.0031	65	-0.703	E	234275.30	314561.71	$3d^5(^4F)4s$	^5F	3	$3d^5(^4F)4p$	$^5F°$	3	R1
1245.997	0.007	1245.9899	0.0050	8	-1.091	E	243266.72	323524.19	$3d^5(^4F)4s$	^3F	2	$3d^5(^4F)4p$	$^3F°$	3	R1
1246.124	0.022	1246.120	0.010	35	-1.008	E	235115.74	315364.82	$3d^5(^4F)4s$	^5F	1	$3d^5(^2F_1)4p$	$^3D°$	2	d,bl,R1

Table A.2 (cont'd)

λ_{obs} [a] (Å)	u_{obs} [b] (Å)	λ_{Ritz} [c] (Å)	u_{Ritz} [d] (Å)	I [e]	$\log(gf_R)$ [f]	$\log(gf_R)$ [g]	E_i [h] (cm^{-1})	E_k [i] (cm^{-1})	Lower Level Configuration	Term	J	Upper Level Configuration	Term [k]	J	Notes [j]
1246.362	0.007	1246.3634	0.0039	25	-0.988	E	232655.80	312889.22	$3d^5(^2D_3)4s$	^{3}D	2	$3d^5(^4F)4p$	^{5}G°	3	R1
1246.544	0.007	1246.5517	0.0056	57	-0.491	E	225617.46	305838.76	$3d^5(^4D)4s$	^{3}D	2	$3d^5(^4D)4p$	^{3}P°	1	R1
1246.830	0.022	1246.824	0.018	71	-0.226	E	268274.36	348478.15	$3d^5(^2D_2)4s$	^{1}D	2	$3d^5(^2D_2)4p$	^{1}P°	1	z,R1*
1246.830	0.022	1246.8205	0.0071	71	-0.249	E	263701.48	343905.49	$3d^5(^2D_2)4s$	^{3}D	1	$3d^5(^2D_2)4p$	^{3}D°	2	z,R1*
1247.367	0.005	1247.3645	0.0044	80	-0.543	E	263736.46	343905.49	$3d^5(^2D_2)4s$	^{3}D	2	$3d^5(^2D_2)4p$	^{3}D°	2	d,bl,W
1247.571	0.005	1247.5878	0.0040	120	-0.044	E	243369.51	323524.19	$3d^5(^4F)4s$	^{3}F	3	$3d^5(^4F)4p$	^{3}F°	3	p,W
1247.673	0.007	1247.6722	0.0026	57	-0.641	E	234412.45	314561.71	$3d^5(^4F)4s$	^{5}F	2	$3d^5(^4F)4p$	^{5}F°	3	R1
1248.050	0.002	1248.0513	0.0017	90	-0.424	E	234083.15	314208.06	$3d^5(^4F)4s$	^{5}F	5	$3d^5(^2F_1)4p$	^{3}F°	4	W
1248.091	0.022	1248.0900	0.0061	38	-0.897	E	240960.04	321082.47	$3d^5(^2H)4s$	^{3}H	4	$3d^5(^2F_1)4p$	^{1}F°	3	p,R1
1248.227	0.022	1248.2280	0.0044	24	-0.789	E	242504.64	322618.21	$3d^5(^2G_2)4s$	^{3}G	4	$3d^5(^4F)4p$	^{3}D°	3	l,R1
1248.445	0.022	1248.4513	0.0049	55	-0.425	E	263806.25	343905.49	$3d^5(^2D_2)4s$	^{3}D	3	$3d^5(^2D_2)4p$	^{3}D°	2	p,R1
1248.495	0.007	1248.4910	0.0033	73	-0.181	E	246241.70	326338.39	$3d^5(^2H)4s$	^{1}H	5	$3d^5(^2G_2)4p$	^{1}H°	5	R1
1248.826	0.002	1248.8266	0.0018	80	-0.338	E	247282.20	327357.37	$3d^5(^2F_2)4s$	^{3}F	4	$3d^5(^2H)4p$	^{1}H°	5	W
1249.442	0.007	1249.4370	0.0050	93	-0.595	E	235115.74	315151.79	$3d^5(^4F)4s$	^{5}F	1	$3d^5(^4F)4p$	^{5}F°	1	R1
1249.534	0.002	1249.5327	0.0019	410	0.096	C+	208131.05	288160.97	$3d^5(^4G)4s$	^{5}G	5	$3d^5(^4G)4p$	^{5}F°	4	I,W
1250.043	0.022	1250.0483	0.0041	83	-0.402	E	208164.06	288160.97	$3d^5(^4G)4s$	^{5}G	4	$3d^5(^4G)4p$	^{5}F°	4	z,R1*
1250.043	0.022	1250.065	0.012	83	-0.825	E	208165.11	288160.97	$3d^5(^4G)4s$	^{5}G	3	$3d^5(^4G)4p$	^{5}F°	4	z,R1*
1250.397	0.004	1250.4081	0.0038	2540	-0.394	E	241082.67	321056.56	$3d^5(^2H)4s$	^{3}H	5	$3d^5(^2G_2)4p$	^{3}F°	4	I,w,z,W*
1250.397	0.004	1250.3970	0.0044	2540	0.610	B+	208046.61	288021.21	$3d^5(^4G)4s$	^{5}G	6	$3d^5(^4G)4p$	^{5}H°	7	I,w,W*
1250.397	0.004	1250.3458	0.0052	2540	-0.400	E	216596.2	296574.09	$3d^5(^4D)4s$	^{5}D	3	$3d^5(^4D)4p$	^{5}D°	3	I,w,z,W*
1250.543	0.005	1250.5426	0.0029	2540	-0.133	E	239107.85	319073.14	$3d^5(^2D_3)4s$	^{1}D	2	$3d^5(^2D_3)4p$	^{1}P°	1	I,p,W
1250.685	0.007	1250.6797	0.0048	43	-0.892	E	247165.79	327122.31	$3d^5(^2F_2)4s$	^{3}F	2	$3d^5(^2F_2)4p$	^{1}D°	2	R1
1250.782	0.007	1250.7961	0.0031	48	-0.677	E	235421.42	315370.50	$3d^5(^2F_1)4s$	^{3}F	4	$3d^5(^2G_2)4p$	^{3}H°	4	R1
1250.903	0.022	1250.900	0.021	26	-0.329	E	307025.84	386968.3	$3d^5(^2D_1)4s$	^{3}D	2	$3d^5(^2D_1)4p$	^{3}F°	2	l,R1
1251.293	0.007	1251.2884	0.0044	22	-1.225	E	232546.14	312463.76	$3d^5(^2D_3)4s$	^{3}D	3	$3d^5(^2F_1)4p$	^{3}G°	3	R1
1251.837	0.002	1251.8359	0.0019	440	0.426	B+	217049.7	296932.37	$3d^5(^4G)4s$	^{3}G	5	$3d^5(^4G)4p$	^{3}G°	5	W
1252.073	0.005	1252.0733	0.0030	5	-0.328	E	232910.84	312778.37	$3d^5(^2D_3)4s$	^{3}D	1	$3d^5(^4F)4p$	^{5}G°	2	I,p,W
1252.169	0.002	1252.188	0.018	570	0.268	C+	208046.61	287906.8	$3d^5(^4G)4s$	^{5}G	6	$3d^5(^4G)4p$	^{5}F°	5	z,W*
1252.169	0.002	1252.145	0.031	570	-0.127	E	307105.32	386968.3	$3d^5(^2D_1)4s$	^{3}D	1	$3d^5(^2D_1)4p$	^{3}F°	2	z,W*
1252.282	0.004	1252.2828	0.0033	50	-0.034	E	229409.73	309263.90	$3d^5(^2I)4s$	^{3}I	6	$3d^5(^2I)4p$	^{3}H°	6	I,p,W
1252.346	0.007	1252.3469	0.0040	68	-0.735	E	229413.82	309263.90	$3d^5(^2I)4s$	^{3}I	5	$3d^5(^2I)4p$	^{3}H°	6	R1
1252.393	0.007	1252.3989	0.0038	62	-1.015	E	217049.7	296896.46	$3d^5(^4G)4s$	^{3}G	5	$3d^5(^4G)4p$	^{3}G°	4	R1
1252.477	0.007	1252.4823	0.0064	44	-0.885	E	225545.70	305387.15	$3d^5(^4D)4s$	^{3}D	1	$3d^5(^4D)4p$	^{3}P°	0	R1
1252.717	0.022	1252.7140	0.0069	72	-0.573	E	236454.05	316280.73	$3d^5(^2F_1)4s$	^{3}F	3	$3d^5(^2F_1)4p$	^{3}F°	3	p,R1
1252.777	0.004	1252.7751	0.0037	620	0.338	C+	229441.11	309263.90	$3d^5(^2I)4s$	^{3}I	7	$3d^5(^2I)4p$	^{3}H°	6	q,W
1253.025	0.004	1253.0078	0.0057	150	-0.535	E	232655.80	312463.76	$3d^5(^2D_3)4s$	^{3}D	2	$3d^5(^2F_1)4p$	^{3}G°	3	p,z,W*

Table A.2 (cont'd)

λ_{obs} [a] (Å)	u_{obs} [b] (Å)	λ_{Ritz} [c] (Å)	u_{Ritz} [d] (Å)	I [e]	$\log(gf_R)$ [f]	$\log(gf_R)$ [g]	E_i [h] (cm^{-1})	E_k [i] (cm^{-1})	Lower Level Configuration	Term	J	Upper Level Configuration	Term [k]	J	Notes [j]
1253.025	0.004	1253.0182	0.0051	150	-1.466	E	208152.08	287959.38	$3d^5(^4G)4s$	^5G	2	$3d^5(^4G)4p$	$^5F°$	3	p,z,W*
1253.096	0.007	1253.0967	0.0038	58	-1.071	E	217130.07	296932.37	$3d^5(^4G)4s$	^3G	4	$3d^5(^4G)4p$	$^3G°$	5	R1
1253.205	0.002	1253.2184	0.0060	380	-0.966	E	234125.87	313920.42	$3d^5(^4F)4s$	^5F	4	$3d^5(^2D_3)4p$	$^3D°$	3	z,W*
1253.205	0.002	1253.2063	0.0048	380	-0.361	E	208164.06	287959.38	$3d^5(^4G)4s$	^5G	4	$3d^5(^4G)4p$	$^5F°$	3	z,W*
1253.205	0.002	1253.223	0.011	380	-0.783	E	208165.11	287959.38	$3d^5(^4G)4s$	^5G	3	$3d^5(^4G)4p$	$^5F°$	3	z,W*
1253.300	0.007	1253.2992	0.0045	81	-0.234	E	217130.07	296919.48	$3d^5(^4G)4s$	^3G	4	$3d^5(^4D)4p$	$^5D°$	4	R1
1253.494	0.002	1253.498	0.014	220	-0.362	E	263701.48	343478.21	$3d^5(^2D_2)4s$	^3D	1	$3d^5(^2D_2)4p$	$^3D°$	1	z,W*
1253.494	0.002	1253.514	0.017	220	-0.423	E	208131.05	287906.8	$3d^5(^4G)4s$	^5G	5	$3d^5(^4G)4p$	$^5F°$	5	z,W*
1253.598	0.022	1253.5739	0.0055	61	-0.780	E	247104.70	326876.62	$3d^5(^2F_2)4s$	^3F	3	$3d^5(^2F_2)4p$	$^3F°$	4	p,R1
1253.668	0.004	1253.6608	0.0032	630	0.145	C+	217130.07	296896.46	$3d^5(^4G)4s$	^3G	4	$3d^5(^4G)4p$	$^3G°$	4	q,W
1253.996	0.002	1253.9798	0.0090	480	0.197	C+	217100.94	296847.04	$3d^5(^4G)4s$	^3G	3	$3d^5(^4G)4p$	$^3G°$	3	z,W*
1253.996	0.002	1253.9617	0.0036	480	-0.997	E	235421.42	315168.67	$3d^5(^2F_1)4s$	^3F	4	$3d^5(^4F)4p$	$^5F°$	5	z,W*
1253.996	0.002	1254.033	0.017	480	-0.366	E	208164.06	287906.8	$3d^5(^4G)4s$	^5G	4	$3d^5(^4G)4p$	$^5F°$	5	z,W*
1254.200	0.002	1254.1940	0.0018	110	-0.120	E	240194.22	319926.70	$3d^5(^2F_1)4s$	^1F	3	$3d^5(^2F_1)4p$	$^1D°$	2	W
1254.421	0.002	1254.4214	0.0062	280	-0.580	E	235115.74	314833.77	$3d^5(^4F)4s$	^5F	1	$3d^5(^4F)4p$	$^5F°$	2	z,W*
1254.421	0.002	1254.4218	0.0094	280	-0.263	E	243266.72	322984.72	$3d^5(^4F)4s$	^3F	2	$3d^5(^4F)4p$	$^3D°$	1	z,W*
1254.421	0.002	1254.4380	0.0075	280	-0.804	E	217130.07	296847.04	$3d^5(^4G)4s$	^3G	4	$3d^5(^4G)4p$	$^3G°$	3	z,W*
1254.541	0.007	1254.5344	0.0042	47	-0.860	E	236454.05	316164.90	$3d^5(^2F_1)4s$	^3F	3	$3d^5(^2F_1)4p$	$^3F°$	2	R1
1254.861	0.007	1254.8645	0.0026	55	-0.233	E	247049.61	326739.49	$3d^5(^2G_2)4s$	^1G	4	$3d^5(^2G_2)4p$	$^1F°$	3	R1
1255.576	0.007	1255.5697	0.0057	22	-1.097	E	234275.30	313920.42	$3d^5(^4F)4s$	^5F	3	$3d^5(^2D_3)4p$	$^3D°$	3	R1
1255.748	0.004	1255.7326	0.0050	170	-0.817	E	247104.70	326739.49	$3d^5(^2F_2)4s$	^3F	3	$3d^5(^2G_2)4p$	$^1F°$	3	I,w,z,W*
1255.748	0.004	1255.7338	0.0072	170	-0.233	E	232655.80	312290.51	$3d^5(^2D_3)4s$	^3D	2	$3d^5(^2D_3)4p$	$^3P°$	1	I,w,z,W*
1255.805	0.004	1255.832	0.010	170	-0.694	E	235736.35	315364.82	$3d^5(^2F_1)4s$	^3F	2	$3d^5(^2F_1)4p$	$^3D°$	2	I,w,z,W*
1255.805	0.004	1255.8164	0.0064	170	-1.363	E	208152.08	287781.55	$3d^5(^4G)4s$	^5G	2	$3d^5(^4P)4p$	$^5D°$	2	I,w,z,W*
1256.031	0.002	1256.0386	0.0030	130	-0.307	E	236454.05	316069.44	$3d^5(^2F_1)4s$	^3F	3	$3d^5(^2F_1)4p$	$^3G°$	4	z,W*
1256.031	0.002	1256.022	0.012	130	-0.864	E	208165.11	287781.55	$3d^5(^4G)4s$	^5G	3	$3d^5(^4P)4p$	$^5D°$	2	z,W*
1256.221	0.004	1256.2212	0.0039	130	-1.416	E	208152.08	287755.89	$3d^5(^4G)4s$	^5G	2	$3d^5(^4P)4p$	$^5D°$	1	q,W
1256.303	0.022	1256.3027	0.0092	21	-1.905	E	208046.61	287645.26	$3d^5(^4G)4s$	^5G	6	$3d^5(^4G)4p$	$^5H°$	6	p,R1
1256.379	0.009	1256.4533	0.0059	170	-0.536	E	235736.35	315325.46	$3d^5(^2F_1)4s$	^3F	2	$3d^5(^2D_3)4p$	$^1F°$	3	d,z,W*
1256.379	0.009	1256.3695	0.0038	170	-0.029	E	247282.20	326876.62	$3d^5(^2F_2)4s$	^3F	4	$3d^5(^2F_2)4p$	$^3F°$	4	d,z,W*
1256.829	0.007	1256.8326	0.0059	49	-0.563	E	235736.35	315301.44	$3d^5(^2F_1)4s$	^3F	2	$3d^5(^2F_1)4p$	$^3D°$	1	R1
1256.916	0.002	1256.9159	0.0020	100	0.354	C+	279200.87	358760.69	$3d^5(^2G_1)4s$	^1G	4	$3d^5(^2G_1)4p$	$^1G°$	4	W
1257.000	0.007	1257.0034	0.0041	41	-0.544	E	240960.04	320514.32	$3d^5(^2H)4s$	^3H	4	$3d^5(^2G_2)4p$	$^3F°$	3	R1
1257.136	0.002	1257.1325	0.0018	100	-0.240	E	263736.46	343282.57	$3d^5(^2D_2)4s$	^3D	2	$3d^5(^2D_2)4p$	$^3F°$	3	W
1257.637	0.004	1257.6368	0.0039	2210	0.535	B+	208131.05	287645.26	$3d^5(^4G)4s$	^5G	5	$3d^5(^4G)4p$	$^5H°$	6	w,W
1258.022	0.002	1258.0249	0.0016	190	-0.131	E	243332.00	322821.68	$3d^5(^4F)4s$	^3F	4	$3d^5(^4F)4p$	$^3F°$	4	W

Table A.2 (cont'd)

λ_{obs} [a] (Å)	u_{obs} [b] (Å)	λ_{Ritz} [c] (Å)	u_{Ritz} [d] (Å)	I [e]	$\log(gf_R)$ [f]	$\log(gf_R)$ [g]	E_i [h] (cm^{-1})	E_k [i] (cm^{-1})	Lower Level Configuration	Term	J	Upper Level Configuration	Term [k]	J	Notes [j]
1258.232	0.002	1258.2364	0.0018	160	-0.039	E	263806.25	343282.57	$3d^5(^2D_2)4s$	^3D	3	$3d^5(^2D_2)4p$	$^3F°$	3	W
1258.462	0.002	1258.4578	0.0042	20	-1.076	E	242862.56	322324.90	$3d^5(^2G_2)4s$	^3G	5	$3d^5(^2H)4p$	$^1I°$	6	I,z,W*
1258.462	0.002	1258.4655	0.0041	20	-0.978	E	232546.14	312007.98	$3d^5(^2D_3)4s$	^3D	3	$3d^5(^2F_1)4p$	$^1G°$	4	I,z,W*
1258.538	0.002	1258.5378	0.0018	80	-0.226	E	247282.20	326739.49	$3d^5(^2F_2)4s$	^3F	4	$3d^5(^2G_2)4p$	$^1F°$	3	W
1259.035	0.007	1259.0391	0.0043	53	-0.505	E	240194.22	319619.87	$3d^5(^2F_1)4s$	^1F	3	$3d^5(^4F)4p$	$^3G°$	3	R1
1259.129	0.007	1259.1312	0.0051	78	-0.048	E	232546.14	311965.97	$3d^5(^2D_3)4s$	^3D	3	$3d^5(^2D_3)4p$	$^3P°$	2	R1
1259.195	0.007	1259.2010	0.0048	65	-0.589	E	235736.35	315151.79	$3d^5(^2F_1)4s$	^3F	2	$3d^5(^4F)4p$	$^5F°$	1	R1
1259.589	0.002	1259.5925	0.0031	290	-0.046	E	229413.82	308804.58	$3d^5(^2I)4s$	^3I	5	$3d^5(^2I)4p$	$^1H°$	5	q,W
1259.727	0.004	1259.7289	0.0032	230	-0.038	E	234083.15	313465.31	$3d^5(^4F)4s$	^5F	5	$3d^5(^4F)4p$	$^5G°$	5	q,W
1260.412	0.007	1260.4071	0.0035	82	0.188	C+	234125.87	313465.31	$3d^5(^4F)4s$	^5F	4	$3d^5(^4F)4p$	$^5G°$	5	R1
1260.736	0.01	1260.7601	0.0039	310	-0.680	E	246241.70	325558.93	$3d^5(^2H)4s$	^1H	5	$3d^5(^2F_2)4p$	$^1G°$	4	p,W
1260.881	0.007	1260.8723	0.0052	8	-1.439	E	232655.80	311965.97	$3d^5(^2D_3)4s$	^3D	2	$3d^5(^2D_3)4p$	$^3P°$	2	R1
1261.120	0.007	1261.1199	0.0043	10	-1.249	E	212095.56	291390.15	$3d^5(^4P)4s$	^5P	3	$3d^5(^4P)4p$	$^5P°$	2	R1
1261.233	0.022	1261.2534	0.0045	82	-0.031	E	243332.00	322618.21	$3d^5(^4F)4s$	^3F	4	$3d^5(^4F)4p$	$^3D°$	3	w,z,R1*
1261.233	0.022	1261.2125	0.0030	82	-0.107	E	247049.61	326338.39	$3d^5(^2G_2)4s$	^1G	4	$3d^5(^2G_2)4p$	$^1H°$	5	w,z,R1*
1261.233	0.022	1261.219	0.012	82	-0.592	E	212253.22	291541.60	$3d^5(^4P)4s$	^5P	2	$3d^5(^4P)4p$	$^5P°$	1	w,z,R1*
1261.344	0.006	1261.3426	0.0053	520	0.409	B+	235421.42	314702.02	$3d^5(^2F1)4s$	^3F	4	$3d^5(^2F_1)4p$	$^3G°$	5	I,p,W
1261.447	0.006	1261.4349	0.0051	140	0.431	B+	279200.87	358475.67	$3d^5(^2G1)4s$	^1G	4	$3d^5(^2G_1)4p$	$^1H°$	5	I,p,W
1261.575	0.007	1261.5726	0.0045	9	-1.469	E	234412.45	313678.60	$3d^5(^4F)4s$	^5F	2	$3d^5(^2D_3)4p$	$^3D°$	1	R1
1261.760	0.004	1261.7596	0.0037	1010	0.422	B+	216189.97	295444.37	$3d^5(^4D)4s$	^5D	4	$3d^5(^4D)4p$	$^5F°$	5	w,W
1262.145	0.007	1262.1084	0.0038	2	-1.781	E	212095.56	291328.05	$3d^5(^4P)4s$	^5P	3	$3d^5(^4G)4p$	$^3F°$	3	R1
1262.552	0.002	1262.5520	0.0064	90	0.156	C+	274740.12	353944.78	$3d^5(^2G_1)4s$	^3G	4	$3d^5(^2G_1)4p$	$^3F°$	3	z,W*
1262.552	0.002	1262.559	0.017	90	-0.104	E	311471.22	390675.47	$3d^5(^2D_1)4s$	^1D	2	$3d^5(^2D_1)4p$	$^1D°$	2	z,W*
1262.655	0.007	1262.6636	0.0026	20	-0.948	E	234083.15	313280.81	$3d^5(^4F)4s$	^5F	5	$3d^5(^4F)4p$	$^5G°$	4	R1
1262.754	0.008	1262.7471	0.0061	90	-0.246	E	263701.48	342893.90	$3d^5(^2D_2)4s$	^3D	1	$3d^5(^2D_2)4p$	$^3F°$	2	d,W
1262.985	0.007	1262.9809	0.0026	2	-1.377	E	235421.42	314599.18	$3d^5(^2F_1)4s$	^3F	4	$3d^5(^4F)4p$	$^5F°$	4	R1
1263.101	0.007	1263.1065	0.0056	11	-0.532	E	274774.89	353944.78	$3d^5(^2G_1)4s$	^3G	3	$3d^5(^2G_1)4p$	$^3F°$	3	R1
1263.301	0.007	1263.3051	0.0054	69	-0.261	E	263736.46	342893.90	$3d^5(^2D_2)4s$	^3D	2	$3d^5(^2D_2)4p$	$^3F°$	2	R1
1263.345	0.002	1263.3450	0.0018	260	-0.141	E	234125.87	313280.81	$3d^5(^4F)4s$	^5F	4	$3d^5(^4F)4p$	$^5G°$	4	W
1263.580	0.007	1263.5789	0.0029	41	-0.693	E	235421.42	314561.71	$3d^5(^2F_1)4s$	^3F	4	$3d^5(^4F)4p$	$^5F°$	3	R1
1263.633	0.007	1263.6325	0.0045	33	-1.142	E	212253.22	291390.15	$3d^5(^4P)4s$	^5P	2	$3d^5(^4P)4p$	$^5P°$	2	R1
1264.013	0.007	1264.0037	0.0037	2	-1.302	E	221087.24	300200.93	$3d^5(^4P)4s$	^3P	2	$3d^5(^4D)4p$	$^5P°$	3	R1
1264.264	0.007	1264.2637	0.0048	9	-1.190	E	235736.35	314833.77	$3d^5(^2F_1)4s$	^3F	2	$3d^5(^4F)4p$	$^5F°$	2	R1
1264.437	0.022	1264.4199	0.0058	71	-1.024	E	263806.25	342893.90	$3d^5(^2D_2)4s$	^3D	3	$3d^5(^2D_2)4p$	$^3F°$	2	z,R1*
1264.437	0.022	1264.438	0.013	71	-0.734	E	212455.09	291541.60	$3d^5(^4P)4s$	^5P	1	$3d^5(^4P)4p$	$^5P°$	1	z,R1*
1264.520	0.008	1264.5242	0.0089	4300	-0.473	E	208046.61	287127.74	$3d^5(^4G)4s$	^5G	6	$3d^5(^4G)4p$	$^5H°$	5	w,z,W*

Table A.2 (cont'd)

λ_{obs} [a] (Å)	u_{obs} [b] (Å)	λ_{Ritz} [c] (Å)	u_{Ritz} [d] (Å)	I [e]	$\log(gf_R)$ [f]	$\log(gf_R)$ [g]	E_i [h] (cm^{-1})	E_k [i] (cm^{-1})	Lower Level Configuration	Term	J	Upper Level Configuration	Term [k]	J	Notes [j]
1264.520	0.008	1264.452	0.043	4300	0.267	C+	164523.18	243608.8	$3d^5(^6S)4s$	^7S	3	$3d^5(^6S)4p$	$^7P°$	3	w,z,W*
1264.640	0.022	1264.6249	0.0045	43	-1.758	E	212253.22	291328.05	$3d^5(^4P)4s$	^5P	2	$3d^5(^4G)4p$	$^3F°$	3	p,R1
1264.750	0.007	1264.7490	0.0056	70	-0.155	E	243369.51	322436.58	$3d^5(^4F)4s$	^3F	3	$3d^5(^4F)4p$	$^3D°$	2	R1
1264.931	0.007	1264.9231	0.0029	67	-0.075	E	247282.20	326338.39	$3d^5(^2F_2)4s$	^3F	4	$3d^5(^2G_2)4p$	$^1H°$	5	R1
1265.669	0.005	1265.6666	0.0046	930	0.592	B+	241772.99	320782.74	$3d^5(^2H)4s$	^3H	6	$3d^5(^2H)4p$	$^3I°$	7	w,W
1265.739	0.005	1265.7345	0.0031	370	0.024	E	234275.30	313280.81	$3d^5(^4F)4s$	^5F	3	$3d^5(^4F)4p$	$^5G°$	4	I,p,W
1265.875	0.002	1265.8758	0.0019	220	-1.251	E	208131.05	287127.74	$3d^5(^4G)4s$	^5G	5	$3d^5(^4G)4p$	$^5H°$	5	W
1266.101	0.007	1266.1332	0.0038	330	-0.676	E	247049.61	326030.24	$3d^5(^2G_2)4s$	^1G	4	$3d^5(^2F_2)4p$	$^3F°$	3	p,W
1266.407	0.004	1266.4050	0.0036	1490	0.390	B+	208164.06	287127.74	$3d^5(^4G)4s$	^5G	4	$3d^5(^4G)4p$	$^5H°$	5	w,W
1266.705	0.002	1266.7090	0.0018	50	-0.437	E	240194.22	319138.95	$3d^5(^2F_1)4s$	^1F	3	$3d^5(^2G_2)4p$	$^1G°$	4	W
1266.864	0.002	1266.8642	0.0020	170	-0.145	E	212455.09	291390.15	$3d^5(^4P)4s$	^5P	1	$3d^5(^4P)4p$	$^5P°$	2	W
1267.038	0.007	1267.0170	0.0049	47	-0.424	E	247104.70	326030.24	$3d^5(^2F_2)4s$	^3F	3	$3d^5(^2F_2)4p$	$^3F°$	3	R1
1267.151	0.022	1267.1629	0.0036	26	-0.987	E	236454.05	315370.50	$3d^5(^2F_1)4s$	^3F	3	$3d^5(^2G_2)4p$	$^3H°$	4	l,R1
1267.304	0.004	1267.254	0.010	820	-0.092	E	236454.05	315364.82	$3d^5(^2F_1)4s$	^3F	3	$3d^5(^2F_1)4p$	$^3D°$	2	w,z,W*
1267.304	0.004	1267.3171	0.0038	820	-0.070	E	246241.70	325148.55	$3d^5(^2H)4s$	^1H	5	$3d^5(^2G_2)4p$	$^3H°$	6	w,z,W*
1267.304	0.004	1267.3075	0.0059	820	0.320	C+	229409.73	308317.18	$3d^5(^2I)4s$	^3I	6	$3d^5(^2I)4p$	$^3I°$	7	w,z,W*
1267.812	0.004	1267.8116	0.0039	580	0.259	C+	229441.11	308317.18	$3d^5(^2I)4s$	^3I	7	$3d^5(^2I)4p$	$^3I°$	7	w,W
1267.896	0.007	1267.8866	0.0049	78	-0.202	E	236454.05	315325.46	$3d^5(^2F_1)4s$	^3F	3	$3d^5(^2D_3)4p$	$^1F°$	3	R1
1267.996	0.007	1267.9984	0.0043	39	-0.566	E	247165.79	326030.24	$3d^5(^2F_2)4s$	^3F	2	$3d^5(^2F_2)4p$	$^3F°$	3	R1
1268.181	0.002	1268.1816	0.0018	120	-0.043	E	274696.55	353549.6	$3d^5(^2G_1)4s$	^3G	5	$3d^5(^2G_1)4p$	$^3H°$	5	W
1268.757	0.007	1268.7650	0.0047	48	-0.597	E	247165.79	325982.59	$3d^5(^2F_2)4s$	^3F	2	$3d^5(^2F_2)4p$	$^3F°$	2	R1
1268.883	0.002	1268.8827	0.0018	240	0.254	C+	274740.12	353549.6	$3d^5(^2G_1)4s$	^3G	4	$3d^5(^2G_1)4p$	$^3H°$	5	W
1269.250	0.006	1269.2507	0.0025	190	-0.407	E	235421.42	314208.06	$3d^5(^2F_1)4s$	^3F	4	$3d^5(^2F_1)4p$	$^3F°$	4	p,W
1269.387	0.006	1269.3885	0.0027	320	0.094	C+	241082.67	319860.76	$3d^5(^2H)4s$	^3H	5	$3d^5(^2H)4p$	$^3I°$	6	p,W
1269.628	0.002	1269.6260	0.0017	70	-0.816	E	234125.87	312889.22	$3d^5(^4F)4s$	^5F	4	$3d^5(^4F)4p$	$^5G°$	3	W
1270.205	0.002	1270.2047	0.0019	120	-0.055	E	242290.58	321018.04	$3d^5(^2G_2)4s$	^3G	3	$3d^5(^2G_2)4p$	$^3F°$	2	W
1270.690	0.009	1270.6900	0.0090	1850	0.658	B+	229441.11	308138.51	$3d^5(^2I)4s$	^3I	7	$3d^5(^2I)4p$	$^3K°$	8	w,W
1271.262	0.022	1271.2643	0.0031	64	-0.642	E	212095.56	290757.40	$3d^5(^4P)4s$	^5P	3	$3d^5(^4P)4p$	$^5P°$	3	z,R1*
1271.262	0.022	1271.2969	0.0046	64	-1.189	E	240960.04	319619.87	$3d^5(^2H)4s$	^3H	4	$3d^5(^4F)4p$	$^3G°$	3	z,R1*
1271.442	0.007	1271.4434	0.0039	72	0.136	C+	274696.55	353347.32	$3d^5(^2G_1)4s$	^3G	5	$3d^5(^2G_1)4p$	$^3F°$	4	R1
1272.035	0.007	1272.0394	0.0031	66	-0.346	E	234275.30	312889.22	$3d^5(^4F)4s$	^5F	3	$3d^5(^4F)4p$	$^5G°$	3	R1
1272.158	0.007	1272.1481	0.0039	5	-1.045	E	274740.12	353347.32	$3d^5(^2G_1)4s$	^3G	4	$3d^5(^2G_1)4p$	$^3F°$	4	R1
1272.647	0.022	1272.6236	0.0063	70	-0.418	E	242504.64	321082.47	$3d^5(^2G_2)4s$	^3G	4	$3d^5(^2F_1)4p$	$^1F°$	3	w,z,R1*
1272.647	0.022	1272.662	0.040	70	-1.070	E	208131.05	286706.5	$3d^5(^4G)4s$	^5G	5	$3d^5(^4G)4p$	$^5H°$	4	w,z,R1*
1272.720	0.007	1272.7111	0.0043	66	-0.160	E	274774.89	353347.32	$3d^5(^2G_1)4s$	^3G	3	$3d^5(^2G_1)4p$	$^3F°$	4	R1
1272.785	0.022	1272.7318	0.0074	11	-0.909	E	235115.74	313686.89	$3d^5(^4F)4s$	^5F	1	$3d^5(^2D_3)4p$	$^3D°$	2	d,R1

Table A.2 (cont'd)

λ_{obs} [a] (Å)	u_{obs} [b] (Å)	λ_{Ritz} [c] (Å)	u_{Ritz} [d] (Å)	I [e]	$\log(gf_R)$ [f]	$\log(gf_R)$ [g]	E_i [h] (cm^{-1})	E_k [i] (cm^{-1})	Lower Level Configuration	Term	J	Upper Level Configuration	Term [k]	J	Notes [j]
1272.867	0.007	1272.8661	0.0049	3	-1.223	E	235115.74	313678.60	$3d^5(^4F)4s$	^5F	1	$3d^5(^2D_3)4p$	$^3D°$	1	R1
1273.207	0.009	1273.2207	0.0033	1440	-1.112	E	234412.45	312953.43	$3d^5(^4F)4s$	^5F	2	$3d^5(^2F_1)4p$	$^3D°$	3	w,z,W*
1273.207	0.009	1273.197	0.040	1440	-1.220	E	208164.06	286706.5	$3d^5(^4G)4s$	^5G	4	$3d^5(^4G)4p$	$^5H°$	4	w,z,W*
1273.207	0.009	1273.214	0.041	1440	0.339	C+	208165.11	286706.5	$3d^5(^4G)4s$	^5G	3	$3d^5(^4G)4p$	$^5H°$	4	w,z,W*
1273.738	0.007	1273.7341	0.0035	56	-0.492	E	247049.61	325558.93	$3d^5(^2G_2)4s$	^1G	4	$3d^5(^2F_2)4p$	$^1G°$	4	R1
1273.818	0.004	1273.8175	0.0031	360	-0.093	E	212253.22	290757.40	$3d^5(^4P)4s$	^5P	2	$3d^5(^4P)4p$	$^5P°$	3	p,W
1274.261	0.002	1274.2624	0.0018	210	-0.082	E	234412.45	312889.22	$3d^5(^4F)4s$	^5F	2	$3d^5(^4F)4p$	$^5G°$	3	W
1274.501	0.022	1274.5093	0.0077	2	-1.506	E	235115.74	313577.31	$3d^5(^4F)4s$	^5F	1	$3d^5(^2D_3)4p$	$^3P°$	0	d,R1
1275.925	0.002	1275.9233	0.0018	140	-0.124	E	274696.55	353071.17	$3d^5(^2G_1)4s$	^3G	5	$3d^5(^2G_1)4p$	$^3H°$	4	W
1276.431	0.002	1276.4312	0.0019	750	0.254	C+	216596.2	294939.65	$3d^5(^4D)4s$	^5D	3	$3d^5(^4D)4p$	$^5F°$	4	W
1276.632	0.005	1276.6330	0.0026	190	-0.323	E	274740.12	353071.17	$3d^5(^2G_1)4s$	^3G	4	$3d^5(^2G_1)4p$	$^3H°$	4	w,W
1276.891	0.022	1276.9060	0.0051	36	-1.553	E	217130.07	295444.37	$3d^5(^4G)4s$	^3G	4	$3d^5(^4D)4p$	$^5F°$	5	l,R1
1276.944	0.01	1276.9456	0.0097	2730	0.120	C+	164523.18	242835.05	$3d^5(^6S)4s$	^7S	3	$3d^5(^6S)4p$	$^7P°$	2	s,W
1277.187	0.01	1277.1999	0.0042	110	0.026	E	274774.89	353071.17	$3d^5(^2G_1)4s$	^3G	3	$3d^5(^2G_1)4p$	$^3H°$	4	p,W
1277.667	0.007	1277.6635	0.0050	29	-1.020	E	239107.85	317375.72	$3d^5(^2D_3)4s$	^1D	2	$3d^5(^2H)4p$	$^3G°$	3	R1
1278.396	0.022	1278.3842	0.0045	2	-0.596	E	242290.58	320514.32	$3d^5(^2G_2)4s$	^3G	3	$3d^5(^2G_2)4p$	$^3F°$	3	H,R1
1278.872	0.004	1278.8705	0.0035	160	-0.192	E	242862.56	321056.56	$3d^5(^2G_2)4s$	^3G	5	$3d^5(^2G_2)4p$	$^3F°$	4	q,W
1279.058	0.022	1279.0329	0.0067	17	-0.571	E	235736.35	313920.42	$3d^5(^2F_1)4s$	^3F	2	$3d^5(^2D_3)4p$	$^3D°$	3	p,R1
1279.329	0.002	1279.3329	0.0018	660	0.139	C+	212095.56	290261.29	$3d^5(^4P)4s$	^5P	3	$3d^5(^4P)4p$	$^5D°$	4	W
1279.713	0.002	1279.7130	0.0020	1190	0.243	C+	208152.08	286294.60	$3d^5(^4G)4s$	^5G	2	$3d^5(^4G)4p$	$^5H°$	3	W
1279.934	0.022	1279.926	0.013	12	-1.265	E	208165.11	286294.60	$3d^5(^4G)4s$	^5G	3	$3d^5(^4G)4p$	$^5H°$	3	H,z,R1*
1279.934	0.022	1279.9092	0.0071	12	-1.748	E	208164.06	286294.60	$3d^5(^4G)4s$	^5G	4	$3d^5(^4G)4p$	$^5H°$	3	H,z,R1*
1280.113	0.022	1280.1172	0.0045	52	0.172	C+	240960.04	319077.89	$3d^5(^2H)4s$	^3H	4	$3d^5(^2H)4p$	$^3I°$	5	z,R1*
1280.113	0.022	1280.0960	0.0066	52	-0.251	E	247104.70	325223.84	$3d^5(^2F_2)4s$	^3F	3	$3d^5(^2G_2)4p$	$^3G°$	4	z,R1*
1280.282	0.022	1280.2842	0.0036	8	-1.201	E	236454.05	314561.71	$3d^5(^2F_1)4s$	^3F	3	$3d^5(^4F)4p$	$^5F°$	3	H,z,R1*
1280.282	0.022	1280.2868	0.0065	8	-0.634	E	247104.70	325212.20	$3d^5(^2F_2)4s$	^3F	3	$3d^5(^2G_2)4p$	$^3G°$	3	H,z,R1*
1281.277	0.022	1281.2889	0.0057	21	-0.287	E	247165.79	325212.20	$3d^5(^2F_2)4s$	^3F	2	$3d^5(^2G_2)4p$	$^3G°$	3	w,z,R1*
1281.277	0.022	1281.2085	0.0050	21	-0.659	E	234412.45	312463.76	$3d^5(^4F)4s$	^5F	2	$3d^5(^2F_1)4p$	$^3G°$	3	w,z,R1*
1281.277	0.022	1281.3303	0.0040	21	-1.006	E	235421.42	313465.31	$3d^5(^2F_1)4s$	^3F	4	$3d^5(^4F)4p$	$^5G°$	5	w,z,R1*
1281.882	0.007	1281.8922	0.0042	6	-0.520	E	242504.64	320514.32	$3d^5(^2G_2)4s$	^3G	4	$3d^5(^2G_2)4p$	$^3F°$	3	R1
1282.282	0.006	1282.2127	0.0083	460	0.002	E	229409.73	307399.91	$3d^5(^2I)4s$	^3I	6	$3d^5(^2I)4p$	$^3I°$	6	w,z,W*
1282.282	0.006	1282.2800	0.0081	460	0.147	C+	229413.82	307399.91	$3d^5(^2I)4s$	^3I	5	$3d^5(^2I)4p$	$^3I°$	6	w,z,W*
1282.747	0.022	1282.7323	0.0046	55	-1.449	E	221087.24	299045.83	$3d^5(^4P)4s$	^3P	2	$3d^5(^4D)4p$	$^5P°$	2	z,R1*
1282.747	0.022	1282.7288	0.0089	55	-0.059	E	229441.11	307399.91	$3d^5(^2I)4s$	^3I	7	$3d^5(^2I)4p$	$^3I°$	6	z,R1*
1283.184	0.007	1283.1830	0.0028	12	-0.155	E	247049.61	324980.8	$3d^5(^2G_2)4s$	^1G	4	$3d^5(^2G_2)4p$	$^3G°$	5	R1
1283.948	0.022	1283.9365	0.0056	16	-0.682	E	221087.24	298972.71	$3d^5(^4P)4s$	^3P	2	$3d^5(^4D)4p$	$^3D°$	3	l,z,R1*

Table A.2 (cont'd)

λ_{obs} [a] (Å)	u_{obs} [b] (Å)	λ_{Ritz} [c] (Å)	u_{Ritz} [d] (Å)	I [e]	$\log(gf_R)$ [f]	$\log(gf_R)$ [g]	E_i [h] (cm^{-1})	E_k [i] (cm^{-1})	Lower Level Configuration	Term	J	Upper Level Configuration	Term [k]	J	Notes [j]
1283.948	0.022	1283.9919	0.0043	16	-1.293	E	234125.87	312007.98	$3d^5(^4F)4s$	^5F	4	$3d^5(^2F_1)4p$	$^1G°$	4	l,z,R1*
1284.476	0.007	1284.4753	0.0057	56	0.068	C+	216590.56	294443.35	$3d^5(^4D)4s$	^5D	2	$3d^5(^4D)4p$	$^5F°$	3	R1
1284.556	0.022	1284.5688	0.0062	47	-0.447	E	216596.2	294443.35	$3d^5(^4D)4s$	^5D	3	$3d^5(^4D)4p$	$^5F°$	3	p,R1
1285.814	0.022	1285.794	0.015	30	-0.012	E	253905.16	331678.14	$3d^5(^2S)4s$	^3S	1	$3d^5(^2S)4p$	$^3P°$	2	H,R1
1286.117	0.007	1286.1073	0.0032	27	-0.110	E	236454.05	314208.06	$3d^5(^2F_1)4s$	^3F	3	$3d^5(^2F_1)4p$	$^3F°$	4	R1
1286.470	0.022	1286.4602	0.0049	2	-1.002	E	234275.30	312007.98	$3d^5(^4F)4s$	^5F	3	$3d^5(^2F_1)4p$	$^1G°$	4	H,R1
1287.572	0.002	1287.5717	0.0020	390	0.080	C+	232546.14	310211.71	$3d^5(^2D_3)4s$	^3D	3	$3d^5(^2D_3)4p$	$^3F°$	4	W
1287.661	0.022	1287.6206	0.0064	59	-0.433	E	235115.74	312778.37	$3d^5(^4F)4s$	^5F	1	$3d^5(^4F)4p$	$^5G°$	2	p,z,R1*
1287.661	0.022	1287.621	0.013	59	0.119	C+	268274.36	345936.97	$3d^5(^2D_2)4s$	^1D	2	$3d^5(^2D_2)4p$	$^1F°$	3	p,z,R1*
1287.805	0.007	1287.8080	0.0051	48	-0.201	E	216434.77	294086.09	$3d^5(^4D)4s$	^5D	1	$3d^5(^4D)4p$	$^5F°$	2	R1
1288.523	0.022	1288.5124	0.0071	3	-0.961	E	242290.58	319899.45	$3d^5(^2G_2)4s$	^3G	3	$3d^5(^4F)4p$	$^3G°$	4	G,R1
1289.834	0.022	1289.852	0.022	31	-0.563	E	216305.74	293834.0	$3d^5(^4D)4s$	^5D	0	$3d^5(^4D)4p$	$^5F°$	1	z,R1*
1289.834	0.022	1289.7899	0.0031	31	-0.334	E	235421.42	312953.43	$3d^5(^2F_1)4s$	^3F	4	$3d^5(^2F_1)4p$	$^3D°$	3	z,R1*
1290.397	0.002	1290.3968	0.0019	150	-0.404	E	216590.56	294086.09	$3d^5(^4D)4s$	^5D	2	$3d^5(^4D)4p$	$^5F°$	2	W
1290.482	0.022	1290.4912	0.0037	22	-1.684	E	216596.2	294086.09	$3d^5(^4D)4s$	^5D	3	$3d^5(^4D)4p$	$^5F°$	2	p,R1
1290.875	0.022	1290.8827	0.0068	2	-0.975	E	236454.05	313920.42	$3d^5(^2F_1)4s$	^3F	3	$3d^5(^2D_3)4p$	$^3D°$	3	H,z,R1*
1290.875	0.022	1290.8589	0.0029	2	-0.964	E	235421.42	312889.22	$3d^5(^2F_1)4s$	^3F	4	$3d^5(^4F)4p$	$^5G°$	3	H,z,R1*
1292.015	0.022	1292.002	0.021	32	-0.573	E	216434.77	293834.0	$3d^5(^4D)4s$	^5D	1	$3d^5(^4D)4p$	$^5F°$	1	l,z,R1*
1292.015	0.022	1292.0763	0.0070	32	-0.360	E	242504.64	319899.45	$3d^5(^2G_2)4s$	^3G	4	$3d^5(^4F)4p$	$^3G°$	4	l,z,R1*
1293.180	0.007	1293.1710	0.0045	5	-0.479	E	242290.58	319619.87	$3d^5(^2G_2)4s$	^3G	3	$3d^5(^4F)4p$	$^3G°$	3	R1
1295.292	0.004	1295.2922	0.0036	190	-0.197	E	212095.56	289298.21	$3d^5(^4P)4s$	^5P	3	$3d^5(^4P)4p$	$^5D°$	3	q,W
1295.761	0.007	1295.7603	0.0058	49	-2.991	E	235115.74	312290.51	$3d^5(^4F)4s$	^5F	1	$3d^5(^2D_3)4p$	$^3P°$	1	R1
1296.198	0.007	1296.2015	0.0025	49	-0.517	E	242504.64	319653.14	$3d^5(^2G_2)4s$	^3G	4	$3d^5(^4F)4p$	$^3G°$	5	R1
1297.729	0.022	1297.7398	0.0059	3	-0.761	E	239107.85	316164.90	$3d^5(^2D_3)4s$	^1D	2	$3d^5(^2F_1)4p$	$^3F°$	2	H,R1
1297.981	0.022	1297.9429	0.0046	7	-1.239	E	212253.22	289298.21	$3d^5(^4P)4s$	^5P	2	$3d^5(^4P)4p$	$^5D°$	3	w,z,R1*
1297.981	0.022	1297.9876	0.0050	7	-1.132	E	235421.42	312463.76	$3d^5(^2F_1)4s$	^3F	4	$3d^5(^2F_1)4p$	$^3G°$	3	w,z,R1*
1298.732	0.002	1298.7317	0.0019	630	0.280	C+	242862.56	319860.76	$3d^5(^2G_2)4s$	^3G	5	$3d^5(^2H)4p$	$^3I°$	6	W
1300.220	0.007	1300.2209	0.0052	16	-1.663	E	212253.22	289163.23	$3d^5(^4P)4s$	^5P	2	$3d^5(^4G)4p$	$^5F°$	1	R1
1300.981	0.002	1300.9808	0.0020	460	-0.114	E	178019.6	254884.70	$3d^5(^6S)4s$	^5S	2	$3d^5(^6S)4p$	$^5P°$	1	W
1301.601	0.022	1301.5786	0.0059	9	-1.009	E	216590.56	293420.33	$3d^5(^4D)4s$	^5D	2	$3d^5(^4P)4p$	$^3P°$	1	H,R4
1302.145	0.01	1302.2431	0.0028	260	-0.227	E	242862.56	319653.14	$3d^5(^2G_2)4s$	^3G	5	$3d^5(^4F)4p$	$^3G°$	5	l,W
1302.386	0.002	1302.3861	0.0020	350	-0.179	E	212095.56	288877.70	$3d^5(^4P)4s$	^5P	3	$3d^5(^4P)4p$	$^5S°$	2	W
1302.835	0.004	1302.8377	0.0034	170	-0.777	E	221087.24	297842.77	$3d^5(^4P)4s$	^3P	2	$3d^5(^4P)4p$	$^3D°$	2	H,W
1303.306	0.008	1303.3152	0.0052	1320	-0.023	E	235736.35	312463.76	$3d^5(^2F_1)4s$	^3F	2	$3d^5(^2F_1)4p$	$^3G°$	3	w,W
1303.969	0.005	1303.9741	0.0045	17	-0.251	E	247165.79	323854.43	$3d^5(^2F_2)4s$	^3F	2	$3d^5(^4F)4p$	$^3F°$	2	R4
1304.870	0.022	1304.8155	0.0039	63	-0.333	E	229409.73	306048.92	$3d^5(^2I)4s$	^3I	6	$3d^5(^2I)4p$	$^3I°$	5	z,R4*

Table A.2 (cont'd)

λ_{obs} [a] (Å)	u_{obs} [b] (Å)	λ_{Ritz} [c] (Å)	u_{Ritz} [d] (Å)	I [e]	$\log(gf_R)$ [f]	$\log(gf_R)$ [g]	E_i [h] (cm^{-1})	E_k [i] (cm^{-1})	Lower Level Configuration	Term	J	Upper Level Configuration	Term [k]	J	Notes [j]
1304.870	0.022	1304.8851	0.0038	63	0.213	C+	229413.82	306048.92	$3d^5(^2I)4s$	^3I	5	$3d^5(^2I)4p$	$^3I°$	5	z,R4*
1304.870	0.022	1304.8986	0.0030	63	-0.808	E	242504.64	319138.95	$3d^5(^2G_2)4s$	^3G	4	$3d^5(^2G_2)4p$	$^1G°$	4	z,R4*
1305.068	0.002	1305.0660	0.0038	160	-0.538	E	212253.22	288877.70	$3d^5(^4P)4s$	^5P	2	$3d^5(^4P)4p$	$^5S°$	2	z,W*
1305.068	0.002	1305.0193	0.0029	160	-0.794	E	247282.20	323909.42	$3d^5(^2F_2)4s$	^3F	4	$3d^5(^2G_2)4p$	$^3H°$	5	z,W*
1305.702	0.004	1305.7062	0.0054	570	0.205	C+	229409.73	305996.64	$3d^5(^2I)4s$	^3I	6	$3d^5(^2I)4p$	$^3K°$	7	q,z,W*
1305.702	0.004	1305.7121	0.0046	570	-1.191	E	235421.42	312007.98	$3d^5(^2F_1)4s$	^3F	4	$3d^5(^2F_1)4p$	$^1G°$	4	q,z,W*
1305.932	0.005	1305.9391	0.0043	55	0.041	C+	242504.64	319077.89	$3d^5(^2G_2)4s$	^3G	4	$3d^5(^2H)4p$	$^3I°$	5	R4
1306.241	0.002	1306.2414	0.0020	870	0.291	C+	229441.11	305996.64	$3d^5(^2I)4s$	^3I	7	$3d^5(^2I)4p$	$^3K°$	7	W
1306.613	0.022	1306.614	0.020	70	0.508	B+	208046.61	284580.3	$3d^5(^4G)4s$	^5G	6	$3d^5(^4G)4p$	$^5G°$	6	w,R4
1307.599	0.002	1307.5990	0.0020	720	0.101	C+	178019.6	254495.66	$3d^5(^6S)4s$	^5S	2	$3d^5(^6S)4p$	$^5P°$	2	W
1307.754	0.022	1307.772	0.015	10	-0.349	E	253905.16	330371.06	$3d^5(^2S)4s$	^3S	1	$3d^5(^2S)4p$	$^3P°$	1	p,R4
1308.646	0.002	1308.6575	0.0059	710	-0.224	E	221428.58	297842.77	$3d^5(^4P)4s$	^3P	1	$3d^5(^4P)4p$	$^3D°$	2	z,W*
1308.646	0.002	1308.6319	0.0054	710	-0.637	E	240960.04	317375.72	$3d^5(^2H)4s$	^3H	4	$3d^5(^2H)4p$	$^3G°$	3	z,W*
1308.646	0.002	1308.5667	0.0064	710	-0.345	E	247104.70	323524.19	$3d^5(^2F_2)4s$	^3F	3	$3d^5(^4F)4p$	$^3F°$	3	z,W*
1309.147	0.022	1309.1383	0.0053	10	-0.920	E	216596.2	292982.34	$3d^5(^4D)4s$	^5D	3	$3d^5(^4P)4p$	$^3P°$	2	p,R4
1309.654	0.005	1309.6539	0.0050	53	-0.338	E	208046.61	284402.66	$3d^5(^4G)4s$	^5G	6	$3d^5(^4G)4p$	$^5G°$	5	R4
1310.078	0.002	1310.0906	0.0049	310	-1.364	E	221087.24	297417.84	$3d^5(^4P)4s$	^3P	2	$3d^5(^4D)4p$	$^5D°$	1	z,W*
1310.078	0.002	1310.0772	0.0057	310	0.035	E	221087.24	297418.62	$3d^5(^4P)4s$	^3P	2	$3d^5(^4P)4p$	$^3D°$	3	z,W*
1310.257	0.002	1310.2530	0.0019	280	0.206	C+	243332.00	319653.14	$3d^5(^4F)4s$	^3F	4	$3d^5(^4F)4p$	$^3G°$	5	W
1310.819	0.022	1310.8634	0.0059	25	-0.882	E	232655.80	308941.40	$3d^5(^2D_3)4s$	^3D	2	$3d^5(^2D_3)4p$	$^1D°$	2	z,R4*
1310.819	0.022	1310.8244	0.0049	25	-0.874	E	243332.00	319619.87	$3d^5(^4F)4s$	^3F	4	$3d^5(^4F)4p$	$^3G°$	3	z,R4*
1311.111	0.002	1311.104	0.011	1860	0.362	B+	208131.05	284402.66	$3d^5(^4G)4s$	^5G	5	$3d^5(^4G).4p$	$^5G°$	5	z,W*
1311.111	0.002	1311.0217	0.0032	1860	-0.214	E	242862.56	319138.95	$3d^5(^2G_2)4s$	^3G	5	$3d^5(^2G2).4p$	$^1G°$	4	z,W*
1311.559	0.002	1311.5573	0.0019	330	-0.081	E	241082.67	317327.91	$3d^5(^2H)4s$	^3H	5	$3d^5(^2H)4p$	$^3H°$	6	W
1312.031	0.01	1312.0327	0.0060	450	-0.212	E	239107.85	315325.46	$3d^5(^2D_3)4s$	^1D	2	$3d^5(^2D_3)4p$	$^1F°$	3	d,bl,W
1312.709	0.022	1312.7368	0.0046	65	-0.266	E	208131.05	284307.78	$3d^5(^4G)4s$	^5G	5	$3d^5(^4G)4p$	$^5G°$	4	z,R4*
1312.709	0.022	1312.655	0.014	65	0.141	C+	229409.73	305591.23	$3d^5(^2I)4s$	^3I	6	$3d^5(^2I)4p$	$^3K°$	6	z,R4*
1312.709	0.022	1312.725	0.014	65	0.251	C+	229413.82	305591.23	$3d^5(^2I)4s$	^3I	5	$3d^5(^2I)4p$	$^3K°$	6	z,R4*
1313.306	0.002	1313.3059	0.0020	1220	0.232	C+	208164.06	284307.78	$3d^5(^4G)4s$	^5G	4	$3d^5(^4G)4p$	$^5G°$	4	W
1314.333	0.002	1314.299	0.029	1680	0.100	C+	208165.11	284251.3	$3d^5(^4G)4s$	^5G	3	$3d^5(^4G)4p$	$^5G°$	3	z,W*
1314.333	0.002	1314.281	0.027	1680	-0.334	E	208164.06	284251.3	$3d^5(^4G)4s$	^5G	4	$3d^5(^4G)4p$	$^5G°$	3	z,W*
1314.333	0.002	1314.3506	0.0054	1680	0.354	C+	246241.70	322324.90	$3d^5(^2H)4s$	^1H	5	$3d^5(^2H)4p$	$^1I°$	6	z,W*
1314.687	0.002	1314.687	0.044	890	-0.026	E	208152.08	284215.8	$3d^5(^4G)4s$	^5G	2	$3d^5(^4G)4p$	$^5G°$	2	z,W*
1314.687	0.002	1314.6578	0.0041	890	-0.705	E	212095.56	288160.97	$3d^5(^4P)4s$	^5P	3	$3d^5(^4G)4p$	$^5F°$	4	z,W*
1314.939	0.022	1314.912	0.045	63	-0.562	E	208165.11	284215.8	$3d^5(^4G)4s$	^5G	3	$3d^5(^4G)4p$	$^5G°$	2	w,z,R4*
1314.939	0.022	1314.9922	0.0099	63	-0.162	E	232546.14	308592.21	$3d^5(^2D_3)4s$	^3D	3	$3d^5(^2D_3)4p$	$^3F°$	3	w,z,R4*

Table A.2 (cont'd)

λ_{obs} [a] (Å)	u_{obs} [b] (Å)	λ_{Ritz} [c] (Å)	u_{Ritz} [d] (Å)	I [e]	$\log(gf_R)$ [f]	$\log(gf_R)$ [g]	E_i [h] (cm^{-1})	E_k [i] (cm^{-1})	Lower Level Configuration	Term	J	Upper Level Configuration	Term [k]	J	Notes [j]
1315.267	0.005	1315.2606	0.0042	55	-0.489	E	232910.84	308941.40	$3d^5(^2D_3)4s$	^3D	1	$3d^5(^2D_3)4p$	$^1D°$	2	R4
1315.668	0.002	1315.6679	0.0020	240	-0.079	E	225545.70	301552.72	$3d^5(^4D)4s$	^3D	1	$3d^5(^4D)4p$	$^3F°$	2	W
1315.973	0.022	1315.9754	0.0062	11	-1.126	E	221428.58	297417.84	$3d^5(^4P)4s$	^3P	1	$3d^5(^4D)4p$	$^5D°$	1	H,R4
1316.305	0.022	1316.2973	0.0048	5	-0.921	E	240194.22	316164.90	$3d^5(^2F_1)4s$	^1F	3	$3d^5(^2F_1)4p$	$^3F°$	2	H,R4
1316.909	0.022	1316.9113	0.0079	59	-0.553	E	225617.46	301552.72	$3d^5(^4D)4s$	^3D	2	$3d^5(^4D)4p$	$^3F°$	2	z,R4*
1316.909	0.022	1316.891	0.011	59	-0.184	E	232655.80	308592.21	$3d^5(^2D_3)4s$	^3D	2	$3d^5(^2D_3)4p$	$^3F°$	3	z,R4*
1317.039	0.022	1317.0575	0.0044	42	-0.760	E	221087.24	297014.07	$3d^5(^4P)4s$	^3P	2	$3d^5(^4D)4p$	$^5D°$	2	p,z,R4*
1317.039	0.022	1317.0259	0.0031	42	-0.912	E	240960.04	316888.69	$3d^5(^2H)4s$	^3H	4	$3d^5(^2H)4p$	$^3G°$	4	p,z,R4*
1317.444	0.002	1317.4446	0.0019	1030	0.548	B+	233840.06	309744.57	$3d^5(^2I)4s$	^1I	6	$3d^5(^2I)4p$	$^1K°$	7	W
1317.960	0.005	1317.9533	0.0029	33	-0.301	E	240194.22	316069.44	$3d^5(^2F_1)4s$	^1F	3	$3d^5(^2F_1)4p$	$^3G°$	4	R4
1318.152	0.002	1318.1512	0.0019	360	-0.180	E	212095.56	287959.38	$3d^5(^4P)4s$	^5P	3	$3d^5(^4G)4p$	$^5F°$	3	W
1318.358	0.005	1318.3544	0.0045	67	0.138	C+	225617.46	301469.60	$3d^5(^4D)4s$	^3D	2	$3d^5(^4D)4p$	$^3F°$	3	R4
1318.511	0.002	1318.5111	0.0020	970	0.240	C+	178019.6	253862.74	$3d^5(^6S)4s$	^5S	2	$3d^5(^6S)4p$	$^5P°$	3	W
1318.918	0.022	1318.9318	0.0094	7	-0.813	E	247165.79	322984.72	$3d^5(^2F_2)4s$	^3F	2	$3d^5(^4F)4p$	$^3D°$	1	d,R4
1319.158	0.002	1319.1564	0.0019	140	-0.150	E	241082.67	316888.69	$3d^5(^2H)4s$	^3H	5	$3d^5(^2H)4p$	$^3G°$	4	W
1319.743	0.005	1319.7475	0.0028	22	-0.141	E	247049.61	322821.68	$3d^5(^2G_2)4s$	^1G	4	$3d^5(^4F)4p$	$^3F°$	4	R4
1320.198	0.022	1320.2036	0.0048	10	-0.877	E	243332.00	319077.89	$3d^5(^4F)4s$	^3F	4	$3d^5(^2H)4p$	$^3I°$	5	d,R4
1320.715	0.002	1320.7151	0.0019	530	0.283	C+	225202.1	300918.68	$3d^5(^4D)4s$	^3D	3	$3d^5(^4D)4p$	$^3F°$	4	W
1320.894	0.005	1320.8965	0.0034	24	-0.638	E	212253.22	287959.38	$3d^5(^4P)4s$	^5P	2	$3d^5(^4G)4p$	$^5F°$	3	R4
1321.250	0.005	1321.2483	0.0045	35	-0.574	E	212095.56	287781.55	$3d^5(^4P)4s$	^5P	3	$3d^5(^4P)4p$	$^5D°$	2	R4
1323.293	0.022	1323.3009	0.0050	6	-0.708	E	247049.61	322618.21	$3d^5(^2G_2)4s$	^1G	4	$3d^5(^4F)4p$	$^3D°$	3	d,R4
1323.549	0.022	1323.5579	0.0049	56	-0.308	E	236454.05	312007.98	$3d^5(^2F_1)4s$	^3F	3	$3d^5(^2F_1)4p$	$^1G°$	4	z,R4*
1323.549	0.022	1323.5405	0.0039	56	0.215	C+	241772.99	317327.91	$3d^5(^2H)4s$	^3H	6	$3d^5(^2H)4p$	$^3H°$	6	z,R4*
1323.989	0.022	1324.0065	0.0056	65	-0.276	E	212253.22	287781.55	$3d^5(^4P)4s$	^5P	2	$3d^5(^4P)4p$	$^5D°$	2	z,R4*
1323.989	0.022	1323.970	0.013	65	0.324	C+	217100.94	292631.33	$3d^5(^4G)4s$	^3G	3	$3d^5(^4G)4p$	$^3H°$	4	z,R4*
1324.467	0.002	1324.4565	0.0068	240	-0.559	E	212253.22	287755.89	$3d^5(^4P)4s$	^5P	2	$3d^5(^4P)4p$	$^5D°$	1	z,W*
1324.467	0.002	1324.481	0.011	240	-1.046	E	217130.07	292631.33	$3d^5(^4G)4s$	^3G	4	$3d^5(^4G)4p$	$^3H°$	4	z,W*
1324.748	0.022	1324.7340	0.0067	44	-0.535	E	221087.24	296574.09	$3d^5(^4P)4s$	^3P	2	$3d^5(^4D)4p$	$^5D°$	3	p,R4
1325.094	0.008	1325.0939	0.0056	160	-0.014	E	251655.96	327122.31	$3d^5(^2F_2)4s$	^1F	3	$3d^5(^2F_2)4p$	$^1D°$	2	s,W
1325.818	0.022	1325.8406	0.0044	2	-1.422	E	233840.06	309263.90	$3d^5(^2I)4s$	^1I	6	$3d^5(^2I)4p$	$^3H°$	6	d,R4
1327.469	0.022	1327.4592	0.0077	21	-0.569	E	247104.70	322436.58	$3d^5(^2F_2)4s$	^3F	3	$3d^5(^4F)4p$	$^3D°$	2	p,R4
1327.636	0.022	1327.6565	0.0076	59	-0.976	E	240960.04	316280.73	$3d^5(^2H)4s$	^3H	4	$3d^5(^2F_1)4p$	$^3F°$	3	d,bl,R4
1328.015	0.022	1328.0071	0.0080	61	-0.430	E	212455.09	287755.89	$3d^5(^4P)4s$	^5P	1	$3d^5(^4P)4p$	$^5D°$	1	p,R4
1329.371	0.002	1329.3704	0.0020	270	0.403	B+	217130.07	292353.65	$3d^5(^4G)4s$	^3G	4	$3d^5(^4G)4p$	$^3H°$	5	W
1330.059	0.005	1330.0598	0.0034	15	-0.694	E	232546.14	307730.72	$3d^5(^2D_3)4s$	^3D	3	$3d^5(^2D_3)4p$	$^3F°$	2	R4
1331.409	0.022	1331.437	0.014	7	-0.950	E	216434.77	291541.60	$3d^5(^4D)4s$	^5D	1	$3d^5(^4P)4p$	$^5P°$	1	H,z,R4*

Table A.2 (cont'd)

λ_{obs} [a] (Å)	u_{obs} [b] (Å)	λ_{Ritz} [c] (Å)	u_{Ritz} [d] (Å)	I [e]	$\log(gf_R)$ [f]	$\log(gf_R)$ [g]	E_i [h] (cm^{-1})	E_k [i] (cm^{-1})	Lower Level Configuration	Term	J	Upper Level Configuration	Term [k]	J	Notes [j]
1331.409	0.022	1331.3913	0.0031	7	-0.979	E	240960.04	316069.44	$3d^5(^2H)4s$	^3H	4	$3d^5(^2F_1)4p$	$^3G°$	4	H,z,R4*
1332.000	0.005	1332.0028	0.0040	23	-0.537	E	232655.80	307730.72	$3d^5(^2D_3)4s$	^3D	2	$3d^5(^2D_3)4p$	$^3F°$	2	R4
1332.840	0.022	1332.8015	0.0031	61	-0.303	E	240960.04	315989.97	$3d^5(^2H)4s$	^3H	4	$3d^5(^2H)4p$	$^3H°$	5	d,bl,R4
1332.988	0.022	1332.9324	0.0050	47	-0.637	E	225202.1	300224.68	$3d^5(^4D)4s$	^3D	3	$3d^5(^4D)4p$	$^3D°$	2	p,z,R4*
1332.988	0.022	1333.019	0.014	47	-0.392	E	225545.70	300563.36	$3d^5(^4D)4s$	^3D	1	$3d^5(^4D)4p$	$^3D°$	1	p,z,R4*
1333.356	0.002	1333.3545	0.0019	250	-0.017	E	225202.1	300200.93	$3d^5(^4D)4s$	^3D	3	$3d^5(^4D)4p$	$^5P°$	3	W
1333.556	0.005	1333.5686	0.0028	12	-1.004	E	241082.67	316069.44	$3d^5(^2H)4s$	^3H	5	$3d^5(^2F_1)4p$	$^3G°$	4	R4
1333.965	0.002	1333.9642	0.0019	350	0.188	C+	233840.06	308804.58	$3d^5(^2I)4s$	^1I	6	$3d^5(^2I)4p$	$^1H°$	5	W
1334.178	0.022	1334.204	0.014	51	-0.902	E	216590.56	291541.60	$3d^5(^4D)4s$	^5D	2	$3d^5(^4P)4p$	$^5P°$	1	l,z,R4*
1334.178	0.022	1334.296	0.012	51	-0.746	E	225617.46	300563.36	$3d^5(^4D)4s$	^3D	2	$3d^5(^4D)4p$	$^3D°$	1	l,z,R4*
1334.178	0.022	1334.1735	0.0048	51	0.201	C+	241772.99	316725.76	$3d^5(^2H)4s$	^3H	6	$3d^5(^2H)4p$	$^3G°$	5	l,z,R4*
1334.984	0.002	1334.9834	0.0019	350	0.191	C+	241082.67	315989.97	$3d^5(^2H)4s$	^3H	5	$3d^5(^2H)4p$	$^3H°$	5	W
1336.161	0.002	1336.1605	0.0019	1080	0.487	B+	217049.7	291891.00	$3d^5(^4G)4s$	^3G	5	$3d^5(^4G)4p$	$^3H°$	6	W
1336.534	0.022	1336.5432	0.0057	18	-0.755	E	232910.84	307730.72	$3d^5(^2D_3)4s$	^3D	1	$3d^5(^2D_3)4p$	$^3F°$	2	H,R4
1336.631	0.022	1336.6329	0.0050	17	-0.495	E	246241.70	321056.56	$3d^5(^2H)4s$	^1H	5	$3d^5(^2G_2)4p$	$^3F°$	4	H,R4
1337.048	0.022	1337.0068	0.0050	56	-0.464	E	216596.2	291390.15	$3d^5(^4D)4s$	^5D	3	$3d^5(^4P)4p$	$^5P°$	2	w,z,R4*
1337.048	0.022	1337.0720	0.0033	56	-0.126	E	235421.42	310211.71	$3d^5(^2F_1)4s$	^3F	4	$3d^5(^2D_3)4p$	$^3F°$	4	w,z,R4*
1339.070	0.01	1339.0649	0.0078	600	-0.614	E	225545.70	300224.68	$3d^5(^4D)4s$	^3D	1	$3d^5(^4D)4p$	$^3D°$	2	d,bl,W
1340.353	0.002	1340.3529	0.0020	130	-0.269	E	225617.46	300224.68	$3d^5(^4D)4s$	^3D	2	$3d^5(^4D)4p$	$^3D°$	2	W
1341.068	0.002	1341.0680	0.0019	170	-0.176	E	216189.97	290757.40	$3d^5(^4D)4s$	^5D	4	$3d^5(^4P)4p$	$^5P°$	3	W
1342.179	0.002	1342.1800	0.0019	660	0.268	C+	217049.7	291555.35	$3d^5(^4G)4s$	^3G	5	$3d^5(^4G)4p$	$^3F°$	4	W
1342.895	0.005	1342.9065	0.0029	23	-0.286	E	242862.56	317327.91	$3d^5(^2G_2)4s$	^3G	5	$3d^5(^2H)4p$	$^3H°$	6	R4
1343.626	0.022	1343.6295	0.0045	19	-0.801	E	217130.07	291555.35	$3d^5(^4G)4s$	^3G	4	$3d^5(^4G)4p$	$^3F°$	4	H,R4
1343.898	0.002	1343.8971	0.0019	160	-0.021	E	240960.04	315370.50	$3d^5(^2H)4s$	^3H	4	$3d^5(^2G_2)4p$	$^3H°$	4	W
1347.215	0.022	1347.2167	0.0079	17	-0.861	E	217100.94	291328.05	$3d^5(^4G)4s$	^3G	3	$3d^5(^4G)4p$	$^3F°$	3	w,R4
1347.736	0.005	1347.7456	0.0039	55	0.130	C+	217130.07	291328.05	$3d^5(^4G)4s$	^3G	4	$3d^5(^4G)4p$	$^3F°$	3	R4
1348.676	0.005	1348.6822	0.0044	11	-1.078	E	279200.87	353347.32	$3d^5(^2G_1)4s$	^1G	4	$3d^5(^2G_1)4p$	$^3F°$	4	R4
1350.058	0.005	1350.0501	0.0030	56	-0.372	E	216189.97	290261.29	$3d^5(^4D)4s$	^5D	4	$3d^5(^4P)4p$	$^5D°$	4	R4
1350.861	0.022	1350.8743	0.0032	19	-0.710	E	242862.56	316888.69	$3d^5(^2G_2)4s$	^3G	5	$3d^5(^2H)4p$	$^3G°$	4	s,R4
1351.063	0.022	1351.0987	0.0033	22	-1.695	E	240194.22	314208.06	$3d^5(^2F_1)4s$	^1F	3	$3d^5(^2F_1)4p$	$^3F°$	4	w,R4
1351.414	0.002	1351.4140	0.0020	440	0.024	C+	217100.94	291097.51	$3d^5(^4G)4s$	^3G	3	$3d^5(^4G)4p$	$^3F°$	2	W
1353.127	0.005	1353.1256	0.0042	18	-0.179	E	251655.96	325558.93	$3d^5(^2F_2)4s$	^1F	3	$3d^5(^2F_2)4p$	$^1G°$	4	R4
1353.871	0.005	1353.8542	0.0040	26	-0.520	E	242862.56	316725.76	$3d^5(^2G_2)4s$	^3G	5	$3d^5(^2H)4p$	$^3G°$	5	R4
1354.528	0.022	1354.5426	0.0062	12	-1.220	E	235115.74	308941.40	$3d^5(^4F)4s$	^5F	1	$3d^5(^2D_3)4p$	$^1D°$	2	G,R4
1355.538	0.022	1355.5538	0.0056	37	-0.470	E	225202.1	298972.71	$3d^5(^4D)4s$	^3D	3	$3d^5(^4D)4p$	$^3D°$	3	s,z,R4*
1355.538	0.022	1355.4845	0.0047	37	-0.380	E	247282.20	321056.56	$3d^5(^2F_2)4s$	^3F	4	$3d^5(^2G_2)4p$	$^3F°$	4	s,z,R4*

Table A.2 (cont'd)

λ_{obs} [a] (Å)	u_{obs} [b] (Å)	λ_{Ritz} [c] (Å)	u_{Ritz} [d] (Å)	I [e]	$\log(gf_R)$ [f]	$\log(gf_R)$ [g]	E_i [h] (cm^{-1})	E_k [i] (cm^{-1})	Lower Level Configuration	Term	J	Upper Level Configuration	Term [k]	J	Notes [j]
1357.498	0.002	1357.4954	0.0018	150	-0.760	E	216596.2	290261.29	$3d^5(^4D)4s$	^5D	3	$3d^5(^4P)4p$	$^5D^\circ$	4	W
1358.158	0.022	1358.1913	0.0045	10	-1.751	E	217130.07	290757.40	$3d^5(^4G)4s$	^3G	4	$3d^5(^4P)4p$	$^5P^\circ$	3	w,R4
1358.338	0.022	1358.3385	0.0068	15	-1.435	E	241082.67	314702.02	$3d^5(^2H)4s$	^3H	5	$3d^5(^2F_1)4p$	$^3G^\circ$	5	H,z,R4*
1358.338	0.022	1358.3439	0.0043	15	-0.772	E	246241.70	319860.76	$3d^5(^2H)4s$	^1H	5	$3d^5(^2H)4p$	$^3I^\circ$	6	H,z,R4*
1360.807	0.022	1360.8158	0.0031	5	-0.671	E	242504.64	315989.97	$3d^5(^2G_2)4s$	^3G	4	$3d^5(^2H)4p$	$^3H^\circ$	5	H,R4
1361.872	0.022	1361.8714	0.0060	2	-4.222	E	225617.46	299045.83	$3d^5(^4D)4s$	^3D	2	$3d^5(^4D)4p$	$^5P^\circ$	2	w,R4
1363.921	0.005	1363.9165	0.0035	8	-0.887	E	234412.45	307730.72	$3d^5(^4F)4s$	^5F	2	$3d^5(^2D_3)4p$	$^3F^\circ$	2	R4
1366.029	0.022	1366.0260	0.0059	15	-1.026	E	235736.35	308941.40	$3d^5(^2F_1)4s$	^3F	2	$3d^5(^2D_3)4p$	$^1D^\circ$	2	H,z,R4*
1366.029	0.022	1365.9918	0.0033	15	-0.937	E	242862.56	316069.44	$3d^5(^2G_2)4s$	^3G	5	$3d^5(^2F_1)4p$	$^3G^\circ$	4	H,z,R4*
1366.682	0.022	1366.666	0.011	7	-1.073	E	235421.42	308592.21	$3d^5(^2F_1)4s$	^3F	4	$3d^5(^2D_3)4p$	$^3F^\circ$	3	d,R4
1368.363	0.022	1368.3648	0.0034	27	-0.292	E	242290.58	315370.50	$3d^5(^2G_2)4s$	^3G	3	$3d^5(^2G_2)4p$	$^3H^\circ$	4	H,R4
1372.549	0.022	1372.542	0.012	13	-1.088	E	216305.74	289163.23	$3d^5(^4D)4s$	^5D	0	$3d^5(^4G)4p$	$^5F^\circ$	1	H,z,R4*
1372.549	0.022	1372.5306	0.0080	13	-1.555	E	239107.85	311965.97	$3d^5(^2D_3)4s$	^1D	2	$3d^5(^2D_3)4p$	$^3P^\circ$	2	H,z,R4*
1372.549	0.022	1372.573	0.011	13	-1.659	E	235736.35	308592.21	$3d^5(^2F_1)4s$	^3F	2	$3d^5(^2D_3)4p$	$^3F^\circ$	3	H,z,R4*
1373.405	0.005	1373.4048	0.0049	29	-0.935	E	216434.77	289246.51	$3d^5(^4D)4s$	^5D	1	$3d^5(^4G)4p$	$^5F^\circ$	2	R4
1375.368	0.022	1375.3709	0.0055	20	-0.786	E	216590.56	289298.21	$3d^5(^4D)4s$	^5D	2	$3d^5(^4P)4p$	$^5D^\circ$	3	H,R4
1376.187	0.005	1376.1967	0.0035	44	-1.688	E	242504.64	315168.67	$3d^5(^2G_2)4s$	^3G	4	$3d^5(^4F)4p$	$^5F^\circ$	5	R4
1376.307	0.022	1376.3115	0.0034	24	-0.580	E	243332.00	315989.97	$3d^5(^4F)4s$	^3F	4	$3d^5(^2H)4p$	$^3H^\circ$	5	H,R4
1379.220	0.022	1379.2101	0.0049	16	-1.516	E	240960.04	313465.31	$3d^5(^2H)4s$	^3H	4	$3d^5(^4F)4p$	$^5G^\circ$	5	H,z,R4*
1379.220	0.022	1379.1593	0.0035	16	-1.494	E	242862.56	315370.50	$3d^5(^2G_2)4s$	^3G	5	$3d^5(^2G_2)4p$	$^3H^\circ$	4	H,z,R4*
1379.549	0.005	1379.5511	0.0042	3	-1.237	E	236454.05	308941.40	$3d^5(^2F_1)4s$	^3F	3	$3d^5(^2D_3)4p$	$^1D^\circ$	2	R4
1380.510	0.022	1380.483	0.015	10	-0.993	E	221428.58	293867.02	$3d^5(^4P)4s$	^3P	1	$3d^5(^4P)4p$	$^3P^\circ$	0	H,z,R4*
1380.510	0.022	1380.512	0.010	10	-2.132	E	225545.70	297982.60	$3d^5(^4D)4s$	^3D	1	$3d^5(^4D)4p$	$^5P^\circ$	1	H,z,R4*
1383.011	0.005	1383.0090	0.0035	17	-2.156	E	242862.56	315168.67	$3d^5(^2G_2)4s$	^3G	5	$3d^5(^4F)4p$	$^5F^\circ$	5	R4
1383.483	0.022	1383.4802	0.0034	2	-1.477	E	216596.2	288877.70	$3d^5(^4D)4s$	^5D	3	$3d^5(^4P)4p$	$^5S^\circ$	2	d,R4
1384.871	0.002	1384.8715	0.0020	230	-0.268	E	233840.06	306048.92	$3d^5(^2I)4s$	^1I	6	$3d^5(^2I)4p$	$^3I^\circ$	5	W
1385.918	0.022	1385.8748	0.0064	53	-0.546	E	233840.06	305996.64	$3d^5(^2I)4s$	^1I	6	$3d^5(^2I)4p$	$^3K^\circ$	7	d,bl,R4
1387.170	0.005	1387.1676	0.0031	7	-0.646	E	247049.61	319138.95	$3d^5(^2G_2)4s$	^1G	4	$3d^5(^2G_2)4p$	$^1G^\circ$	4	R4
1388.875	0.022	1388.8698	0.0057	2	-0.998	E	243369.51	315370.50	$3d^5(^4F)4s$	^3F	3	$3d^5(^2G_2)4p$	$^3H^\circ$	4	w,R4
1389.043	0.005	1389.0481	0.0045	24	-0.799	E	221428.58	293420.33	$3d^5(^4P)4s$	^3P	1	$3d^5(^4P)4p$	$^3P^\circ$	1	R4
1389.443	0.005	1389.4485	0.0039	22	-0.712	E	216189.97	288160.97	$3d^5(^4D)4s$	^5D	4	$3d^5(^4G)4p$	$^5F^\circ$	4	R4
1390.917	0.005	1390.9154	0.0046	49	-0.225	E	221087.24	292982.34	$3d^5(^4P)4s$	^3P	2	$3d^5(^4P)4p$	$^3P^\circ$	2	R4
1391.667	0.005	1391.6577	0.0031	12	-0.704	E	247282.20	319138.95	$3d^5(^2F_2)4s$	^3F	4	$3d^5(^2G_2)4p$	$^1G^\circ$	4	R4
1392.480	0.022	1392.4908	0.0052	60	-0.171	E	240194.22	312007.98	$3d^5(^2F_1)4s$	^1F	3	$3d^5(^2F_1)4p$	$^1G^\circ$	4	p,R4
1394.371	0.022	1394.373	0.020	56	-0.856	E	216189.97	287906.8	$3d^5(^4D)4s$	^5D	4	$3d^5(^4G)4p$	$^5F^\circ$	5	d,bl,R4
1397.548	0.022	1397.5506	0.0073	46	-0.731	E	221428.58	292982.34	$3d^5(^4P)4s$	^3P	1	$3d^5(^4P)4p$	$^3P^\circ$	2	d,bl,R4

Table A.2 (cont'd)

λ_{obs} [a] (Å)	u_{obs} [b] (Å)	λ_{Ritz} [c] (Å)	u_{Ritz} [d] (Å)	I [e]	$\log(gf_R)$ [f]	$\log(gf_R)$ [g]	E_i [h] (cm^{-1})	E_k [i] (cm^{-1})	Lower Level Configuration	Term	J	Upper Level Configuration	Term [k]	J	Notes [j]
2472.65		2473.367	0.019				1489.82	41920.54	$3d^6$	^5D	2	$3d^6$	^3D	3	R4
2514.62		2515.353	0.025				1871.38	41627.23	$3d^6$	^5D	1	$3d^6$	^3D	2	R4
2521.72		2522.484	0.033				2057.52	41700.99	$3d^6$	^5D	0	$3d^6$	^3D	1	R4
2934.99		2935.824	0.025				0.00	34061.99	$3d^6$	^5D	4	$3d^6$	^3G	4	R4
3036.18		3037.070	0.032				1489.82	34416.29	$3d^6$	^5D	2	$3d^6$	^3G	3	R4
3380.74		3381.717	0.034				0.00	29570.78	$3d^6$	^5D	4	$3d^6$	$^3F_2$	3	R4
3446.16		3447.185	0.038				889.61	29898.79	$3d^6$	^5D	3	$3d^6$	$^3F_2$	2	R4

[a]Experimentally measured wavelengths.

[b]One standard uncertainty of the wavelength value in the previous column.

[c]Ritz wavelengths derived from the optimized energy levels calculated by LOPT [19].

[d] Estimated uncertainty of the ritz wavelengths reported in the previous column.
The uncertainty of the ritz wavelength is determined as part of the level optimization routine in LOPT [19].

[e]Relative Intensity.

[f]$\log(gf)$ values calculated by A. J. J. Raassen and P. H. M. Uylings.

[g] Estimated uncertainty of the $\log(gf)$ values reported in the previous column:
B+ – Uncertainty $\leq 7\%$, C+ – Uncertainty $\leq 18\%$, E – Uncertainty $> 50\%$.

[h]Energy of the lower level from the level optimization. See Table A.3 for energy level uncertainty

[i]Energy of the upper level from the level optimization. See Table A.3 for energy level uncertainty

[j] Additional line information: d – diffuse, bl – blended, l – shaded longer, p – perturbed by close line, w – wide, s – shaded shorter, H – very hazy, G – rough estimate for line position, I – line intensity is unreliable, * – line is multiply classified, z – transition weighted out of level optimization, R1, R2, R3, R4 – Line intensity and experimental wavelength taken from Raassen et al. or Raassen and van Kleff with the wavelength shifted according to section **??**, W – line information based on measurements made in this work.

[k]°– Odd Parity.

Table A.3 Energy Levels of Ni V

Configuration	Term [a]	J	Energy (cm^{-1})	u_E [b] (cm^{-1})	Number of Transitions [c] Determining Level
$3d^6$	^5D	4	0.00	0.00	33
$3d^6$	^5D	3	889.61	0.29	37
$3d^6$	^5D	2	1489.82	0.32	32
$3d^6$	^5D	1	1871.38	0.35	25
$3d^6$	^5D	0	2057.52	0.46	10
$3d^6$	$^3P_2$	2	26152.49	0.38	24
$3d^6$	^3H	6	27111.40	0.33	28
$3d^6$	^3H	5	27578.61	0.32	40
$3d^6$	^3H	4	27858.94	0.32	41
$3d^6$	$^3P_2$	1	28697.33	0.40	20
$3d^6$	$^3F_2$	4	29123.90	0.30	49
$3d^6$	$^3F_2$	3	29570.78	0.29	41
$3d^6$	$^3P_2$	0	29640.25	0.50	9
$3d^6$	$^3F_2$	2	29898.79	0.34	33
$3d^6$	^3G	5	33256.49	0.30	35
$3d^6$	^3G	4	34061.99	0.29	43
$3d^6$	^3G	3	34416.29	0.34	39
$3d^6$	^1I	6	41252.65	0.39	19
$3d^6$	^3D	2	41627.23	0.36	33
$3d^6$	^3D	1	41700.99	0.39	23
$3d^6$	^3D	3	41920.54	0.31	34
$3d^6$	$^1G_2$	4	42208.47	0.32	28
$3d^6$	$^1S_2$	0	47699.96	0.61	3
$3d^6$	$^1D_2$	2	48607.12	0.39	18
$3d^6$	^1F	3	57924.12	0.35	20
$3d^6$	$^3P_1$	0	66738.13	0.67	8
$3d^6$	$^3P_1$	1	67548.05	0.48	21
$3d^6$	$^3F_1$	2	68632.25	0.44	16
$3d^6$	$^3F_1$	4	68719.26	0.34	24
$3d^6$	$^3F_1$	3	68855.07	0.35	26
$3d^6$	$^3P_1$	2	69156.49	0.36	18
$3d^6$	$^1G_1$	4	77900.04	0.42	13
$3d^6$	$^1D_1$	2	104421.97	0.75	5
$3d^5(^6S)4s$	^7S	3	164523.18	1.34	3
$3d^5(^6S)4s$	^5S	2	178019.6	0.3	3
$3d^5(^4G)4s$	^5G	6	208046.61	0.57	8
$3d^5(^4G)4s$	^5G	5	208131.05	0.29	13
$3d^5(^4G)4s$	^5G	2	208152.08	0.39	10
$3d^5(^4G)4s$	^5G	4	208164.06	0.34	14
$3d^5(^4G)4s$	^5G	3	208165.11	0.75	13
$3d^5(^4P)4s$	^5P	3	212095.56	0.26	17
$3d^5(^4P)4s$	^5P	2	212253.22	0.29	15
$3d^5(^4P)4s$	^5P	1	212455.09	0.36	8
$3d^5(^4D)4s$	^5D	4	216189.97	0.26	13
$3d^5(^4D)4s$	^5D	0	216305.74	0.61	4
$3d^5(^4D)4s$	^5D	1	216434.77	0.38	9
$3d^5(^4D)4s$	^5D	2	216590.56	0.29	13
$3d^5(^4D)4s$	^5D	3	216596.2	0.3	18
$3d^5(^4G)4s$	^3G	5	217049.7	0.3	5
$3d^5(^4G)4s$	^3G	3	217100.94	0.45	5
$3d^5(^4G)4s$	^3G	4	217130.07	0.29	11
$3d^5(^4P)4s$	^3P	2	221087.24	0.31	12
$3d^5(^4P)4s$	^3P	1	221428.58	0.38	8
$3d^5(^4D)4s$	^3D	3	225202.1	0.3	9
$3d^5(^4D)4s$	^3D	1	225545.70	0.50	9
$3d^5(^4D)4s$	^3D	2	225617.46	0.34	8
$3d^5(^2I)4s$	^3I	6	229409.73	0.33	11

Table A.3 (cont'd)

Configuration	Term [a]	J	Energy (cm^{-1})	u_E [b] (cm^{-1})	Number of Transitions [c] Determining Level
$3d^5(^2I)4s$	^3I	5	229413.82	0.31	11
$3d^5(^2I)4s$	^3I	7	229441.11	0.40	8
$3d^5(^2D_3)4s$	^3D	3	232546.14	0.26	15
$3d^5(^2D_3)4s$	^3D	2	232655.80	0.34	10
$3d^5(^2D_3)4s$	^3D	1	232910.84	0.36	8
$3d^5(^2I)4s$	^1I	6	233840.06	0.31	8
$3d^5(^4F)4s$	^5F	5	234083.15	0.26	11
$3d^5(^4F)4s$	^5F	4	234125.87	0.26	15
$3d^5(^4F)4s$	^5F	3	234275.30	0.29	14
$3d^5(^4F)4s$	^5F	2	234412.45	0.27	13
$3d^5(^4F)4s$	^5F	1	235115.74	0.36	13
$3d^5(^2F_1)4s$	^3F	4	235421.42	0.27	19
$3d^5(^2F_1)4s$	^3F	2	235736.35	0.32	14
$3d^5(^2F_1)4s$	^3F	3	236454.05	0.28	15
$3d^5(^2D_3)4s$	^1D	2	239107.85	0.35	11
$3d^5(^2F_1)4s$	^1F	3	240194.22	0.27	14
$3d^5(^2H)4s$	^3H	4	240960.04	0.27	14
$3d^5(^2H)4s$	^3H	5	241082.67	0.27	13
$3d^5(^2H)4s$	^3H	6	241772.99	0.31	8
$3d^5(^2G_2)4s$	^3G	3	242290.58	0.28	13
$3d^5(^2G_2)4s$	^3G	4	242504.64	0.26	19
$3d^5(^6S)4p$	$^7P^\circ$	2	242835.05	1.32	3
$3d^5(^2G_2)4s$	^3G	5	242862.56	0.27	16
$3d^5(^4F)4s$	^3F	2	243266.72	0.40	8
$3d^5(^4F)4s$	^3F	4	243332.00	0.26	15
$3d^5(^4F)4s$	^3F	3	243369.51	0.36	9
$3d^5(^6S)4p$	$^7P^\circ$	3	243608.8	2.3	2
$3d^5(^6S)4p$	$^7P^\circ$	4	244897.1	2.0	1
$3d^5(^2H)4s$	^1H	5	246241.70	0.30	9
$3d^5(^2G_2)4s$	^1G	4	247049.61	0.28	12
$3d^5(^2F_2)4s$	^3F	3	247104.70	0.37	11
$3d^5(^2F_2)4s$	^3F	2	247165.79	0.33	12
$3d^5(^2F_2)4s$	^3F	4	247282.20	0.27	12
$3d^5(^2F_2)4s$	^1F	3	251655.96	0.36	5
$3d^5(^6S)4p$	$^5P^\circ$	3	253862.74	0.35	5
$3d^5(^2S)4s$	^3S	1	253905.16	0.86	5
$3d^5(^6S)4p$	$^5P^\circ$	2	254495.66	0.35	4
$3d^5(^6S)4p$	$^5P^\circ$	1	254884.70	0.35	4
$3d^5(^2D_2)4s$	^3D	1	263701.48	0.50	6
$3d^5(^2D_2)4s$	^3D	2	263736.46	0.38	7
$3d^5(^2D_2)4s$	^3D	3	263806.25	0.38	7
$3d^5(^2D_2)4s$	^1D	2	268274.36	0.67	4
$3d^5(^2G_1)4s$	^3G	5	274696.55	0.34	6
$3d^5(^2G_1)4s$	^3G	4	274740.12	0.34	7
$3d^5(^2G_1)4s$	^3G	3	274774.89	0.34	6
$3d^5(^2G_1)4s$	^1G	4	279200.87	0.39	4
$3d^5(^4G)4p$	$^5G^\circ$	2	284215.8	2.5	4
$3d^5(^4G)4p$	$^5G^\circ$	3	284251.3	1.5	3
$3d^5(^4G)4p$	$^5G^\circ$	4	284307.78	0.36	4
$3d^5(^4G)4p$	$^5G^\circ$	5	284402.66	0.64	4
$3d^5(^4G)4p$	$^5G^\circ$	6	284580.3	1.3	2
$3d^5(^4G)4p$	$^5H^\circ$	3	286294.60	0.41	5
$3d^5(^4G)4p$	$^5H^\circ$	4	286706.5	2.4	7
$3d^5(^4G)4p$	$^5H^\circ$	5	287127.74	0.30	6
$3d^5(^4G)4p$	$^5H^\circ$	6	287645.26	0.38	3
$3d^5(^4P)4p$	$^5D^\circ$	1	287755.89	0.45	6
$3d^5(^4P)4p$	$^5D^\circ$	2	287781.55	0.36	7

Table A.3 (cont'd)

Configuration	Term [a]	J	Energy (cm^{-1})	u_E [b] (cm^{-1})	Number of Transitions [c] Determining Level
$3d^5(^4G)4p$	$^5F^\circ$	5	287906.8	1.1	5
$3d^5(^4G)4p$	$^5F^\circ$	3	287959.38	0.28	8
$3d^5(^4G)4p$	$^5H^\circ$	7	288021.21	0.64	1
$3d^5(^4G)4p$	$^5F^\circ$	4	288160.97	0.29	8
$3d^5(^4P)4p$	$^5S^\circ$	2	288877.70	0.29	7
$3d^5(^4G)4p$	$^5F^\circ$	1	289163.23	0.39	5
$3d^5(^4G)4p$	$^5F^\circ$	2	289246.51	0.45	5
$3d^5(^4P)4p$	$^5D^\circ$	3	289298.21	0.33	9
$3d^5(^4P)4p$	$^5D^\circ$	4	290261.29	0.25	7
$3d^5(^4P)4p$	$^5P^\circ$	3	290757.40	0.27	7
$3d^5(^4G)4p$	$^3F^\circ$	2	291097.51	0.44	6
$3d^5(^4G)4p$	$^3F^\circ$	3	291328.05	0.30	14
$3d^5(^4P)4p$	$^5P^\circ$	2	291390.15	0.35	7
$3d^5(^4P)4p$	$^5P^\circ$	1	291541.60	0.79	8
$3d^5(^4G)4p$	$^3F^\circ$	4	291555.35	0.30	11
$3d^5(^4G)4p$	$^3H^\circ$	6	291891.00	0.31	5
$3d^5(^4G)4p$	$^3H^\circ$	5	292353.65	0.31	7
$3d^5(^4G)4p$	$^3H^\circ$	4	292631.33	0.65	7
$3d^5(^4P)4p$	$^3P^\circ$	2	292982.34	0.37	7
$3d^5(^4P)4p$	$^3P^\circ$	1	293420.33	0.39	7
$3d^5(^4D)4p$	$^5F^\circ$	1	293834.0	1.2	5
$3d^5(^4P)4p$	$^3P^\circ$	0	293867.02	0.78	3
$3d^5(^4D)4p$	$^5F^\circ$	2	294086.09	0.30	8
$3d^5(^4D)4p$	$^5F^\circ$	3	294443.35	0.42	6
$3d^5(^4D)4p$	$^5F^\circ$	4	294939.65	0.27	6
$3d^5(^4D)4p$	$^5F^\circ$	5	295444.37	0.33	5
$3d^5(^4D)4p$	$^5D^\circ$	3	296574.09	0.37	8
$3d^5(^4G)4p$	$^3G^\circ$	3	296847.04	0.49	6
$3d^5(^4G)4p$	$^3G^\circ$	4	296896.46	0.30	11
$3d^5(^4D)4p$	$^5D^\circ$	4	296919.48	0.33	11
$3d^5(^4G)4p$	$^3G^\circ$	5	296932.37	0.30	8
$3d^5(^4D)4p$	$^5D^\circ$	2	297014.07	0.27	11
$3d^5(^4D)4p$	$^5D^\circ$	1	297417.84	0.31	9
$3d^5(^4P)4p$	$^3D^\circ$	3	297418.62	0.33	10
$3d^5(^4P)4p$	$^3D^\circ$	2	297842.77	0.31	12
$3d^5(^4D)4p$	$^5P^\circ$	1	297982.60	0.39	8
$3d^5(^4D)4p$	$^5D^\circ$	0	298059.89	0.40	3
$3d^5(^4P)4p$	$^3D^\circ$	1	298600.17	0.47	6
$3d^5(^4D)4p$	$^3D^\circ$	3	298972.71	0.34	12
$3d^5(^4D)4p$	$^5P^\circ$	2	299045.83	0.30	12
$3d^5(^4D)4p$	$^5P^\circ$	3	300200.93	0.26	13
$3d^5(^4D)4p$	$^3D^\circ$	2	300224.68	0.34	8
$3d^5(^4D)4p$	$^3D^\circ$	1	300563.36	0.68	6
$3d^5(^4D)4p$	$^3F^\circ$	4	300918.68	0.28	9
$3d^5(^4D)4p$	$^3F^\circ$	3	301469.60	0.39	8
$3d^5(^4D)4p$	$^3F^\circ$	2	301552.72	0.51	4
$3d^5(^4P)4p$	$^3S^\circ$	1	303249.35	0.32	6
$3d^5(^4D)4p$	$^3P^\circ$	0	305387.15	0.58	5
$3d^5(^2I)4p$	$^3K^\circ$	6	305591.23	0.83	3
$3d^5(^4D)4p$	$^3P^\circ$	1	305838.76	0.45	9
$3d^5(^2I)4p$	$^3K^\circ$	7	305996.64	0.41	5
$3d^5(^2I)4p$	$^3I^\circ$	5	306048.92	0.32	9
$3d^5(^4D)4p$	$^3P^\circ$	2	306378.72	0.29	9
$3d^5(^2D_1)4s$	^3D	3	306962.95	0.74	6
$3d^5(^2D_1)4s$	^3D	2	307025.84	1.27	6
$3d^5(^2D_1)4s$	^3D	1	307105.32	1.84	3
$3d^5(^2I)4p$	$^3I^\circ$	6	307399.91	0.51	7

Table A.3 (cont'd)

Configuration	Term [a]	J	Energy (cm^{-1})	u_E [b] (cm^{-1})	Number of Transitions [c] Determining Level
$3d^5(^2D_3)4p$	$^3F^\circ$	2	307730.72	0.30	7
$3d^5(^2I)4p$	$^3K^\circ$	8	308138.51	0.68	1
$3d^5(^2I)4p$	$^3I^\circ$	7	308317.18	0.45	3
$3d^5(^2D_3)4p$	$^3F^\circ$	3	308592.21	0.61	10
$3d^5(^2I)4p$	$^1H^\circ$	5	308804.58	0.31	8
$3d^5(^2D_3)4p$	$^1D^\circ$	2	308941.40	0.33	10
$3d^5(^2I)4p$	$^3H^\circ$	6	309263.90	0.35	6
$3d^5(^2I)4p$	$^1K^\circ$	7	309744.57	0.32	4
$3d^5(^2I)4p$	$^3H^\circ$	5	309919.84	0.34	8
$3d^5(^2I)4p$	$^3H^\circ$	4	309952.42	0.33	5
$3d^5(^2D_3)4p$	$^3F^\circ$	4	310211.71	0.28	6
$3d^5(^2D_1)4s$	^1D	2	311471.22	0.81	3
$3d^5(^2D_3)4p$	$^3P^\circ$	2	311965.97	0.40	8
$3d^5(^2F_1)4p$	$^1G^\circ$	4	312007.98	0.33	14
$3d^5(^2D_3)4p$	$^3P^\circ$	1	312290.51	0.45	7
$3d^5(^2F_1)4p$	$^3G^\circ$	3	312463.76	0.36	11
$3d^5(^4F)4p$	$^5G^\circ$	2	312778.37	0.40	6
$3d^5(^4F)4p$	$^5G^\circ$	3	312889.22	0.27	11
$3d^5(^2F_1)4p$	$^3D^\circ$	3	312953.43	0.28	10
$3d^5(^4F)4p$	$^5G^\circ$	4	313280.81	0.28	8
$3d^5(^4F)4p$	$^5G^\circ$	5	313465.31	0.31	11
$3d^5(^2D_3)4p$	$^3P^\circ$	0	313577.31	0.49	4
$3d^5(^2D_3)4p$	$^3D^\circ$	1	313678.60	0.36	8
$3d^5(^2D_3)4p$	$^3D^\circ$	2	313686.89	0.47	8
$3d^5(^2D_3)4p$	$^3D^\circ$	3	313920.42	0.44	10
$3d^5(^2F_1)4p$	$^3F^\circ$	4	314208.06	0.26	14
$3d^5(^2I)4p$	$^1I^\circ$	6	314392.43	0.84	3
$3d^5(^4F)4p$	$^5F^\circ$	3	314561.71	0.28	13
$3d^5(^4F)4p$	$^5F^\circ$	4	314599.18	0.26	12
$3d^5(^2F_1)4p$	$^3G^\circ$	5	314702.02	0.42	8
$3d^5(^4F)4p$	$^5G^\circ$	6	314756.83	0.32	5
$3d^5(^4F)4p$	$^5F^\circ$	2	314833.77	0.38	6
$3d^5(^4F)4p$	$^5F^\circ$	1	315151.79	0.37	7
$3d^5(^4F)4p$	$^5F^\circ$	5	315168.67	0.30	9
$3d^5(^2F_1)4p$	$^3D^\circ$	1	315301.44	0.46	7
$3d^5(^2D_3)4p$	$^1F^\circ$	3	315325.46	0.39	10
$3d^5(^2F_1)4p$	$^3D^\circ$	2	315364.82	0.66	9
$3d^5(^2G_2)4p$	$^3H^\circ$	4	315370.50	0.28	13
$3d^5(^2H)4p$	$^3H^\circ$	5	315989.97	0.28	11
$3d^5(^2F_1)4p$	$^3G^\circ$	4	316069.44	0.26	15
$3d^5(^2F_1)4p$	$^3F^\circ$	2	316164.90	0.34	10
$3d^5(^2F_1)4p$	$^3F^\circ$	3	316280.73	0.48	14
$3d^5(^2H)4p$	$^3G^\circ$	5	316725.76	0.32	9
$3d^5(^4F)4p$	$^5D^\circ$	4	316743.28	0.28	8
$3d^5(^2H)4p$	$^3G^\circ$	4	316888.69	0.28	16
$3d^5(^4F)4p$	$^5D^\circ$	3	317232.17	0.31	10
$3d^5(^2H)4p$	$^3H^\circ$	6	317327.91	0.28	7
$3d^5(^2H)4p$	$^3G^\circ$	3	317375.72	0.36	12
$3d^5(^4F)4p$	$^5D^\circ$	0	317460.78	0.53	3
$3d^5(^4F)4p$	$^5D^\circ$	1	317478.19	0.51	7
$3d^5(^4F)4p$	$^5D^\circ$	2	317517.50	0.36	12
$3d^5(^2D_3)4p$	$^1P^\circ$	1	319073.14	0.39	4
$3d^5(^2H)4p$	$^3I^\circ$	5	319077.89	0.35	7
$3d^5(^2G_2)4p$	$^1G^\circ$	4	319138.95	0.28	15
$3d^5(^4F)4p$	$^3G^\circ$	3	319619.87	0.35	11
$3d^5(^4F)4p$	$^3G^\circ$	5	319653.14	0.28	11
$3d^5(^2H)4p$	$^3I^\circ$	6	319860.76	0.28	7

Table A.3 (cont'd)

Configuration	Term [a]	J	Energy (cm^{-1})	u_E [b] (cm^{-1})	Number of Transitions [c] Determining Level
$3d^5(^4F)4p$	$^3G^\circ$	4	319899.45	0.47	10
$3d^5(^2F_1)4p$	$^1D^\circ$	2	319926.70	0.28	7
$3d^5(^2G_2)4p$	$^3F^\circ$	3	320514.32	0.35	14
$3d^5(^2H)4p$	$^3I^\circ$	7	320782.74	0.41	4
$3d^5(^2G_2)4p$	$^3F^\circ$	2	321018.04	0.30	8
$3d^5(^2G_2)4p$	$^3F^\circ$	4	321056.56	0.33	13
$3d^5(^2F_1)4p$	$^1F^\circ$	3	321082.47	0.44	12
$3d^5(^2H)4p$	$^1I^\circ$	6	322324.90	0.35	8
$3d^5(^4F)4p$	$^3D^\circ$	2	322436.58	0.44	10
$3d^5(^4F)4p$	$^3D^\circ$	3	322618.21	0.35	13
$3d^5(^4F)4p$	$^3F^\circ$	4	322821.68	0.27	9
$3d^5(^4F)4p$	$^3D^\circ$	1	322984.72	0.57	7
$3d^5(^4F)4p$	$^3F^\circ$	3	323524.19	0.35	14
$3d^5(^4F)4p$	$^3F^\circ$	2	323854.43	0.39	10
$3d^5(^2G_2)4p$	$^3H^\circ$	5	323909.42	0.26	12
$3d^5(^2H)4p$	$^3H^\circ$	4	323926.69	0.27	12
$3d^5(^2G_2)4p$	$^3G^\circ$	5	324980.8	0.3	10
$3d^5(^2G_2)4p$	$^3H^\circ$	6	325148.55	0.29	7
$3d^5(^2G_2)4p$	$^3G^\circ$	3	325212.20	0.37	11
$3d^5(^2G_2)4p$	$^3G^\circ$	4	325223.84	0.37	12
$3d^5(^2F_2)4p$	$^1G^\circ$	4	325558.93	0.31	15
$3d^5(^2F_2)4p$	$^3F^\circ$	2	325982.59	0.36	10
$3d^5(^2F_2)4p$	$^3F^\circ$	3	326030.24	0.33	13
$3d^5(^2G_2)4p$	$^1H^\circ$	5	326338.39	0.29	9
$3d^5(^2G_2)4p$	$^1F^\circ$	3	326739.49	0.29	13
$3d^5(^2F_2)4p$	$^3F^\circ$	4	326876.62	0.33	16
$3d^5(^2F_2)4p$	$^1D^\circ$	2	327122.31	0.38	8
$3d^5(^2H)4p$	$^1H^\circ$	5	327357.37	0.29	7
$3d^5(^2F_2)4p$	$^3D^\circ$	1	329462.64	0.79	4
$3d^5(^2F_2)4p$	$^3G^\circ$	3	329614.63	0.29	13
$3d^5(^2S)4p$	$^3P^\circ$	0	329618.3	2.7	2
$3d^5(^2F_2)4p$	$^3D^\circ$	2	329776.40	0.43	11
$3d^5(^2F_2)4p$	$^3D^\circ$	3	329872.79	0.37	15
$3d^5(^2F_2)4p$	$^3G^\circ$	4	330297.45	0.42	8
$3d^5(^2S)4p$	$^3P^\circ$	1	330371.06	0.60	4
$3d^5(^2F_2)4p$	$^3G^\circ$	5	330718.47	0.28	5
$3d^5(^2S)4p$	$^3P^\circ$	2	331678.14	0.69	4
$3d^5(^2H)4p$	$^1G^\circ$	4	332995.93	0.49	6
$3d^5(^2S)4p$	$^1P^\circ$	1	334477.49	0.91	2
$3d^5(^2F_2)4p$	$^1F^\circ$	3	334728.09	0.37	7
$3d^5(^2D_2)4p$	$^3F^\circ$	2	342893.90	0.47	7
$3d^5(^2D_2)4p$	$^3F^\circ$	3	343282.57	0.38	6
$3d^5(^2D_2)4p$	$^3D^\circ$	1	343478.21	0.84	5
$3d^5(^2D_2)4p$	$^3D^\circ$	2	343905.49	0.44	8
$3d^5(^2D_2)4p$	$^3D^\circ$	3	344805.43	0.39	6
$3d^5(^2D_2)4p$	$^3F^\circ$	4	344911.17	0.44	4
$3d^5(^2D_2)4p$	$^1F^\circ$	3	345936.97	0.56	7
$3d^5(^2D_2)4p$	$^3P^\circ$	2	346913.07	0.39	8
$3d^5(^2D_2)4p$	$^3P^\circ$	0	346921.34	0.69	2
$3d^5(^2D_2)4p$	$^3P^\circ$	1	346960.07	0.49	7
$3d^5(^2D_2)4p$	$^1P^\circ$	1	348478.15	1.03	3
$3d^5(^2D_2)4p$	$^1D^\circ$	2	349546.19	0.62	5
$3d^5(^2G_1)4p$	$^3H^\circ$	4	353071.17	0.34	8
$3d^5(^2G_1)4p$	$^3F^\circ$	4	353347.32	0.35	10
$3d^5(^2G_1)4p$	$^3H^\circ$	5	353549.6	0.3	8
$3d^5(^2G_1)4p$	$^3F^\circ$	3	353944.78	0.45	8
$3d^5(^2G_1)4p$	$^3H^\circ$	6	354989.9	3.1	2

Table A.3 (cont'd)

Configuration	Term [a]	J	Energy (cm^{-1})	u_E [b] (cm^{-1})	Number of Transitions [c] Determining Level
$3d^5(^2G_1)4p$	$^3F°$	2	355148.90	0.39	5
$3d^5(^2G_1)4p$	$^3G°$	3	355399.16	0.35	9
$3d^5(^2G_1)4p$	$^3G°$	4	355765.96	0.36	8
$3d^5(^2G_1)4p$	$^3G°$	5	356036.38	0.40	6
$3d^5(^2G_1)4p$	$^1H°$	5	358475.67	0.46	5
$3d^5(^2G_1)4p$	$^1G°$	4	358760.69	0.40	4
$3d^5(^2G_1)4p$	$^1F°$	3	360060.86	0.56	4
$3d^5(^2P)4p$	$^3P°$	0	368440.41	0.98	2
$3d^5(^2P)4p$	$^3P°$	1	368746.9	2.3	2
$3d^5(^2P)4p$	$^3P°$	2	369649.07	0.74	4
$3d^5(^2P)4p$	$^3D°$	2	374804.6	1.5	3
$3d^5(^2P)4p$	$^3D°$	1	374829	2	1
$3d^5(^2P)4p$	$^3D°$	3	376472.01	0.96	2
$3d^5(^2P)4p$	$^1D°$	2	377060	1	1
$3d^5(^2P)4p$	$^3S°$	1	378555.63	0.75	3
$3d^5(^2P)4p$	$^1P°$	1	380167	1	1
$3d^5(^2D_1)4p$	$^3F°$	2	386968.3	1.8	3
$3d^5(^2D_1)4p$	$^3F°$	3	387332.2	1.2	4
$3d^5(^2D_1)4p$	$^3F°$	4	388699.29	0.84	2
$3d^5(^2D_1)4p$	$^3D°$	1	388746.2	1.8	3
$3d^5(^2D_1)4p$	$^3D°$	2	389572.0	1.3	5
$3d^5(^2D_1)4p$	$^3D°$	3	390479.36	0.75	3
$3d^5(^2D_1)4p$	$^1D°$	2	390675.47	0.89	4
$3d^5(^2D_1)4p$	$^3P°$	2	392414.38	0.83	5
$3d^5(^2D_1)4p$	$^1F°$	3	392958.32	0.81	3
$3d^5(^6S)5p$	$^5P°$	3	423532.8	2.4	2
$3d^5(^6S)5p$	$^5P°$	2	423782.2	2.4	2
$3d^5(^6S)5p$	$^5P°$	1	423935.1	2.4	2
$3d^5(^6S)4f$	$^5F°$	2	439419.3	3.7	1
$3d^5(^6S)4f$	$^5F°$	1	439419.6	3.7	1
$3d^5(^6S)4f$	$^5F°$	3	439422.9	3.7	1
$3d^5(^6S)4f$	$^5F°$	4	439426.7	3.7	1
$3d^5(^6S)4f$	$^5F°$	5	439433.9	3.7	1
$3d^5(^6S)5f$	$^5F°$	5	502124.0	4.8	1
$3d^5(^6S)5f$	$^5F°$	4	502132.7	4.8	1
$3d^5(^6S)5f$	$^5F°$	3	502136.9	4.8	1
$3d^5(^6S)5f$	$^5F°$	1	502142.5	4.8	1
$3d^5(^6S)5f$	$^5F°$	2	502150	10	1

[a]Note: °– Odd Parity.

[b]Estimate of one standard uncertainty.

[c] Not all transitions included in table A.2 for a given level are used to determine that level. The number of transitions given in the this table includes only the significant transitions that were used to determine the level.

Appendix B: Extended Transition Probability Table

Table B.1 Fe II Transition Probabilities

Upper Level	Lower Level	λ (Å)	σ (cm^{-1})	BF (%)	$\mu(BF)$ (%)	A (s^{-1})	$\mu(A)$ (%)
$3d^6(^3P_2)4p\ y^4P_{1/2}$	$3d^7\ a^4F_{5/2}$	1709.5543	58494.78	2.04	10	5.797E+06	14
	$3d^7\ a^4P_{3/2}$	2097.5496	47659.542	3.22	5	9.135E+06	11
$E = 61332.753\ cm^{-1}$	$3d^7\ a^4P_{1/2}$	2107.7960	47427.888	1.04	17	2.947E+06	20
$\tau = 3.5 \pm 0.4$ ns	$3d^7\ a^2P_{1/2}$	2355.2159	42445.968	8.32	4	2.364E+07	11
	$3d^7\ a^2D2_{5/2}$	2449.2907	40815.784	0.39	12	1.102E+06	16
	$3d^6(^3P_2)4s\ b^4P_{5/2}$	2468.2567	40502.179	0.96	6	2.729E+06	12
	$3d^6(^3P_2)4s\ b^4P_{3/2}$	2529.5592	39520.698	67.45	1	1.916E+08	10
	$3d^6(^3P_2)4s\ b^4P_{1/2}$	2568.4097	38922.935	15.52	3	4.409E+07	10
	$3d^6(^3P_2)4s\ b^2P_{3/2}$	2812.4956	35545.14	1.07	13	3.035E+06	17
Residual				3.0			
$3d^6(^3F_2)4p\ y^4G_{9/2}$	$3d^7\ a^4F_{9/2}$	1610.9229	62076.218	5.30	8	2.048E+07	13
	$3d^7\ a^4F_{7/2}$	1625.5229	61518.664	11.59	4	4.473E+07	11
$E = 63948.803\ cm^{-1}$	$3d^7\ a^2G_{9/2}$	2078.1607	48104.141	1.78	7	6.857E+06	12
$\tau = 3.6 \pm 0.4$ ns	$3d^7\ a^2H_{11/2}$	2292.4210	43608.56	0.33	14	1.276E+06	18
	$3d^6(^3H)4s\ a^4H_{11/2}$	2351.2007	42518.447	20.38	3	7.869E+07	10
	$3d^6(^3H)4s\ a^4H_{9/2}$	2359.5956	42367.188	6.60	4	2.548E+07	11
	$3d^6(^3H)4s\ a^4H_{7/2}$	2366.875	42236.90	1.30	4	5.032E+06	11
	$3d^6(^3F_2)4s\ b^4F_{9/2}$	2419.8936	41311.581	0.46	8	1.755E+06	13
	$3d^6(^3F_2)4s\ b^4F_{7/2}$	2430.0780	41138.457	49.57	2	1.914E+08	10
	$3d^6(^3G)4s\ a^4G_{11/2}$	2595.2764	38520.024	0.30	12	1.164E+06	15
	$3d^6(^3H)4s\ b^2H_{11/2}$	2646.2133	37778.598	0.26	12	1.013E+06	16
	$3d^6(^3F_2)4s\ a^2F_{7/2}$	2728.9050	36633.887	2.14	4	8.250E+06	11
Residual				1.0			
$3d^6(^3F_2)4p\ y^4G_{7/2}$	$3d^7\ a^4F_{7/2}$	1623.0929	61610.769	5.44	8	2.092E+07	13
	$3d^7\ a^4F_{5/2}$	1633.9093	61202.909	10.36	4	3.983E+07	11
$E = 64040.891\ cm^{-1}$	$3d^7\ a^2G_{9/2}$	2074.1886	48196.251	1.66	9	6.379E+06	13
$\tau = 2.6 \pm 0.3$ ns	$3d^7\ a^2H_{9/2}$	2312.2255	43235.083	0.25	17	9.46 E+05	19
	$3d^6(^3H)4s\ a^4H_{9/2}$	2354.4776	42459.276	22.99	2	8.843E+07	10
	$3d^6(^3H)4s\ a^4H_{7/2}$	2361.7258	42328.977	6.32	4	2.431E+07	11
	$3d^6(^3F_2)4s\ b^4F_{7/2}$	2424.6509	41230.530	1.58	4	6.059E+06	11
	$3d^6(^3F_2)4s\ b^4F_{5/2}$	2432.2609	41101.540	39.77	2	1.529E+08	10
	$3d^6(^3G)4s\ a^4G_{7/2}$	2626.6969	38059.277	0.50	13	1.912E+06	16
	$3d^6(^3H)4s\ b^2H_{9/2}$	2652.5665	37688.119	1.03	5	3.954E+06	11
	$3d^6(^3F_2)4s\ a^2F_{7/2}$	2722.0625	36725.970	2.70	4	1.038E+07	11
	$3d^6(^3F_2)4s\ a^2F_{5/2}$	2744.8940	36420.507	5.16	10	1.986E+07	14
	$3d^6(^3G)4s\ b^2G_{9/2}$	2970.6935	33652.348	0.61	42	2.336E+06	43
	$3d^7\ b^2F_{5/2}$	3101.885	32229.110	1.65	17	6.350E+06	20
Residual				2.0			
$3d^6(^3G)4p\ x^4G_{11/2}$	$3d^7\ a^4F_{9/2}$	1569.6753	63707.444	5.66	18	1.724E+07	20
	$3d^7\ a^2H_{11/2}$	2209.7534	45239.814	0.69	9	2.101E+06	13
$E = 65580.065\ cm^{-1}$	$3d^6(^3H)4s\ a^4H_{13/2}$	2255.1867	44328.495	0.84	7	2.571E+06	12
$\tau = 3.3 \pm 0.3$ ns	$3d^6(^3H)4s\ a^4H_{11/2}$	2264.3199	44149.713	0.88	7	2.669E+06	12
	$3d^6(^3F_2)4s\ b^4F_{9/2}$	2327.9608	42942.870	1.998	5	6.090E+06	11
	$3d^6(^3G)4s\ a^4G_{11/2}$	2489.8296	40151.277	63.75	2	1.944E+08	10
	$3d^6(^3G)4s\ a^4G_{9/2}$	2424.6509	39774.737	0.51	9	1.557E+06	13
	$3d^6(^3H)4s\ b^2H_{11/2}$	2432.2609	39409.885	20.73	3	6.321E+07	10
	$3d^6(^3G)4s\ a^2G_{9/2}$	2840.7580	35191.525	4.94	4	1.507E+07	11

Table B.1 (cont'd)

Upper Level	Lower Level	λ (Å)	σ (cm^{-1})	BF (%)	$\mu(BF)$ (%)	A (s^{-1})	$\mu(A)$ (%)
Residual				1.0			
$3d^6(^3G)4p\ x^4G_{9/2}$	$3d^7\ a^4F_{9/2}$	1566.8221	63823.454	12.28	9	4.892E+07	13
	$3d^7\ a^4F_{7/2}$	1580.6300	63265.913	11.51	7	4.585E+07	12
$E = 65696.053\ cm^{-1}$	$3d^6(^3H)4s\ a^4H_{11/2}$	2258.3855	44265.713	0.34	18	1.346E+06	20
$\tau = 2.5 \pm 0.3$ ns	$3d^6(^3F_2)4s\ b^4F_{9/2}$	2321.6895	43058.857	3.31	4	1.319E+07	11
	$3d^6(^3G)4s\ a^4G_{11/2}$	2482.6573	40267.265	35.33	2	1.408E+08	10
	$3d^6(^3G)4s\ a^4G_{9/2}$	2506.0933	39890.727	26.23	3	1.045E+08	10
	$3d^6(^3G)4s\ a^4G_{7/2}$	2517.2203	39714.408	1.48	5	5.890E+06	11
	$3d^6(^3H)4s\ b^2H_{11/2}$	2529.2281	39525.871	8.29	3	3.303E+07	11
	$3d^6(^3F_2)4s\ a^2F_{7/2}$	2604.6690	38381.127	0.17	21	6.85 E+05	23
		2922.025	34212.830	1.06	16	4.230E+06	19
Residual				1.0			
$3d^6(^3G)4p\ x^4G_{7/2}$	$3d^7\ a^4F_{5/2}$	1584.9524	63093.377	12.45	7	4.461E+07	12
	$3d^6(^3H)4s\ a^4H_{9/2}$	2254.1069	44349.728	0.38	18	1.358E+06	21
$E = 65931.358\ cm^{-1}$	$3d^6(^3F_2)4s\ b^4F_{7/2}$	2318.3430	43121.006	1.65	5	5.924E+06	11
$\tau = 2.8 \pm 0.3$ ns	$3d^6(^3G)4s\ a^4G_{9/2}$	2491.3962	40126.030	30.72	2	1.101E+08	10
	$3d^6(^3G)4s\ a^4G_{7/2}$	2502.3927	39949.713	43.52	2	1.560E+08	10
	$3d^6(^3G)4s\ a^4G_{5/2}$	2507.0221	39875.949	2.65	4	9.488E+06	11
	$3d^6(^3G)4s\ a^4G_{7/2}$	2517.2203	39578.548	4.64	4	1.664E+07	11
	$3d^6(^3H)4s\ b^2H_{9/2}$	2525.8616	38616.438	2.41	5	8.636E+06	11
	$3d^6(^3F_2)4s\ a^2F_{5/2}$	2609.4402	38310.953	1.58	5	5.677E+06	11
Residual				4.0			
$3d^6(^3G)4p\ x^4F_{9/2}$	$3d^7\ a^4F_{9/2}$	1559.0852	64140.179	17.71	7	6.999E+07	12
	$3d^6(^3D)4s\ a^4D_{7/2}$	1722.430	58057.520	1.11	21	4.368E+06	24
$E = 66012.775\ cm^{-1}$	$3d^6(^3H)4s\ a^4H_{11/2}$	2242.3422	44582.391	0.36	13	1.428E+06	17
$\tau = 2.5 \pm 0.3$ ns	$3d^6(^3F_2)4s\ b^4F_{9/2}$	2304.7348	43375.589	4.62	4	1.826E+07	11
	$3d^6(^3F_2)4s\ b^4F_{7/2}$	2313.9746	43202.405	1.03	6	4.077E+06	12
	$3d^6(^3G)4s\ a^4G_{11/2}$	2463.2812	40583.983	21.64	3	8.553E+07	10
	$3d^6(^3G)4s\ a^4G_{9/2}$	2486.3508	40207.451	43.00	2	1.670E+08	10
	$3d^6(^3G)4s\ a^4G_{7/2}$	2497.3029	40031.130	0.86	5	3.405E+06	11
	$3d^6(^3H)4s\ b^2H_{11/2}$	2509.1210	39842.594	4.94	4	1.954E+07	11
	$3d^6(^3H)4s\ b^2H_{9/2}$	2520.6733	39660.006	1.93	5	7.609E+06	11
	$3d^6(^3F_2)4s\ a^2F_{7/2}$	2583.3491	38697.859	0.26	15	1.018E+06	18
	$3d^6(^3D)4s\ b^4D_{7/2}$	2895.2192	34529.577	2.55	6	1.007E+07	12
Residual				0.5			
$3d^6(^3G)4p\ x^4F_{7/2}$	$3d^7\ a^4F_{7/2}$	1563.7906	63947.180	25.63	6	1.149E+08	12
	$3d^7\ a^4F_{5/2}$	1573.8280	63539.344	3.95	38	1.771E+07	39
$E = 66377.315\ cm^{-1}$	$3d^6(^3F_2)4s\ b^4H_{7/2}$	2294.6099	43566.967	4.00	5	1.795E+07	11
$\tau = 2.2 \pm 0.2$ ns	$3d^6(^3G)4s\ a^4G_{9/2}$	2464.0095	40571.987	33.32	3	1.494E+08	10
	$3d^6(^3G)4s\ a^4G_{7/2}$	2474.7650	40395.671	23.30	3	1.045E+08	11
	$3d^6(^3G)4s\ a^4G_{7/2}$	2479.2928	40321.905	0.53	10	2.363E+06	14
	$3d^6(^3H)4s\ b^2H_{9/2}$	2497.7138	40024.545	2.71	5	1.216E+07	11
	$3d^6(^3F_2)4s\ a^2F_{7/2}$	2559.2393	39062.397	1.59	5	7.112E+06	11
	$3d^6(^3F_2)4s\ a^2F_{5/2}$	2579.4121	38756.921	1.35	5	6.046E+06	11
	$3d^6(^3D)4s\ b^4D_{5/2}$	2857.1722	34989.362	2.61	7	1.171E+07	12
	$3d^6(^3F_2)4s\ a^2F_{7/2}$	2864.970	34894.130	1.02	19	4.569E+06	21

Table B.1 (cont'd)

Upper Level	Lower Level	λ ($\AA$)	σ (cm^{-1})	BF (%)	$\mu(BF)$ (%)	A (s^{-1})	$\mu(A)$ (%)
Residual				4.0			
$3d^6(^3G_2)4p\ y^4H_{7/2}$	$3d^6(^3H)4s\ a^4H_{9/2}$	2217.0608	45090.720	1.33	7	4.123E+06	12
	$3d^6(^3H)4s\ a^4H_{7/2}$	2223.4857	44960.440	10.16	4	3.156E+07	11
$E = 66672.336\ cm^{-1}$	$3d^6(^3G)4s\ a^4G_{9/2}$	2446.2202	40867.012	0.63	11	1.945E+06	15
$\tau = 3.2 \pm 0.3$ ns	$3d^6(^3G)4s\ a^4G_{7/2}$	2456.8210	40690.690	4.60	4	1.428E+07	11
	$3d^6(^3G)4s\ a^4G_{5/2}$	2461.2833	40616.924	75.25	1	2.337E+08	10
	$3d^6(^3F_2)4s\ a^2F_{5/2}$	2559.9251	39051.932	8.04	4	2.495E+07	11
Residual				0.7			
$3d^6(^3G)4p\ x^2G_{7/2}$	$3d^7\ a^2G_{7/2}$	1846.5758	54154.289	5.35	7	2.209E+07	12
	$3d^7\ a^2H_{9/2}$	2010.6969	49717.931	25.95	3	1.072E+08	10
$E = 70523.694\ cm^{-1}$	$3d^6(^3G)4s\ a^4G_{9/2}$	2235.5252	44718.328	0.60	21	2.471E+06	23
$\tau = 2.4 \pm 0.2$ ns	$3d^6(^3H)4s\ b^2H_{9/2}$	2263.2320	44170.932	8.76	4	3.621E+07	11
	$3d^6(^3G)4s\ b^2G_{9/2}$	2490.8300	40135.152	2.81	7	1.160E+07	12
	$3d^6(^3G)4s\ b^2G_{7/2}$	2514.3830	39759.219	41.93	2	1.733E+08	10
	$3d^7\ b^2F_{5/2}$	2582.4134	38711.880	5.59	4	2.311E+07	11
	$3d^7\ b^2F_{7/2}$	2594.9651	38524.644	2.87	8	1.184E+07	13
	$3d^6(^1D_2)4s\ c^2D_{5/2}$	3089.391	32359.440	6.15	8	2.539E+07	13
Residual				1.5			
$3d^6(^1I)4p\ y^2I_{11/2}$	$3d^7\ a^2H_{11/2}$	1864.6453	53629.502	6.32	9	2.282E+07	14
	$3d^7\ a^2H_{9/2}$	1880.9725	53163.988	18.18	4	6.564E+07	11
$E = 73969.761\ cm^{-1}$	$3d^6(^3I)4s\ a^2I_{13/2}$	2432.7002	41094.118	2.10	7	7.573E+06	12
$\tau = 2.8 \pm 0.3$ ns	$3d^6(^3I)4s\ a^2I_{11/2}$	2434.7290	41059.878	71.72	1	2.589E+08	10
	$d^6(^1G_2)4s\ c^2G_{9/2}$	2468.1926	40503.231	1.68	8	6.071E+06	13
Residual				1.4			

Bibliography

[1] Gillian Nave, Paul Barklem, Maria Teresa Belmonte, Nancy Brickhouse, Paul Butler, Frances Cashman, M. Chatzikos, Charles R. Cowley, Elizabeth Den Hartog, Steven Federman, Gary Ferland, Michael Fogle, Henrik Hartman, Francisco Guzman, Sara Heap, Florian Kerber, Alexander Kramida, Varsha P. Kulkarni, James E. Lawler, Joan Marler, Sultana Nahar, Juliet Pickering, Pascal Quinet, Yur Ralchenko, Daniel Savin, Chris Sneden, Endre Takacs, Glenn Wahlgren, John Webb, Jennifer Wiseman, and Mike Wood. Atomic data for astrophysics: Needs and challenges. *Bulletin of the AAS*, 51(7), 9 2019. URL `https://baas.aas.org/pub/2020n7i001`. https://baas.aas.org/pub/2020n7i001.

[2] Katharina Lodders. Solar system abundances of the elements. In Aruna Goswami and B. Eswar Reddy, editors, *Principles and Perspectives in Cosmochemistry*, pages 379–417, Berlin, Heidelberg, 2010. Springer Berlin Heidelberg. ISBN 978-3-642-10352-0.

[3] C J A P Martins. The status of varying constants: a review of the physics, searches and implications. *Reports on Progress in Physics*, 80(12):126902, nov 2017. doi: 10.1088/1361-6633/aa860e. URL `https://doi.org/10.1088/1361-6633/aa860e`.

[4] John D. Barrow, João Magueijo, and Håvard Bunes Sandvik. Variations of alpha in space and time. *Phys. Rev. D*, 66:043515, Aug 2002. doi: 10.1103/PhysRevD.66.043515. URL `https://link.aps.org/doi/10.1103/PhysRevD.66.043515`.

[5] John D. Barrow and Sean Z. W. Lip. Generalized theory of varying alpha. *Phys. Rev. D*, 85:023514, Jan 2012. doi: 10.1103/PhysRevD.85.023514. URL `https://link.aps.org/doi/10.1103/PhysRevD.85.023514`.

[6] Jacob D. Bekenstein. Fine-structure constant: Is it really a constant? *Phys. Rev. D*, 25:1527–1539, Mar 1982. doi: 10.1103/PhysRevD.25.1527. URL `https://link.aps.org/doi/10.1103/PhysRevD.25.1527`.

[7] J. C. Berengut and V. V. Flambaum. Manifestations of a spatial variation of fundamental constants in atomic and nuclear clocks, oklo, meteorites, and cosmological phenomena. *EPL (Europhysics Letters)*, 97(2):20006, jan 2012. doi: 10.1209/0295-5075/97/20006. URL https://doi.org/10.1209/0295-5075/97/20006.

[8] S. Blatt, A. D. Ludlow, G. K. Campbell, J. W. Thomsen, T. Zelevinsky, M. M. Boyd, J. Ye, X. Baillard, M. Fouché, R. Le Targat, A. Brusch, P. Lemonde, M. Takamoto, F.-L. Hong, H. Katori, and V. V. Flambaum. New limits on coupling of fundamental constants to gravity using ^{87}Sr optical lattice clocks. *Phys. Rev. Lett.*, 100:140801, Apr 2008. doi: 10.1103/PhysRevLett.100.140801. URL https://link.aps.org/doi/10.1103/PhysRevLett.100.140801.

[9] A. Bauch and S. Weyers. New experimental limit on the validity of local position invariance. *Phys. Rev. D*, 65:081101, Apr 2002. doi: 10.1103/PhysRevD.65.081101. URL https://link.aps.org/doi/10.1103/PhysRevD.65.081101.

[10] John K. Webb, Victor V. Flambaum, Christopher W. Churchill, Michael J. Drinkwater, and John D. Barrow. Search for time variation of the fine structure constant. *Phys. Rev. Lett.*, 82:884–887, Feb 1999. doi: 10.1103/PhysRevLett.82.884. URL https://link.aps.org/doi/10.1103/PhysRevLett.82.884.

[11] V. A. Dzuba, V. V. Flambaum, and J. K. Webb. Space-time variation of physical constants and relativistic corrections in atoms. *Phys. Rev. Lett.*, 82:888–891, Feb 1999. doi: 10.1103/PhysRevLett.82.888. URL https://link.aps.org/doi/10.1103/PhysRevLett.82.888.

[12] J. C. Berengut, V. V. Flambaum, A. Ong, J. K. Webb, John D. Barrow, M. A. Barstow, S. P. Preval, and J. B. Holberg. Limits on the dependence of the fine-structure constant on gravitational potential from white-dwarf spectra. *Phys. Rev. Lett.*, 111:010801, Jul 2013. doi: 10.1103/PhysRevLett.111.010801. URL https://link.aps.org/doi/10.1103/PhysRevLett.111.010801.

[13] S. P. Preval, M. A. Barstow, J. B. Holberg, and N. J. Dickinson. A comprehensive near- and far-ultraviolet spectroscopic study of the hot DA white dwarf G191-B2B. *Monthly Notices of the Royal Astronomical Society*, 436 (1):659–674, 09 2013. ISSN 0035-8711. doi: 10.1093/mnras/stt1604. URL https://doi.org/10.1093/mnras/stt1604.

[14] A.J.J. Raassen and Th.A.M. van Kleff. Extended analysis and ionization potential of the fifth spectrum of nickel (Ni V). *Physica B+C*, 85(1):180–190, 1977. ISSN 0378-4363. doi: https://doi.org/10.1016/0378-4363(76)90112-1. URL https://www.sciencedirect.com/science/article/pii/0378436376901121.

[15] Jan Olof Ekberg. Term analysis of Fe V. *Physica Scripta*, 12(1-2):42–57, jul 1975. doi: 10.1088/0031-8949/12/1-2/004. URL https://doi.org/10.1088/0031-8949/12/1-2/004.

[16] J. W. Ward, A. J. J. Raassen, A. Kramida, and G. Nave. Spectra of Ni V and Fe V in the vacuum ultraviolet. *The Astrophysical Journal Supplement Series*, 245(2):22, Nov 2019. doi: 10.3847/1538-4365/ab4ea3. URL https://doi.org/10.3847/1538-4365/ab4ea3.

[17] A. Kramida, Yu. Ralchenko, J. Reader, and NIST ASD Team (2020). Atomic spectra database version 5.8. URL Available:https://physics.nist.gov/asd. [Accessed: 09-21-2020]. National Institute of Standards and Technology, Gaithersburg, MD.

[18] Vladilen Letokhov and Sveneric Johansson. *Astrophysical Lasers*. Oxford University Press, 2009.

[19] A.E. Kramida. The program LOPT for least-squares optimization of energy levels. *Computer Physics Communications*, 182(2):419–434, 2011. ISSN 0010-4655. doi: https://doi.org/10.1016/j.cpc.2010.09.019. URL https://www.sciencedirect.com/science/article/pii/S0010465510003784.

[20] V I Azarov, W-Ü L Tchang-Brillet, J-F Wyart, F Launay, and M Benharrous. Determination of the $3d^3 4d$ and $3d^3 5s$ configurations of Fe V. *Physica Scripta*, 63(6):438–461, jun 2001. doi: 10.1238/physica.regular.063a00438. URL https://doi.org/10.1238/physica.regular.063a00438.

[21] A.E. Kramida. Energy levels and spectral lines of quadruply ionized iron (Fe V). *The Astrophysical Journal Supplement Series*, 212(1):11, apr 2014. doi: 10.1088/0067-0049/212/1/11. URL https://doi.org/10.1088/0067-0049/212/1/11.

[22] F. C. McKenna, F. P. Keenan, N. C. Hambly, C. Allende Prieto, W. R. J. Rolleston, L. H. Aller, and W. A. Feibelman. The optical spectral line list of RR telescopii. *The Astrophysical Journal Supplement Series*, 109(1):225–239, mar 1997. doi: 10.1086/312977. URL https://doi.org/10.1086/312977.

[23] A. J. J. Raassen. Additional identifications of high ionization stages of iron and nickel in the ultraviolet spectrum of the slow nova RR telescopii. *Physica Scripta*, 292(1):696–698, may 1985. doi: 10.1086/163201. URL https://doi.org/10.1086/163201.

[24] A.J.J. Raassen, Th.A.M. van Kleef, and B.C. Metsch. Term analysis of the system $3d^6$-$3d^5 4p$ of the fifth spectrum of nickel (Ni V). *Physica B+C*, 84(1):133–146, 1976. ISSN 0378-4363. doi: https://doi.org/10.1016/0378-4363(76)90015-2. URL https://www.sciencedirect.com/science/article/pii/0378436376900152.

[25] A.J.J. Raassen. Analysis of the sixth spectrum of nickel (Ni VI). *Physica B+C*, 100(3):404–424, 1980. ISSN 0378-4363. doi: https://doi.org/10.1016/0378-4363(80)90026-1. URL https://www.sciencedirect.com/science/article/pii/0378436380900261.

[26] J. C. Pickering, Sveneric Johansson, and P. L. Smith. The ferrum project: Branching ratios and atomic transition probabilities of Fe II transitions from the $3d^6(a^3f)4p$ subconfiguration in the visible to vuv spectral region. 377:361–367, 2001. ISSN 0004-6361. doi: 10.1051/0004-6361:20010943. URL https://lup.lub.lu.se/search/ws/files/4640986/624123.pdf.

[27] J. C. Pickering, M. P. Donnelly, Hampus Nilsson, A. Hibbert, and Sveneric Johansson. The FERRUM Project: Experimental oscillator strengths of the UV 8 multiplet and other uv transitions from the y^6p levels of Fe II. *Astronomy & Astrophysics*, 396(2):715–722, 2002. ISSN 1432-0746. doi: 10.1051/0004-6361:20021388.

[28] Gillian Nave and Sveneric Johansson. The spectrum of Fe II. *The Astrophysical Journal Supplement Series*, 204(1):1, dec 2012. doi: 10.1088/0067-0049/204/1/1. URL https://doi.org/10.1088/0067-0049/204/1/1.

[29] B. Vodar and N. Astoin. New source of light for the far ultra-violet. *Nature*, 166(1):1029–1030, Dec 1950. doi: https://doi.org/10.1038/1661029b0.

[30] R.E. Beverly. VI Light emission from high-current surface-spark discharges. volume 16 of *Progress in Optics*, pages 357–411. Elsevier, 1978. doi: https://doi.org/10.1016/S0079-6638(08)70075-1. URL https://www.sciencedirect.com/science/article/pii/S0079663808700751.

[31] Joseph Reader and Gabriel L. Epstein. Analysis of the spectrum of quadruply ionized yttrium (Y V). *J. Opt. Soc. Am.*, 62(5):619–622, May 1972. doi: 10.1364/JOSA.62.000619. URL http://www.osapublishing.org/abstract.cfm?URI=josa-62-5-619.

[32] Karsten Danzmann, Mathias Günther, Joachim Fischer, Manfred Kock, and Michael Kühne. High current hollow cathode as a radiometric transfer standard source for the extreme vacuum ultraviolet. *Appl. Opt.*, 27(23):4947–4951, Dec 1988. doi: 10.1364/AO.27.004947. URL http://www.osapublishing.org/ao/abstract.cfm?URI=ao-27-23-4947.

[33] R.S. Hudson, L.L. Skrumeda, and W. Whaling. Fe II level populations in a hollow cathode discharge. *Journal of Quantitative Spectroscopy and Radiative Transfer*, 38(1):1–4, 1987. ISSN 0022-4073. doi: https://doi.org/10.1016/0022-4073(87)90103-8. URL https://www.sciencedirect.com/science/article/pii/0022407387901038.

[34] Jules Z. Klose, George F. Hartig, and William J. Rosenberg. Characterization of a Pt-Ne hollow cathode spectral line source. *Appl. Opt.*, 29(19):2951–2959, Jul 1990. doi: 10.1364/AO.29.002951. URL http://www.osapublishing.org/ao/abstract.cfm?URI=ao-29-19-2951.

[35] J. E. Sansonetti, J. Reader, C. J. Sansonetti, and A. Nicolo. Atlas of the spectrum of a platinum/neon hollow-cathode reference lamp in the region 1130-4330 å. *NIST Journal of Research*, 97(1):1–211, Jan 1992.

[36] Craig J. Sansonetti, F. Kerber, Joseph Reader, and M. R. Rosa. Characterization of the far-ultraviolet spectrum of Pt/Cr-Ne hollow cathode lamps as used on the Space Telescope Imaging Spectrograph on board the Hubble Space Telescope. *The Astrophysical Journal Supplement Series*, 153(2):555–579, aug 2004. doi: 10.1086/421874. URL https://doi.org/10.1086/421874.

[37] R. D. Saunders, W. R. Ott, and J. M. Bridges. Spectral irradiance standard for the ultraviolet: the deuterium lamp. *Appl. Opt.*, 17(4):593–600, Feb 1978. doi: 10.1364/AO.17.000593. URL http://www.osapublishing.org/ao/abstract.cfm?URI=ao-17-4-593.

[38] Roman Klein, Simone Kroth, Wolfgang Paustian, Mathias Richter, and Reiner Thornagel. PTB's radiometric scales for UV and VUV source calibration based on synchrotron radiation. *Metrologia*, 55(3):386–391, apr 2018. doi: 10.1088/1681-7575/aab803. URL https://doi.org/10.1088/1681-7575/aab803.

[39] Ulf Griesmann and Rainer Kling. Interferometric measurement of resonance transition wavelengths in C IV, Si IV, Al III, Al II, and Si II. *The Astrophysical Journal*, 536(2):L113–L115, jun 2000. doi: 10.1086/312741. URL https://doi.org/10.1086/312741.

[40] J. M. McCrea. Ion-sensitive plate detectors in mass spectrometry. *Applied Spectroscopy*, 25(2):246–252, 1971. doi: 10.1366/000370271779948547. URL https://doi.org/10.1366/000370271779948547.

[41] Gillian Nave, Craig J. Sansonetti, Csilla I. Szabo, John J. Curry, and Darren G. Smillie. Use of phosphor image plates for measuring intensities in vacuum ultraviolet spectra. *Review of Scientific Instruments*, 82(1):013107, 2011. doi: 10.1063/1.3529879. URL https://doi.org/10.1063/1.3529879.

[42] Frank S. Tomkins and Mark Fred. A photoelectric setting device for a spectrum plate comparator. *J. Opt. Soc. Am.*, 41(9):641–643, Sep 1951. doi: 10.1364/JOSA.41.000641. URL http://www.osapublishing.org/abstract.cfm?URI=josa-41-9-641.

[43] B. A. Searle. FT500 ultra-violet Fourier transform spectrometer user guide, 1981.

[44] Ulf Griesmann, Rainier Kling, John H. Burnett, and Lukasz Bratasz. NIST FT700 Vacuum Ultraviolet Fourier Transform Spectrometer: applications in ultraviolet spectrometry and radiometry. In George R. Carruthers and Kenneth F. Dymond, editors, *Ultraviolet Atmospheric and Space Remote Sensing: Methods and Instrumentation II*, volume 3818, pages 180 – 188. International

Society for Optics and Photonics, SPIE, 1999. URL https://doi.org/10.1117/12.364153.

[45] G. Nave, U. Griesmann, J. W. Brault, and M. C. Abrams. Xgremlin: Interferograms and spectra from Fourier transform spectrometers analysis, Nov 2015.

[46] J. W. Brault and M. C. Abrams. Fourier transform spectroscopy: New methods and applications. *OSA Technical Digest Series: Optical Society of America*, 6: 386–391, 1989.

[47] Gabriel L. Epstein and Joseph Reader. Spectrum and energy levels of triply ionized yttrium (Y IV): erratum. *J. Opt. Soc. Am.*, 72(8):1100–1102, Aug 1982. doi: 10.1364/JOSA.72.001100. URL http://www.osapublishing.org/abstract.cfm?URI=josa-72-8-1100.

[48] D. G. Smillie, J. C. Pickering, G. Nave, and P. L. Smith. THE SPECTRUM AND TERM ANALYSIS OF CO III MEASURED USING FOURIER TRANSFORM AND GRATING SPECTROSCOPY. *The Astrophysical Journal Supplement Series*, 223(1):12, Mar 2016. doi: 10.3847/0067-0049/223/1/12. URL https://doi.org/10.3847/0067-0049/223/1/12.

[49] A.J.J. Raassen and S.Ortí Ortin. Extension of the analysis of the three lowest configurations in the third spectrum of cobalt (Co III). *Physica B+C*, 123(3): 353–369, 1984. ISSN 0378-4363. doi: https://doi.org/10.1016/0378-4363(84)90111-6. URL https://www.sciencedirect.com/science/article/pii/0378436384901116.

[50] A J J Raassen and P H M Uylings. The use of complete sets of orthogonal operators in spectroscopic studies. *Physica Scripta*, T65:84–87, jan 1996. doi: 10.1088/0031-8949/1996/t65/011. URL https://doi.org/10.1088/0031-8949/1996/t65/011.

[51] L. R. Kurucz. gf2804.pos, Nov 2011. URL http://kurucz.harvard.edu/atoms/2804/.

[52] J. R. Fuhr and W. L. Wiese. A critical compilation of atomic transition probabilities for neutral and singly ionized iron. *Journal of Physical and Chemical Reference Data*, 35(4):1669–1809, 2006. doi: 10.1063/1.2218876. URL https://doi.org/10.1063/1.2218876.

[53] Werner, K., Rauch, T., and Kruk, J. W. The hot white dwarf in the peculiar binary nucleus of the planetary nebula EGB 6. *A&A*, 616:A73, 2018. doi: 10.1051/0004-6361/201833200. URL https://doi.org/10.1051/0004-6361/201833200.

[54] S. P. Preval, M. A. Barstow, N. R. Badnell, I. Hubeny, and J. B. Holberg. Hot DA white dwarf model atmosphere calculations: including improved Ni

PI cross-sections. *Monthly Notices of the Royal Astronomical Society*, 465(1): 269–280, 11 2016. ISSN 0035-8711. doi: 10.1093/mnras/stw2800. URL https://doi.org/10.1093/mnras/stw2800.

[55] Anne Thorne. *Spectrophysics*. Springer Netherlands, 1988. doi: 10.1007/978-94-009-1193-2.

[56] A J J Raassen and P H M Uylings. Critical evaluation of calculated and experimental transition probabilities and lifetimes for singly ionized iron group elements. 31(14):3137–3146, jul 1998. doi: 10.1088/0953-4075/31/14/012. URL https://doi.org/10.1088/0953-4075/31/14/012.

[57] Uylings P.H.M. Raassen A.J.J. VizieR Online Data Catalog: Fe II oscillator strengths, 1998.

[58] Roman Schnabel, M. Johanning, and Manfred Kock. Fe II lifetimes and transition probabilities. *Astronomy and Astrophysics*, 414, 09 2003. doi: 10.1051/0004-6361:20031685.

[59] W Schade, B Mundt, and V Helbig. Radiative lifetimes of fe II levels. 21 (15):2691–2696, aug 1988. doi: 10.1088/0953-4075/21/15/014. URL https://doi.org/10.1088/0953-4075/21/15/014.

[60] E. A. Den Hartog, J. E. Lawler, C. Sneden, J. J. Cowan, and A. Brukhovesky. Atomic transition probabilities for UV and blue lines of fe ii and abundance determinations in the photospheres of the sun and metal-poor star HD 84937. 243(2):33, aug 2019. doi: 10.3847/1538-4365/ab322e. URL https://doi.org/10.3847/1538-4365/ab322e.

[61] Z S Li, H Lundberg, U Berzinsh, S Johansson, and S Svanberg. 33(24):5593–5600, dec 2000. doi: 10.1088/0953-4075/33/24/311. URL https://doi.org/10.1088/0953-4075/33/24/311.

[62] C.M. Sikström, H. Nilsson, U. Litzén, A. Blom, and H. Lundberg. Uncertainty of oscillator strengths derived from lifetimes and branching fractions. *Journal of Quantitative Spectroscopy and Radiative Transfer*, 74(3):355–368, 2002. ISSN 0022-4073. doi: https://doi.org/10.1016/S0022-4073(01)00258-8. URL https://www.sciencedirect.com/science/article/pii/S0022407301002588.

[63] Blom A. Influence of noise on fitted position and intensity of spectral lineshapes. *Lund Reports on Atomic Physics*, 262, 2000.